UNIVERSIDAD DE MURCIA

ESCUELA INTERNACIONAL DE DOCTORADO

Threshold Detection and Analysis: MARS Methodology in Macroeconomics and Public Health

Detección y Análisis de Umbrales: Metodología MARS en Macroeconomía y Salud Pública

D. César Nebot Monferrer

2018

UNIVERSIDAD DE MURCIA

Escuela Internacional de Doctorado

Threshold detection and analysis:

MARS methodology in Macroeconomics and Public Health.

D. César Nebot Monferrer

Supervisors:

Prof. Dr. José García Solanes

Prof. Dr. Arielle Beyaert

2018

A mi mujer y a mis hijos.

Santi: Gracias, sin tu apoyo y fortaleza en el hogar esta tesis no habría sido posible.

Ignasi y Xavi: por tantos momentos que esta tesis nos debe.

Nunca es demasiado tarde para aprender. Si bien la genialidad es la semilla, sólo la constancia y el esfuerzo la convierten en fruto.

Acknowledgments

This thesis would not have been possible without the invaluable guidance of my supervisors. I am deeply indebted to José García Solanes and Arielle Beyaert. I am unable to calculate how many lives I need to live to thank you for all your encouragement, effort, advice and help. You have believed in me so much more than I am capable of doing.

I want to specially thank José María López Lozano, Tim Lawes, and Ian Gould for their tenacity and passion in the fight against bacterial resistance. Thank you for how much you have taught me. We will continue fighting. I want to thank the co-authors of the article on bacterial resistance presented in this thesis and all members of the Threshold study group for their professionalism and dedication to make Science advance and a more hopeful future.

Contents

List of Tables

List of Figures

1 Introducción.

La presente tesis tiene como objeto detectar, con una metodología altamente flexible, la existencia de umbrales, para analizar relaciones macroeconómicas como la Regla de Taylor, (que establece la asociación entre el estado coyuntural de la economía y las decisiones de reacción sobre el tipo de interés de la autoridad monetaria), y la Ley de Okun (que relaciona las variaciones de la actividad económica y las variaciones en la tasa de desempleo); y, a su vez, aplicar la metodología desarrollada para abordar, en un marco altamente interdisciplinar, el análisis de una de las preocupaciones actuales más importantes de la Organización Mundial de la Salud (OMS) en materia de Salud Pública: el desarrollo de la resistencia bacteriana a los antibióticos.

Desde el punto de vista de la teoría económica, aunque se ha debatido mucho acerca de la no linealidad de la Regla de Taylor y de la Ley de Okun, y de sus implicaciones para las políticas macroeconómicas, no se han alcanzado estimaciones ni resultados que permitan implicaciones directas en el diseño de políticas públicas.

Desde el punto de vista de Salud Pública, el debate de la no linealidad entre el uso de antibióticos y el cada vez más preocupante fenómeno de la resistencia bacteriana a los antimicrobianos todavía se encuentra en sus fases iniciales. No obstante, la preocupación mostrada tanto por la OMS (WHO, 2017) como por el G7 no sólo nos impele a explorar la no linealidad de esta relación sino que además entendemos como urgente la detección de umbrales, si existen, en la intensidad de uso de antibióticos, para permitir orientar mejor el diseño de las necesarias políticas de Salud Pública.

Si estas relaciones macroeconómicas como la Regla de Taylor o la Ley de Okun, así como la relación entre la resistencia bacteriana a los antibióticos y el uso de los mismos tuvieran un comportamiento puramente lineal para todo el rango de las variables explicativas, la evidencia empírica no debería mostrar comportamientos no lineales y menos la existencia de umbrales. Así mismo, si existen umbrales en estas relaciones, la metodología adecuada no debería imponer previamente modelos lineales sin una fundamentación suficiente. Ésta debería permitir que sean los datos

los que hablen, no sólo para estimar el modelo, sino también para seleccionarlo.

A diferencia de lo métodos paramétricos que estiman los parámetros de un modelo seleccionado previamente, los métodos no paramétricos permiten una flexibilidad mayor, necesaria para estimar y analizar las relaciones objeto de esta tesis. La metodología no paramétrica Multiple Adaptive Regression Splines (MARS) desarrollada por Friedman (1991) permite seleccionar y estimar modelos detectando múltiples umbrales en los efectos de varias variables explicativas a la vez, e incluso en los efectos de interacción entre ellas si los hubiere. Si bien los modelos lineales pueden ofrecer resultados interesantes en entornos locales, la metodología MARS permite identificar cuándo esta linealidad cambia por regiones en las diferentes variables explicativas.

De hecho, en las relaciones entre variables que se derivan de modelos macroeconómicos, la linealidad suele ser producto de la linearización del comportamiento del sistema en un entorno local, para así aprovechar la versatilidad y simplicidad que entrañan las estimaciones lineales. No obstante, en el comportamiento de las series temporales macroeconómicas no solamente existen fundadas sospechas de que los procesos no lineales subyacen a los modelos de coyuntura económica (Hamilton, 2010), sino que además estos modelos pueden mostrar procesos de sobrerreacción. Por eso, entre otras razones, en las últimas décadas, el análisis no lineal de series temporales económicas ha profundizado en la estimación con métodos no paramétricos.

Desde el trabajo pionero de Tong (1983), han proliferado los estudios en los que se estiman cambios de régimen de comportamiento de las series temporales económicas. Tong desarrolla modelos de umbral para estimar los cambios de comportamiento en la variable dependiente en función de la región de valores del dominio de una variable explicativa, o incluso de la propia variable dependiente retardada. En una primera aproximación Tong (1987) supone la existencia de diferentes funciones lineales en diferentes regiones del espacio de los estados de forma que “el análisis de un sistema estocástico complejo puede ser realizado mediante su descomposición en subsistemas más sencillos”. La metodología TAR (Threshold Autoregression) para series temporales, desarrollada a partir de las ideas de Tong, ha dado lugar a una prolífica literatura y a multitud de estimaciones de series temporales económicas como el PIB de EEUU (Potter, 1995; Pesaran and Potter, 1997). Como refinamientos de esta metodología surgieron métodos de estimación como SETAR (Self-exciting

Threshold Autorregresive) y los que permiten una transición suavizada entre las regiones, como los modelos STAR (Smooth Threshold Autoregression) desarrollados fundamentalmente por Chan and Tong (1986). No obstante, Lewis and Stevens (1991) señalan que si bien la metodología TAR detecta regiones disjuntas, no lo hace necesariamente para regiones de varias variables que puedan interactuar. Cuando los fenómenos económicos son tales que el comportamiento no lineal de una variable depende del comportamiento no lineal de otra, se debe poder definir regiones que recojan efectos de interacción y se precisa el uso de funciones *spline*. En su crítica, proponen el uso de la metodología MARS (Multivariate Adaptative Regression Spline) de Friedman (1991).

En el capítulo 2 de la presente tesis, realizamos una descripción y un análisis en profundidad de la metodología MARS. Se expone paso por paso cómo funciona el algoritmo iterativo de selección del modelo y de estimación. Partiendo del modelo más simple, MARS aproxima la función que relaciona los datos construyendo funciones base mediante la inclusión iterativa de funciones splines truncadas linealmente. En un proceso denominado "forward pass", cada iteración selecciona umbrales, variables y coeficientes de forma que minimiza la suma de los cuadrados de los errores resultantes. Tras este paso, con la intención de reducir la complejidad innecesaria del modelo, se procede a un "backward pass" en el que se reducen iterativamente los términos seleccionados en el paso anterior. Usando el criterio Modified Gross Cross Validation (MGCV) basado en Craven and Wahba (1979) que penaliza la complejidad del modelo, en cada iteración se elimina aquel término cuya aportación al poder explicativo del modelo no compensa la complejidad que induce.

Para comprobar la utilidad de la metodología hemos desarrollado simulaciones de Monte Carlo sobre cuatro modelos diferentes de generación de datos. Estimamos cada muestra tanto con MARS como linealmente y obtenemos las distribuciones empíricas de los parámetros estimados. Demostramos que la metodología MARS se revela como una metodología anidadora: si las relaciones subyacentes son en realidad lineales, el procedimiento de estimación lo seleccionaría y estimaría como tal, y en el caso de existir no linealidades y umbrales también los detectaría. Esto entraña una gran ventaja, sujetarnos a un modelo lineal o a una función no lineal paramétrica nos limita a encajar los datos en ese marco y, por lo tanto, nos expone al riesgo de modelos mal especificados, mientras que con el método no paramétrico MARS los datos permiten no sólo estimar la función sino también seleccionar un mejor modelo (Friedman, 1991, 1993; Lewis and Stevens, 1991).

Para acabar el capítulo sobre la metodología, describimos paso a paso un protocolo básico de estimación que aprovecha las ventajas de MARS. Los pasos de este protocolo siguen una estructura lógica de estimación: en primer lugar, se contempla la selección de variables relevantes aprovechando las capacidades del Generalized Additive Models (GAM) de Hastie and Tibshirani (1990); Hastie (2017) con la intención de evitar problemas de concurvidad habituales en los procesos de selección de modelos; se sugiere también el recurso al test de raíz unitaria con múltiples cambios estructurales propuesto por Carrion-i Silvestre et al. (2009) y al test de cointegración MARS de Sephton (1994), cuando la naturaleza del fenómeno a estudiar lo justifique; en segundo lugar, se procede al diseño del modelo econométrico general y a su estimación con MARS; en tercer lugar, se obtienen medidas de la bondad del ajuste; y, en cuarto lugar, se aplica una innovación metodológica de la presente tesis que consiste en un procedimiento para la obtención de intervalos de confianza de los múltiples umbrales detectados y localizados por MARS, adaptando para ello la metodología propuesta por Hansen (2000) y mejorada por Donayre et al. (2018). Finalmente, para completar el capítulo, describimos un protocolo particularizado para cada relación objeto de estudio de esta tesis, de acuerdo con la naturaleza de los datos o de los modelos existentes previamente en la literatura.

En el capítulo 3, abordamos el estudio de la Regla de Taylor desarrollando un modelo teórico que generaliza el modelo gradual dinámico de Svensson (1997) de metas de inflación. Nos centramos, tal y como hacen otros estudios (Cukierman and Muscatelli, 2008; Surico, 2002, 2007a; Ruge-Murcia, 2002), en que la fuente de no linealidad de la Regla de Taylor provenga de las características de la función de preferencias de la autoridad monetaria sobre las desviaciones de la tasa de inflación y del producto de la economía. En esta tesis proponemos y justificamos una generalización de las funciones de preferencia sobre cada una de estas variables de forma que puedan estar definidas como funciones continuas por partes, estrictamente convexas y con una segunda derivada no continua. En el caso de que la función de preferencia sea cuadrática y se defina igual para todo el dominio, tendríamos el modelo típico de Svensson con una Regla de Taylor lineal. Nuestra estrategia consiste en que si las funciones de preferencia pueden estar definidas de la forma indicada, la regla de Taylor a estimar también pueda estar definida por regiones y así albergar umbrales, incluso múltiples umbrales en efectos de interacción. Así pues, sin imponer una forma funcional concreta, definiendo sus características necesarias y permitiendo la posibilidad de estar definida por partes, nos dotamos de un fundamento teórico más

flexible para estimar, en el caso de que existan, múltiples regímenes y umbrales en la Regla de Taylor. Para acabar el capítulo, se calibran las respuestas en el tiempo del tipo de interés, la tasa de inflación y las desviaciones del producto ante diferentes shocks de oferta y demanda en un modelo con umbrales. Los resultados avalan que el modelo con umbrales muestra ajustes más intensos y que se extienden más en el tiempo ante los shocks que sin umbrales.

En el capítulo 4, incluimos el artículo de investigación en el que estimamos la Regla de Taylor para la Reserva Federal de Estados Unidos aplicando el protocolo correspondiente expuesto en el capítulo 2. Si bien la literatura empírica avala la evidencia de no linealidad de la Regla de Taylor, son diversas las aproximaciones que ofrecen resultados parciales. Los Smooth Transition AutoRegressive (STAR) (Granger et al., 1993) utilizados por (Petersen et al., 2007; Cukierman and Muscatelli, 2008; Gerlach and Lewis, 2014b; Lamarche and Koustasy, 2012; Kazanas et al., 2011; Gnabo and Moccero, 2015) estiman transiciones entre regímenes en una sola variable explicativa. Aunque el refinamiento de Ahmad (2016) usando Multiple Regime MRSTAR permite estimar umbrales simultáneamente para las desviaciones del output y de la inflación, esta metodología no aborda posibles efectos de interacción con umbrales ni estima intervalos de confianza para cada umbral.

En nuestro artículo, aprovechamos la flexibilidad de MARS para estimar la Regla de Taylor para la Reserva Federal de los Estados Unidos. No sólo detectamos umbrales razonables en los efectos principales de las variables explicativas sino también en los efectos de interacción. Además encontramos diferencias significativas en la reacción de la Reserva Federal vinculadas a las diferentes presidencias. Otra de las innovaciones que aportamos es la estimación de intervalos de confianza de los umbrales detectados de forma que ofrecemos una caracterización más completa de la Regla de Taylor que las existentes hasta el momento. En consecuencia, este artículo aporta innovaciones teóricas y empíricas en el continuado debate sobre la Regla de Taylor.

Dado que en el modelo expuesto en el capítulo 3 la fuente de la no linealidad de la Regla de Taylor recae en las preferencias de la autoridad monetaria, resulta interesante estimar la Regla de Taylor para el Banco Central Europeo con la metodología propuesta en esta tesis y observar las diferencias con la estimación obtenida para la Reserva Federal de Estados Unidos. En el capítulo 5, aportamos el artículo de investigación en el que estimamos esta Regla de Taylor para la Eurozona aplicando el protocolo correspondiente expuesto en el capítulo 2. De nuevo, en la literatura

encontramos estimaciones de la Regla de Taylor para el Banco Central Europeo mediante regresiones no lineales por umbrales definidos sobre solo una de las variables explicativas (Gerdesmeier and Roffia, 2004; Gerlach and Schnabel, 2000; Surico, 2007b; Aguiar and Martins, 2008; Ikeda, 2010; Klose, 2011; Kulikauskas, 2014). Otras estimaciones se centran en la existencia de cambios estructurales en torno a la Crisis del 2008 (Gerlach and Lewis, 2014a,b). Dado que MARS no excluye la existencia de cambios estructurales, todos los modelos mencionados se pueden ver como casos particulares de los modelos que MARS puede obtener y, por lo tanto, no están excluidos de nuestro análisis. En nuestra estimación detectamos umbrales tanto en las desviaciones del producto como en la tasa de inflación, y aportamos sus respectivos intervalos de confianza. Concluimos que el BCE tiene en cuenta la actividad económica más de lo que oficialmente declara y reacciona de forma más intensa a las desviaciones de la inflación una vez que éstas han excedido con suficiente margen el objetivo oficial del 2%. Por otra parte, si bien no se encuentran diferencias significativas entre las tres presidencias del BCE, sí se evidencia una caída abrupta en los tipos de interés asociada a la Crisis del 2008.

En el capítulo 6, proponemos un modelo simple para la Ley de Okun basado en la hipótesis de que los empleadores en las empresas son aversos al riesgo. Desde que Okun (1962) estableciera la existencia de esta relación entre las variaciones de la actividad económica y las variaciones del desempleo, no han sido muchos los esfuerzos que se han dedicado en ofrecer su fundamentación teórica para identificar los factores que dan lugar a esta relación y menos para dar una justificación de su no linealidad (Neftci, 1984; Prachowny, 1993; Zerbo et al., 2018; Adachi et al., 2015).

Silvapulle et al. (2004), en su revisión de las posibles causas de la no linealidad de la Ley de Okun, recoge tres hipótesis principales: la “Hipótesis de la rigidez institucional”, relacionada con el coste del despido provocado por causas institucionales; la “Hipótesis del acaparamiento de trabajo” que reflejaría la reticencia de los empleadores a deshacerse de mano de obra en la que han invertido recursos de formación; y, finalmente, la “Hipótesis de la aversión al riesgo de las empresas” que justificaría una mayor reacción del desempleo en momentos de recesión que en momentos de expansión, simplemente porque los empleadores suelen ponderar de forma más importante las malas noticias que las buenas. Silvapulle concluye que sólo la “Hipótesis de la aversión al riesgo de las empresas” tiene sustento en la evidencia empírica.

El modelo que proponemos se basa en la “Hipótesis de empresas aversas al riesgo“

con un coeficiente de aversión que no se mantiene constante. Suponemos que es una función que refleja las preferencias de aversión al riesgo de los empleadores y se define por partes dependiendo de la variación de la actividad económica. Los umbrales en la ley de Okun serían una consecuencia de los saltos que pueden darse en esta función de aversión al riesgo. Por lo tanto, es razonable que pueda haber más de un umbral y en un lugar del crecimiento económico diferente de cero. De hecho, la ubicación de los umbrales tiene su relevancia porque permite debatir si la forma de la Ley de Okun se debe a una combinación de hipótesis, en lugar de una hipótesis única excluyendo a las demás. En concreto, se argumenta que una combinación de la "Hipótesis de aversión al riesgo" y de la "Hipótesis de rigidez institucional" puede dar lugar a una Ley de Okun convexa no lineal con al menos un umbral en la zona de recesión (crecimiento negativo y aumento de la tasa de desempleo). La explicación consistiría en que, en una economía con altos costes de despido, el valor absoluto del coeficiente de Okun aumenta cuando la recesión resulta ser suficientemente intensa superando ciertos niveles. De manera similar, la combinación de la "Hipótesis de aversión al riesgo" con la "Hipótesis del acaparamiento de trabajo" puede dar lugar a una Ley de Okun convexa no lineal con al menos un umbral en la zona de expansión (crecimiento positivo y tasa de desempleo decreciente). Esto significaría que en una economía donde las empresas invierten en la capacitación de sus trabajadores, el valor absoluto del coeficiente de Okun disminuye cuando la expansión se vuelve suficientemente intensiva más allá de ciertos niveles; de modo que las empresas desaceleran la tasa de contratación de nuevos trabajadores por invertir en la capacitación de los ya contratados. Todo esto implicaría que las estimaciones empíricas de la Ley de Okun no deberían imponer previamente ni el número de umbrales, ni su ubicación.

En el capítulo 7, incluimos el artículo de investigación sobre la estimación de la Ley de Okun. La literatura ha explorado ampliamente la evidencia empírica de la Ley de Okun mientras que su su fundamentación teórcia ha sido bastante pobre. Su estudio es relevante para el conocimiento del comportamiento del mercado laboral de una economía, para la implementación y efectividad de las políticas en materia laboral y para comprender la recuperación europea tras la crisis del 2008 con altas tasas de desempleo.

Las investigaciones recientes evidencian cada vez más su naturaleza no lineal pero con limitaciones que procuramos paliar en este capítulo. La mayoría de estudios empíricos sobre la Ley de Okun utilizan modelos paramétricos imponiendo exógenamente la posición de un umbral (Economou and Psarianos, 2016; Huang and Chang,

2005; Holmes and Silverstone, 2006; Valadkhani and Smyth, 2015; Tang and Bethencourt, 2017; Koutroulis et al., 2016). En cambio, Jardin and Gaétan (2012) utilizan un método semiparamétrico más flexible que confirma la no linealidad de la Ley de Okun para 16 países europeos pero sin cuantificar la relación de dependencia entre las variables ni estimar la posición de umbrales.

Creemos que para esta tarea se precisa un procedimiento de estimación flexible e integral para alcanzar tres objetivos principales: cuantificar la relación no lineal entre el crecimiento del producto y la variación de la tasa de desempleo; detectar y localizar, si existen, varios umbrales; y, finalmente, estimar posibles cambios estructurales así como las diferencias entre países.

Para este propósito, en este artículo de investigación, estimamos la Ley de Okun con MARS, aplicando el protocolo correspondiente expuesto en el capítulo 2, para cuatro países de Europa: España, Alemania, los Países Bajos y Francia. Además, en consonancia con la "Hipótesis de la aversión al riesgo de las empresas" hemos incluido una variable dicotómica para controlar el posible efecto de la crisis en la Eurozona para la Ley de Okun de cada uno de estos países.

A pesar de que nuestra metodología no impone un número preestablecido de regímenes y, por lo tanto, de umbrales, nuestros resultados para cada país confirman la existencia de únicamente dos regímenes pero con umbrales cuyas posiciones difieren entre países. De acuedo con los intervalos de confianza estimados, los umbrales son significativamente distintos, salvo para Francia y Alemania donde no difieren entre sí significativamente. Por un lado, nuestras estimaciones revelan que la Ley de Okun de un país periférico como España tiene pendientes mucho más acusadas que las de los países del núcleo. Por otro lado, las diferencias entre los coeficientes de Okun por debajo y por encima del umbral son consistentes con la "Hipótesis de aversión al riesgo de las empresas" según la cual el desempleo responde más fuertemente durante las recesiones que durante las expansiones. Además, las diferencias estadísticamente significativas entre las posiciones de los umbrales contribuyen al debate de que en España la combinación de la aversión al riesgo con la "Hipótesis de rigidez institucional" tiene más fuerza que en el resto de países analizados, donde a su vez la combinación con la "Hipótesis de acaparamiento laboral" sería más importante. Finalmente, los períodos de crisis económica en la zona del euro afectan la ley de Okun en Francia, lo que refuerza la idea de que los empleadores aversos al riesgo están preocupados por la información del área económica en la que están operando. A la

luz de todos estos resultados, este artículo aporta innovaciones teóricas y empíricas en el debate de la Ley de Okun.

Tal como señalábamos al principio de esta introducción, ante la preocupante amenaza para la Salud Pública que entraña la resistencia bacteriana a los antibióticos, el interés actual y el paralelismo por su no linealidad y la posible existencia de umbrales nos han llevado a aplicar esta metodología de forma sistemática. Por lo tanto, en el capítulo 8, incluimos un artículo de investigación, realizado en colaboración con un equipo interdisciplinar de investigadores europeos, en el que hemos analizado, utilizando MARS, la relación entre la intensidad de uso de antibióticos en diferentes centros hospitalarios y de atención primaria de Europa y la aparición de cepas resistentes a estos antibióticos.

Esta aplicación nos permite, además, particularizar el protocolo de estimación para series temporales diferentes a las macroeconómicas y que se recoge en el capítulo 2. A su vez, podemos contribuir de forma práctica en la detección de umbrales en la intensidad de uso de antibióticos que ayuden a orientar el diseño de ciertas políticas de Salud Pública, con resultados que pueden ser muy relevantes para un problema objeto de preocupación en el más alto nivel de las autoridades sanitarios mundiales.

A pesar de que la mayoría de los estudios que investigan esta relación utilizan métodos de estimación lineal, hace varias décadas Levy (1994) formuló la hipótesis de que la aparición de cepas resistentes a los antimicrobianos podía estar asociada a que la intensidad de uso de los antibióticos superase ciertos umbrales, estableciendo así las bases para una relación no lineal. A su vez, una de las vertientes más fructíferas del estudio epidemiológico de este grave problema de Salud Pública consiste en el uso de la econometría de series temporales en la estimación de esta relación (López-Lozano et al., 2000). Si bien la metodología hasta ahora empleada para este problema se ha ceñido a modelos lineales, se revela cada vez más importante el uso de métodos econométricos no lineales (Monnet et al., 2004; Lawes et al., 2015b,a, 2017).

Los resultados del artículo no sólo detectan umbrales precisos en la intensidad de uso de los antibióticos en los centros hospitalarios y de atención primaria objeto de estudio sino que además aportan intervalos de confianza que facilitan dar soporte significativo a las recomendaciones de política sanitaria del uso restringido de antibióticos. Esta línea de estudio nos ha permitido la publicación de tres artículos más en revistas de impacto (Lawes et al., 2015b,a, 2017). El artículo de investigación de este capítulo contribuye con varias innovaciones empíricas en el debate de

la racionalización en el uso de los antibióticos para hacer frente a la amenaza de la resistencia bacteriana.

Finalmente, el capítulo 9 resume, a modo de conclusión, las principales contribuciones de la presente tesis y apunta las futuras líneas de investigación a desarrollar.

2 Methodology.

2.1 Overview.

This chapter describes the methodology we employ in this thesis to estimate different nonlinear relationships. Firstly, we introduce a nonparametric data driven procedure that allows to select and estimate a model, detecting regions of the domain delimited by thresholds. This is Multiple Adaptive Regression Spline (MARS) from Friedman (1991). To demonstrate that this estimation procedure is more general, comprehensive and flexible, we provide Monte Carlo experiments with different models. Afterwards, we introduce a basic protocol to estimate a nonlinear model with possible multiple thresholds in the explanatory variables. Finally, we adapt the basic protocol to three diverse relationships: Taylor rule, that relates interest rate driven by the monetary authority to the inflation rate and the output gap of an economy; Okun's law, that associates variations in unemployment rate of an economy to its output growth; and Antibiotic resistance, that links the antimicrobial resistance to the use of antibiotics at medical centre level.

2.2 Multiple Adaptive Regression Splines.

Over the last decades, nonlinear time series techniques have been developed to model complex dynamics that linear model is not able to represent. Nonparametric regression analysis avoid imposing linearity assumptions in modeling and enables more flexibility to approach data. However, although this data mining provides flexibility, it also quickly results into unreliable in high dimensions. This is the so-called curse of dimensionality due to sparseness of data when the number of possible structural relationship increases fast with dimension. Indeed, for a large dimensionality any dataset tends to be sparse and almost all dataset shows concurvity that makes

prediction unstable in certain regions Morlini (2006). Concurvity is the nonparametric generalization of multicollineatiry; while multicollinearity takes place when some of the explanatory variables are linearly dependent, concurvity occurs when they lie close with a non linear dependency. The greater the number of explanatory variables, the greater the possibility of concurvity to happen by chance (Bozdogan, 2003).

To exploit flexibility of nonparametric modeling and overcome the curse of dimensionality, researchers have proposed some nonparametric methods with backfitting algorithm to penalize complexity and overfitted models. One of them is the Multivariate Adaptive Regression Splines (MARS) procedure by Friedman (1991, 1993); Friedman and Roosen (1995).

MARS is a nonparametric method that estimates nonlinear regression functions without imposing previously functional forms, it means that data-based methodology not only estimates but also selects the model. Given a set of explanatory variables, it fits a model as an expansion in product of truncated linear spline functions selected through a forward and backward recursive partitioning strategy. Hence, the procedure accommodates both nonlinearities and interactions among the explanatory variables as a generalization of Recursive Partitioning (RP) (Friedman, 1977) or Classification and Regression Trees (CART) (Friedman et al., 1984) and additive modeling (Hastie and Tibshirani, 1984, 1987, 1990) that uses spline fitting instead of other simple functions. RP is an approximation of an unknown function $f(x)$ at x using an expansion in a set of basis functions, where each basis function is a product of univariate indicator functions [1]. But Friedman (1991) and Lewis and Stevens (1991) report some weaknesses associated with the RP. One of them is that basis functions composed by indicator functions makes the estimated function to be not continuous at the boundaries even when the true underlying function $f(x)$ is continuous. In addition, RP fails for a large number of explanatory variables or or estimating additive models (Chung, 2012). MARS procedure solves these weaknesses.

First, in order to tackle problems of RP in estimating linear and additive models, Friedman (1991) proposes a simple innovation in the algorithm of MARS. On the contrary to recursive partitioning, for each iteration the parent regions during the

[1] Given $\{Rj\}_{j=1}^{s}$ a set of S disjoint subregions being a partitioning of the domain D, each basis function is an indicator function $B_j(x) = I\{x \epsilon R_j\}$ that takes value one if it accomplishes the condition $x \epsilon R_j$ and zero otherwise.

creation of its related subregions are not automatically eliminated. Consequently both the parent and its related subregions are can be chosen for further partitioning in the next iterations resulting into possible overlapping subregions of the whole domain. This innovation allows the algorithm to produce linear models with the iterative partitioning of the initial region by different explanatory variables and the addition of successive partitioning with different predictor variables.

The second innovation in MARS procedures consist of a modeling approach with linear truncated splines (hinges) instead of indicator functions to eliminate discontinuities at the boundaries of adjacent subregions. Thus, it produces models with continuous functions and with discontinuous first partial derivative of $f(x)$ at the knot points of each explanatory variable. Even more, MARS also may produce additive models allowing interactions and trading off the interaction order and model complexity of the additive functions and interactions with a global criterion (Frank, 1995). Therefore, MARS produces a more flexible approach than ordinary linear regression and additive modeling. In addition, MARS procedure endogenously detect knots locations, i.e. thresholds, without previously imposing their existence, which are the explanatory variables with thresholds and the number of them.

Lewis and Stevens (1991) extend this technique to nonlinear time series analysis using lagged values of the time series as explanatory variables in MARS algorithm. The models from this procedure are called Adaptive Spline Threshold AutoRegressive (ASTAR) time series models that can be considered as a generalizations of the Threshold Autoregresive (TAR) models initially introduced by Tong and Lim (1980), Tong (1983), and Tong (1990).

To date, compared to the TAR models, the MARS methodology has not received much attention in economics in spite of its great flexibility. Tong's pioneering contribution gave rise to a very extensive line of research that explores possible thresholds in economics; Hansen (2011) provides an excellent review of the prolific line of research derived from Tong's work. The basic TAR model assumes that the autoregressive structure of a variable varies according to the value reached by the variable itself in the recent past.

A related line of research in recent decades examines using a threshold specification in the context of a traditional regression model. In these studies, two distinct regression models are defined and simultaneously estimated for two disjoint regions defined in a threshold variable, which needs not be the explained variable. However, even

the more sophisticated threshold regression models consider the existence of only one threshold variable and only one set of disjoint threshold-defined regions. These are serious limitations if we suspect that $f(x)$ could exhibit multiple thresholds associated with various threshold variables and even interactions between them. Lewis and Stevens (1991) present a general criticism of the limitations of traditional threshold models and propose the MARS as a solution. Consequently, in contrast with the traditional TAR and threshold regression models, it is unnecessary to determine which variable generates a threshold behavior.

MARS for time series initiated by Lewis and Stevens (1991) has been extensively explored by Keogh (2010) with different autoregressive orders and temporal terms (TSMARS). While Self-Exciting Threshold AutoRegressive (SETAR) and Open Loop Threshold AutoRegressive (TARSO) models introduced by Tong and Lim (1980) estimate piecewise linear functions over disjoint subregions but discontinuous at their boundaries, TSMARS methodology obtains nonlinear threshold models continuous in the domain of the explanatory variables and possible interactions between lagged explanatory variables. Therefore TSMARS constitutes a generalization of Tong's models (Chung, 2012).

MARS procedure has been widely used to estimate functions in diverse fields of knowledge as Natural Science: Ecology and Environmental Science (Kilinc et al., 2017; Zhang and Hepner, 2017) or Oceanography (Lewis and Ray, 1997); Medical and Health Science: Epidemiology (Lawes et al., 2015b,a, 2017) or Public Health (Vanegas and Vásquez, 2017); Engineering and Technology: (Dey and Das, 2016; Goh et al., 2018); Social Science: Economics and Finance (De Gooijer et al., 1998; Sephton, 2001); Agricultural Science: (Deo et al., 2017; Mehdizadeh et al., 2017). Some studies as Kuhnert et al. (2000); Muñoz and Felicísimo (2004); Mukkamala et al. (2006); Mehdizadeh et al. (2017) also check the better performance of MARS than other parametric and nonparametric techniques in terms of accuracy and flexibility. Leathwick et al. (2006) provide evidence of MARS models are also parsimonious with better predictions than General Additive Models from Hastie and Tibshirani (1987, 1990). Ture et al. (2005); Alvarado et al. (2010) remark the superior computation efficiency of MARS procedure, its accuracy and interpretability of its results.

On the other hand, although Friedman (1991) establishes a minimum required data of 50 observations, Jin et al. (2001) argue that small sample size deteriorates MARS performance. Moreover Briand et al. (2000) note that MARS is sensitive to outlier

effect and to strong collinearities among explanatory variables. These weaknesses should be taken into account when the pool of explanatory variables and their lags can be great or under the suspicion of the existence of outliers due to any problem in data gathering procedure. Lawes et al. (2015b,a, 2017) propose to reduce the initial pool of possible explanatory variables using Generalized Additive Models to discard no significant potential predictors in the research on the effect of multiple antibiotic use on the antimicrobial resistance. Thus, this previous step may collaborate with backward fitting algorithm of MARS to tackle the curse of dimensionality.

2.2.1 MARS algorithm.

MARS algorithm is composed by some steps. The objective is to model the dependence of variable y_t on explanatory variables $x_t^1, ..., x_t^p$. We define the model

$$y_t = f(x_t^1, ..., x_t^p) + \varepsilon_t$$

over some domain $D \epsilon \mathbf{R}^p$ containing the data and the error term ε_t is assumed to be independently distributed with $E(\varepsilon_t) = 0$ and variance $E(\varepsilon_t^2) = \sigma^2$. The function $f(x)$ is the true relationship between outcome time-series (y_t) and a vector of p explanatory variables $x_t = (x_t^1 \ldots . x_t^p)$ that we want to estimate from the data.

MARS procedure approximates this function[2] as:

$$y_t = \beta_0 + \sum_{m=1}^{M} \beta_m b_m (x_t) + \varepsilon_t$$

where;

[2]It is easy to see that a model specification with a threshold can be expressed as a combination of hinge functions. Without loss of generality, let us consider a function with two regions delimited by a threshold τ. For each region we have different slopes β_1 and β_2.

$$\begin{cases} y = a_1 + \beta_1 x + \varepsilon & x \leq \tau \\ y = a_2 + \beta_2 x + \varepsilon & x > \tau \end{cases}$$

This specification can be rewritten as the sum of basis functions

$$y = \alpha + c_1 max(x - \tau, 0) - c_2 max(\tau - x, 0) + \varepsilon$$

where τ is the knot, and each basis function is composed by a hinge or truncated spline function $max()$ and coefficients that correspond to the previous specification $c_1 \equiv \beta_1$ and $c_2 \equiv \beta_2$.

β_0 is a constant

β_m is the coefficient for the m^{th} basis function, $m = 1, ..., M$

$b_m(x_t)$ is the m^{th} basis function, $m = 1, ..., M$

ε_t is an independently distributed error term with $E(\varepsilon_t) = 0$ and variance $E(\varepsilon_t^2) = \sigma^2$

The basis functions are products of up to a maximum interaction order mi truncated linear splines or hinge functions (we usually restrict $mi = 2$), describing the relationship between one or more explanatory variables and the outcome in terms of segments of stable association separated by knots or thresholds values. These interacting hinge functions allow us to identify possible interactions between variables. Namely, for a $mi = 2$ the m^{th} basis function takes one of the following two forms:

No interaction: $b_m(x_t) = h\left(x_t^k, \tau_{k,m}\right)$ for some $k = 1, \ldots, p$

With interaction: $b_m(x_t) = h_m\left(x_t^k, \tau_{k,m}\right) \cdot h_m\left(x_t^j, \tau_{j,m}\right)$

for some $k,\ j = 1, \ldots, p,\ k \neq j$

where $\tau_{k,m}$ is the threshold value of x_t^k in the m^{th} basis function and where $h\left(x_t^k, \tau_{k,m}\right)$ is a hinge function (or truncated linear spline) that takes the following form depending on whether the basis function takes effect above or below the threshold $\tau_{k,m}$ (See Figure 2.1)

a) above the threshold: $h_m\left(x_t^k, \tau_{k,m}\right) = max(x_t^k - \tau_{k,m},\ 0)$

b) below the threshold: $h_m\left(x_t^k, \tau_{k,m}\right) = max(\tau_{km} - x_t^k,\ 0)$

Figure 2.1: Graph of the two truncated linear spline or hinge functions.

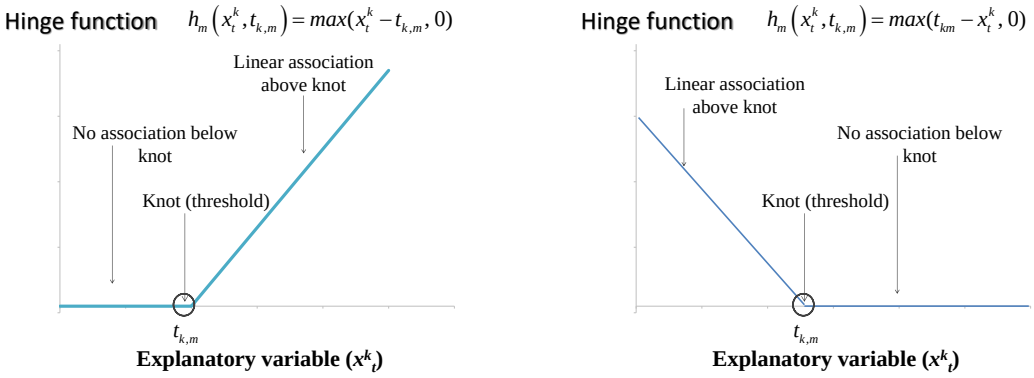

If no knot (threshold) is detected, then a simple linear association between explanatory and outcome variable can be specified as a single function applied across the total range of values of the explanatory variable.

In the algorithm, once we define $x_t = (x_t^1 \ldots . x_t^p)$ with all potentially significant explanatory variables, including the associated lags, the model identification and estimation proceed by an automated and iterative process. The description that follows is mainly based on Friedman (1991, 1993); Chung (2012).

Forward pass: In general terms, MARS starts with the simplest model containing only a constant basis function and iteratively generates a matrix of basis functions in a forward stepwise manner. Candidate basis functions are added in order of ability to improve model fit by minimizing the residual sum of squares (RSS) until the model reaches a predefined limit of complexity. The candidate basis functions are identified by a nested exhaustive search looping over the existing set of basis functions, and all other possible explanatory variables (or interactions) and knot (threshold) positions.

In more exhaustive terms, the forward pass proceeds in the following way. To estimate $f(x_t)$ with data $\{y_t, x_t^k\}_{t=1}^T$, , for $k = 1, ..., p$ let $\{R_m\}_{m=1}^S$ be a set of disjoint subregions of the domain such that $D \mid D = \cup_{m=1}^S R_m$. MARS estimates the function $f(x_t)$ at x_t with

$$\hat{f}(x_t) = \sum_{m=1}^{S} \beta_m b_m(x_t)$$

where b_m are the basis functions associated with the subregions R_m. These basis functions are of the form

$$b_m(x) = \begin{cases} 1, & m = 1 \\ \prod_{j=1}^{mi} h_{jm}\left(x_t^{k(jm)}, \tau_{jm}\right) & m \geq 2 \end{cases}$$

where mi is the number of interaction order in the m^{th} basis function, h_{jm} indicates the hinge function, $k(jm)$ is the index of the explanatory variables and τ_{jm} is a knot location on each of the corresponding variables.

MARS algorithm starts with only one basis function $b_1(x_t) = 1$ in the model which

corresponds to selecting the initial subregion as $R_1 = D$, the whole domain. After the initial step, the algorithm first adds a pair of basis functions:

$$b_2(x_t) = b_1(x_t)max(x_t^k - \tau,\ 0) \text{ and } b_3(x_t) = b_1(x_t)max(\tau - x_t^k,\ 0)$$

where $t \in \{x_t^k : 1 \leq i \leq N; 1 \leq k \leq p\}$. The pair (x_t^k, τ) is found by minimizing the RSS

$$\sum_{i=1}^{N}[y_t - \beta_1 - \beta_2 max(x_t^k - \tau,\ 0) + \beta_3 max(x_t^k - \tau,\ 0)]^2$$

for $k = 1, ..., p$. The estimation procedure is an exhaustive search method.

For every $t \in \{x_t^k : 1 \leq i \leq N; 1 \leq k \leq p\}$ and $k = 1, ..., p$, the ordinary least squares method is performed and the pair (x_t^k, τ) with the minimum RSS is chosen. The resulting model has the form $\hat{f}(x) = \beta_1 + \beta_2 max(x_t^{k*} - \tau^*,\ 0) + \beta_3 max(x_t^{k*} - \tau^*,\ 0)$

For the next iteration, a pair of products are included such that

$$b_m(x_t)max(x_t^k - \tau,\ 0) \text{ and } b_m(x_t)max(\tau - x_t^k,\ 0)$$

where for $b_m(x_t)$ we have the previously selected basis functions:

$$b_1(x_t) = 1,\ b_2(x_t) = max(x_t^{k*} -\ \tau^*,\ 0) \text{ and } b_3(x) = max(\tau^* - x_t^{k*},\ 0)$$

The selection of basis function depends on the RSS. The model shall contain $2M+1$ basis functions after the Mth iteration. The next $M + 1$ iteration adds two new basis functions:

$$b_{2M+2}(x_t) = b_l(x_t)max(x_t^k - \tau,\ 0) \text{ and } b_{2M+3}(x_t) = b_l(x)max(\tau - x_t^k,\ 0)$$

where $1 \leq l \leq 2M + 1$ and the $b_l(x_t)$ is already in the model. Therefore, l, k and τ minimize the RSS. That is

$$(l, k, \tau) = \underset{l,k,t}{argmin} \sum_{i=1}^{N}[y_t - \sum_{m=1}^{2M+1}(\beta_m b_m(x_t) - \beta_{2M+2} b_l(x_t)max(x_t^k - \tau,\ 0) -$$
$$- \beta_{2M+3} b_l(x)max(\tau - x_t^k,\ 0)]^2$$

The algorithm iterates this forward step until the maximum number of basis functions M_{max} (chosen by the user) is reached. This forward pass procedure provides a model that overfits the data. Therefore, it is necessary a pruning pass to eliminate those subregions whose basis functions do not sufficiently contribute to the accuracy of the model.

Backwards (pruning) pass: During the subsequent pruning pass MARS removes basis functions contributing least to model fit, until no significant improvement is seen in a modified form of the generalized cross validation (MGCV) criterion that penalizes model complexity, based on Craven and Wahba (1979). This criterion is defined as

$$\text{MGCV} = \frac{\frac{1}{T}\ \sum_{t=1}^{T}(y_t - \hat{f_M}\,(x_t))^2}{[1 - C\,(M)\,/T]^2}$$

where T is the number of observations; $C(M)$ is the model complexity penalty function which is defined as $C(M) = (M+1) + dM$, where M is the number of basis functions retained in the model and $M + 1$ the number of parameters in $\hat{f_M}\,(x_t))$ and d represents the degree of additional contribution brought by a basis function to the model complexity, Friedman (1991) suggests a value for d between 2 and 4; usually $d = 3$.

Therefore, this MGCV criterion accounts for the inherent improvement in explained variance associated with increasing numbers of basis-functions, and its calculation allows estimates of the relative importance of each basis function. Model selection converges on a set of basis functions that most efficiently explain variation in dependent variable.

Figure 2.2 illustrates the scheme of MARS procedure with forward and backward passes compared with Ordinary Least Squares (OLS) estimation. It can be clearly understood as a particular case of MARS where forward stepwise and pruning pass do not detect any threshold for each of the explanatory variables.

According to the steps in forward pass in MARS procedure, the variable x is split into two variables $z_1 = max(x - \tau, 0)$ and $z_2 = max(\tau - x, 0)$. Therefore, one of

Figure 2.2: Scheme for the Multiple Adaptive Regression Spline (MARS) procedure and its comparison to the Ordinary Least Squares (OLS) estimation.

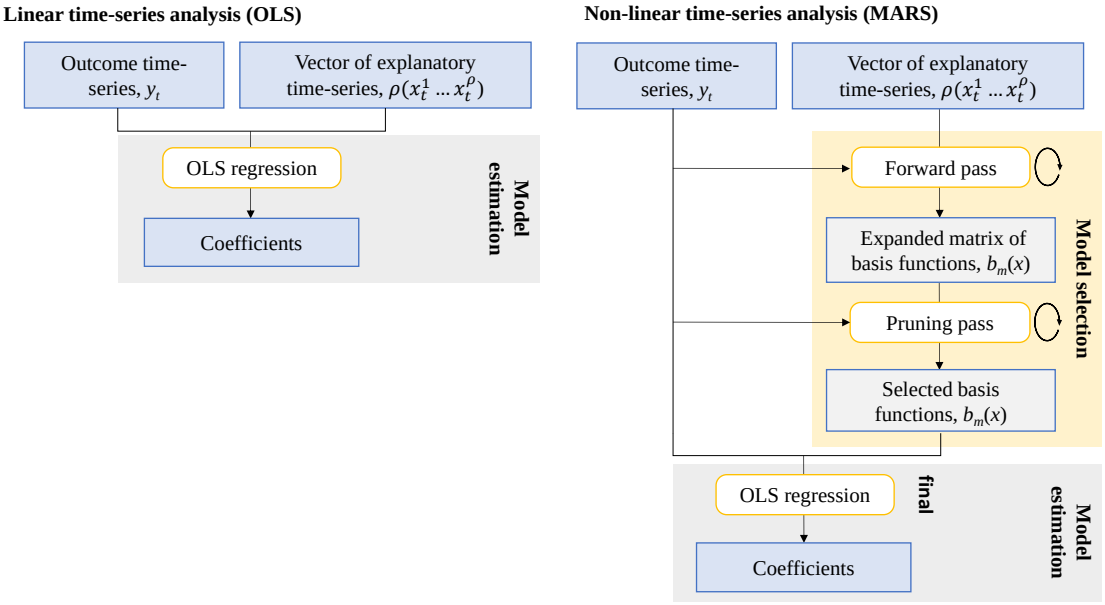

the outputs we can obtain from MARS procedure is the matrix of split explanatory variables corresponding to each basis function detected.

From the output of MARS model, it is useful to generate contribution charts illustrating how the outcome time-series depends on each explanatory variables across the observed ranges. See Figure 2.3 for different examples of contributions[3].

[3]For MARS estimations and plotting contributions, we created codes in R using packages *Earth* and Plotmo (Milborrow, 2009, 2015). Also we use B34S programming language with SCAB34S Splines module (available in SCA Workbench, Scientific Computing Associates Corp, Illinois, USA) (Stokes and Lattyak, 2005, 2008b).

Figure 2.3: Example illustrations of contributions from MARS.

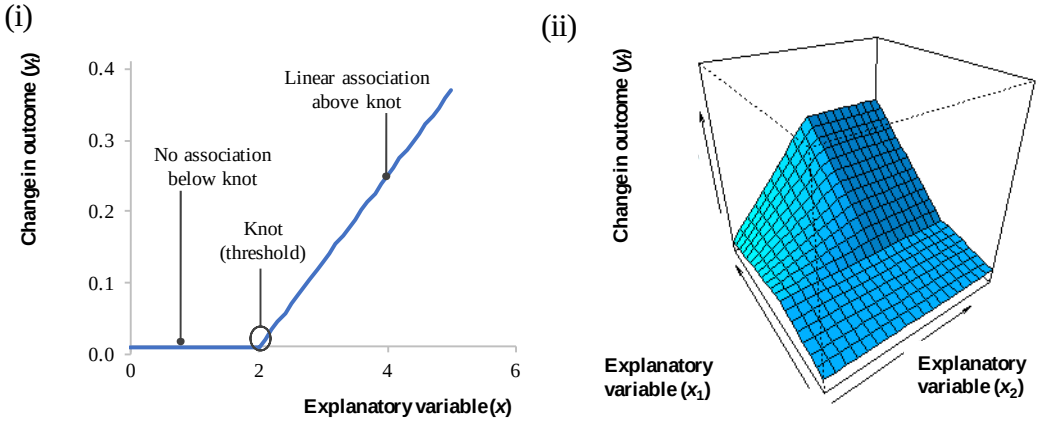

Contribution charts illustrating the case of basis functions of the relationship between the outcome (y_t) and (i) a single explanatory variable with positive impact only above threshold and (ii) interacting explanatory variables (x_1, x_2) with various types of impact depending on the regions of the interacting variables

2.2.2 Monte Carlo experiments.

To impose strict linearity in estimations when the underlying relationship is non-linear can result into misspecification with an important loss of information and biased model coefficients. It is useful to run Monte Carlo experiments for demonstrating this. In this subsection, we present some Monte Carlo experiments to check the properties of the estimators and to compare them with that ones resulting from linear estimation.

a) Comparing linear and non-linear time-series model performance.

We used a Monte Carlo experiment to compare the ability of linear (Ordinary Least Squares, OLS) and non-linear (Multivariate Adaptive Regression Splines, MARS) time-series models in identifying various predefined functional relationships between simulated explanatory and outcome time-series. We hypothesized that for time-series related by simple linear processes MARS and OLS regression methods would perform equally well, but that only MARS would accurately identify non-linear associations. We generated 10000 simulated datasets using simple stochastic processes incorporating the following predefined functional relationships (see Figure 2.4):

- (A) Non-autoregressive without threshold

$$y_t = -4 + 2x_t + u_t \quad u_t \sim N\left(0, \sigma^2 = 0.1\right) \quad \forall t = 1, \cdots, 200$$

- (B) Non-autoregressive with threshold

$$\begin{cases} if\ x_t \leq 2 \ \ y_t = u_t & u_t \sim N\left(0, \sigma^2 = 0.1\right) \\ if\ x_t \leq 2_t \ \ y_t = -4 + 2x_t + u_t & u_t \sim N\left(0, \sigma^2 = 0.1\right) \end{cases} \quad \forall t = 1, \cdots, 200$$

- (C) Autoregressive with threshold

$$\begin{cases} if\ x_t \leq 0 \ \ y_t = 0.5y_{t-1} + u_t & u_t \sim N\left(0,\ \sigma^2 = 0.1\right) \\ if\ x_t > 0 \ \ y_t = 0.5y_{t-1} + 1x_t + u_t & u_t \sim N\left(0,\ \sigma^2 = 0.1\right) \end{cases} \quad \forall t = 1, \cdots, 200$$

- (D) Threshold Autoregression

$$\begin{cases} if\ x_t \leq 0 \ \ y_t = 0 + 0.25y_{t-1} + u_t & u_t \sim N\left(0,\ \sigma^2 = 0.1\right) \\ if\ x_t > 0 \ \ y_t = 0 + 0.75y_{t-1} + u_t & u_t \sim N\left(0,\ \sigma^2 = 0.1\right) \end{cases} \quad \forall t = 1, \cdots, 200$$

Where:

x_t is the explanatory (independent) time-series variable at time t

y_t is the outcome (dependent) time-series variable at time t

u_t is the error term at time t , with Normal distribution, zero mean and variance σ^2

y_{t-1} is an autoregressive term of order 1 (i.e. dated at *t-1*)

For each dataset we fitted both linear and non-linear time-series analyses with MARS, and recorded sample parameter estimates (a constant, b slope, and s^2 as the estimate of variance of error), a measure of goodness of fit (R^2) and threshold. Figure 2.4 illustrates histograms for the distributions of R^2 values and parameter estimates from both linear and non-linear models with MARS. Each column contains the analysis from the Monte Carlo experiment associated to the (A) to (D) models. They are headed by their respective mathematical model expression and scatter plots representing one sample generated by the model and the actual model for each experiment with solid lines. Each row, from the second to the fifth one, contains the histograms of each estimated parameter distribution from both linear and MARS, blue and red respectively. Red vertical lines are the actual values of the parameters of each respectively model. Last row contains histograms of the distribution for threshold estimates.

The model (A), in the first column, is a simple linear association between an explanatory variable x_t and the explained variable y_t with no threshold. The violet color of the histograms reflects overlapped distributions of linear and MARS parameter

estimates[4]. They show that MARS and Ordinary Least Square give practically the same estimate distributions.

The model (B), in the second column, is similar to the model (A) but with a threshold in the predictor variable at 2. In this case, MARS identifies the lack of an association below the threshold and correctly estimates the association above the threshold in the defined stochastic process. By contrast, the linear approach results in biased estimations of coefficients with constant and slope at all levels of x_t (see histograms in 2.4 (B)). Moreover, the variance of residuals in the linear model is significantly greater than the one in MARS which reflects the value in the predefined stochastic process. This indicates that linear estimation ignores valuable information on predictable variation in y_t by describing it as error. This is reflected in a lower proportion of total variation in the dependent variable explained by the independent variable in OLS compared to MARS models.

The model (C) is a transfer function with an autoregressive term y_{t-1} and a transfer variable x_t with a threshold. In this case, as for the model (B) OLS is clearly worse than MARS to approach the actual model.

[4]In this Monte Carlo experiment, we reject possible detected thresholds when the slopes of the basis functions and not significantly different using the computed distributions in the experiment for the slopes.

Figure 2.4: Monte Carlo experiments comparing linear and non-linear time-series analyses (MARS).

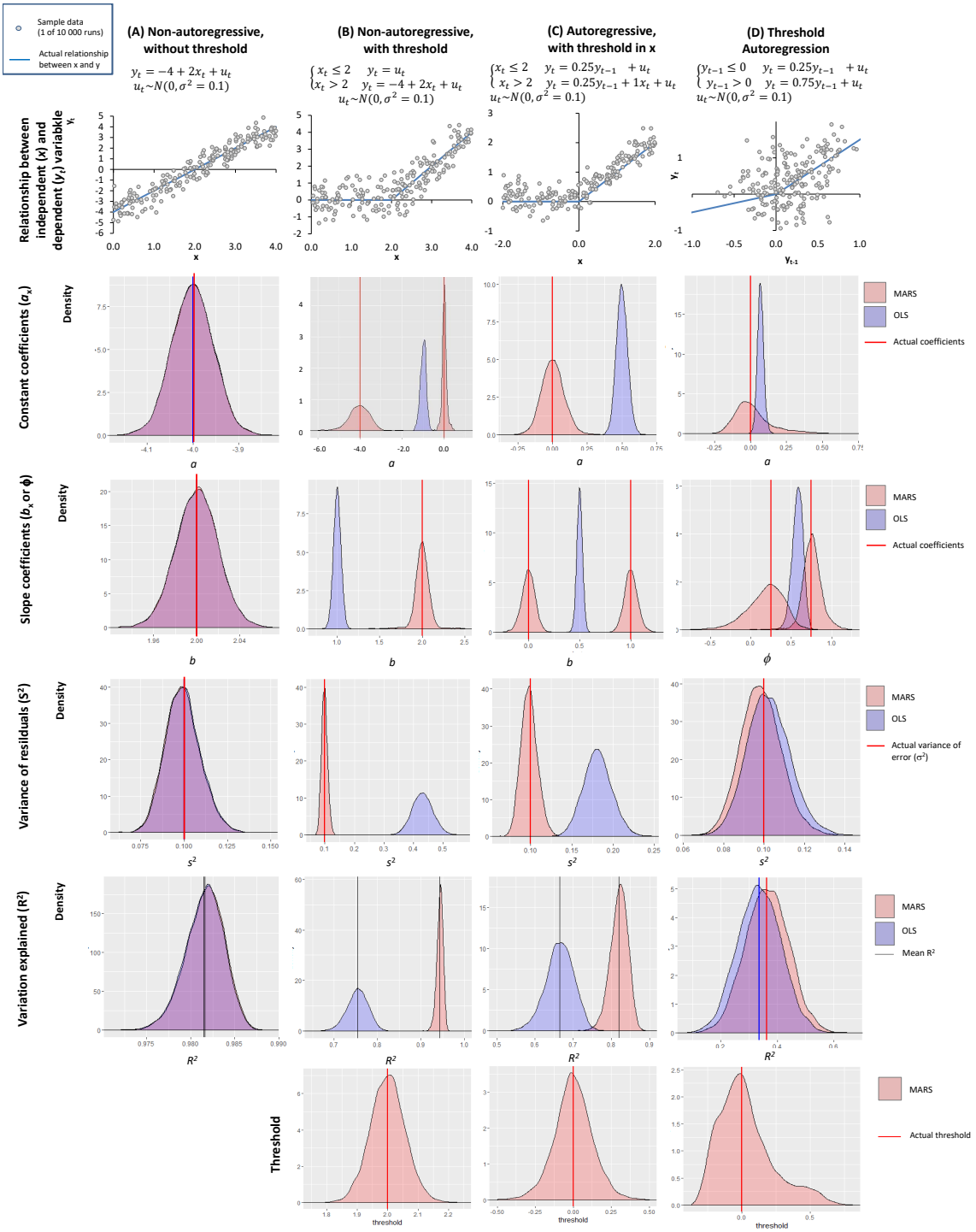

Ability to identify known relationships between explanatory (x) and outcome (y_t) time-series was assessed by applying both linear (ordinary least squares, OLS) and non-linear (Multivariate Adaptive Regression Splines, MARS) models to 10, 000 datasets generated through simple predefined stochastic processes (A) to (D). Frequency distributions indicate estimates from these 10,000 models of coefficients (constant a, slope b), and variance (s^2) as well as summary of model fit (R^2). Comparison can be made to predefined values for coefficients and variance of error.

The model (D) is a simple Threshold Autoregressive model (TAR) with a threshold in the autoregressive term y_{t-1}. In this case, variance of residuals and the explained variation are quite similar between both estimation procedures but MARS provides unbiased estimators. On contrary to the previous models with thresholds, the distribution of the estimated threshold for this model is not symmetric. Table 2.1 contains four sections, one for each model from (A) to (D). Actual values of each parameter are in the Actual column, while OLS and MARS column include the mean of each parameter estimates and its 95% confidence interval calculated from the distributions extracted from the previous Monte Carlo experiments. Median of distribution for each estimated parameters with MARS are provided in the last column; therefore we can check the asymmetric distribution of the estimated parameters with MARS in case of a TAR model as in (D). According to these values, we can conclude that for each nonlinear model, MARS not only provides a better fit to data than OLS, as expected, but also a comprehensive methodology which detects thresholds delimiting regions for each independent variable with a distinct functional relationship with the dependent variable, and estimates OLS for each of those regions.

Threshold distribution from the model (D) in table 2.1 is skew. To check the behavior of the threshold distribution from the model (D) we have run Monte Carlo experiments for a range of the variance of errors σ^2 from 0.01 to 0.25. Figure 2.5 illustrates how the 95% confidence interval of the distribution of threshold estimates, its mean and median depend on the variance of errors σ^2. As logically, the greater is the variance of errors, the lower is the accuracy of threshold detection and therefore the greater is the 95% confidence interval. We have also computed Pearson's coefficient of skewness for threshold distribution depending on the variance of errors, σ^2; the number of samples, N; and the number of periods for each sample, T. Pearson's coefficient of skewness is constant on σ^2 and N [5] and decreases on sample periods but not monotonically (see Figure 2.6). Therefore, the greater the number of period of the sample, the lower is the skewness of the threshold distribution, therefore its mean and its median become closer.

[5] Given $N = 10.000$ and $t = 200$, Pearson's coefficient of skewness is 0.91 for all the range of $\sigma^2 \epsilon (0.01, 0.25)$. And for $\sigma^2 = 0.1$ and $t = 200$, coefficient of skewness is hardly constant 0.9 for all the range of $N \epsilon (500, 10.000)$,

Table 2.1: Results from Monte Carlo experiments

Model	Actual	OLS coefficients	MARS coefficients	MARS median
(A) Non-autoregressive without threshold				
Constant coefficient (a)	-4.00	-4 (-4.09, -3.91)	-4 (-4.09, -3.91)	-4
Slope coefficient (b)	2.00	2 (1.96, 2.04)	2 (1.96, 2.04)	2
σ^2	0.10	0.1 (0.08, 0.12)	0.1 (0.08, 0.12)	0.1
R^2	-	0.98 (0.98, 0.99)	0.98 (0.98, 0.99)	0.98
(B) Non-autoregressive with threshold				
Constant coefficient (a)		-1 (-1.21, -0.82)		
Slope coefficient (b)		1 (0.91, 1.09)		
Constant coeff. (ai) below threshold	0.00		0 (-0.13, 0.12)	0
Slope coefficient (bi) below threshold	0.00		0 (-0.12, 0.12)	0
Constant coeff. (aii) above threshold	-4.00		-4 (-4.53, -3.53)	-4
Slope coefficient (bii) above threshold	2.00		2 (1.83, 2.19)	2
Threshold	2.00		2 (1.89, 2.11)	2
σ^2	0.10	0.43 (0.36, 0.5)	0.1 (0.08, 0.12)	0.1
R^2	-	0.75 (0.7, 0.8)	0.94 (0.93, 0.96)	0.94
(C) Autoregressive with threshold				
Constant coefficient (a)	0.00	0.5 (0.44, 0.56)	0 (-0.15, 0.17)	0
Slope coefficient (b)		0.5 (0.44, 0.56)		
Slope coefficient (bi) below threshold	0.00		0 (-0.14, 0.12)	0
Slope coefficient (bii) above threshold	1.00		1 (0.88, 1.14)	1
AR(1) coefficient (ϕ)	0.25	0.25 (0.16, 0.33)	0.25 (0.18, 0.31)	0.25
Threshold	0.00		0 (-0.26, 0.26)	0
σ^2	0.05	0.18 (0.15, 0.22)	0.1 (0.08, 0.12)	0.1
R^2	-	0.66 (0.59, 0.73)	0.82 (0.77, 0.86)	0.82
(D) Threshold Autoregressive				
Constant coefficient (a)	0	0.07 (0.03, 0.12)	0.02 (-0.17, 0.36)	-0.01
AR(1) coefficient (ϕ)		0.58 (0.44, 0.7)		
AR(1) coefficient (ϕi) above threshold	0.75		0.76 (0.53, 1.02)	0.76
AR(1) coefficient (ϕii) below threshold	0.25		0.18 (-0.34, 0.56)	0.21
Threshold	0		0.03 (-0.26, 0.54)	0
σ^2	0.1	0.1 (0.08, 0.12)	0.1 (0.08, 0.12)	0.1
R^2		0.34 (0.19, 0.48)	0.36 (0.22, 0.51)	0.36

Figure 2.5: Distributions of threshold estimates on different values σ^2.

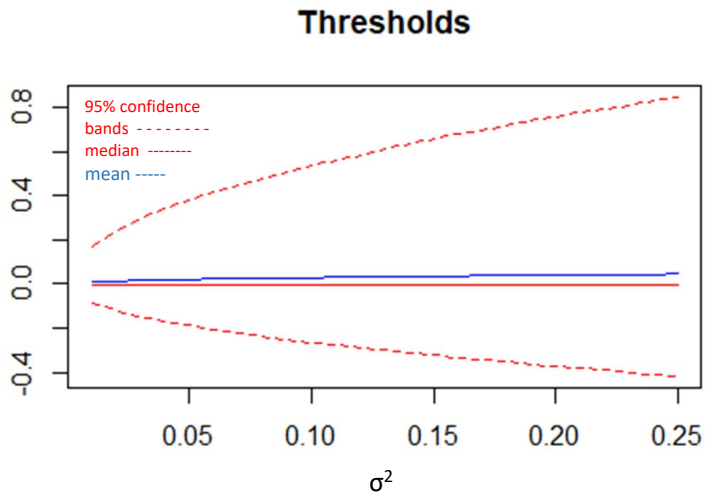

This Figure illustrates how the 95% confidence interval of the distribution of threshold estimates, its mean and median depend on the variance of errors σ^2 we use for the model to run Monte Carlo experiments.

Figure 2.6: Pearson's coefficient of skewness for the threshold distribution the model (D) depending on sample periods T

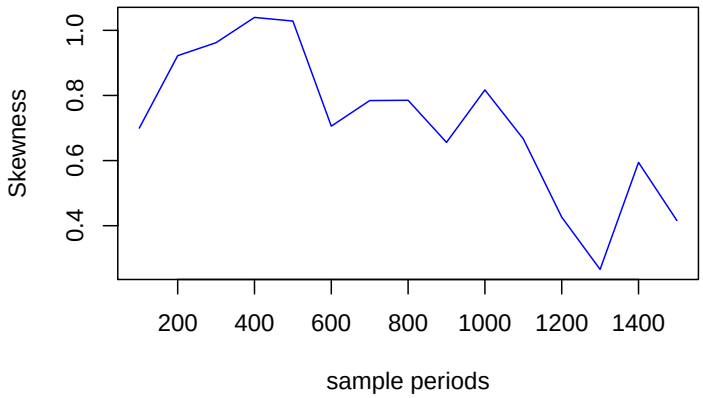

2.3 Estimation protocols.

Our purpose in this thesis consist of approaching nonlinear relationships with MARS methodology. In this subsection, we present a basic protocol, it means a list of some basic steps for estimating nonlinear functions we suspect that contains thresholds in the explaining variables. Afterwards, according to the nature of each time series we adapt the basic protocol adding some steps. We use our methodology on three different functional relationships.

The first one is Taylor rule: the reaction of the interest rate driven by the monetary authority with respect to inflation rate and output gap of the economy; many studies have attempted to estimate Taylor rule with nonlinear and both parametric and non parametric methods but although the possible existence of multiple thresholds in this function not many efforts have been addressed to estimate them. The flexibility and comprehensiveness MARS methodology may allow to contribute with enrich Taylor rule estimations not only with multiple thresholds but also with combined thresholds in interaction effects if they exist.

The second one is Okun's law: the relationship between the change in unemployment rate of an economy and its output growth; even though researchers have devoted efforts to estimating nonlinear Okun's law, they usually impose the existence of only one threshold and even its level. This strong assumption implies that only one of the theoretical hypothesis that shape Okun's law can be verified. Once more again, flexibility of MARS methodology can provide richer estimations with multiple and not previously imposed thresholds. This may shed light in the theoretical debate about the hypothesis that shape Okun's law.

The third one is the relationship between the antimicrobial resistence (AMR) and the use of antibiotics. This is absolutely different to the previous two relationships but it is of major current interest because of the World Heath Organization concerns (WHO, 2017). In addition, it is a chance to apply MARS methodology to very diverse data as epidemiological time series. Incipient research efforts have been devoted (Lawes et al., 2015b,a, 2017) to detect possible thresholds in this relationship as hypothesized Levy (Levy, 1994).

As it seems logical, in order to apply the basic protocol to each time series of the relationships we want to model, it turns to be necessary to adapt it to the nature of the data. For instance, unlike time series from national statistics offices Official

Statistical Offices, quality of antibiotic use data gathered from hospital laboratories may require an outlier treatment of the time series. Also, it is different if we need to check previously which are the explanatory variables or if they come out directly from a theoretical model. In the next subsections, we present the basic protocol and the enhanced protocols we employ to estimate these mentioned relationships.

2.3.1 Basic protocol.

We propose a basic protocol composed by four steps. The first step consists of selecting explanatory variables and their lags. The second one is the estimation with MARS procedure and the contributions charts to understand the nonlinear relationship between the explained variable and each one of the significant predictors. The following step consists in some diagnostic checks to evaluate performance of estimation. Finally, the last step is addressed to obtain 95% confidence bands for each detected threshold.

Step 1. Set the pool of explanatory variables and their lags.

MARS is a data driven procedure that both selects and estimates the model. It provides a high degree of flexibility but it may be affected by curse of dimensionality or concurvity problem in high dimensions that makes prediction unstable in certain regions (Morlini, 2006). Concurvity is the nonparametric generalization of multicollineatiry. Therefore, the greater the number of explanatory variables, the greater the possibility of concurvity to happen by chance (Bozdogan, 2003).

In case we obtain the pool of explanatory variables and their lags from a theoretical model, we can proceed with MARS relying on its ability to discard no significant predictors but it is likely to come out a concurvity problem. We propose to carry out optionally an additional *a priori* data-based selection of candidate explanatory variables and lags. This would be done through inspection of outputs from fitting a General Additive Model (GAM) to the data. GAM is a very general procedure that can be used for the identification of the most likely predictors, since it runs a nonparametric estimation of the functional relationships between explanatory and outcome time-series, based upon iterative data fitting, rather than prior assumptions. It also allows for variability in the functional relationships across different values of the explanatory variables and can therefore capture nonlinear associations[6].

[6]We use GAM package in B34S programming language with SCAB34S Splines module (available

GAM estimates the relationship between p explanatory (x_t) and the outcome (y_t) time-series as a sum of smooth, or spline, functions:

$$E(y_t \mid x_{1t}, x_{2t}, \ldots, x_{pt}) = s_0 + \sum_{j=1}^{p} s_j(x_{jt})$$

where $\{s_j(x_{jt})\}$ are spline functions; they are standardised such that, after removal of free constants (s_o) their expected contribution to the outcome (y) is zero (i.e. $E[s_j(x_{jt})] = 0$ for each j). The splines are obtained by a process of splitting the time-series into sections, join at knot points, and fitting simple curves described by cubic functions to the data in each section. The GAM methodology identifies the optimal combination of spline functions $s_j(x_j)$ following the iterative procedure suggested by Hastie and Tibshirani (1990). Combining a local scoring algorithm and a backfitting procedure reducing complexity in the association for each explanatory variable, this method converges on a solution balancing data fit with smoothness.

To identify the most relevant explanatory time series from the initial pool, we run iteratively by removing first those variables and lag combinations whose contributions were nonsignificant before re-running the GAM model on a reduced subset of variables and lags. The process stops when the model contains only significant contributions of variables and lags that are identified on contribution charts by the zero line of nonassociation falling outside of 95% confidence intervals around the estimate (see some examples of contribution charts from GAM in Figure 2.7). These constitute the restricted set of explanatory variables for the next step.

in SCA Workbench, Scientific Computing Associates Corp, Illinois, USA)(Stokes and Lattyak, 2008a). Also we created R codes using GAM package (Hastie, 2013).

Figure 2.7: Illustrations of GAM contribution charts with significant bands.

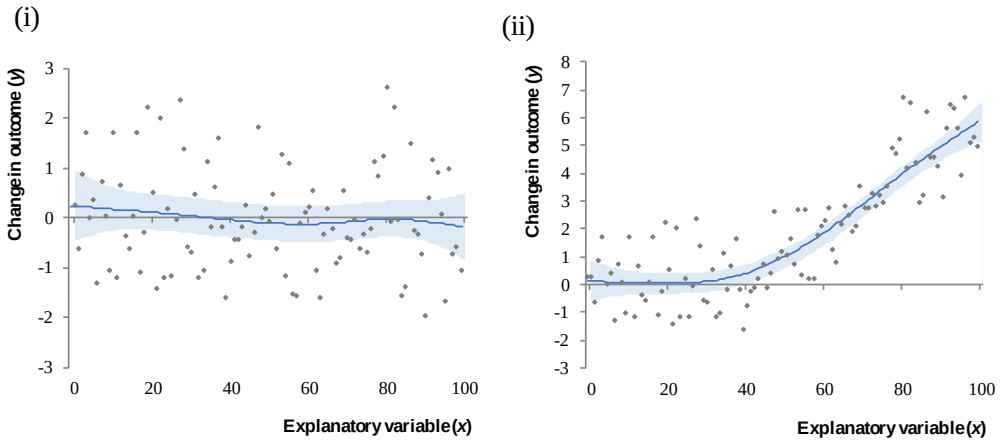

Examples of contribution charts from GAM procedure in (i) the absence and (ii) the presence of significant relationships between (x) and the outcome (y) variables. The blue bands represent the 95% confidence bands.

Step 2. Model estimation with MARS

After setting the pool of explanatory variables (and lags), and whether associations with the outcome series were linear or non-linear, we used the MARS procedure[7] to obtain an easily interpretable characterization of these associations (Friedman, 1991) detecting thresholds values of the explanatory variables, if they exist, delimiting regions of individual or interacting explanatory variables within which associations with the outcome differs substantially from those in other regions. MARS also provides the most efficient explanation of the variation in outcomes with a systematic estimation and automatic selection of the combination of explanatory variables and threshold values. This combination can be obtained as an enhanced matrix.

It is necessary to compute the autocorrelation function (ACF) of the MARS residuals to check they are whitened, otherwise statistical inference of the parameters of the final model would be not reliable. Then, we run the Box Pierce test to detect a significant autocorrelation in the residuals. If so, we iteratively estimate an ARIMAX transfer function with the vectors of the enhanced matrix as regressors. In each loop, the least significant variable is eliminated until the estimation process converges to a model in which all the estimated coefficients are significant and the errors are compatible with a white noise to make a more reliable statistical inference

[7] As usual for MARS estimations, we discard detection of possible thresholds in the 15% of extreme values of the sample.

of the parameters of the final model. In this sense, our procedure applies MARS on time series data following TSMARS developed by Keogh (2010).

It is useful to generate contribution chart for each basis function to illustrate how each significant explanatory variables from MARS contributes to the outcome variables . It is also interesting to estimate linear model as a benchmark for comparing with MARS performance.

Step 3. Diagnostic checks.

Adequacy of model fit is defined by different criteria as normally distributed residuals with homogeneous variance and mean equal to zero evaluated by a normality test; also the absence of significant residual autoregression, that can be checked with Box Pierce test (Box and Pierce, 1970): and the absence of residual nonlinearities evaluated by a Hinich's test (Hinich, 1982).

In addition some measures of goodness of fit can be reported as the modified generalized cross validation (MGCV) based on Craven and Wahba (1979), the mean absolute percentage error (MAPE), Akaike Information Criterion (Akaike, 1987) (AIC) or its corrected bias version for small samples AICc (Hurvich and Tsai, 1989), Schwarz criterion also known as Bayesian Information criterion (BIC) (Schwarz et al., 1978) and the Log-likelihood criterion.

Step 4. Confidence intervals for thresholds values.

In the absence of an existing method for deriving measures of uncertainty around thresholds derived from nonparametric MARS models, we develop a procedure inspired by Hansen (2000) to compute confidence intervals for thresholds detected by MARS model. To the best of our knowledge, the computation of confidence intervals for thresholds parameters in MARS model is an innovation of this. Hansen considers a simple threshold model with only one variable affected by a threshold effect, and obtains a distribution theory for the threshold parameter (τ) from which asymptotic confidence intervals can be built. He first derives the limiting distribution of a Likelihood Ratio test (LR) for the null hypothesis that the threshold parameter $\tau = \tau_0$. He then builds confidence intervals through the inversion of LR: the $(1-\alpha)$ Inverted Likelihood Ratio (ILR) confidence interval consisting of all the possible values of τ for which the null hypothesis would not be rejected at the α level. Donayre et al. (2018) examine improvements of Hansen's ILR confidence interval, increasing its quality in finite samples with large threshold effects (i.e. when the change in slope

from one side of the threshold to the other is large). They show that a "conservative modification" enlarging Hansen's ILR confidence interval is optimal. In this "conservative ILR confidence interval" the lower end of the interval is enlarged from the first value lower than τ_l (lower bound of the confidence interval) for which the null hypothesis is rejected, up to τ_l; at the upper end, it is enlarged from τ_u (upper bound of the confidence interval) up to the first value greater than τ_u for which the null hypothesis is rejected. According to Donayre et al. (2018), this modification provides intervals at a confidence level at least as high as the nominal one that are still informative.

We adapted this procedure for MARS estimations with more than one explanatory variable containing thresholds, and one or more thresholds per variable, by using the partial residuals – i.e. the estimated part of the outcome not explained by other explanatory variables and their thresholds. To simplify the explanation, let us suppose that in modeling y, we have two explanatory variables, x_1 and x_2, and that a threshold has been detected by MARS for each one, at τ_{x_1} and τ_{x_2} respectively. To obtain the confidence interval associated with τ_{x_1}, we obtain the "partial residuals relative to x_1" , say $y(x_1)$, which is the part of y not explained byx_2 (and its threshold). We obtain it by subtracting from y the part of the full model related exclusively with x_2. Once $y(x_1)$ is obtained, we can apply on the data of $y(x_1)$ and x_1 the procedure of Hansen (2000) improved by Donayre et al. (2018). In that way we obtain a conservative ILR confidence interval for $\tau(x_1)$ conditional on the estimated values of the parameters (slopes and thresholds) related to x_2. We then repeat the same procedure interchanging the roles of x_1 and x_2, and we now obtain the conservative ILR confidence intervals for $\tau(x_2)$ conditional on the estimated values of the parameters related to x_1.

Under suspicion of heteroskedasticity, we follow the correction algorithm proposed by Hansen (2000). It basically consists of dividing the ILR function by an estimation of the nuisance parameter η^2 that appears in the distribution of the Likelihood Ratio statistic when heteroskedasticity is present (Hansen, 2000). The correcting factor is computed with the following steps.

Firstly, given the k^{th} explanatory variable x_k with a threshold $\tau(x_k)$ estimated by MARS and its partial residual $y(x_k)$, we compute $\delta_k = \hat{\theta}_{1,1,k} - \hat{\theta}_{1,2,k}$ from the threshold regression:

$$\begin{cases} y(x_k) = \theta_{0,1,k} + \theta_{1,1,k}x_k + e_{1,k} & x_k \leq \tau(x_k) \\ y(x_k) = \theta_{0,2,k} + \theta_{1,2,k}x_k + e_{2,k} & x_k > \tau(x_k) \end{cases}$$

where $\hat{\theta}_{i,j,k}$ is the estimator of coefficient i in the equation j for variable k.

In a second step, we calculate a new pair of variables $\hat{r}_{1,k}$ and $\hat{r}_{2,k}$ as follows

$$\hat{r}_{1,k} = (\delta_k x_k)^2(\hat{e}_k I_{TxT}\hat{e}'_k)/\hat{\sigma}^2$$
$$\hat{r}_{2,k} = (\delta_k x_k)^2$$

where $\hat{\sigma}^2 = \hat{e}'_k\hat{e}_k/(n-2k)$, $\hat{e}_k$ is the full vector of residuals that combines $\hat{e}_{1,k}$ and $\hat{e}_{2,k}$, k is the number of estimated parameters for each regression and I_{TxT} is the identity matrix TxT. (It is easy to see that $(\hat{e}'_k I_{TxT}\hat{e}_k)$ is a vector with components that are the square of the components of $\hat{e}_k$)

Thirdly, we estimate $\hat{\mu}_{i,j,,k,}$ with the following regressions:

$$\hat{r}_{1,k} = \hat{\mu}_{0,1,k} + \hat{\mu}_{1.1,k}x_k + \hat{\mu}_{2,1,k}x_k^2 + \hat{\nu}_{1,k}$$
$$\hat{r}_{2,k} = \hat{\mu}_{0,2,k} + \hat{\mu}_{1,2,k}x_k + \hat{\mu}_{2,2,k}x_k^2 + \hat{\nu}_{2,k}$$

where $\hat{\nu}_{j,k}$ are the residuals.

Finally, the nuisance parameter is estimated as follows

$$\hat{\eta}^2 = \frac{\hat{\mu}_{0,1,k} + \hat{\mu}_{1.1,k}\tau(x_k) + \hat{\mu}_{2,1,k}\tau(x_k)^2}{\hat{\mu}_{0,2,k} + \hat{\mu}_{1,2,k}\tau(x_k) + \hat{\mu}_{2,2,k}\tau(x_k)^2}$$

We use the nuisance parameter to calculate the Inverted Likelihood Ratio (ILR) under heteroskedasticity as $ILRh = ILR/\hat{\eta}^2$

With the new $ILRh$, we proceed as in Donayre et al. (2018) to obtain the conservative $ILRh$ confidence intervals for $\tau(x_k)$ conditional on the estimated values of the parameters related to the rest of $x_{l\neq k}$. We call the resulting interval the Condidtional Conservative ILR interval (CCILR in the sequel).

Performance evaluation of the procedure for threshold confidence intervals.

In order to evaluate the performance of our procedure to estimate 95% confidence intervals for thresholds, we examine the empirical coverage rates and the average lengths of the confidence intervals obtained with Monte Carlo experiments. The coverage rate is calculated as the frequency of constructed intervals containing the true value of the threshold parameter. We define the average length of the confidence interval as the difference between the upper and the lower boundaries of the

confidence interval averaged across repetitions. We consider both homoscedastic and heteroskedastic data generating processes from a basic model. The explanatory variables are generated with a uniform distribution, so that the position of the threshold in the variable range should not have any relevant effect on the results. We evaluate the performance of the proposed procedure with 1000 replications for each experiment with different sample size ranging from 50 to 1000 data with increments of 50.

The homoscedastic data generating process contains a normally distributed error term with a constant variance whatever the subregion in the domain:

$$y_t = 2max(x_{1t} - 1, 0) + max(x_{2t} - 2, 0) + e_t \quad e_t \sim N(\mu = 0, \sigma^2 = 0.1) \quad (2.1)$$

So the model contains the following regions;

$$\begin{cases} if\ x_1 \leq 1,\ x_2 \leq 2 & y_t = 0x_{1t} + 0x_{2t} + e_t \\ if\ x_1 \leq 1,\ x_2 > 2_t & y = 0x_{1t} + 1(x_{2t} - 2) + e_t \\ if\ x_1 > 1,\ x_2 \leq 2 & y_t = 2(x_{1t} - 1) + 0x_{2t} + e_t \\ if\ x_1 > 1,\ x_2 > 2 & y = 2(x_{1t} - 1) + 1(x_{2t} - 2) + e_t \end{cases}$$

Figure 2.8 is the graphical representation of the systematic part of the model.

Figure 2.8: Basic model for the data generating processes (2.1) and (2.2).

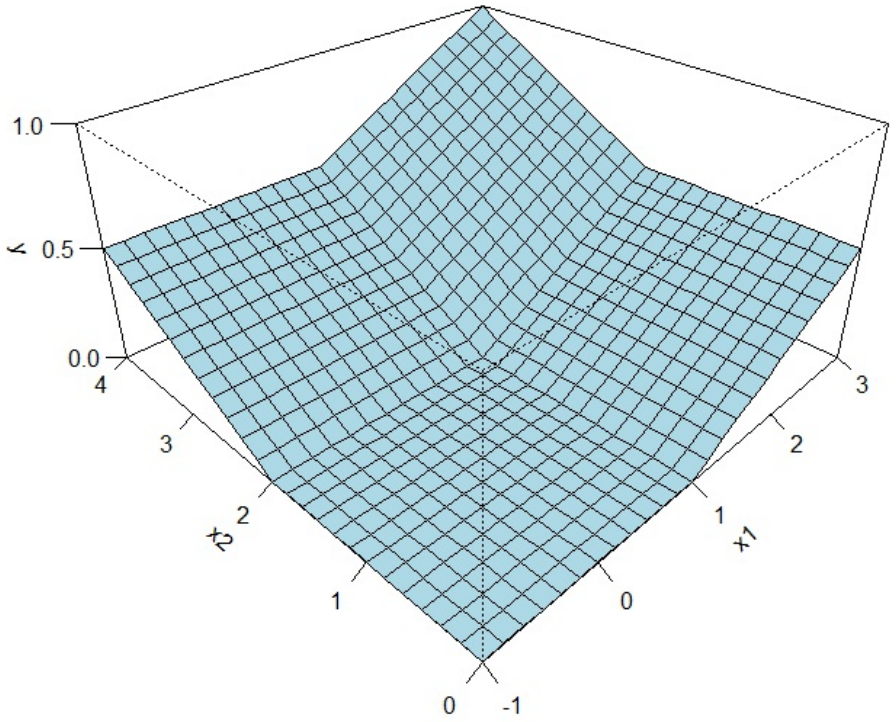

Tables 2.2 and 2.3 summarize the results from the experiments, for the homoscedastic and heteroskedastic models, respectively. Each table reflects the coverage rates and the average length of the CCILR confidence intervals for each threshold. Each row refers to the Monte Carlo experiment for sample size T. We also compute a synthetic measure to compare the informative content of the CCILR confidence intervals with that of an alternative approach discussed below. Let the "coverage efficiency measure" be the ratio between the coverage rate and the length of the confidence interval. This ratio is of interest because for the same coverage rate, a confidence interval obtained by one procedure is more informative than the other if its length is shorter.

Table 2.2: Monte Carlo experiments with homoscedastic data.

	Homoscedastic data generated by (2.1)					
	Confidence Interval for threshold in x_1, $\tau(x_1) = 1$			Confidence Interval for threshold in x_2, $\tau(x_2) = 2$		
Sample size T	Coverage rate (A1)	Average length (B1)	Coverage efficiency (A1)/(B1)=(E1)	Coverage rate (A2)	Average length (B2)	Coverage efficiency (A2)/(B2)=(E2)
50	0.971	0.5330	1.8219	0.975	0.9126	1.0684
100	0.981	0.3351	2.9272	0.978	0.5954	1.6427
150	0.986	0.2581	3.8201	0.986	0.4673	2.1101
200	0.98	0.2162	4.5338	0.981	0.3966	2.4734
250	0.982	0.1878	5.2278	0.985	0.3494	2.8193
300	0.982	0.1696	5.7903	0.99	0.3158	3.1353
350	0.979	0.1543	6.3467	0.984	0.2903	3.3895
400	0.98	0.1424	6.8837	0.981	0.2692	3.6445
450	0.982	0.1325	7.4140	0.986	0.2525	3.9043
500	0.971	0.1263	7.6884	0.985	0.2388	4.1248
550	0.981	0.1186	8.2697	0.988	0.2264	4.3643
600	0.976	0.1127	8.6597	0.989	0.2158	4.5826
650	0.968	0.1082	8.9491	0.985	0.2055	4.7933
700	0.973	0.1038	9.3697	0.99	0.1974	5.0157
750	0.979	0.1001	9.7820	0.988	0.1902	5.1936
800	0.973	0.0967	10.0641	0.989	0.1838	5.3806
850	0.968	0.0933	10.3800	0.991	0.1780	5.5660
900	0.976	0.0904	10.8002	0.986	0.1724	5.7202
950	0.979	0.0878	11.1515	0.987	0.1675	5.8941
1000	0.969	0.0850	11.4006	0.987	0.1630	6.0563

For all the sample sizes considered in the experiments, we do not obtain any undercoverage: all coverage rates are at least equal the the nominal size of 95%. On the basis of the results of Donayre et al. (2018), the coverage rate of the confidence interval is expected to be greater than the nominal confidence level and at least asymptotically in the case of normally distributed errors. As expected, the greater the sample size, the shorter the average confidence interval length and the more accurate the location of the estimated threshold. Logically, the coverage efficiency increases with the sample size.

The heteroskedastic data generating process is similar to the homoscedastic one described above except for the variance of the error term that depends on whether the evaluated point is above or below the threshold on x_{1t}.

$$\begin{aligned} y_t &= 2max(x_{1t} - 1, 0) + max(x_{2t} - 2, 0) + e_{it} \quad e_{it} \sim N(\mu = 0, \sigma_i^2) \\ &if\ x_{1t} \leq 1 \;\; e_{1t} \sim N(\mu = 0, \sigma_1^2 = 0.05) \\ &if\ x_{1t} > 1 \;\; e_{2t} \sim N(\mu = 0, \sigma_2^2 = 0.1) \end{aligned} \tag{2.2}$$

$$\begin{cases} if\ x_{1t} \leq 1,\ x_{2t} \leq 2 & y_t = 0x_{1t} + 0x_{2t} + e_{1t} \\ if\ x_{1t} \leq 1,\ x_{2t} > 2_t & y = 0x_{1t} + 1(x_{2t} - 2) + e_{1t} \\ if\ x_{1t} > 1,\ x_{2t} \leq 2 & y_t = 2(x_{1t} - 1) + 0x_{2t} + e_{2t} \\ if\ x_{1t} > 1,\ x_{2t} > 2 & y = 2(x_{1t} - 1) + 1(x_{2t} - 2) + e_{2t} \end{cases}$$

Table 2.3: Monte Carlo experiments with heteroskedastic data.

	Heteroskedastic data generated by (2.2)					
	Confidence Interval for threshold in x_1, $\tau(x_1) = 1$			Confidence Interval for threshold in x_2, $\tau(x_2) = 2$		
Sample size T	Coverage rate (C1)	Average length (D1)	Coverage efficiency (C1)/(D1)=(F1)	Coverage rate (C2)	Average length (D2)	Coverage efficiency (C2)/(D2)=(F2)
50	0.956	0.5145	1.8581	0.954	0.7817	1.2204
100	0.968	0.3147	3.0759	0.977	0.5157	1.8944
150	0.982	0.2456	3.9986	0.98	0.4011	2.4432
200	0.979	0.2055	4.7647	0.981	0.3447	2.8460
250	0.969	0.1804	5.3719	0.977	0.3041	3.2128
300	0.976	0.1617	6.0347	0.988	0.2734	3.6131
350	0.979	0.1481	6.6093	0.99	0.2533	3.9082
400	0.973	0.1371	7.0947	0.984	0.2339	4.2067
450	0.973	0.1288	7.5542	0.983	0.2181	4.5062
500	0.97	0.1200	8.0829	0.989	0.2065	4.7894
550	0.976	0.1148	8.5032	0.99	0.1957	5.0595
600	0.972	0.1096	8.8703	0.985	0.1874	5.2556
650	0.97	0.1044	9.2938	0.99	0.1808	5.4771
700	0.969	0.1000	9.6889	0.983	0.1715	5.7322
750	0.97	0.0963	10.0753	0.985	0.1657	5.9438
800	0.978	0.0930	10.5132	0.982	0.1595	6.1561
850	0.979	0.0904	10.8289	0.988	0.1554	6.3590
900	0.973	0.0874	11.1282	0.982	0.1504	6.5274
950	0.976	0.0847	11.5184	0.985	0.1466	6.7208
1000	0.973	0.0821	11.8568	0.98	0.1423	6.8852

Table 2.3 for heteroskedastic data generated process by (2.2) summarizes coverage rates and averages of the length of the confidence intervals for each threshold. As in the previous table, for all the sample sizes considered in the experiments, all coverage rates are at least 95%; as before and as expected, the average length decreases with sample size; whereas the coverage efficiency increases.

We also compare the performance of our procedure with an alternative procedure suggested by an anonymous referee for one of the papers of this thesis. The suggestion consisted of computing the intervals by only conditioning on the rest of thresholds (RTproc), letting the associated slopes free, i.e, reestimating these slopes at each estimation point of the building process of the intervals. There are pros

and cons for each procedure. The "Partial Residuals" approach (PRproc) has the advantage of working with the final "optimal" pairs of thresholds and associated slopes and to estimate the conditional likelihood profile for a much simpler model, with only one variable and one threshold; this conditional model in fact constitutes a particular case of Hansen's model. It has the drawback of conditioning on more parameters. The alternative RTproc approach has the advantage of conditioning on less parameters but at the cost of computing the conditional likelihood profile in a more complex model and obtaining the conditional intervals to some extent with less sample information (less degrees of freedom) since it works works with a much more general, and maybe complex, version of Hansen's model. The conditional confidence intervals of RTproc are therefore expected to be, in general, wider than those based on PRproc. As a result, the former are also expected to have larger coverage rates than the latter. So there is presumably a trade-off between coverage rate and length of the interval, and in case both approaches reach coverage rates at least as large as the nominal confidence level, it is interesting to compare the relative gains and costs of each approach and see whether some pattern emerge from such a comparison.

So, we ran the same Monte Carlo experiments with the RTproc procedure. For each sample size, we computed the coverage rate, the average length of the intervals and the synthetic coverage efficiency measure.

The coverage rate never falls below the nominal level of 95% in the RTproc procedure. So, it is important to examine which of the two procedures offers the best information concerning the location of the threshold at the given level of confidence. There is a necessary tradeoff between coverage and length (in the sense that we prefer a large coverage rate with small intervals), therefore we built a ratio of the coverage efficiency ratios ($rCER$) as a synthetic measure of which approach works better.

$$rCER = \frac{\text{coverage efficiency ratio PRrproc}}{\text{coverage efficiency ratio RTproc}}$$

A value of $rCER$ above 1 favours the PRproc procedure developed in this thesis, whereas a value below 1 favours the RTproc procedure. This $rCER$ is presented in Table 2.4 for both the homoscedastic and heteroskedastic cases, for each sample size. Figure 2.9 represents the computed rCER for each threshold for homoscedastic and heteroskedastic data. All the values, without exception, stand above 1 for all sample

sizes and for both thresholds. So, these experiments suggest our Partial Residual approach PRproc is more informative than the alternative RTproc for application purposes.

Table 2.4: Ratio of the coverage efficiency ratios for PRproc and alternative RTproc

rCER	Comparison between procedures			
	Homoscedasticity		Heteroskedasticity	
Sample size T	Confidence Interval for $\tau(x_1) = 1$	Confidence Interval for $\tau(x_2) = 2$	Confidence Interval for $\tau(x_1) = 1$	Confidence Interval for $\tau(x_2) = 2$
50	1.0174	1.0581	1.0001	1.0073
100	1.0039	1.0461	1.0004	1.0349
150	1.0177	1.0519	1.0111	1.0354
200	1.0186	1.0405	1.0171	1.0430
250	1.0189	1.0417	1.0162	1.0253
300	1.0174	1.0521	1.0022	1.0391
350	1.0181	1.0395	1.0132	1.0454
400	1.0172	1.0396	1.0108	1.0413
450	1.0207	1.0456	1.0114	1.0490
500	1.0018	1.0428	1.0193	1.0473
550	1.0188	1.0391	1.0161	1.0418
600	1.0088	1.0387	1.0064	1.0420
650	1.0071	1.0517	1.0030	1.0399
700	1.0104	1.0442	1.0083	1.0399
750	1.0207	1.0433	0.9996	1.0421
800	1.0035	1.0386	1.0156	1.0309
850	1.0044	1.0462	1.0161	1.0436
900	1.0131	1.0413	1.0083	1.0338
950	1.0181	1.0412	1.0080	1.0419
1000	1.0066	1.0420	1.0158	1.0440

Figure 2.9: Ratios rCER for each threshold for homoscedastic (—) and heteroskedastic (- - -) data

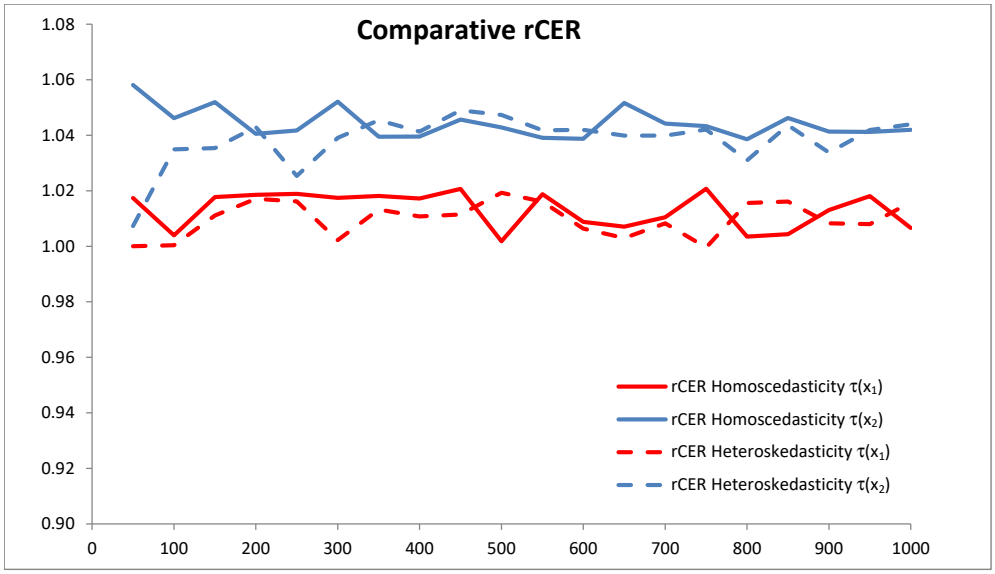

As a result, we recommend the partial residual approach. On the one hand, given the presence of multiple thresholds, other alternatives, such as bootstrapped methods, are not likely to give satisfactory results. They may be prohibitively time-consuming; even in the case of only one threshold, bootstrapping is very time consuming and has been shown to yield non informative confidence intervals (Enders et al., 2007).

2.3.2 Protocol for estimating Taylor Rule.

Here we introduce some specificities in the basic protocol to estimate TR.

Step 1. Set the pool of explanatory variables and their lags.

To estimate TR, we use monthly data to have time series as large as possible and because it is consistent with the frequency of the monetary authority meetings. We calculate the inflation rate, expressed in annual rates, from the seasonally adjusted monthly Consumer Prices Index accessible in Statistics office of the monetary authority. To compute the monthly output gap, we apply the Hodrick-Prescott filter with a smoothing parameter equal to 14400 (see Hodrick and Prescott (1997)) to the logarithm of the Industrial Production Index, that is usually available in the

Statistics Office databases of the economic region. Using lagged values for the explanatory variables tackles the endogeneity problem and is also consistent with the idea that the monetary authority decisions on nominal interest rates require information that is time-consuming to collect. In addition, when data covers periods defined by different chairmanships of the monetary authority or some abrupt changes in the economy as a Crisis or an economic area enlargement (as in the European Union) we include dummies variables in the model to capture possible effects.

Step 2. Model estimation with MARS.

To estimate TR we employ the partial adjustment specification from Judd and Rudebusch (1998) that incorporates interest rate smoothing. Let us assume i_t^* is the interest rate recommended by the monetary authority such that

$$i_t^* = r^* + \pi_t + \alpha(\pi_t - \pi^*) + \beta_1 \widetilde{y}_t + \beta_2 \widetilde{y}_{t-1}$$

and we use the partial adjustment process

$$\Delta i_t = \gamma(i_t^* - i_{t-1}) + \rho \Delta i_{t-1}$$

where γ is the gradual adjustment coefficient. Therefore, we firstly construct the MARS specification with the basis functions and possible interactions:

$$\begin{aligned} i_t^* = (\beta_0 + \delta d_t) &+ \sum_{m_\pi=1}^{M_\pi} (\beta_{m_\pi} + \delta_{m_\pi} d_t) b[\pi_{t-1}, \tau_{m_\pi}] + \\ &+ \sum_{m_y=1}^{M_y} (\beta_{m_y} + \delta_{m_y} d_t) b[\widetilde{y}_{t-1}, \tau_{m_y}] + \\ &+ \sum_{m_{y\pi}=1}^{M_{y\pi}} (\beta_{m_{y\pi}} + \delta_{m_{y\pi}} d_t) b[\pi_{t-1}, \tau_{\pi,m_{y\pi}}] b[\widetilde{y}_{t-1}, \tau_{y,m_{y\pi}}] + \rho \Delta i_{t-1} + \varepsilon_t \end{aligned}$$

d_t : dummy variable

After MARS estimation, we estimate the partial adjustment process of the interest rate considered in Judd and Rudebusch (1998) with an ARIMAX transfer function taking into account thresholds detected in i_t^*.

Step 3 for diagnostic checks and the Step 4 for computing confidence intervals for thresholds values are the same as in the basic protocol.

2.3.3 Protocol for Okun's Law

Here we introduce some specificities in the basic protocol to estimate Okun's law.

Step 1. Set the pool of explanatory variables and their lags.

To estimate Okun's law we use quarterly data due to the frequency of unemployment rate data release from Statistics offices. We also calculate quarterly output growth rate from real GDP and introduce dummy variable for economic crisis periods according to Research institutions dating[8].

Variables such that unemployment rate u_t and the Gross Domestic Product (GDP) of an economy may be cointegrated. Therefore, we firstly proceed to check the integration order of the unemployment rate using the unit root test with multiple structural change proposed by Carrion-i Silvestre et al. (2009). We need this more complex unit root test that checks even up to for five possible structural changes in the time series because it would be possible that outcome time series may be stationary by periods with different levels depending on possible different regions delimited by thresholds of the explanatory variables.

In case of unit root of unemployment rate, we use the MARS cointegration test proposed by Sephton (1994) to check for cointegration between the unemployment rate and real GDP to determine whether we have to discriminate between long term and short term effects in Okun's law. These two substeps allow us if we should introduce a cointegration term in the specification of the MARS model.

Step 2. Model estimation with MARS.

The MARS specification for the Okun's law that we propose is[9]:

$$\triangle u_t = (\beta_0 + \delta_1 d_{Ct}) + \sum_{m=1}^{M} \beta_m b[\gamma_t, \tau_m] + \rho_1 \triangle u_{t-1} + \rho_2 \triangle u_{t-2} + \varepsilon_t$$

$\mathrm{u_t}$: unemployment rate d_{Ct}: crisis dummy, γ_t : quarterly growth rate

Step 3 for diagnostic checks and the Step 4 for computing confidence intervals for thresholds values are the same as in the basic protocol.

[8] CEPR Euro Area Business Cycle Dating Committee establishes the chronology of recessions and expansions in Eurozone and NBER also stablishes it in USA.

[9] In case of cointegrated times series, we should also include as explanatory variable a cointegration term that would reflect the long term association between unemployment rate and real GDP in the following model specification.

2.3.4 Protocol for Antibiotic resistance

Due to several specificities and differences in this field with respect to the previous two, we need to add some special considerations to the basic protocol. In summary, we start by defining a set of explanatory variables (antibiotic use, infection control time-series, population interactions, resistance in previous months, etc.). This set is defined by (a) expert opinion informed by prior risk-factor studies, molecular epidemiology in the region; and (b) inspection of resistance profiles of the pathogen of interest. We consider delays between changes in explanatory time-series and associated change in outcome time-series (lags) of up to 6 months.

Before analysis we check time-series and make adjustments for extreme values (outliers) or unexpected shifts in mean (structural changes). We also use vector autoregression (VAR) models to help distinguish any reverse causality in relationships between explanatory and outcome series: this might occur, for example, if prescribing behaviour was altered by resistance rates in the population in previous months. Next, we restrict the set of explanatory variables, and lags, to be put into final multivariable models. We use a procedure that fits smooth functions to relationships between explanatory and outcome time-series, and allows visual inspection of likely significant associations. After identifying the most promising explanatory variables (and lags of effects), we estimate MARS model which both identifies significant predictors, and defines any non-linear relations as a series of linear relationships connected by 'knots' or thresholds. Model fit is checked by ensuring residuals were normally distributed without unexplained nonlinearities. Confidence intervals around each threshold were fit by a conditional conservative inverted likelihood ratio (CCILR) method, using partial residuals. Finally we converted thresholds from models into suggested maximum total treatment courses per month in the population by multiplying model thresholds by the size of the population and dividing by an average treatment course. It is useful to evaluate projections for alternative antibiotic stewardship policy options by a counterfactual analysis.

Step 1. Set the pool of explanatory variables and their lags.

Subtep 1.1: Theoretical foundation

Participating centres identify *a priori* a minimum dataset of antibiotic sub-groups or agents they consider most likely to affect the epidemiology of the resistant organism under investigation (target organism). Decisions are based upon: previous empirical evidence of risk factors and molecular epidemiology in the study region

or related contexts. Additionally, using antibiogram data from the study period and population, we review co-resistances to other antibiotics among isolates of the target organism with and without the resistance under investigation. We consider antibiotics with the largest absolute rates of co-resistance in the resistant isolates to be most likely to exert significant selection pressures (Søgaard, 1989; Møller, 1989). Where data is available we integrate additional dummy explanatory variables on hospital activity or infection control activities, associated with the outcome variable in previous studies.

Substep 1.2: Data validation

To ensure consistent time-series we first account for known changes in exogenous conditions, such as changes in laboratory method. We capture immediate and gradual effects by entering a dummy variable and its interaction with an autoregressive term, as explanatory variables. We then examine time series to detect potential unknown measurement errors as follows. Visual inspection identify potential structural changes that can be seen for example as a large stepwise change in mean or outliers that can be observed as values deviating largely from surrounding values. We apply successive Chow tests in the time series to automatically detect the most probable dates of structural changes and, where necessary, to disaggregate the sample into two or more segments, each with a stable mean. For each segment we apply an outlier detection technique using the following criterion: an observation is considered as an outlier if Cook's distance at this point is greater than five times the mean of Cook's distances of all the observations of the segment. Finally, we replace outlier values with the mean of the three preceding and three following observations.

Subtep 1.3 Identifying the most likely predictors and their lags

Given the potentially complex relationships between ecological variables under investigation, we seek to refine our understanding of potential associations before applying MARS model.

Firstly, situations of reverse causality could exist when ecological exposures- such as rates of infections with resistant pathogens connected populations, or use of some antibiotic groups in a given population- respond to, rather than predict, rates of resistance. In order to minimise this risk, we check the direction of relationships between explanatory and outcome time-series by applying Granger-causality test and Vector Autoregression (VAR) models. Secondly, nonlinear models of the type used in this study are potentially complex and difficult to extract form the data if too

many predictors are used at the same time. Therefore, we carry out an additional *a priori* data-based selection of candidate explanatory variables and lags. For each centre we include all theoretically relevant variables at lags of 1 to 6 months and autoregressive terms at lags 1 and 2 to fit a GAM. We limit lags to 6-months based on widespread evidence of declining relevance of antibiotic exposures by time-since exposure, and prior experience that considerations of longer lags lead to problems of concurvity. On the basis of the GAM outputs, an explanatory variable with a specific lag is retained in the model only if its contribution is significantly different from zero at any part of its domain.

Step 2. MARS Multivariable model estimation.

The MARS specification that we propose for analyzing the model of Antimicrobial Resistance AMR_tseries with K antibiotic use time series $Abx_{i,t}$ and a dummy variable for the Infection control campaign if it has been undertaken in the cenrtre. To avoid a possible excess of complexity in the model, we restrict the MARS specification with no interaction basis functions between antibiotic use time series.

$$\begin{aligned} AMR_t = (\beta_0 + \delta_1 d_t) + \sum_{m=1}^{M_{AR1}} \beta_{AR1,m} b_m \left(AMR_{t-1}\right) + \sum_{m=1}^{M_{AR1}} \delta_{AR1,m} b_m \left(d_1 AMR_{t-1}\right) \\ \sum_{m=1}^{M_1} \beta_{Abx1,m} b_m \left(Abx_{1,t}\right) + \sum_{m=1}^{M_2} \beta_{Abx2,m} b_m \left(Abx_{2,t}\right) + \ldots \\ + \sum_{m=1}^{M_i} \beta_{Abxi,m} b_m \left(Abx_{i,t}\right) + \ldots + \sum_{m=1}^{M_K} \beta_{AbxK,m} b_m \left(Abx_{K,t}\right) + \varepsilon_t \end{aligned}$$

d_t : Infection Control dummy variable

Step 3 for diagnostic checks and the Step 4 for computing confidence intervals for thresholds values are the same as in the basic protocol.

Step 5. Interpretation

The minimum in the estimated confidence interval of the thresholds identified for each significantly associated antibiotic group are translated into suggested maximum numbers of patient treatments per month not expected to adversely affect resistance at population levels. We multipliy the threshold, expressed in Defined Daily Doses (DDD) per 1000 Occupied Bed Days (OBD) (or Inhabitants Days (ID)), by the size of the monthly patient population (in thousands of OBDs or IDs), and then divide by an average patient treatment course of 7 DDDs (except for aminoglycosides

which were considered as 3 DDDs). These maximums are further compared to contemporary levels of antibiotic use in the last year of study, to provide indications of how current use of antibiotics should be modified to avoid resistance spread.

In addition, to illustrate the potential effects of restricting antibiotics to threshold levels, we perform a counterfactual analysis to compare the expected evolution AMR under a 'business as usual' scenario in which antibiotic use continued as in last year of study to projected time-series with antibiotics restricted to threshold levels. We use a breakpoint analysis to identify the last stationary segment in AMR time-series from the study period. From this point we recursively evaluate MARS models using means from these stationary segments as starting points to derive steady states for AMR in community and hospital populations. Based on steady state values and MARS models for the study period (baseline) it can be simulated 1000 samples of 24-month projections, incorporating random error term with variance as derived in the baseline MARS model. For each sample projection we enter mean antibiotic levels in the last year of the study period ('business as usual') and alternative levels set at identified thresholds (antibiotic stewardship options). It can be calculated the mean difference between business as usual and each policy option for every month along with 95% confidence intervals. Finally, it is useful to illustrate alternative projections and differences using medians of distributions from the 1000 sample projections.

3 A model for nonlinear Taylor rule.

3.1 Introduction.

Implementing optimal monetary policy corresponds to automatically set the policy interest rate following an optimal policy function (Svensson, 2010). Optimal policy functions obtained by targeting rules are more efficient than those obtained by instrument rules as Svensson (1999) demonstrates. Although main concerns of monetary authorities focus on stabilising inflation rate, inflation targeting does not imply that monetary policy does not care about the stability of the real economy (Svensson, 2010). Ball (1999) and Svensson (1999) expose that concern about output gap stability as an intermediate target rule provides an explanation of gradual transmission mechanism of the monetary policy. Therefore, an optimal policy function will reflect the relative importance of both factors depending on their weights in the monetary authority preference function (Ball, 1999; Taylor, 1999; Clarida et al., 2000). These preferences are typically represented by a quadratic loss function defined over the inflation deviation and the output gap. A linear dynamic system describing the economy completes the linear-quadratic framework that generates linear optimal policy functions with a proportional adjustment of nominal interest rates to the inflation deviations and the output gaps.

A quadratic loss function may provide a reasonable approach to the monetary authority preferences around a point in the short term but it does not imply that the same quadratic function can give a reasonable approach for wider ranges; nonlinear Taylor rules may be reasonable. The literature reports asymmetric preferences as one of the main theoretical sources of nonlinearities in monetary authority behaviour. Ruge-Murcia (2002) and Cukierman and Muscatelli (2008) consider asymmetric preferences of central banks and their rationale. Surico (2002); Ruge-Murcia (2002); Cukierman and Muscatelli (2008) demonstrate that asymmetric preferences of central banks generate nonlinearities in the interest-rate reaction rule using specific

functions that nest a quadratic function as a particular case. Cukierman and Muscatelli (2008) propose a generic function but they impose an exogenous threshold on the inflation rate target imposing two different regimes.

In this chapter, we introduce targeting rule models beyond the linear quadratic framework using a generic loss function that nests the quadratic function as a particular case and that does not previously impose neither the number nor the location of thresholds on the inflation rate and on the output gap. The first model we present is a static version that allows a changing behavior of the central bank by regions with piecewise continuous and strictly convex preference functions with noncontinuous second derivative on the inflation rate and the output gap. Noncontinuous second derivatives of these functions imply nonlinear Taylor rule defined by regions delimited by thresholds. The second model is a generalization of the dynamic and partial adjustment model of Svensson (1999) with the central bank preference function defined as in the static version.

In section 2, we present these two models; in section 3, we perform calibrations to compare the response to diverse shocks of a model with thresholds to a model without them.

3.2 Model: the optimal central bank behavior.

3.2.1 Static targeting model.

Let us consider a monetary authority minimising a loss function defined for the inflation rate deviations and the output gap. We only assume that the loss function is composed by two separable preference functions $g(\widetilde{\pi})$ defined for the inflation rate deviation and $h(\widetilde{y})$ defined for the output gap of the economy. The parameter λ weights the importance of preferences on the inflation gap with respect to the preferences on the output gap in the loss function; it is assumed to be greater than 1 reflecting the central bank's concern about inflation rate deviations. Also, the central bank takes its decisions observing the Aggregate Supply (3.1) in the economy, the IS (3.2) and the Fisher equation (3.3).

i Policymaker Loss objective function

$$L(\widetilde{\pi},\widetilde{y}) = \lambda g(\widetilde{\pi}) + h(\widetilde{y})$$
$$\widetilde{\pi} = (\pi - \pi^*),\ \widetilde{y} = (y - y^*)$$
π^* : inflation rate target
y^* : potential output

ii Aggregate Supply:

$$\pi = \pi^e + \alpha\widetilde{y} + u_\pi \tag{3.1}$$

u_π : inflation rate error term
π^e : expected inflation rate

iii IS

$$\widetilde{y} = A - \phi(r - \overline{r}) + u_y \tag{3.2}$$

u_y : output gap error term
r : real interest rate
$\bar{r}$: long term equilibrium real interest rate

iv Fisher equation

$$r = i - \pi^e \tag{3.3}$$

Therefore, the optimization problem of the monetary authority is

$$\min_i \left[\lambda g(\widetilde{\pi}) + h(\widetilde{y})\right]$$
$$s.t. \begin{cases} \pi = \pi^e + \alpha\widetilde{y} + u_\pi \\ r = i - \pi^e \\ \widetilde{y} = A - \phi(r - \overline{r}) + u_y \end{cases} \tag{3.4}$$

The Taylor rule will be the solution of this minimisation problem. With these generic functions, the coefficient for the inflation rate will depend on the second derivatives of the central bank preference functions. Therefore, if the preference functions of the central bank are defined as piecewise continuous and strictly convex functions with noncontinuous second derivatives at the boundaries of the regions of their domains (Figure 3.1), the Taylor rule would be nonlinear, different from one region to another and delimited by thresholds. We are not previously imposing any threshold but generalizing the preference function to any partitioning set of the domain. This type of general function adapts the idea that the sensitivity reaction of the monetary authority to the inflation rate or the output gap may differ if they are above or below targets. Indeed, declarations of the governors suggest that

a differentiated sensitivity is very likely, and this fact can not be reflected in the preference functions considered so far. Therefore, we shall allow preference functions may take this general piecewise-continuous form, to check implications in the TR.

In order to solve the (3.4) we take derivatives with respect to interest rate i .

$$\begin{cases} \lambda \dfrac{\partial g(\widetilde{\pi})}{\partial \widetilde{\pi}} \dfrac{\partial \widetilde{\pi}}{\partial \widetilde{y}} \dfrac{\partial \widetilde{y}}{\partial r} \dfrac{\partial r}{\partial i} + \dfrac{\partial h(\widetilde{y})}{\partial \widetilde{y}} \dfrac{\partial \widetilde{y}}{\partial r} \dfrac{\partial r}{\partial i} = 0 \\ \dfrac{\partial \widetilde{\pi}}{\partial \widetilde{y}} = \alpha;\ \dfrac{\partial r}{\partial i} = 1;\ \dfrac{\partial \widetilde{y}}{\partial r} = -\phi \end{cases} \Longrightarrow$$

$$\Longrightarrow \lambda \frac{\partial g(\widetilde{\pi})}{\partial \widetilde{\pi}} \alpha(-\phi) + \frac{\partial h(\widetilde{y})}{\partial \widetilde{y}}(-\phi) = 0$$

to obtain the optimal condition

$$\frac{\partial g(\widetilde{\pi})}{\partial \widetilde{\pi}} = \frac{1}{\lambda \alpha} \frac{\partial h(\widetilde{y})}{\partial \widetilde{y}} \tag{3.5}$$

The Taylor rule that solves (3.4) will be an interest rate function depending on the inflation rate. The first derivative of the interest rate with respect to inflation rate comes out from derivatives of the optimal condition (3.5) and the system (3.4).

$$\frac{\partial^2 g(\widetilde{\pi})}{\partial \widetilde{\pi}^2} = \frac{1}{\lambda \alpha} \frac{\partial^2 h(\widetilde{y})}{\partial \widetilde{y}^2} \frac{\partial \widetilde{y}}{\partial \widetilde{\pi}}$$

$$\frac{\partial \widetilde{y}}{\partial \widetilde{\pi}} = \phi \left(\frac{\partial i}{\partial \widetilde{\pi}} - 1 \right)$$

Therefore, we obtain the following expression for $\dfrac{\partial i}{\partial \widetilde{\pi}}$ in the case of the static model for the Taylor rule:

$$\frac{\partial i}{\partial \widetilde{\pi}} = 1 + \frac{1}{\phi} \lambda \alpha \frac{\dfrac{\partial^2 g(\widetilde{\pi})}{\partial \widetilde{\pi}^2}}{\dfrac{\partial^2 h(\widetilde{y})}{\partial \widetilde{y}^2}} \tag{3.6}$$

Not imposing a specific functional form for $g()$ and $h()$ allows us to demonstrate that the coefficient for the inflation rate and the output gap in the Taylor rule clearly depends on the second derivatives of the monetary authority's preference functions.

3.2.2 Dynamic and gradualist targeting model.

Once we have demonstrated the relevance of the second derivative of the monetary authority preference functions in a static model for shaping the Taylor rule, we move to the dynamic and gradualist environment of Svensson (1999). We assume that the central bank minimises an intertemporal loss function defined on the inflation rate deviations and the output gap but considering now time path decisions subject to the information set at the moment. Let us assume time separated loss functions with time discounting parameter ,β. Also, the central bank takes its decisions observing for each period the dynamic aggregate supply (3.7) in the economy, the IS function (3.8) and the Fisher equation (3.9).

1. Policymaker loss function

$$E_t \sum_{s=0}^{\infty} \beta^s L(\widetilde{\pi}_{t+s}, \widetilde{y}_{t+s})$$

$$L(\widetilde{\pi}_{t+s}, \widetilde{y}_{t+s}) = [\lambda g(\widetilde{\pi}_{t+s}) + h(\widetilde{y}_{t+s})]$$

$$\widetilde{\pi}_{t+s} = \pi_{t+s} - \pi^*, \ \widetilde{y}_{t+s} = \ y_{t+s} - y^*_{t+s}$$

2. Aggregate Supply

$$\pi_{t+1} = \pi_t + \alpha \widetilde{y}_t + u_{\pi,t+1} \tag{3.7}$$

3. IS

$$\widetilde{y}_{t+1} = \delta \widetilde{y}_t + \eta x_t - \xi r_t + u_{y,t+1} \tag{3.8}$$

4. Fisher equation

$$r_t = i_t - E_t(\pi_{t+1}) \tag{3.9}$$

The central bank faces now the optimal dynamic problem

$$\min_{i_t} E_t \sum_{s=0}^{\infty} \beta^s \left[\lambda g(\widetilde{\pi}_{t+s}) + h(\widetilde{y}_{t+s})\right] \tag{3.10}$$

$$s.t. \begin{cases} \pi_{t+1} = \pi_t + \alpha \widetilde{y}_t + u_{\pi,t+1} \\ \widetilde{y}_{t+1} = \delta \widetilde{y}_t + \eta x_t - \xi r_t + u_{y,t+1} \\ r_t = i_t - E_t(\pi_{t+1}) \end{cases}$$

Equation (3.8) is a dynamic IS where the output gap exhibits sluggish adjustment and depends on the real interest rate and on predetermined variable where x_t may capture other determinants of interest rate setting in open economies (Ball, 1999). The transmission mechanism of the monetary policy is treated either in Svensson (1999) or Ball (1999): monetary authority changes i_t and this implies a change

in r_t; from (3.10), it would affect $\widetilde{y}_{t+1}$but not $\widetilde{y}_t$, and so, $\widetilde{y}_{t+2}$and also $\widetilde{\pi}_{t+2}$. This timing convention is consistent with the literature on the transmission mechanism of monetary policy that establishes a change in monetary policy imply a variation in the output in the short run and a change in the inflation rate slowly later (Christiano et al., 1999). According to this transmission mechanism, this minimisation problem may be simplified considering for each period the two subsequent periods as in Svensson (1999).

We obtain the first order condition taking derivatives with respect to i_t

$$\beta E_t(\frac{\partial h}{\partial \widetilde{y}_{t+1}}\frac{\partial \widetilde{y}_{t+1}}{\partial r_t}\frac{\partial r_t}{\partial i_t}) + \beta^2\lambda E_t(\frac{\partial g}{\partial \widetilde{\pi}_{t+2}}\frac{\partial \widetilde{\pi}_{t+2}}{\partial \widetilde{y}_{t+1}}\frac{\partial \widetilde{y}_{t+1}}{\partial r_t}\frac{\partial r_t}{\partial i_t})+$$
$$+\beta^2 E_t(\frac{\partial h}{\partial \widetilde{y}_{t+2}}\frac{\partial \widetilde{y}_{t+2}}{\partial \widetilde{y}_{t+1}}\frac{\partial \widetilde{y}_{t+1}}{\partial r_t}\frac{\partial r_t}{\partial i_t}) = 0 \tag{3.11}$$

Also we use derivatives from (3.10) and forwarded IS equation

$$\frac{\partial r_t}{\partial i_t} = 1;\ \frac{\partial \widetilde{y}_{t+1}}{\partial r_t} = -\xi;\ \frac{\partial \widetilde{y}_{t+2}}{\partial \widetilde{y}_{t+1}} = \delta;\ \frac{\partial \widetilde{\pi}_{t+2}}{\partial \widetilde{y}_{t+1}} = \alpha$$

in (3.11) $\beta E_t(\frac{\partial h}{\partial \widetilde{y}_{t+1}}(-\xi)) + \beta^2\lambda E_t(\frac{\partial g}{\partial \widetilde{\pi}_{t+2}}\alpha(-\xi)) + \beta^2 E_t(\frac{\partial h}{\partial \widetilde{y}_{t+2}}\delta(-\xi)) = 0$

to obtain Euler equation

$$E_{t-1}(\frac{\partial h}{\partial \widetilde{y}_t}) + \alpha\beta\lambda E_{t-1}(\frac{\partial g}{\partial \widetilde{\pi}_{t+1}}) + \delta\beta E_{t-1}(\frac{\partial h}{\partial \widetilde{y}_{t+1}}) = 0 \tag{3.12}$$

The solution of (3.10) is an implicit function $i_t = i(E_t\widetilde{\pi}_{t+1}, E_t\widetilde{y}_{t+1})$ that fulfills the Euler condition, IS, Aggregate Supply and the Fisher equation.

Taking derivatives of the conditions with respect to the inflation rate deviation we can obtain the slope of the Taylor rule for the inflation rate.

$$\begin{cases} \alpha\beta\lambda E_{t-1}(\frac{\partial^2 g}{\partial \widetilde{\pi}^2_{t+1}}) + \delta\beta E_{t-1}(\frac{\partial^2 h}{\partial \widetilde{y}^2_{t+1}}\frac{\partial \widetilde{y}_{t+1}}{\partial r_t}\frac{\partial r_t}{\partial \pi_{t+1}}) = 0 \\ \frac{\partial \widetilde{y}_{t+1}}{\partial \pi_{t+1}} = -\xi\frac{\partial r_t}{\partial \pi_{t+1}} \\ \frac{\partial r_t}{\partial \pi_{t+1}} = \frac{\partial i_t}{\partial \pi_{t+1}} - 1 \end{cases}$$

$$\frac{\partial i_t}{\partial \pi_{t+1}} = 1 + \frac{\alpha\lambda E_{t-1}(\frac{\partial^2 g}{\partial \widetilde{\pi}^2_{t+1}})}{\delta\xi E_{t-1}(\frac{\partial^2 h}{\partial \widetilde{y}^2_{t+1}})}$$

Similarly, the slope of the Taylor rule for the output gap comes out from taking

derivatives with respect to it:

$$\begin{cases} E_{t-1}\dfrac{\partial^2 h}{\partial \widetilde{y}_t^2} + \alpha\beta\lambda E_{t-1}(\dfrac{\partial^2 g}{\partial \widetilde{\pi}_{t+1}^2}\dfrac{\partial \widetilde{\pi}_{t+1}}{\partial \widetilde{y}_t}) + \delta\beta E_{t-1}(\dfrac{\partial^2 h}{\partial \widetilde{y}_{t+1}^2}\dfrac{\partial \widetilde{y}_{t+1}}{\partial \widetilde{y}_t}) = 0 \\ \dfrac{\partial E_{t-1}\widetilde{y}_{t+1}}{\partial \widetilde{y}_t} = \delta - \xi\dfrac{\partial E_{t-1} r_t}{\partial \widetilde{y}_t} \\ \dfrac{\partial r_t}{\partial \widetilde{y}_t} = \dfrac{\partial i_t}{\partial \widetilde{y}_t} - \dfrac{\partial E_t \widetilde{\pi}_{t+1}}{\partial \widetilde{y}_t} \\ \dfrac{\partial \widetilde{\pi}_{t+1}}{\partial \widetilde{y}_t} = \alpha \end{cases}$$

$$E_{t-1}\frac{\partial^2 h}{\partial \widetilde{y}_t^2} + \alpha\beta\lambda E_{t-1}(\frac{\partial^2 g}{\partial \widetilde{\pi}_{t+1}^2}\alpha) + \delta\beta E_{t-1}(\frac{\partial^2 h}{\partial \widetilde{y}_{t+1}^2}(\delta - \xi[\frac{\partial i_t}{\partial \widetilde{y}_t} - \alpha])) = 0 \implies$$

$$\implies \frac{\partial i_t}{\partial \widetilde{y}_t} = \alpha(1 + \frac{\alpha\lambda E_{t-1}(\frac{\partial^2 g}{\partial \widetilde{\pi}_{t+1}^2})}{\delta\xi E_{t-1}(\frac{\partial^2 h}{\partial \widetilde{y}_{t+1}^2})}) + \frac{\delta}{\xi} + \frac{E_{t-1}(\frac{\partial^2 h}{\partial \widetilde{y}_t^2})}{\delta\beta\xi E_{t-1}(\frac{\partial^2 h}{\partial \widetilde{y}_{t+1}^2})}$$

With these two partial derivatives we can construct the first order Taylor expansion for the Taylor rule

$$i_t \simeq \left[1 + \frac{\alpha\lambda E_{t-1}(\frac{\partial^2 g}{\partial \widetilde{\pi}_{t+1}^2})}{\delta\xi E_{t-1}(\frac{\partial^2 h}{\partial \widetilde{y}_{t+1}^2})}\right] E_t\pi_{t+1} +$$

$$+ \left[\alpha(1 + \frac{\alpha\lambda E_{t-1}(\frac{\partial^2 g}{\partial \widetilde{\pi}_{t+1}^2})}{\delta\xi E_{t-1}(\frac{\partial^2 h}{\partial \widetilde{y}_{t+1}^2})}) + \frac{\delta}{\xi} + \frac{E_{t-1}(\frac{\partial^2 h}{\partial \widetilde{y}_t^2})}{\delta\beta\xi E_{t-1}(\frac{\partial^2 h}{\partial \widetilde{y}_{t+1}^2})}\right] \widetilde{y}_t \tag{3.13}$$

The first point in (3.13) is that the second derivatives of $g()$ and $h()$ are relevant for the coefficients of the Taylor rule. Second, it is easy to check that a cross effect between the inflation rate and the output gap can be obtained considering the second degree Taylor expansion of (3.13). Finally, in case the functions $g()$ and $h()$ are piecewise continuous and strictly convex functions with noncontinuous second derivative, Taylor rule would exhibit nonlinearity defined by different regions delimited by thresholds, as we show below.

3.2.3 Discussion about Taylor Rule Coefficients

We have stressed so far that, for our purpose, the most important feature of the central bank loss function is its second derivatives in the inflation deviation and output

gap. Let us then specify general assumptions about this loss function and explore their consequences in how second derivatives affect the Taylor Rule coefficients.

We consider very general though simple characteristics for $g()$ and $h()$ functions that give rise to interesting nonlinearities in the TR, which will take the form of multiple thresholds: Some of these are associated with the value of a single variable (for instance, the inflation deviation) and others take place for specific combinations of two individual variables that interact with each other (for instance, the interaction between the inflation deviation and the output gap at specific values of each).

Figure 3.1: Examples of preference (loss) functions on inflation deviation with different regimes.

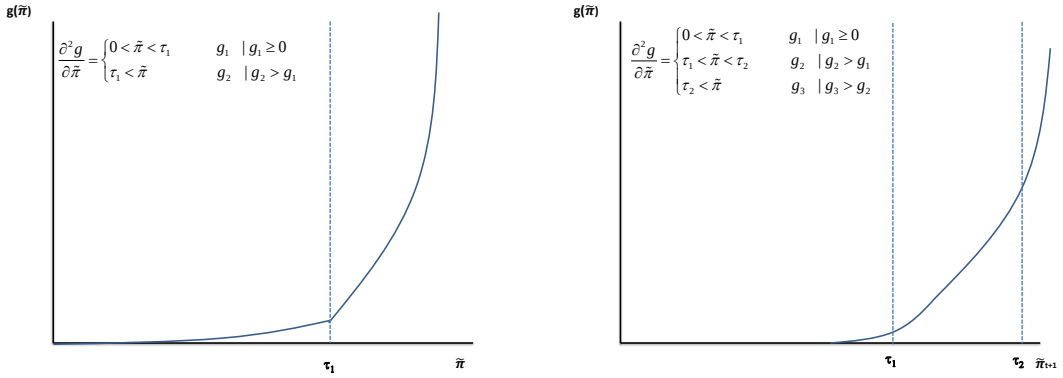

We assume both functions can be piecewise continuous (Figure 3.1). Therefore, the whole domain of $\widetilde{\pi}$ can be split into n disjoint regions $\{R_1^{\pi}, R_2^{\pi}, ..., R_n^{\pi}\}$ Similarly, the whole domain of $\widetilde{y}$ can be split into m disjoint regions $\{R_1^{y}, R_2^{y}, ..., R_m^{y}\}$ We assume that the functions will be strictly convex (i.e., their second derivatives are strictly positive). This implies the higher the marginal loss, the higher the deviation from targets, which is a common-sense assumption.

We will see how the Taylor rule changes as a result of the combination of four elements: (1) the characteristics of the second derivatives with respect to the output gap, on one hand; (2) with respect to the inflation deviation, on the other; (3) the region in which the economy stands at time t, $(\widetilde{y}_t)$; and (4) the region in which the monetary authority wants the economy to stand in the coming period $(\widetilde{y}_{t+1})$.

Case A

The current output gap $\widetilde{y}_t$, as well as the short term output gap $\widetilde{y}_{t+1}$, lie on the same region R_i^y, so that $\dfrac{\partial^2 h}{\partial \widetilde{y}_t^2} = \dfrac{\partial^2 h}{\partial \widetilde{y}_{t+1}^2} = c_2$. For simplicity, let us assume that this second derivative is constant, $\dfrac{\partial^2 h}{\partial \widetilde{y}_{t+1}^2} = c_2$, and similarly for $g()$, $\dfrac{\partial^2 g}{\partial \widetilde{\pi}_{t+1}^2} = c_1$

$$i_t \simeq \left[1 + \frac{\alpha\lambda c_1}{\delta\xi c_2}\right] E_t\pi_{t+1} + \left[\alpha(1 + \frac{\alpha\lambda c_1}{\delta\xi c_2}) + \frac{(1+\delta^2\beta)}{\delta\beta\xi}\right] \widetilde{y}_t$$

So, in this particular case, we obtain a Taylor rule function with constant coefficients in this particular region. In another region these constant coefficients could vary with changes in $c1$ and/or $c2$.

Case B

The current output gap $\widetilde{y}_t$, as well as the short term output gap objective $\widetilde{y}_{t+1}$, lie on the same region R_i^y, so that $\dfrac{\partial^2 h}{\partial \widetilde{y}_t^2} = \dfrac{\partial^2 h}{\partial \widetilde{y}_{t+1}^2}$ and again assume as before$\dfrac{\partial^2 h}{\partial \widetilde{y}_{t+1}^2} = c_2$. By contrast, $g()$ is such that $\dfrac{\partial^2 g}{\partial \widetilde{\pi}_{t+1}^2}$ is not constant for the whole domain of $g()$. Then:

$$i_t \simeq \left[1 + \frac{\alpha\lambda \dfrac{\partial^2 g}{\partial \widetilde{\pi}_{t+1}^2}}{\delta\xi c_2}\right] E_t\pi_{t+1} + \left[\alpha(1 + \frac{\alpha\lambda \dfrac{\partial^2 g}{\partial \widetilde{\pi}_{t+1}^2}}{\delta\xi c_2}) + \frac{(1+\delta^2\beta)}{\delta\beta\xi}\right] \widetilde{y}_t \tag{3.14}$$

Consider two adjacent inflation regions such that:

$$\frac{\partial^2 g}{\partial \widetilde{\pi}_{t+1}^2} = \begin{cases} g_i > 0 \ \text{ if } \ \widetilde{\pi}_{t+1} \in R_i^\pi \\ g_{i+1} > g_i, \text{if } \ \widetilde{\pi}_{t+1} \in R_{i+1}^\pi \end{cases}$$

In these circumstances, the Taylor rule reflects the existence of different regions for the two components of the loss functions and exhibits threshold behavior:

$$i(\widetilde{\pi}_{t+1}, \widetilde{y}_t) \simeq \begin{cases} \left[1 + \dfrac{\alpha\lambda g_i}{\delta\xi c_2}\right] E_t\pi_{t+1} + \left[\alpha(1 + \dfrac{\alpha\lambda g_i}{\delta\xi c_2}) + \dfrac{(1+\delta^2\beta)}{\delta\beta\xi}\right] \widetilde{y}_t \ \text{ if } \ \widetilde{\pi}_{t+1} \in R_i^\pi \\ \left[1 + \dfrac{\alpha\lambda g_{i+1}}{\delta\xi c_2}\right] E_t\pi_{t+1} + \left[\alpha(1 + \dfrac{\alpha\lambda g_{i+1}}{\delta\xi c_2}) + \dfrac{(1+\delta^2\beta)}{\delta\beta\xi}\right] \widetilde{y}_t \ \text{ if } \ \widetilde{\pi}_{t+1} \in R_{i+1}^\pi \end{cases}$$

Case C

If the second derivative with respect to inflation is as in Case B

$$\frac{\partial^2 g}{\partial \widetilde{\pi}_{t+1}^2} = \begin{cases} g_i > 0 \ \text{ if } \ \widetilde{\pi}_{t+1} \in R_i^\pi \\ g_{i+1} > g_i, \text{if } \ \widetilde{\pi}_{t+1} \in R_{i+1}^\pi \end{cases}$$

and the second derivative with respect to the output gap is similarly defined as

$$\frac{\partial^2 h}{\partial \widetilde{y}_t^2} = \begin{cases} h_j > 0 \ \text{ if } \ \widetilde{y}_t \in R_j^y \\ h_{j+1} > h_j \ \text{ if } \ \widetilde{y}_t \in R_{j+1}^y \end{cases}$$

then we may consider two different scenarios:

Scenario 1. The central bank is convinced that its decisions can reduce the output gap by pushing the economy to another (adjacent) region. Then, the output gap $\widetilde{y}_t$ and the short term objective for it, $\widetilde{y}_{t+1}$, lie on different but adjacent regions R_j^y and R_{j+1}^y such that $\dfrac{\partial^2 h}{\partial \widetilde{y}_t^2} = h_{j+1}$, $\dfrac{\partial^2 h}{\partial \widetilde{y}_{t+1}^2} = h_j$, and $h_{j+1} > h_j$.

Therefore, the Taylor rule takes the following form:

$$i(\widetilde{\pi}_{t+1}, \widetilde{y}_t) \simeq \begin{cases} \left[1 + \dfrac{\alpha\lambda g_i}{\delta\xi h_j}\right] E_t\pi_{t+1} + \left[\alpha(1 + \dfrac{\alpha\lambda g_i}{\delta\xi h_j}) + \dfrac{\delta}{\xi} + \dfrac{h_{j+1}}{\delta\beta h_j}\right] \widetilde{y}_t \ \text{ if } \widetilde{\pi}_{t+1} \in R_i^\pi,\ \widetilde{y}_t \in R_j^{\widetilde{y}} \\ \\ \left[1 + \dfrac{\alpha\lambda g_{i+1}}{\delta\xi h_j}\right] E_t\pi_{t+1} + \left[\alpha(1 + \dfrac{\alpha\lambda g_{i+1}}{\delta\xi h_j}) + \dfrac{\delta}{\xi} + \dfrac{h_{j+1}}{\delta\beta h_j}\right] \widetilde{y}_t \ \text{ if } \widetilde{\pi}_{t+1} \in R_{i+1}^\pi,\ \widetilde{y}_t \in R_j^{\widetilde{y}} \end{cases}$$

Scenario 2. The central bank is not convinced of its ability to avoid expanding the output gap. Then, the current output gap $\widetilde{y}_t$ and short term output gap objective $\widetilde{y}_{t+1}$ lie on different but adjacent regions R_1^y and R_2^y but now $\dfrac{\partial^2 h}{\partial \widetilde{y}_t^2} < \dfrac{\partial^2 h}{\partial \widetilde{y}_{t+1}^2}$.

$$\frac{\partial^2 g}{\partial \widetilde{\pi}_{t+1}^2} = \begin{cases} g_i > 0 \ \textit{if} \ \widetilde{\pi}_{t+1} \in R_i^\pi \\ g_{i+1} > g_1 \ \textit{if} \ \widetilde{\pi}_{t+1} \in R_{i+1}^\pi \end{cases} \qquad \frac{\partial^2 h}{\partial \widetilde{y}_t^2} = \begin{cases} h_j > 0 \ \textit{if} \ \widetilde{y}_t \in R_j^y \\ h_{j+1} > h_1 \ \textit{if} \ \widetilde{y}_t \in R_j^y \end{cases}$$

In this case, it can be shown that the Taylor rule takes the following form:

$$i(\widetilde{\pi}_{t+1}, \widetilde{y}_t) = \begin{cases} \left[1 + \dfrac{\alpha\lambda g_i}{\delta\xi h_{j+1}}\right] E_t\pi_{t+1} + \left[\alpha(1 + \dfrac{\alpha\lambda g_i}{\delta\xi h_{j+1}}) + \dfrac{\delta}{\xi} + \dfrac{h_j}{\delta\beta h_{j+1}}\right] \widetilde{y}_t \ \text{ if } \widetilde{\pi}_{t+1} \in R_i^\pi,\ \widetilde{y}_t \in R_j^{\widetilde{y}} \\ \\ \left[1 + \dfrac{\alpha\lambda g_{i+1}}{\delta\xi h_{j+1}}\right] E_t\pi_{t+1} + \left[\alpha(1 + \dfrac{\alpha\lambda g_{i+1}}{\delta\xi h_{j+1}}) + \dfrac{\delta}{\xi} + \dfrac{h_j}{\delta\beta h_{j+1}}\right] \widetilde{y}_t \ \text{ if } \widetilde{\pi}_{t+1} \in R_{i+1}^\pi,\ \widetilde{y}_t \in R_j^{\widetilde{y}} \end{cases}$$

To sum up, these cases allow us to explain how different reactions by the central bank depend upon the region characterized by the value of the second derivatives of functions $g()$ and $h()$. Hence, this Taylor rule could explain different and more intensive central bank reactions when some thresholds have been exceeded. In addition, from this short discussion, a simple conclusion arises: if the components of the central bank loss function concerning the output gap $g()$ and the inflation deviation $h()$ are piecewise continuous and strictly convex functions with non continuous second derivatives, then the Taylor rule will be nonlinear and will exhibit possibly complex threshold behavior. Since there is no reason for thinking that central bank has smooth and homogeneous preferences about the whole domain of the output

gap and the inflation deviations, it is necessary to use sufficiently flexible nonlinear methods, at least in the form of nonconstant parameters with possible multiple thresholds and even interaction effects for a reliable empirical estimation of the TR.

3.3 Calibrating the model

In order to understand how the model with thresholds works compared to the model without thresholds, we calibrate responses of the interest rate to several shocks in the inflation deviations and the output gap.

Our first calibration consists of simulating the response of the model (3.10) to a 2-period impulse in the inflation rate through $u_{\pi,t+1}$ in the Aggregate Supply (3.7). The proposed impulse parameter values and the loss functions with thresholds are as follows:

Parameter values:

$$\alpha = 0.25, \beta = 0.95, \delta = 0.75, \eta = 0.25, \xi = 10, \lambda = 2 \tag{3.15}$$

Preference functions:

$$g(\widetilde{\pi}_t) = \begin{cases} |\widetilde{\pi}_t| \leq 0.02 \Rightarrow 10\widetilde{\pi}_t^2 \\ |\widetilde{\pi}_t| > 0.02 \Longrightarrow \widetilde{\pi}_t^2 \end{cases} \quad h(\widetilde{y}_t) = \begin{cases} |\widetilde{y}_t| \leq 0.02 \Rightarrow 5\widetilde{y}_t^2 \\ |\widetilde{y}_t| > 0.02 \Longrightarrow \widetilde{y}_t^2 \end{cases} \tag{3.16}$$

Impulse [inflation shock]:

$$u_{\pi,1} = 0.1,\ u_{\pi,2} = 0.1,\ u_{\pi,j} = 0,\ \forall j = 3, ...50 \tag{3.17}$$

We consider the model composed by the following (more traditional) preference functions $g(\widetilde{\pi}_t) = \widetilde{\pi}_t^2, \forall \widetilde{\pi}_t$ and $h(\widetilde{y}_t) = \widetilde{y}_t^2, \forall \widetilde{y}_t$ as the benchmark.

Figure 3.2 illustrates the short-run responses of the interest rates to impulses in the inflation rate (3.17). Interest rate positively responses to these positive inflation rate shocks during some periods in the short run. As theoretically expected, this response in the long term is zero for non-permanent shocks. The model with thresholds shows a temporal trajectory of the interest rate response higher and more persistent than that one for the model without thresholds. It means that when a central bank has the proposed piecewise preference functions its reaction will be more intensive and

persistent while the inflation rate and/or output gap of the economy are still above the thresholds.

Figure 3.2: Interest rate short-run responses to impulses in the inflation rate.

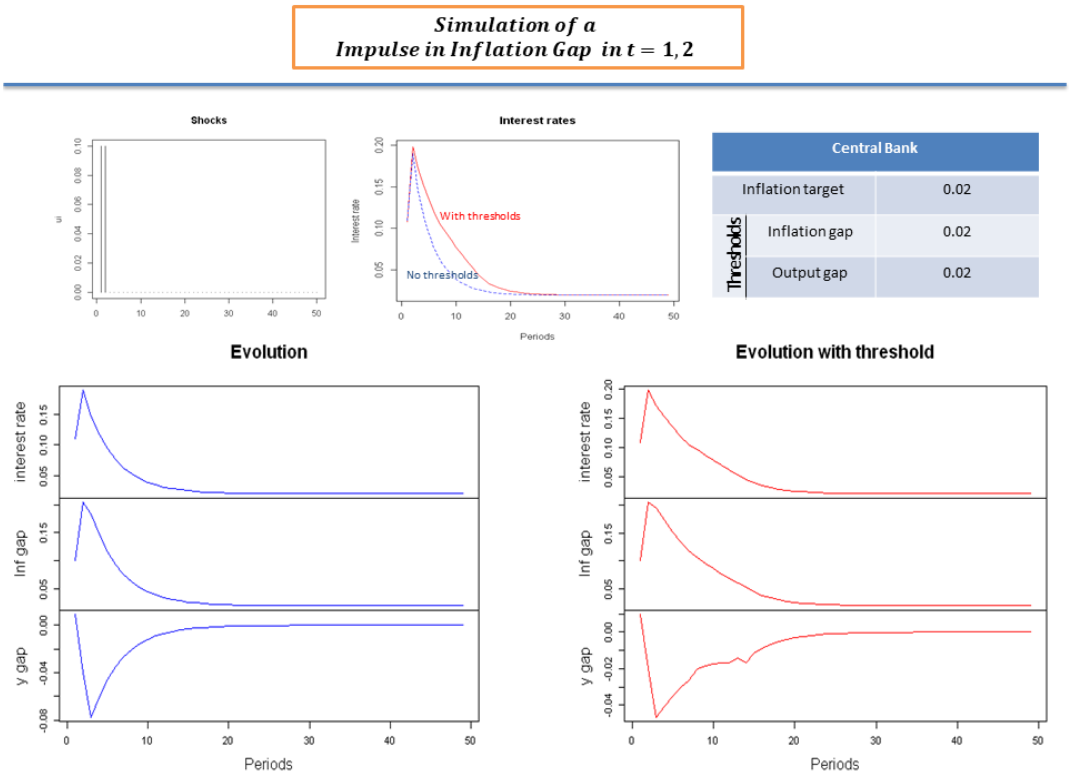

Aggregate supply impulse in a model with and without thresholds.

Figure 3.3 shows different responses of interest rate to the shock in inflation rate depending on the values of the coefficient α in the Aggregate Supply (3.7), and the autoregressive coefficient δ in the IS function (3.8). The greater α, the sharper the decrease of the interest rate after the inflationary shock, because of a the greater sensitivity of the inflation rate to the output gap from the previous period, and so the effectiveness of the monetary authority to control the inflation rate through the interest rate. On the other hand, the greater the autoregressive coefficient δ of the output gap in IS (3.8), the slower the decrease of the interest rate after the inflationary shock because the monetary authority needs to keep higher interest rate during more time to fight against the persistence of the output gap.

Figure 3.3: Responses of interest rate to an impulse in the inflation deviation depending on AS and IS parameters.

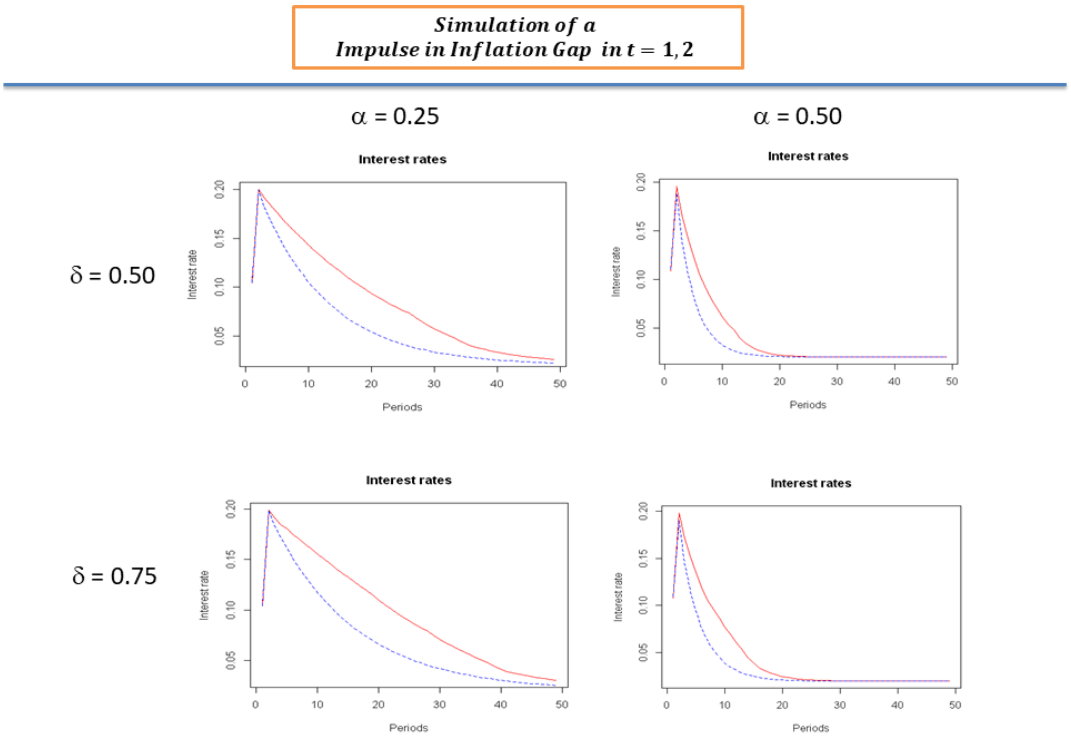

Response to an impulse in the inflation gap for different combinations of parameter values of α and δ.

The second calibration consists of simulating the response of the interest rate to a permanent shock in the output gap in the IS function such that:

$$\text{Permanent impulse [output gap shock]: } u_{y,j} = 0.1 \ \forall j = 1, ...50 \tag{3.18}$$

Figure 3.4 illustrates the response of the interest rate to a permanent shock in the output gap (3.18). As expected in the model, this permanent shock in the output gap permanently increases the nominal interest rate to a new steady state. This interest rate steady state is greater for the model with threshold than the one for the model without threshold, just because the output gap shock makes the monetary authority react with more intensity related to values above the threshold for the output gap.

Figure 3.4: Responses of the interest rate to a permanent shock in the output gap.

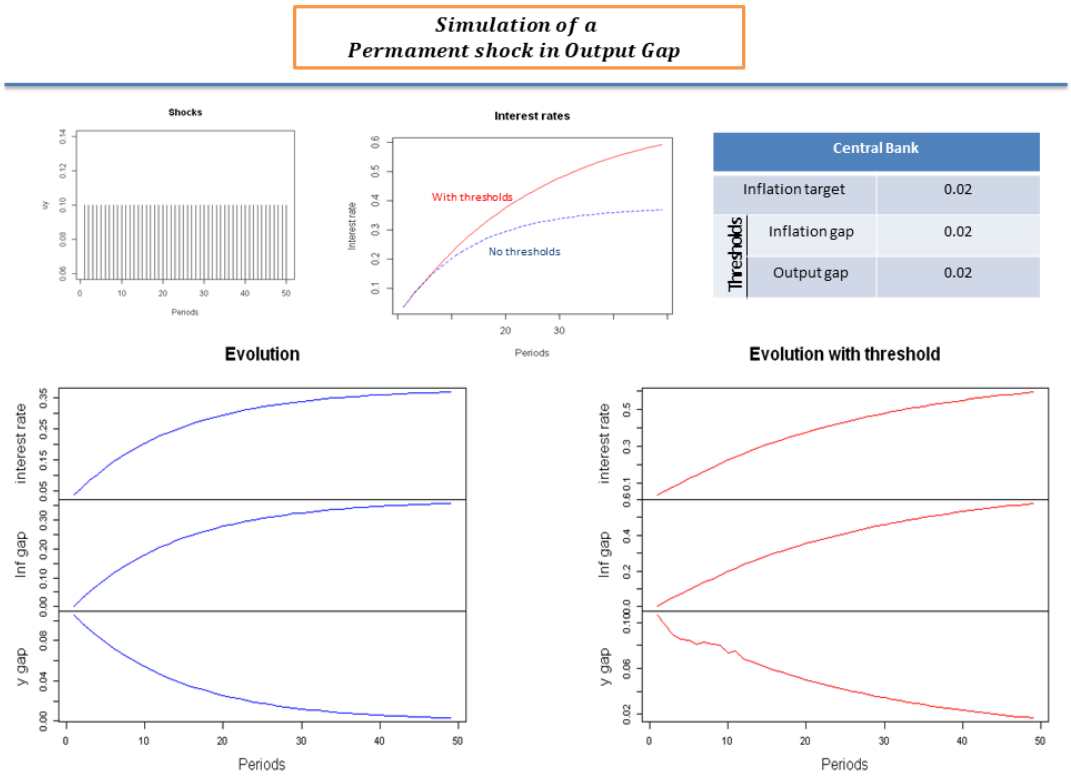

Calibration of a model with thresholds and a model without thresholds response facing an IS permanent shock .

Figure (3.5) depicts the interest rate responses to a permanent shock in the output gap depending on different values of the coefficient α in the Aggregate Supply (3.7), and the autoregressive coefficient δ in the IS function (3.8). The greater α, the lower the new steady state of the interest rate, because of a greater effectiveness of the monetary policy. By contrast, for a greater value of the autoregressive coefficient δ of the output gap in IS (3.8), the greater the new steady state for the interest rate because it is necessary to keep higher interest rate to fight against the persistence of the output gap.

Figure 3.5: Responses of the interest rate to a permanent shock in the output gap depending on AS and IS parameters.

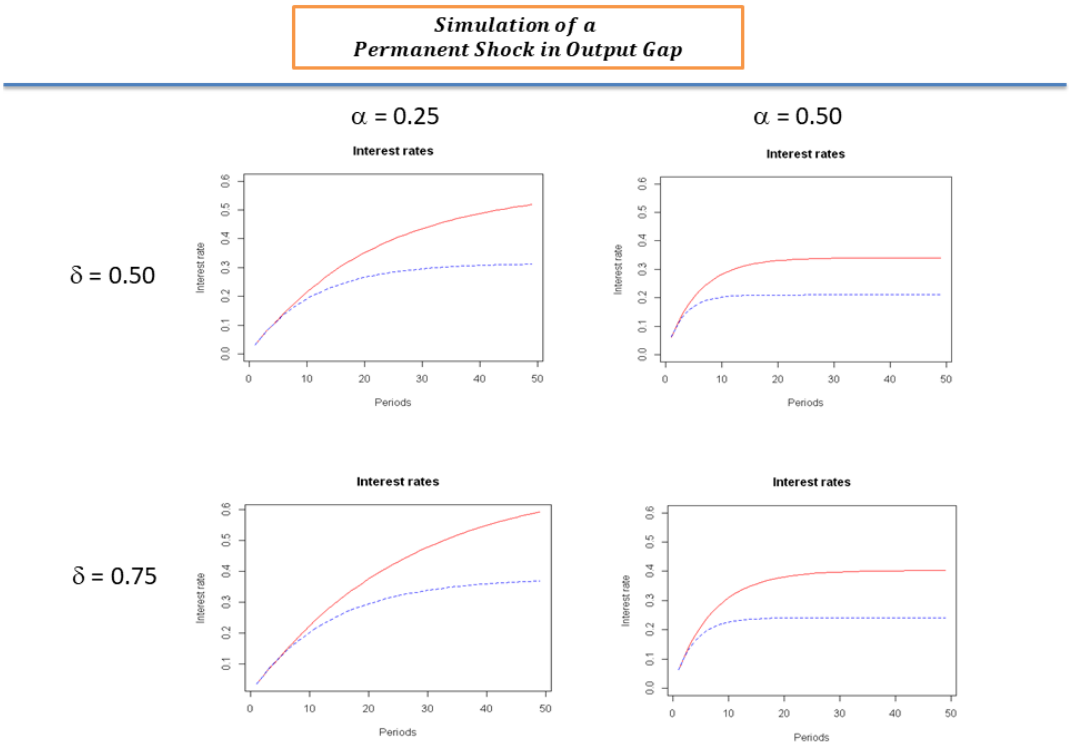

Interest rate response to a permanent shock in the output gap for different combinations of parameter values of α and δ.

The third calibration consists of simulating the response of the interest rate to an output gap shock as before but only taking place during the first half of the total number of periods. We call it as a semi-permanent impulse.

$$\text{Semi-permanent impulse[output gap shock]: } u_{y,j} = 0.1 \ \forall j = 1, ...25 \qquad (3.19)$$
$$u_{y,j} = 0 \ \ \forall j = 26, ...50$$

Figure (3.6)shows the response of the interest rate to this semi-permanent impulse in the output gap (3.19). It may be understood as a number of periods with greater government spending and a sudden cutoff after those periods. During the periods with the positive shock, interest rate increases. As in the second calibration, the model with threshold shows an interest rate time path with greater values than for the model without threshold. For the following periods with no shock, interest rate

decreases and again the model with threshold give us an interest rate trajectory above the one for the model without threshold. Moreover, (3.6) provides the output gap response series to the shock. When the positive impulse starts, the output gap increases but it fades out even if the impulse keeps constant in time. This is because of the monetary authority reaction with the interest rate. On the other hand, when the impulse disappears, the interest rate falls and the output gap becomes negative but smoothly converging to zero.

Figure 3.6: Response of the interest rate to a semi-permanent shock in output.

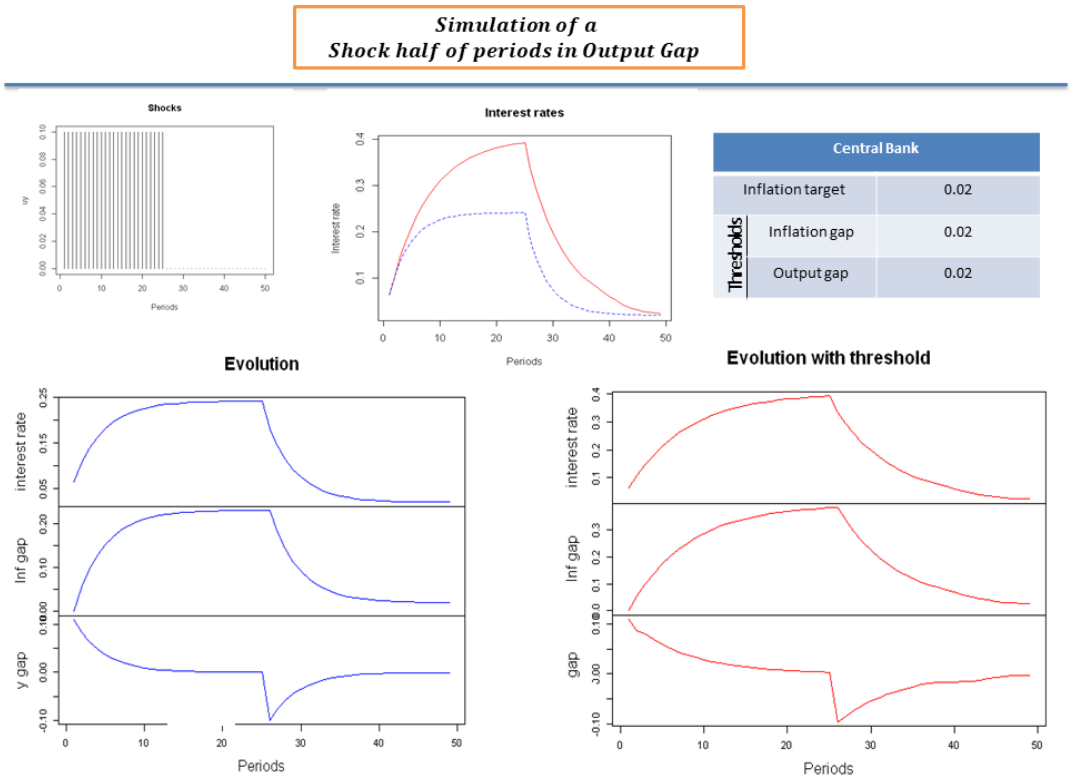

Calibration of a model with thresholds and a model without thresholds response facing a semi-permanent output gap.

As in the previous calibration, we present in (3.7) how the response of the interest rate to this impulse depends on the value of α in the Aggregate Supply (3.7). The greater α, the greater effectiveness of the monetary policy, therefore for greater values of α the interest rate is not only reaching lower maximum values but it also

suffers abrupt reductions. The model with thresholds gives time trajectories for the interest rate above those from the model without threshold.

Figure 3.7: Response of the interest rate to semi permanent shock in output depending on AS parameter.

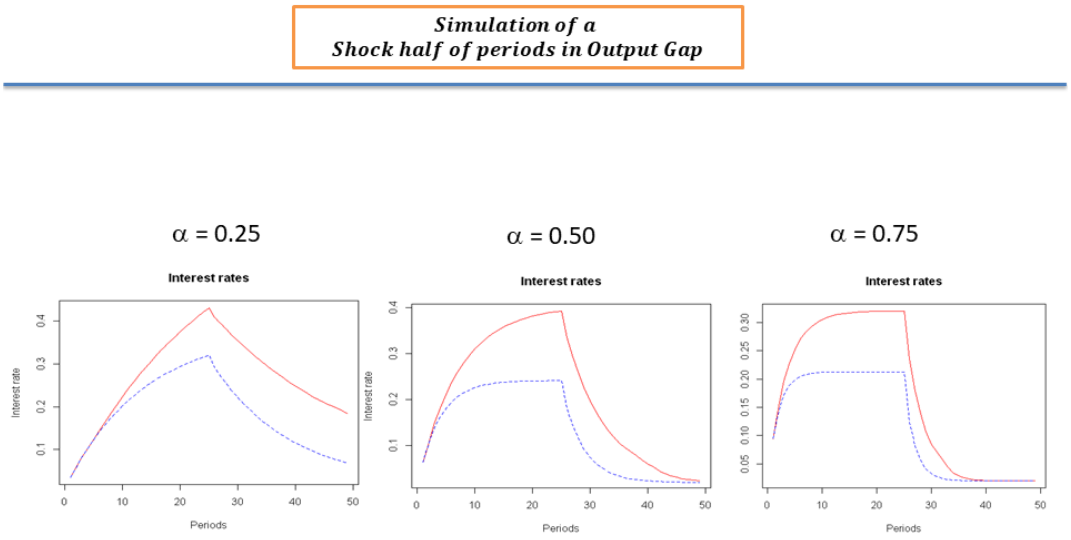

Model response to a semi-permanent shock in the output gap depending on different parameter values of α.

The last calibration we propose consists of simulating the response of the interest rate to combined random inflationary and output gap shocks in (3.7) and (3.8), respectively. In this case, the impulse will be two series of inflationary and output gap normally distributed random shocks, as follows:

Combined impulse series [inflationary and output gap shocks]:

$$\forall t = 1, ...50 \quad u_{\pi,t} \sim N(0, \sigma = 0.1) \qquad u_{y,t} \sim N(0, \sigma = 0.1) \tag{3.20}$$

Figure 3.8: Response of the models to combined inflationary and output gap shocks.

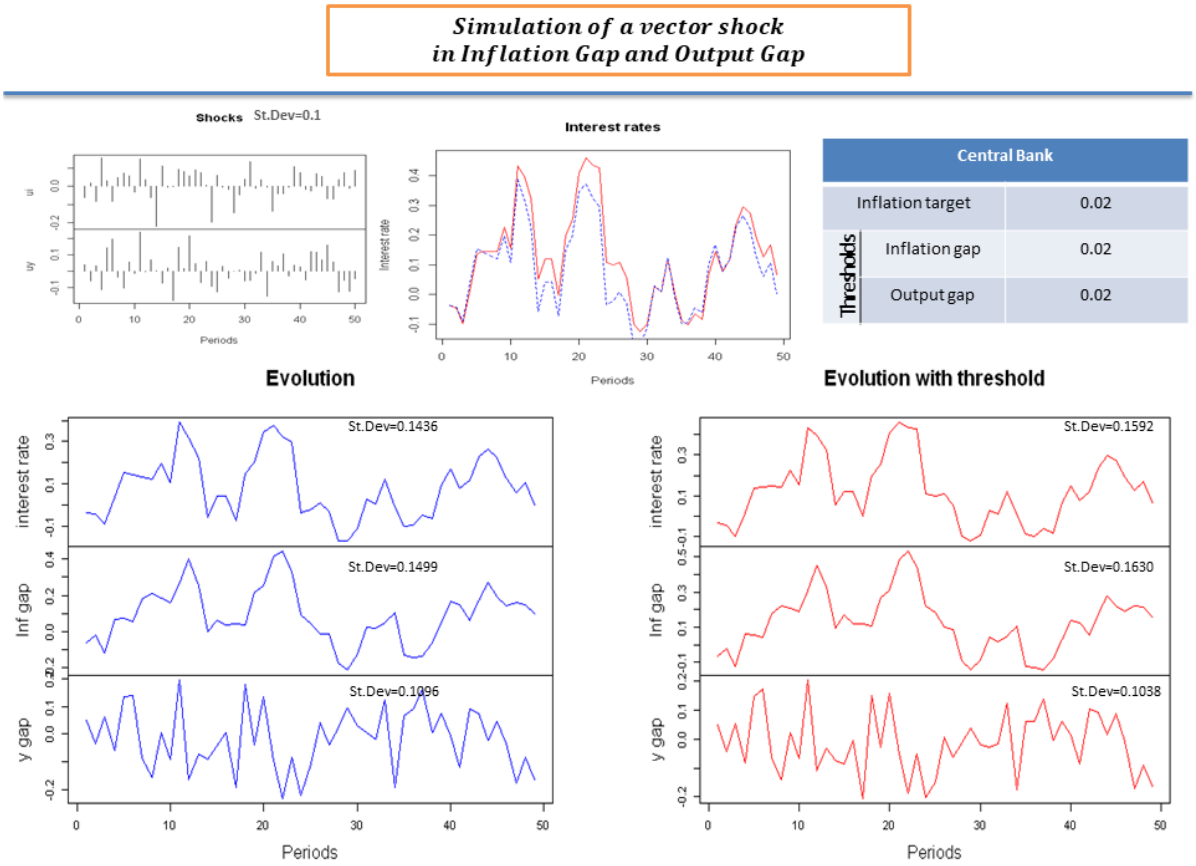

Calibration of the model with thresholds and the model without thresholds, both with an impulse composed by random inflationary and output gap shocks.

Figure 3.8 shows the response of the interest rate, the inflation rate, and the output gap to one sample of random shocks (3.20). According to the previous calibrations the standard deviation of the interest rate results to be greater in the model with thresholds than in the model without thresholds. Let us imagine data is generated by a model with thresholds, if we try to estimate a linear Taylor rule from a model without a threshold, the residuals will exhibit a great variance capturing as noise information that is relevant for the model. Moreover, the estimators will be biased.

In order to check it, we run a Monte Carlo experiment to evaluate the effects of estimating the Taylor rule by Ordinary Least Square: We generate 10000 samples

generated by a nonlinear model with thresholds and random inflationary and output gap shocks.

We use the following monetary authority preference functions for simulating samples:

$g(\widetilde{\pi}_{t+1})$ for the inflation rate deviation with an inflation target (and threshold) of 0.02 ($\widetilde{\pi}_{t+1} = \pi_{t+1} - 0.02$),

$$g(\widetilde{\pi}_{t+1}) = \begin{cases} (\pi_{t+1} - 0.02)^2 & \text{if } \widetilde{\pi}_{t+1} \leq 0.02 \\ 10\,(\pi_{t+1} - 0.02)^2\,, \text{if } \widetilde{\pi}_{t+1} > 0.02 \end{cases}$$

and $h(\widetilde{y}_t)$ for the output gap $\widetilde{y}_t$,

$$h(\widetilde{y}_t) = \begin{cases} (\widetilde{y}_t)^2 & \text{if } \widetilde{y}_t \leq 0.02 \\ 10\,(\widetilde{y}_t)^2\,, \text{if } \widetilde{y}_t > 0.02 \end{cases}$$

In Figure 3.9, we provide the true values of the inflation rate and the output gap coefficients according to the model (3.13). In addition, we provide histograms for the estimators β_π and β_y from the linear specification of the Taylor rule:

$$i_t = \beta_{0+}\beta_\pi \widetilde{\pi}_t + \beta_y \widetilde{y}_t + \varepsilon$$

The histograms show that both estimators are clearly and strongly biased with respect to the true values. Consequently, if the monetary authority follows a nonlinear policy rule as described in our model, the empirical results from a traditional linear Taylor rule estimation can be seriously misleading.

Figure 3.9: OLS estimations of 10.000 samples generated by a model with thresholds.

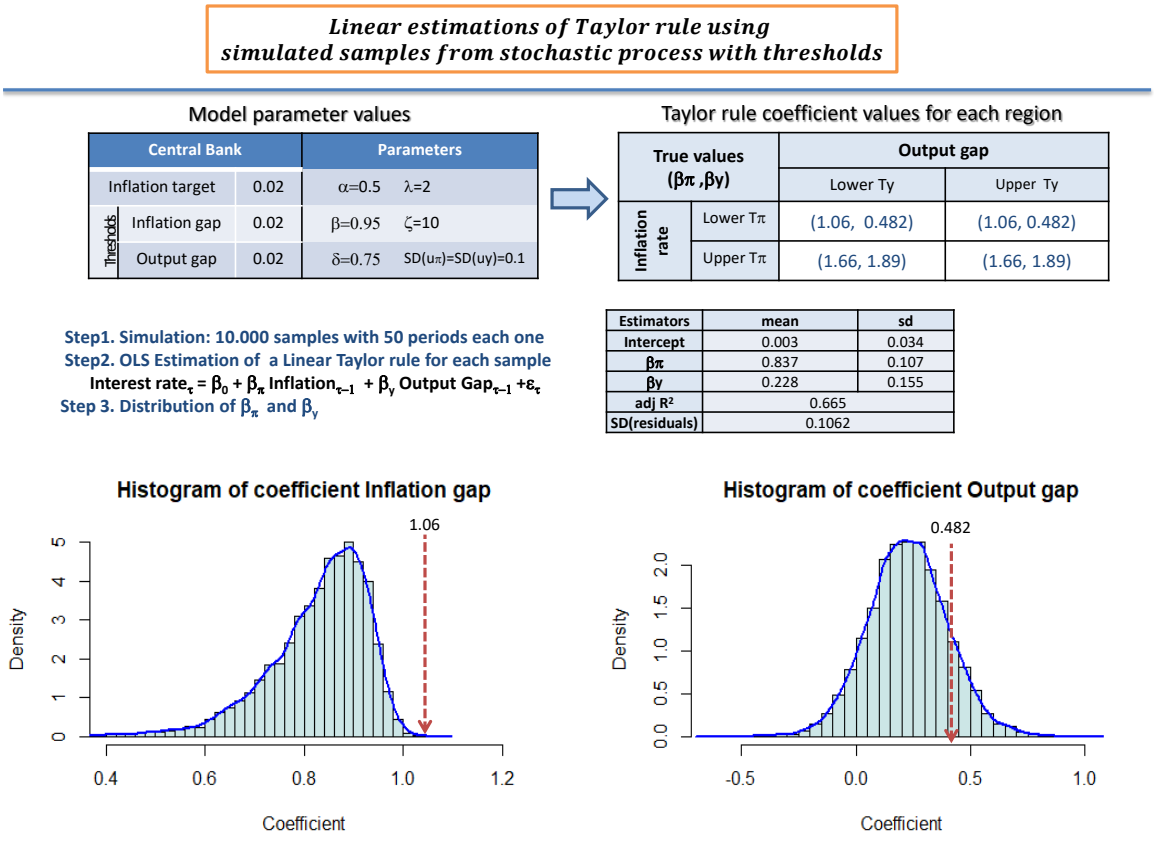

4 Thresholds in the implementation of Monetary Policy: The Taylor Rule revisited.

This paper presents results for endogenous threshold estimations of the Taylor Rule. We first propose and develop a theoretical model in which the central bank's optimal behavior is conveniently described by piecewise defined preference functions on the inflation and the output gaps and we show that this implies thresholds in the implementation of monetary policy. The empirical results we obtain with Multiple Adaptive Regression Splines (MARS) confirm the theoretical conjecture.
We apply MARS to estimate the Fed Taylor rule from 1970 to 2014 with the partial adjustment model from Judd and Rudebusch (1998). MARS not only detects actual thresholds in monetary policy, but also fits the data better than the usual linear models. The main thresholds are detected for inflation rate at 4.31% $95\%CI(3.86\%, 4.89\%)$ and for the output gap at 0.012 $95\%CI(-0.0213, 0.0196)$[1]. As our theoretical framework predicted, an interaction effect appears between the inflation rate and the output gap. Moreover, under Paul Volcker's governance, this methodology detects reactions from the U.S. Federal Reserve Bank that are stronger than in previous periods and reveals that the inflation gap generates reactions at a lower threshold level. Our paper thus innovates both theoretically and empirically, and provides a more complete characterization of the nonlinear feature of the Taylor Rule.

[1] 95%CI corresponds to the Confidence interval at this percentage

4.1 Introduction.

Over the last two decades, researchers have devoted much effort to analyzing the factors responsible for observed nonlinearities in the Taylor Rule (henceforth denoted as TR), and to applying new empirical methodologies to detect and quantify them. It is of utmost importance to correctly tackle this problem since, if TR estimations disregard nonlinearities when they are present, the generated coefficients on the inflation rate and on the output gap will be biased, and the evaluation of the policy reactions of the central banks will be incorrect and misleading.

In this paper we analyze an important source of nonlinearities in the TR, which, to the best of our knowledge, has not been considered in the literature: the discrete changes that the central banks make at certain moments to the weights attached to deviations of the rate of inflation, and/or of the output gap, from their targets once one or the two fundamental determinants reach certain thresholds. Such behavior translates into discrete jumps of the short-term interest rate policy, giving rise to nonlinearities in the monetary policy rule. Indeed, our main theoretical argument in this paper is that complex nonlinearities in the TR may arise as a result of specific -though intuitively simple- characteristics of monetary authority's preferences.

In the theoretical part of this paper, we derive a dynamic and general Taylor Rule from a very general social loss function of the central bank. We substitute the traditional assumption of a quadratic social loss function (that gives rise to a linear TR) by simply assuming that the central bank has a piecewise-defined social loss function that depends on the inflation and output gaps, and we derive from it a monetary policy rule that exhibits thresholds. We show that multiple thresholds may exist and may interact with each other. On the empirical side, we use the MARS procedure, which is a technique particularly well suited to endogenously detecting and quantifying multiple and interacting thresholds in the optimal behavior of the central banks. We believe that our paper is the first application of this methodology for the estimation of Taylor Rules.

We use the initial model specification from Judd and Rudebusch (1998) applying MARS procedure to estimate the U.S. Fed monetary policy rule with monthly data for the period 1970 to 2014. We detect thresholds for the inflation rate 4.31% $95\%CI(3.86\%, 4.89\%)$ and at 0.012 $95\%CI(-0.0213, 0.0196)$ for the output gap. As our theoretical framework predicts, we find an interaction between inflation and output gap. We also estimate a stronger sensitivity of the Fed's reaction in the

Volcker-Greenspan period to inflation rate even at a lower threshold than in the other period which is consistent with the literature; in addition, Bernanke period is also characterized by a less intensive reaction to inflation rate and output gap.

The rest of the paper is organized as follows: In Section 2, we summarize the relevant literature on nonlinearities in the TR. We develop optimal nonlinear threshold Taylor Rules in Section 3, assuming a piecewise-defined structure for the social loss function of the central bank. In Section 4, we explain the MARS methodology, describe the data, estimate the model, and in section 5 we compare our results with the findings. Finally, in Section 6, we present our conclusions and propose a more complete characterization of the Taylor Rule derived from the empirical findings that have confirmed our theoretical conjecture.

4.2 Literature review.

Up till now, the literature reports two main theoretical sources of nonlinearities in the behavior of the central banks. The first one relies upon the asymmetrical preferences of the central banks, in the sense that they give different weights to inflation deviations and the output gap depending on the sign of those deviations. The second source of nonlinearities is nonlinear short run trade-offs between output and inflation (i.e. nonlinear Phillips Curve). It is easy to show that one or both sources of nonlinearities give rise to nonlinear TRs when they are included in the optimization process of the central banks.

As far as the first source is concerned, Robert Nobay and Peel (2003) take the asymmetric preferences of central banks as given and explores which consequences derive from this assumption for the monetary policy under both commitment and discretion. Ruge-Murcia (2002) assumes that central banks have social preferences that are asymmetric around inflation and unemployment targets, which implies that both the size and the sign of the deviations matter to the central banker. Cukierman and Muscatelli (2008) assume that the asymmetries in the social loss function derive from the fact that the central banks have a stronger aversion to recessions than to expansions because they must be accountable to democratically elected politicians. Taking this a step further, some scholars demonstrate that the asymmetric preferences of central banks generate nonlinearities in the interest-rate reaction rule. See, for instance, Orphanides and Wieland (2000), Surico (2002), Ruge-Murcia (2002),

and Cukierman and Muscatelli (2008).

As regards the source of nonlinearities stemming from the structural system, Dolado et al. (2005) review the theoretical evidence on concave and/or convex short-run Phillips curves in the literature, and explain how these nonlinearities generate optimal nonlinear monetary reaction functions. Orphanides and Wieland (2000) use zone-linear Phillips curves to derive an optimal behavior of the central banks that targets an inflation zone instead of an inflation point. Petersen et al. (2007) emphasize that the inflation gap and the output gap are inherently nonlinear processes, with output exhibiting short and sharp recessions, but long and smooth recoveries over the business cycle. Neftci (1984) shows that the rate of unemployment exhibits this asymmetric dynamics using the framework of finite state Markov processes. Under such circumstances, the U.S. Fed responds differently to negative versus positive inflation and output shocks when it tries to stabilize the business cycle.

Turning to the literature on the empirical findings, one strand investigates the presence of nonlinearities by applying parametric modeling techniques. Petersen et al. (2007), Cukierman and Muscatelli (2008) and Gerlach and Lewis (2014b), among others, estimate parametric Smooth Transition AutoRegressive (STAR) models (Granger et al., 1993). Some authors estimate Fed's TR with STAR to identify gradual policy changes between different regimes on the inflation rate (Lamarche and Koustasy, 2012) or on the output gap (Kazanas et al., 2011) or other financial variables (Gnabo and Moccero, 2015). Considering that the observed nonlinearity in Fed's TR may not come from only one threshold variable, Ahmad (2016) proposes to estimate it with a Multiple Regime STAR (MRSTAR) model that simultaneously considers the output gap and the inflation rate as threshold variables. He finds different regimes delimited by three thresholds: one on the output gap at 0.0047 and two on the inflation rate at 1.45% and 3.10%. Although this flexible approach achieves some interesting results, it is needed a measure of uncertainty around thresholds and to allow possible interaction effects between the explanatory variables to provide a more complete description of the regimes in the TR.

On the other hand Kim et al. (2005), Assenmacher-Wesche (2006) and Sims and Zha (2006) apply Markov regime switching models, Dolado et al. (2005) test the statistical significance of the interaction term between inflation deviations and the output gap in the framework of two models: the Euler equation specification, on the one hand, and an ordered probit model designed to analyze adjustments in the

nominal interest rate, on the other. Klose (2011) builds a new approach to estimate nonlinear Taylor reaction functions when asymmetries depend on the state of the economy.

In a new strand of the empirical literature researchers have begun to apply semi-parametric methodologies, which enable the analyst to use more flexible specifications and to estimate nonlinearities using a more data-driven approach. Hayat and Mishra (2010) apply a generalized framework to explain the reaction of the U.S. Fed to substantially different levels of both inflation and output gaps. The authors find that the interaction between deviations in the inflation rate and the output gap is a significant term of the policy rule in the case of forward-looking inflation forecasts. De Sá and Portugal (2015) apply the sieve estimation technique, a fully non parametric approach, to analyze monetary policy in the U.S. and Brazil.

To date, empirical studies on nonlinearities in the TR show contradictory results. Clarida and Gertler (1997) test for the null hypothesis of symmetry and find evidence against it in the case of the Bundesbank's past policy actions. Dolado et al. (2004) obtain a nonlinear rule for U.S. monetary policy during the recession after 1983, but not before 1979. Surico (2007a) reaches the opposite conclusion. He finds that the Fed's interest rate reacted more strongly to output contractions than to output expansions of the same magnitude before 1979. Petersen et al. (2007) find a nonlinear TR for the monetary policy of the U.S. Fed during the 1983-2004 Great Moderation period. They also discover that the Fed's monetary actions during the 1970s are well characterized by a linear reaction function. Castro (2011) finds that the behavior of the U.S. Fed can be accurately described by a linear TR augmented by an index that reflects the financial conditions of the economy.

Hayat and Mishra (2010) find that the U.S. Fed's monetary policy reacted with significantly greater intensity to changes in inflation rates (and in inflation expectations) when these rates reached levels in the range of 6.5% to 8.5%. This effect occurs independently of the prevailing monetary policy regime, which is generally linked to who chairs the Fed. Sims and Zha (2006) estimate a multivariate model, on U.S. data since 1959, with regime switching both in the coefficients and the variances of the model. They conclude that coefficients change as a function of the monetary regime in force, but not enough to account for the rise and decline of the rate of inflation in the U.S. during 1970s and 1980s. So, in their opinion, U.S. monetary policy did not change much from the 1970s to the 1980s. Finally, Cukierman and

Muscatelli (2008) obtain evidence in favor of nonlinearities in the Taylor Rules of both the UK and U.S. except during the Volcker era (from September 1979 until June 1987).

In our paper, we apply the flexible MARS methodology to investigate the monetary policy of the U.S. Fed. We detect various thresholds as well as interaction effects (and their confidence intervals) for both the inflation and the output gaps and we show that MARS provides a more complete characterization of the nonlinear TR than the other empirical techniques previous researchers have employed. By doing so, we also confirm our theoretical conjecture about the existence of a much more general - though simple- social loss function than that used in the previous literature. So, this paper innovates both theoretically by identifying another source of nonlinearities in the TR and empirically by making use of a non parametric method with results that give support to our theoretical approach.

4.3 Central bank behavior with thresholds in preferences.

In this section, we present a new version of the dynamic model of Svensson (1999), in which the optimal central bank behavior is obtained from the minimisation of a generic loss function instead of a quadratic function. We allow this generic function to vary by regions, depending on the values of the inflation deviations on one hand and of the output gaps on the other. We demonstrate that the existence of these regions generates an optimal behavior for the central bank which is described by a Taylor Rule that possibly exhibits multiple thresholds and interaction effects between the inflation rate and the output gap[2].

4.3.1 The Model.

Let us define a generic central bank loss function, which is composed of two separable additive and continuous functions of the deviation of the inflation rate from target, ($\widetilde{\pi} = \pi - \pi^*$), and the output gap ($\widetilde{y} = y - y^*$), respectively:

$$L(\widetilde{\pi}_t, \widetilde{y}_t) = [\lambda g(\widetilde{\pi}_t) + h(\widetilde{y}_t)]$$

[2]We provide the solutions for the model in Chapter 3.

Parameter λ is the relative weight attached to the inflation function, which is assumed to be greater than one to reflect the central bank's particularly high level of concern with the losses caused by the inflation differential.

The central bank decides i_t by minimizing the intertemporal loss function with a time discount $\beta \in (0,1)$

$$E_t \sum_{s=0}^{\infty} \beta^s L(\widetilde{\pi}_{t+s}, \widetilde{y}_{t+s}) \tag{4.1}$$

taking into account the dynamic aggregate supply (4.2), the IS function (4.3), and the Fisher equation (4.4), which are formulated as follows, according to the monetary transmission mechanism adopted in Svensson (1997) :

$$\pi_{t+1} = \pi_t + \alpha \widetilde{y}_t + u_{\pi,t+1} \tag{4.2}$$

$$\widetilde{y}_{t+1} = \delta \widetilde{y}_t + \eta x_t - \xi r_t + u_{y,t+1} \tag{4.3}$$

$$r_t = i_t - E_t(\pi_{t+1}) \tag{4.4}$$

4.3.2 Solving the dynamic model.

The IS equation in (4.3) is a schedule in which the output gap exhibits gradual adjustment and depends on the real interest rate as well as on predetermined variables x_t that may capture other determinants of interest rate setting in open economies as in Ball (1999). The transmission mechanism of the monetary policy is treated both in Svensson (1999) and in Ball (1999): the monetary authority changes i_t and this in turn modifies r_t; equation (4.3) reflects the assumption that this would affect $\widetilde{y}_{t+1}$ but not $\widetilde{y}_t$, and then, $\widetilde{y}_{t+2}$ and $\widetilde{\pi}_{t+2}$ in (4.2). This timing convention is consistent with the extensive literature on the monetary policy transmission mechanism claiming that changes in monetary policy affect output in the short run and slowly alters the inflation rate later on, Christiano et al. (1999). This transmission mechanism allows us to simplify the minimisation problem as follows:

$$\min_{i_t} E_t \beta \left[\lambda g(\widetilde{\pi}_{t+1}) + h(\widetilde{y}_{t+1})\right] + E_t \beta^2 \left[\lambda g(\widetilde{\pi}_{t+2}) + h(\widetilde{y}_{t+2})\right] \tag{4.5}$$

$$s.t. \begin{cases} \pi_{t+1} = \pi_t + \alpha \widetilde{y}_t + u_{\pi,t+1} \\ \widetilde{y}_{t+1} = \delta \widetilde{y}_t + \eta x_t - \xi r_t + u_{y,t+1} \\ r_t = i_t - E_t(\pi_{t+1}) \end{cases}$$

The implicit solution for this problem, available in Chapter 3, is a generic TR such that

$$i_t = i(E_t\widetilde{\pi}_{t+1}, \widetilde{y}_t) \tag{4.6}$$

Taking derivatives with respect to the inflation rate deviation and the output gap helps us to understand how this Taylor Rule works under the generic loss function adopted here.

$$\frac{\partial i_t}{\partial \widetilde{\pi}_{t+1}} = 1 + \frac{\alpha\lambda E_{t-1}(\frac{\partial^2 g}{\partial \widetilde{\pi}^2_{t+1}})}{\delta\xi E_{t-1}(\frac{\partial^2 h}{\partial \widetilde{y}^2_{t+1}})}$$

$$\frac{\partial i_t}{\partial \widetilde{y}_t} = \alpha(1 + \frac{\alpha\lambda E_{t-1}(\frac{\partial^2 g}{\partial \widetilde{\pi}^2_{t+1}})}{\delta\xi E_{t-1}(\frac{\partial^2 h}{\partial \widetilde{y}^2_{t+1}})}) + \frac{\delta}{\xi} + \frac{E_{t-1}(\frac{\partial^2 h}{\partial \widetilde{y}^2_t})}{\delta\beta\xi E_{t-1}(\frac{\partial^2 h}{\partial \widetilde{y}^2_{t+1}})}$$

So, the first order Taylor expansion of this TR will be

$$i_t \simeq \left[1 + \frac{\alpha\lambda E_{t-1}(\frac{\partial^2 g}{\partial \widetilde{\pi}^2_{t+1}})}{\delta\xi E_{t-1}(\frac{\partial^2 h}{\partial \widetilde{y}^2_{t+1}})}\right] E_t\pi_{t+1} +$$
$$+ \left[\alpha(1 + \frac{\alpha\lambda E_{t-1}(\frac{\partial^2 g}{\partial \widetilde{\pi}^2_{t+1}})}{\delta\xi E_{t-1}(\frac{\partial^2 h}{\partial \widetilde{y}^2_{t+1}})}) + \frac{\delta}{\xi} + \frac{E_{t-1}(\frac{\partial^2 h}{\partial \widetilde{y}^2_t})}{\delta\beta\xi E_{t-1}(\frac{\partial^2 h}{\partial \widetilde{y}^2_{t+1}})}\right] \widetilde{y}_t \tag{4.7}$$

It is worth noting the importance of the second derivatives of the loss functions in determining the values of the TR coefficients: when a generic loss function is used, the constant coefficients of the traditional TR are replaced by possibly non-constant coefficients that depend crucially on the values of the second derivatives of the loss function.

In the particular case where the central bank expects no change in the second derivative of the loss function with respect to the output gap of the following period and the next one, $E_{t-1}(\frac{\partial^2 h}{\partial \widetilde{y}^2_t}) = E_{t-1}(\frac{\partial^2 h}{\partial \widetilde{y}^2_{t+1}})$ a simplified version of the Taylor Rule arises.

$$i_t \simeq \left[1 + \frac{\alpha\lambda E_{t-1}(\frac{\partial^2 g}{\partial \widetilde{\pi}^2_{t+1}})}{\delta\xi E_{t-1}(\frac{\partial^2 h}{\partial \widetilde{y}^2_{t+1}})}\right] E_t\widetilde{\pi}_{t+1} + \left[\alpha(1 + \frac{\alpha\lambda E_{t-1}(\frac{\partial^2 g}{\partial \widetilde{\pi}^2_{t+1}})}{\delta\xi E_{t-1}(\frac{\partial^2 h}{\partial \widetilde{y}^2_{t+1}})}) + \frac{(1+\delta^2\beta)}{\delta\beta\xi}\right] \widetilde{y}_t$$

We discuss these expressions and their implications in more detail in the following section.

4.3.3 Discussion: the Taylor Rule Coefficients.

We have stressed so far that, for our purpose, the most important feature of the central bank loss function is its second derivatives in the inflation deviation and output gap. Let us then specify general assumptions about this loss function and explore their consequences in how second derivatives affect the Taylor Rule coefficients.

We consider very general though simple characteristics for $g()$ and $h()$ functions that give rise to interesting non-linearities in the TR, which will take the form of multiple thresholds: Some of these are associated with the value of a single variable (for instance, the inflation deviation) and others take place for specific combinations of two individual variables that interact with each other (for instance, the interaction between the inflation deviation and the output gap at specific values of each).

We assume both functions are piecewise continuous. Therefore, the whole domain of $\widetilde{\pi}$ can be split into n disjoint regions $\{R_1^{\pi}, R_2^{\pi}, ..., R_n^{\pi}\}$ Similarly, the whole domain of $\widetilde{y}$ can be split into m disjoint regions $\{R_1^{y}, R_2^{y}, ..., R_m^{y}\}$ We assume that the functions will be strictly convex (i.e., their second derivatives are strictly positive). This implies that the marginal loss is higher the higher the deviation from targets, which is a common-sense assumption.

We will see how the TR changes as a result of the combination of four elements: (1) the characteristics of the second derivatives with respect to the output gap, on one hand; (2) with respect to the inflation deviation, on the other; (3) the region in which the economy stands at time t, $(\widetilde{y}_t)$; and (4) the region in which the monetary authority wants the economy to stand in the coming period $(\widetilde{y}_{t+1})$.

Let us consider some cases to observe how TR changes. In the case of the current output gap $\widetilde{y}_t$, as well as the short term output gap $\widetilde{y}_{t+1}$, lie on the same region R_i^{y}, so that $\dfrac{\partial^2 h}{\partial \widetilde{y}_t^2} = \dfrac{\partial^2 h}{\partial \widetilde{y}_{t+1}^2} = c_2$. For simplicity let us assume that this second derivative is constant, $\dfrac{\partial^2 h}{\partial \widetilde{y}_{t+1}^2} = c_2$, and similarly for $g()$, $\dfrac{\partial^2 g}{\partial \widetilde{\pi}_{t+1}^2} = c_1$.

$$i_t \simeq \left[1 + \frac{\alpha\lambda c_1}{\delta\xi c_2}\right] E_t\pi_{t+1} + \left[\alpha(1 + \frac{\alpha\lambda c_1}{\delta\xi c_2}) + \frac{(1+\delta^2\beta)}{\delta\beta\xi}\right] \widetilde{y}_t$$

So, in this particular case, we obtain a TR function with constant coefficients in this particular region. In another region these constant coefficients could vary with changes in $c1$ and/or $c2$.

In the case of the current output gap $\widetilde{y}_t$, as well as the short term output gap objective $\widetilde{y}_{t+1}$, lie on the same region R_i^y, so that $\dfrac{\partial^2 h}{\partial \widetilde{y}_t^2} = \dfrac{\partial^2 h}{\partial \widetilde{y}_{t+1}^2}$ and again assume as before$\dfrac{\partial^2 h}{\partial \widetilde{y}_{t+1}^2} = c_2$. By contrast, $g()$ is such that $\dfrac{\partial^2 g}{\partial \widetilde{\pi}_{t+1}^2}$ is not constant for the whole domain of $g()$. Then:

$$i_t \simeq \left[1 + \frac{\alpha\lambda \dfrac{\partial^2 g}{\partial \widetilde{\pi}_{t+1}^2}}{\delta\xi c_2}\right] E_t\pi_{t+1} + \left[\alpha(1 + \frac{\alpha\lambda \dfrac{\partial^2 g}{\partial \widetilde{\pi}_{t+1}^2}}{\delta\xi c_2}) + \frac{(1+\delta^2\beta)}{\delta\beta\xi}\right] \widetilde{y}_t \tag{4.8}$$

Consider two adjacent inflation regions such that:

$$\frac{\partial^2 g}{\partial \widetilde{\pi}_{t+1}^2} = \begin{cases} g_i > 0 \ \text{ if } \ \widetilde{\pi}_{t+1} \in R_i^\pi \\ g_{i+1} > g_i, \text{if } \ \widetilde{\pi}_{t+1} \in R_{i+1}^\pi \end{cases}$$

In these circumstances, the TR reflects the existence of different regions for the two components of the loss functions and exhibits threshold behavior:

$$i(\widetilde{\pi}_{t+1}, \widetilde{y}_t) \simeq \begin{cases} \left[1 + \dfrac{\alpha\lambda g_i}{\delta\xi c_2}\right] E_t\pi_{t+1} + \left[\alpha(1 + \dfrac{\alpha\lambda g_i}{\delta\xi c_2}) + \dfrac{(1+\delta^2\beta)}{\delta\beta\xi}\right] \widetilde{y}_t \ \ if \ \ \widetilde{\pi}_{t+1} \in R_i^\pi \\ \left[1 + \dfrac{\alpha\lambda g_{i+1}}{\delta\xi c_2}\right] E_t\pi_{t+1} + \left[\alpha(1 + \dfrac{\alpha\lambda g_{i+1}}{\delta\xi c_2}) + \dfrac{(1+\delta^2\beta)}{\delta\beta\xi}\right] \widetilde{y}_t \ \ if \ \ \widetilde{\pi}_{t+1} \in R_{i+1}^\pi \end{cases}$$

Consequently, this TR allows us to explain how different reactions by the central bank depend upon the region characterized by the value of the second derivatives of functions $g()$ and $h()$. Moreover, it could explain different and more intensive central bank reactions when some thresholds have been exceeded. A clear conclusion arises: If the component of the central bank loss function concerning the output gap $g()$ and the inflation deviation $h()$ are piecewise continuous and strictly convex functions, then the TR will be nonlinear and will exhibit possibly complex threshold behavior. Therefore, since there is no reason for thinking that the central bank has smooth and homogeneous preferences about the whole domain of the output gap and inflation deviations, for reliable empirical estimation of the TR, it is necessary to use sufficiently flexible nonlinear methods, at least in the form of non-constant parameters with possible multiple thresholds and even interaction effects.

4.4 Methodology and estimation procedure.

In order to estimate TR that is possibly nonlinear with multiple and interacting thresholds, we avoid imposing a predefined parametric model. Our strategy consists of using a data-based methodology to select the model, as well as to estimate it. Multiple adaptive regression splines (MARS) is a nonparametric procedure that allows us to endogenously select the best model and estimate it, as well as to endogenously detect and estimate thresholds if there are any. To date, compared to the Threshold Autoregressive (TAR) models initially introduced by Tong and Lim (1980),Tong (1983), and Tong (1990), the MARS methodology has not received much attention in economics in spite of its great flexibility. Tong's pioneering contribution gave rise to a very extensive line of research that explores possible thresholds in economics; Hansen (2011) provides an excellent review of the prolific line of research derived from Tong's work. The basic TAR model assumes that the autoregressive structure of a variable varies according to the value reached by the variable itself in the recent past. A related line of research in recent decades examines using a threshold specification in the context of a traditional regression model. In these studies, two distinct regression models are defined and simultaneously estimated for two disjoint regions defined in a threshold variable, which needs not be the explained variable. The study by Shen et al. (1995) is probably the first instance of the use of this type of model to fit the reaction function of the central bank. In this case, the threshold parameter is estimated, whereas the threshold variable and its delay parameter are exogenously determined; they use the current value of the inflation rate as threshold variable. Baum and Karasulu (1997) go a step further and combine cointegration and threshold models using the technique of threshold cointegration developed by Balke and Fomby (1997) to model the Federal Reserve discount policy.

However, even the more sophisticated threshold regression models consider the existence of only one threshold variable and only one set of disjoint threshold-defined regions. These are serious limitations for our purpose since we demonstrate that the TR could exhibit multiple thresholds associated with various threshold variables and even interactions between them. Lewis and Stevens (1991) present a general criticism of this double limitation of traditional threshold models and propose the MARS methodology from Friedman (1991, 1993) to endogenously detect and estimate possible thresholds for each independent variable of the model under study, together with possible interactions between them. Consequently, in contrast with

the traditional TAR and threshold regression models, it is unnecessary to determine which variable generates a threshold behavior.

MARS is a nonparametric estimation procedure that selects and fits the model endogenously detecting and quantifying thresholds and complex nonlinearities if they exist. Given a set of explanatory variables, MARS fits a model as an expansion in products of truncated linear spline functions (hinge functions), which are selected through recursive partitioning strategy with forward and backward passes. By using products of hinge functions, the procedure accommodates both nonlinearities and interactions among the explanatory variables as a generalization of Recursive Partitioning (RP) (Friedman, 1977). MARS for time series (TSMARS) initiated by Lewis and Stevens (1991) has been extensively explored by Keogh (2010). While SETAR and the self-exciting open-loop threshold autoregressive (TARSO) models of Tong (1990) identify piecewise linear functions over disjoint subregions, with discontinuities at the boundaries of the regions, TSMARS methodology obtains nonlinear threshold models continuous in the domain of the predictor variables and with possible interactions among lagged predictor variables. Therefore TSMARS constitutes a further generalization of Tong's models (Chung, 2012).

MARS seeks to model the dependence of variable y_t on a set of explanatory variables $x_t^1, ..., x_t^p$ (where some of these variables may be lagged values of other, i.e. x_t^pmight be x_{t-1}^1 for instance). The true unknown model

$$y_t = f(x_t^1, ..., x_t^p) + \varepsilon_t$$

over some domain $D \epsilon \mathbf{R}^p$ containing the data and the error term ε_t is assumed to be independently distributed with $E(\varepsilon_t) = 0$ and variance $E(\varepsilon_t^2) = \sigma^2$. The function $f(x)$ is the true relationship between outcome time-series (y_t) and a vector of p explanatory variables $x_t = (x_t^1 \ldots . x_t^p)$ that we want to estimate from the data.

MARS procedure approximates this function as:

$$y_t = \beta_0 + \sum_{m=1}^{M} \beta_m b_m (x_t) + \varepsilon_t \tag{4.9}$$

where;

β_0 is a constant

β_m is the coefficient for the m^{th} basis function, $m = 1, ..., M$

$b_m(x_t)$ is the m^{th} basis function, $m = 1, ..., M$

ε_t is an independently distributed error term with $E(\varepsilon_t) = 0$ and $E(\varepsilon_t^2) = \sigma^2$

The basis functions are products of up to a maximum interaction order mi truncated linear splines or hinge functions (we usually restrict $mi = 2$), describing the relationship between one or more explanatory variables and the outcome in terms of segments of stable association separated by knots or threshold values. These interacting hinge functions allow us to identify possible interactions between variables. Namely, for $mi = 2$ the m^{th} basis function takes one of the following two forms:

No interaction: $b_m(x_t) = h_m\left(x_t^k, \tau_{k,m}\right)$ for some $k = 1, \ldots, p$

With interaction: $b_m(x_t) = h_m\left(x_t^k, \tau_{k,m}\right) \cdot h_m\left(x_t^j, \tau_{j,m}\right)$

for some $k,\ j = 1, \ldots, p,\ k \neq j$

where $\tau_{k,m}$ is the threshold value of x_t^k in the m^{th} basis function and where $h\left(x_t^k, \tau_{k,m}\right)$ is a hinge function (or truncated linear spline) that takes the following form depending on whether the basis function takes effect above or below the threshold $\tau_{k,m}$(See Figure 4.1)

a) above the threshold: $h_m\left(x_t^k, \tau_{k,m}\right) = max(x_t^k - \tau_{k,m},\ 0)$

b) below the threshold: $h_m\left(x_t^k, \tau_{k,m}\right) = max(\tau_{km} - x_t^k,\ 0)$

Figure 4.1: Graph of the two truncated linear spline or hinge functions.

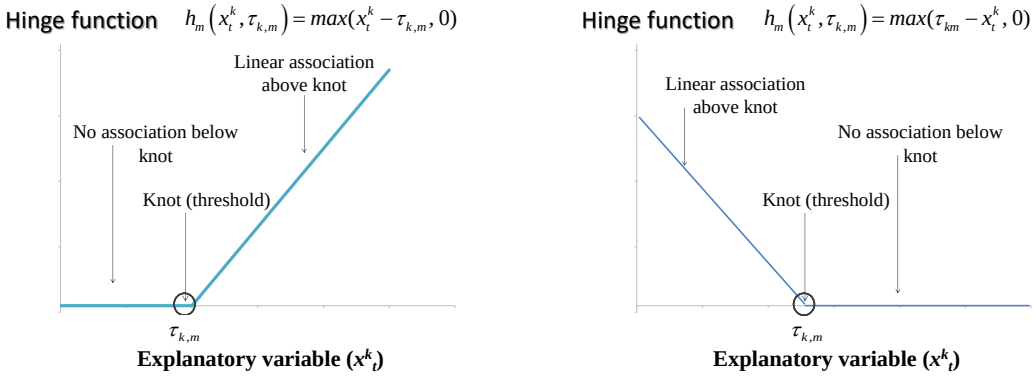

If no knot (threshold) is detected, then a simple linear association between explanatory and outcome variables can be specified as a single function applied across the total range of values of the explanatory variable.

In the algorithm, once we define $x_t = (x_t^1 \ldots . x_t^p)$ with all potentially significant explanatory variables, including the associated lags, the model identification and estimation proceed by an automated and iterative process. The description that follows is mainly based on Friedman (1991, 1993); Chung (2012).

Forward pass: In general terms, starting with the simplest model containing only a constant basis function, MARS iteratively generates a matrix of basis functions in a forward stepwise manner. Candidate basis functions are added according to their ability to improve model fit by minimizing the residual sum of squares (RSS) until the model reaches a predefined limit of complexity. The candidate basis functions are identified by a nested exhaustive search looping over the existing set of basis functions, and all other possible explanatory variables (or interactions) and knot (threshold) positions.

This forward pass procedure provides a model that overfits the data. Therefore, a pruning process is required to remove the subregions whose product basis functions do not sufficiently contribute to the accuracy of the model.

Backward (pruning) pass: During the backward pass, MARS iteratively prunes the model obtained from the forward pass. It removes basis functions to reduce the value of a modified form of the generalized cross validation ($MGCV$) criterion that penalizes model complexity, based on Craven and Wahba (1979) This pruning pass runs until MGCV cannot be further reduced. This criterion is defined as

$$\text{MGCV} = \frac{\frac{1}{T}\sum_{t=1}^{T}(y_t - \hat{f_M}(x_t))^2}{[1 - C(M)/T]^2}$$

where T is the number of observations; $C(M)$ is the model complexity penalty function which is defined as $C(M) = (M+1) + dM$, where M is the number of basis functions retained in the model and M+1 the number of parameters in $\hat{f_M}(x_t))$ and d represents the degree of additional contribution brought by a basis function to the model complexity, Friedman (1991) suggests a value for d between 2 and 4; usually $d = 3$.

Therefore, this MGCV criterion accounts for the inherent improvement in explained variance associated with increasing numbers of basis-functions, and its calculation allows estimates of the relative importance of each basis function so the model selection process converges on a set of basis functions that most efficiently explain variation in the dependent variable.

For easier understanding, we provide Figure 7.3 that schematize OLS procedure in the left column and MARS procedure in the right one. While OLS directly proceeds to estimate model parameters using the data, MARS uses them in each iteration of forward and backward passes to select and estimate the final model. During these passes, each variable x may be split into two variables $z_1 = max(x - \tau, 0)$ and $z_2 = max(\tau - x, 0)$; therefore, at the end, MARS estimates a linear model with a matrix of split explanatory variables corresponding to each basis function detected for the final model. Consequently, OLS can be understood as a particular case of MARS where forward and pruning passes do not detect any threshold for any of the explanatory variables.

Figure 4.2: Comparison between the Ordinary Least Squares (OLS) estimation and Multiple Adaptive Regression Spline (MARS) procedure.

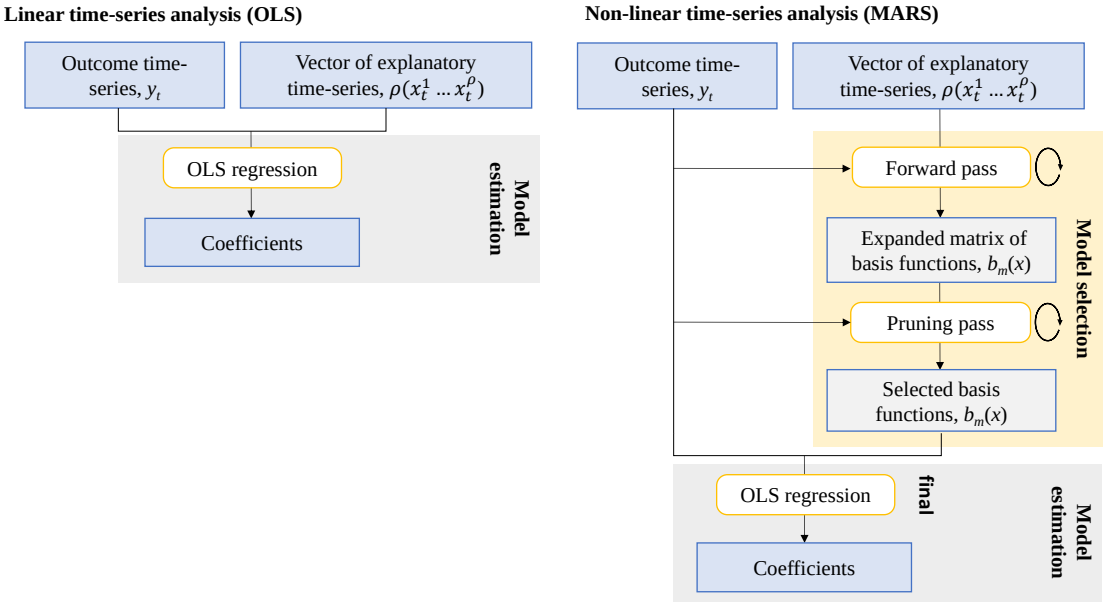

To exploit MARS capabilities for estimating TR for US Fed, we propose the following protocol.

Step 1. Set the pool of explanatory variables and their lags.

To estimate TR, we use monthly data to have time series as large as possible and because it is consistent with the frequency of the monetary authority meetings. We calculate inflation rate, expressed in annual rates, from the seasonally adjusted monthly Consumer Prices Index accessible in statistics office of the monetary authority. To compute the monthly output gap, we apply the Hodrick-Prescott filter with a smoothing parameter equal to 14400 (see Hodrick and Prescott (1997)) to the logarithm of the Industrial Production Index, that is usually available in the Statistics Office databases of the economic region. Using lagged values for the explanatory variables tackles the endogeneity problem and is also consistent with the idea that the monetary authority decisions on nominal interest rates require information that is time-consuming to collect. In addition, when data covers periods defined by different chairmanships of the monetary authority or some abrupt changes in the economy as a Crisis or an enlargement (as in the European Union) we include dummies variables in the model to capture possible effects.

Step 2. Model estimation with MARS.

To estimate TR we employ the partial adjustment specification from Judd and Rudebusch (1998) that incorporates interest rate smoothing. Let us assume i_t^* is the interest rate recommended by the monetary authority such that

$$i_t^* = r^* + \pi_t + \alpha(\pi_t - \pi^*) + \beta_1 \widetilde{y}_t + \beta_2 \widetilde{y}_{t-1}$$

and we use the partial adjustment process

$$\Delta i_t = \gamma(i_t^* - i_{t-1}) + \rho \Delta i_{t-1} \tag{4.10}$$

where γ is the gradual adjustment coefficient. Therefore, we firstly construct the MARS specification with the basis functions and possible interactions:

$$\begin{aligned} i_t^* = (\beta_0 + \delta d_t) + \sum_{m_\pi=1}^{M_\pi} (\beta_{m_\pi} + \delta_{m_\pi} d_t) b[\pi_{t-1}, \tau_{m_\pi}] + \\ + \sum_{m_y=1}^{M_y} (\beta_{m_y} + \delta_{m_y} d_t) b[\widetilde{y}_{t-1}, \tau_{m_y}] + \\ + \sum_{m_{y\pi}=1}^{M_{y\pi}} (\beta_{m_{y\pi}} + \delta_{m_{y\pi}} d_t) b[\pi_{t-1}, \tau_{\pi,m_{y\pi}}] b[\widetilde{y}_{t-1}, \tau_{y,m_{y\pi}}] + \rho \Delta i_{t-1} + \varepsilon_t \end{aligned} \tag{4.11}$$

d_t : dummy variable

The model incorporates dummy variables to distinguish between the three US Fed

chairmanship periods if relevant.

After estimating 4.11, we estimate 4.10with an ARIMA transfer function taking into account thresholds detected in i_t^*.

Step 3. Diagnostic checks.

For the adequacy of model fit, we provide Box Pierce test (Box and Pierce, 1970)to check the absence of significant residual autoregression and the Akaike Information Criterion (Akaike, 1987)(AIC) or its corrected bias version for small samples $AICc$ (Hurvich and Tsai, 1989), Schwarz criterion also known as Bayesian Information criterion (BIC) (Schwarz et al., 1978) and the Log-likelihood criterion for comparison purposes between models. (See Table 4.1)

Step 4. Confidence intervals for thresholds values.

In the absence of an existing method for deriving measures of uncertainty around thresholds derived from non-parametric MARS models, we adapt to MARS model a procedure inspired by Hansen (2000) and improved by Donayre et al. (2018) to compute confidence intervals for thresholds parameters that constitutes an innovation by itself. We adapted this procedure for MARS estimations with more than one explanatory variable containing thresholds, and one or more thresholds per variable, by using the partial residuals – i.e. the estimated part of the outcome not explained by other explanatory variables and their thresholds. To simplify the explanation, let us suppose that in modeling y, we have two explanatory variables, x_1 and x_2, and that a threshold has been detected by MARS for each one, at τ_{x_1} and τ_{x_2} respectively. To obtain the confidence interval associated with τ_{x_1}, we obtain the "partial residuals relative to x_1" , say $y(x_1)$, which is the part of y not explained byx_2 (and its threshold). We obtain it by subtracting from y the part of the full model related exclusively with x_2. Once $y(x_1)$ is obtained, we can apply on the data of $y(x_1)$ and x_1 the procedure of Hansen (2000) improved by Donayre et al. (2018). In that way we obtain a confidence interval for $\tau(x_1)$ conditional on the estimated values of the parameters (slopes and thresholds) related to x_2. We then repeat the same procedure interchanging the roles of x_1 and x_2, and we now obtain the confidence intervals for $\tau(x_2)$ conditional on the estimated values of the parameters related tox_1. We also use the correction procedure for heteroskedasticity proposed by Hansen (2000).

4.5 Results.

We summarize linear Least Square (OLS) and MARS estimations in a table; the column for the detected thresholds also provides significant coefficients for second degree of interaction between variables such as the inflation and output gap and dummies for different periods of the Fed. For instance, interaction between the inflation deviation and the output gap gives us the estimated coefficient and the threshold values related to each variable involved in it. In the case of an interaction that results from an explanatory variable and a dummy variable, the coefficient reflects the contribution of that variable in the fulfillment of the TR, conditioned on the period defined by the dummy variable. In other words, given the definition of the dummy variables, the coefficient indicates the amount by which the contribution of the explanatory variable changes with respect to the pre-Volcker period. At the bottom of the table we provide the AIC, $AICc$, and BIC criteria, as well as the value of the log-likelihood function and a measure of the relative advantage of the MARS procedure over OLS for evaluating the improvements in goodness of fit.

Additionally, for each MARS estimation we present three-dimensional graphs that reflect the contributions of the variables to the interest rate evolution, which allow us to understand the behavior of the TR over different regions of the relevant variables. We also present three-dimensional graphs for OLS estimation in order to compare it with the MARS methodology. Additionally, we offer the autocorrelation functions of the residuals in each case.

Table 4.1 is structured in two sections: the upper one contains the estimations for the coefficients of the variables of the model. There are two columns, one for the thresholds and the second for the coefficients respectively under MARS estimation and one column for OLS coefficients. Each threshold is presented with its 95% confidence interval (CI). The sign "<" or ">" before the value of the detected threshold indicates how the estimated coefficient of the same row is related to the threshold. The interactions between two variables with a significant coefficient, selected by the MARS procedure, appear in a row with the name of both variables together with the threshold associated with each variable, except for cases where a dummy variable is involved. The second section displays different measures of fit for MARS and linear estimations; the middle column allows a comparison between both approaches since it contains the improvement yielded by fitting with MARS instead of OLS.

The MARS estimation of the model 4.8 reveals that the most important detected

threshold for inflation rate is located at 4.31% $95\%CI(3.86\%, 4.89\%)$ for the main effect and it is also located at 4.31% but with a wider $95\%CI(2.77\%, 6.56\%)$ for the interaction effect with output gap. Clearly, the intensity of the Fed's reaction above this threshold increases and as our flexible and comprehensive theoretical model permits, we find an interaction effect between the inflation rate and the output gap. The threshold for the output gap in this interaction effect is at 0.012 $95\%CI(-0.0213, 0.0196)$.

Significant coefficients are found for Volcker and Bernanke dummy variables. According to this, following the model, the different governance periods in the Fed are detected as affecting changes in the interest rate. While Bernanke affects lowering in parallel the contribution of inflation and output gap to the change in interest rate, Volcker-Greenspan period shows a systematically greater sensitivity of the interest rate to inflation then in other periods. This stronger reaction of the monetary authority to inflation rate starts from a lower threshold than in other periods, at 2.87% $95\%CI(2.74\%, 3.17\%)$ and also to output gap with a threshold at zero -0.001 $95\%CI(-0.0062, 0.0045)$

According to the substantial improvements in the measures of fit, AIC, $AICc$, BIC and Log-Likelihood, the MARS estimation achieves a better fit than linear estimation.

Table 4.1: Main results of the each country estimation.

Dependent variable $\triangle interest_t$	***MARS***		***Linear***
variables	**thresholds**	**coefficients**	**coefficients**
$intercept$		0.0067 *	0.0012 *
$inflation_{t-1}$	<0.0431 (0.0386, 0.0489) >0.0431 (0.0386, 0.0489) > 0.0761 (0.0714, 0.0925)	0.0614 0.1145 * -0.2722 *	0.0278 *
$inflation_{t-1}$ x $output_{t-1}$	>0.0431 (0.0277, 0.0656) > 0.0012 (-0.0213, 0.0196)	3.4363 *	
$inflation_{t-1}$ x $Volcker_t$	> 0.0287 (0.0274, 0.0317)	0.0991 *	
$output_{t-1}$ x $Volcker_t$	< -0.001 (-0.0062, 0.0045) > -0.001 (-0.0062, 0.0045)	0.1006 · 0.1878 *	
$Bernanke_t$		-0.0035 *	-0.0015 *
$interest_{t-1}$		-0.1483 *	-0.0392 *
$\triangle interest_{t-1}$		0.4876 *	0.3801 *
ACF residual Box Pierce Test p-value	0.1732		0.1601
Improvements of measure of fit MARS vs Linear			
AIC	-4141.74	16.38	-4125.36
AICc	-4141.39	16.25	-4125.15
BIC	-4103.34	7.84	-4095.49
LogLik	2079.87	10.19	2069.68

Figure 4.3 shows the three dimensional contribution of the independent variables by pairs to the change of the interest rate for both in MARS and linear estimation[3]. We also provide the autocorrelation function of the residuals to demonstrate they are compatible with white noise.

[3]In these graphs, contribution of the inflation rate to the interest rate in the MARS estimation shows planes with close to zero slope for a very high level of inflation gaps, data related to both oil crisis.

Figure 4.3: Graphs of the model 4.11.

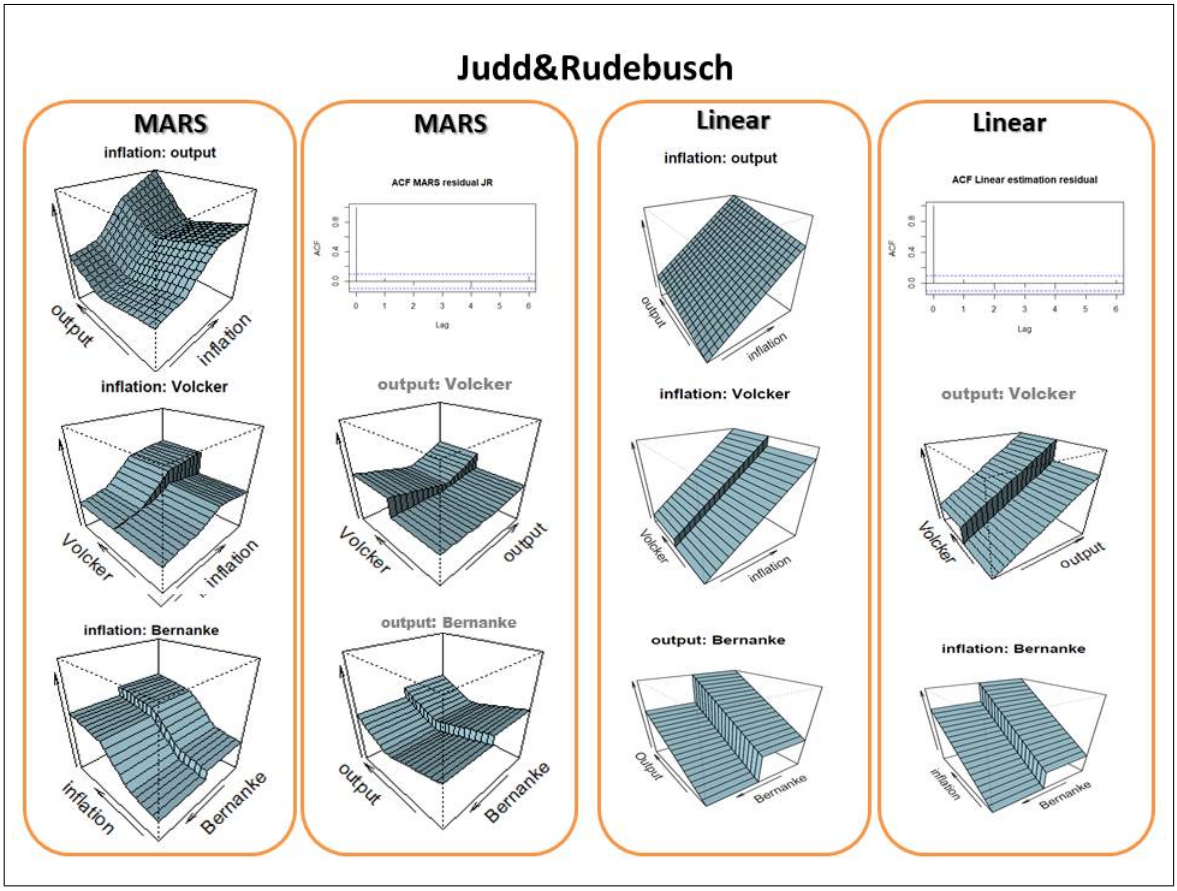

The three-dimensional contribution graphs clearly illustrate that flexibility of MARS provides a better adjustment to data; they also illustrate that the Fed behavior is fully compatible with the assumption of variable curvature of the social loss function over regions that we stated in our theoretical model and that we expected in the empirical application. In addition, it is easy to visualize the combined effect between inflation and output gap.

4.6 Conclusions.

In this paper we focus on the nonlinearities in Taylor Rules that we derived theoretically from the characteristics of the preferences of the central banks. Unlike the traditional approach, which imposes specific functional forms, we propose using

central bank's generic piecewise-defined social preferences. We show that the social preferences of the central bank are a source of multiple thresholds and interaction effects in the resulting TR. Also, we propose to estimate this nonlinear TR with Multiple Adaptive Regression Splines, a flexible nonparametric estimation procedure that enables us to endogenously detect various forms and combinations of thresholds in the monetary policy responses. To the best of our knowledge, our paper is the first application of this methodology to the estimation of TRs. We estimate the TR for the United States from 1970 to 2014 with monthly data. For the estimated model, the measures of fit AIC,$AICc$,BIC, and Log-Likelihood criteria indicate that MARS fits better data than linear estimation. Moreover, we detect thresholds for the inflation rate at 4.31% $95\%CI(3.86\%, 4.89\%)$ and for the output gap at 0.0012 $95\%CI(-0.0213, 0.0196)$. As the theoretical framework predicts, we also find an interaction between inflation and output gap. We also estimate a stronger sensitivity of the Fed's reaction in the Volcker-Greenspan period to inflation rate even at a lower threshold than in the other period which is consistent with the literature; in addition, Bernanke period is also characterized by a less intensive reaction to inflation and output gap.

Our empirical methodology also allows us to assess in a clearer and more rigorous way the behavior of the Fed in each governance period compared with previous analysis. All in all, the application of the MARS methodology, which is particularly well suited to detecting and quantifying thresholds in the TR, not only gives support to our theoretical conjecture but also provides a more complete characterization of the nonlinear TR than alternative empirical techniques applied so far in the literature.

4.7 Appendix.

4.7.1 Time Series with detected thresholds.

In order to illustrate the estimation of 5.2, we provide a graph of interest rate time series in which periods where inflation values above the detected threshold, 4.31%, are clearly identified.

Figure 4.4: Federal fund rate and periods where inflation was above the detected threshold, 0.043.

4.7.2 From MARS to contributions of the variables.

In a linear estimation, the provided coefficients directly correspond to the contributions of each explanatory variable to the dependent variable. However, in MARS, we have a group of basis functions setting up different regions and therefore we should combine coefficients of each basis function to obtain the contribution of an explanatory variable to the dependent variable on each region.

If we are interested in quantifying the contribution of a given variable at a specific point of the variables space, we must first identify the region in which that point is located; then, we need to identify the basis functions that are active in that region for the relevant variables in order to compute the corresponding contribution. The

contribution will be a composition of the $\beta's$ of those relevant variables. For a better understanding, let us consider an example presented in Table 4.1. For example, let us consider to evaluate the estimated contribution of the inflation rate to the change of the interest rate during the previous Volcker period at the point where the inflation rate is 5% and the output gap is 0.05 [point $(\pi = 0.05, \tilde{y} = 0.05, d_V = 0, d_B = 0)$]. We first identify all the coefficients that are relevant in the region of this point to compute the contribution of the inflation rateβ: 0.0067 0.1145, 3.4363

From Table 4.1, we can construct the estimated equation which is active in the region at the point:

$\triangle i_t = 0.0067 + 0.1145max[(\pi_{t-1} - 0.0431), 0] + 3.4363max[(\pi_{t-1} - 0.0431)(\widetilde{y}_{t-1} - 0.0012), 0] - 0.1483i_{t-1} + 0.4876\triangle i_{t-1}$

Once the relevant equation is built, we can obtain the contribution of each explanatory variable in that region.

$\triangle i_t = 0.0067 + 0.1145\pi_{t-1} - 0.004935 + 3.4363\pi_{t-1}\widetilde{y}_{t-1} - 0.0385\pi_{t-1} - 0.1481\widetilde{y}_{t-1} - 0.00166 - 0.1483i_{t-1} + 0.4876\triangle i_{t-1}$

$$\triangle i_t = 0.000105 + 0.076\pi_{t-1} + 3.4363\pi_{t-1}\widetilde{y}_{t-1} - 0.1481\widetilde{y}_{t-1} - 0.1483i_{t-1} + 0.4876\triangle i_{t-1}$$

For the $\widetilde{y}_{t-1} = 0.05$ the slope of the contribution of the inflation rate will be 0.2478 and for the $\pi_{t-1} = 0.05$ the slope of the contribution of the output gap will be 0.0275

If we consider the same point but in the Volcker period we will obtain

$\triangle i_t = 0.0067 + 0.1145max[(\pi_{t-1} - 0.0431), 0] + 3.4363max[(\pi_{t-1} - 0.0431)(\widetilde{y}_{t-1} - 0.0012), 0] + 0.1878 * max[\widetilde{y}_{t-1} - (-0.001), 0] - 0.1483i_{t-1} + 0.4876\triangle i_{t-1}$

$$\begin{aligned}\triangle i_t = {} & 0.000105 + 0.076\pi_{t-1} + 3.4363\pi_{t-1}\widetilde{y}_{t-1} - 0.1481\widetilde{y}_{t-1} + 0.1878\widetilde{y}_{t-1} + \\ & + 0.1878 * 0.001 - 0.1483i_{t-1} + 0.4876\triangle i_{t-1}\end{aligned}$$

$$\triangle i_t = 0.0002928 + 0.076\pi_{t-1} + 3.4363\pi_{t-1}\widetilde{y}_{t-1} + 0.0397\widetilde{y}_{t-1} - 0.1483i_{t-1} + 0.4876\triangle i_{t-1}$$

5 New insights into the nonlinearity of the ECB Taylor Rule.

We apply a nonparametric procedure, Multiple Adaptive Regression Splines (MARS), to endogenously select the best multiple threshold model for the European Central Bank (ECB) Taylor Rule (TR). MARS offers the advantage of not excluding simpler models if they better fit the data. On monthly data from 1/2000 to 9/2016, the TR exhibits thresholds for both the output gap and inflation and uncover interesting information about the different sensitivity of the ECB to each variable. We conclude that the ECB cares more about the economic activity than officially declared and reacts to inflation deviations only if they sufficiently exceed the official 2% target. We also detect an overall shift in the monetary policy during the 2008 financial crisis that pushed the system towards the Zero Lower Bound (ZLB). We reach a more complete description of the ECB TR than published so far.

5.1 Introduction

We estimate a non linear TR for the ECB within a very flexible empirical framework. We use the nonparametric MARS methodology (Friedman, 1991; Lewis and Stevens, 1991; Keogh, 2010) which endogenously detects whether the ECB decisions concerning changes in the interest rate varies with the magnitude and the sign of the output gap and inflation, and whether it is sensitive to certain combinations of both magnitudes. This method can estimate models with multiple and endogenously detected thresholds and transition variables with possible interactions. Therefore, it offers empirical results of the ECB Taylor rule much more general than those published to date. Most nonlinear ECB reaction functions estimated so far assume that the Taylor rule is asymmetric around exogenously fixed targets for the output gap (zero value) and for the inflation rate (2% value), assuming that these targets

actually are the relevant ones for the ECB. See Surico (2007b), Aguiar and Martins (2008), Ikeda (2010) and Klose (2011). Kulikauskas (2014) on the other hand, inspired in Gerdesmeier and Roffia (2004) and Gerlach and Schnabel (2000), uses nonlinear threshold regressions with only one transition variable at a time. Finally, Gerlach and Lewis (2014a,b) address the existence of a structural break around the 2008 crisis within an otherwise linear Taylor rule. Since MARS does not preclude the existence of structural changes, all the aforementioned models are in fact particular cases of the models that MARS is able to reveal, and are thus not excluded from our analysis.

Using monthly data for the period 1/2000 to 9/2016 we obtain a data-based TR that exhibits thresholds for both the output gap and the inflation rate and obtain interesting information about the different sensitivity of the ECB to each variable[1]. We also detect an overall shift in the monetary policy as a result of the 2008 financial crisis that pushed the system into the vecinity of the Zero Lower Bound (ZLB). We therefore reach a more complex and complete description of the ECB reaction function than published so far.

5.2 The model and estimations

The decision of estimating the TR with MARS stems from theoretical results obtained by Nebot et al. (2016). They assume a generic CB loss function with the only characteristic that the amount of the loss may vary by region per inflation deviations and output gaps, reflecting that the ECB is more sensitive to inflation and/or output gaps in some intervals of these variables than in others. They show that this loss function can generate a TR with multiple thresholds for inflation and output gaps and even interaction effects. Their loss function is composed of two separable additive piecewise-continuous functions of the deviation of inflation from target ($\widetilde{\pi} = \pi - \pi^*$) and the output gap ($\widetilde{y} = y - y^*$), respectively:

$$L(\widetilde{\pi}_t, \widetilde{y}_t) = [g(\widetilde{\pi}_t) + h(\widetilde{y}_t)]$$

[1]We use data of monthly frequency because MARS needs an important amount of data to select and estimate the best model. Our sample period starts in 1/2000 for the following reasons: a) Eurostat Industrial Production Index are estimated values for 1999 in contrast with the normal values from 2000 onwards; b) computation of the inflation rates of 1999 needs the monthly HCPI of 1998, a year in which the euro was not operating yet. Even so, we also estimated the model with data from 1/1999 to 9/2016, and obtained no significant differences neither between coefficients nor between thresholds.

From that generic form they demonstrate that the constant coefficients of the traditional TR are replaced by possibly non-constant coefficients that depend crucially on the values of the second derivatives of the loss function and can vary by region:

$$i_t^* \simeq \phi_\pi \left[E_{t-1}(\frac{\partial^2 g}{\partial \widetilde{\pi}_{t+1}^2}), E_{t-1}(\frac{\partial^2 h}{\partial \widetilde{y}_{t+1}^2}) \right] E_t \widetilde{\pi}_{t+1} + \phi_y \left[E_{t-1}(\frac{\partial^2 g}{\partial \widetilde{\pi}_{t+1}^2}), E_{t-1}(\frac{\partial^2 h}{\partial \widetilde{y}_t^2}), E_{t-1}(\frac{\partial^2 h}{\partial \widetilde{y}_{t+1}^2}) \right] \widetilde{y}_t \qquad (5.1)$$

The estimation of the TR should then avoid imposing a predefined nonlinear parametric model. The non parametric MARS procedure allows for endogenously detecting possible thresholds for each independent variable, as well as interactions, without excluding simpler (or even linear) specifications if they fit better.

In spite of its great flexibility, MARS has not received as much attention in economics as the TAR models introduced by Tong and Lim (1980) and Tong (1983). However, estimations of the TR with TAR or Threshold Regression models impose one specific threshold variable and assume a unique threshold (Shen et al. (1995) and Baum and Karasulu (1997)). Furthermore, since the TR can exhibit multiple thresholds associated with various variables this is too limiting. For such situations, Lewis and Stevens (1991) propose employing the greater generality of MARS, which avoids presetting which variable generates a threshold behaviour.

Thus, we use MARS to estimate the TR on monthly eurozone data covering three ECB chairmanship periods (Duisenberg, 1/2000 to 10/2003; Trichet, 11/2003 to 10/2011; Draghi, 11/2011 to 9/2016). Per the literature we use the Euro Overnight Index Average (EONIA) to derive the nominal interest. rate[2]. We compute the inflation rate, expressed in annual rates, from the seasonally-adjusted monthly Harmonized Consumer Prices Index. We compute the monthly output gap by applying the Hodrick-Prescott filter to Industrial Production Index in logarithm (see Hodrick and Prescott (1997)). The model specification is based on two ideas.

First, we introduce thresholds in the basic TR specification (Taylor (1999)), including dummy variables -dated in October 2008, after the Lehman-Brothers bankruptcy[3] to account for a general structural change that might have occurred in the

[2]Working with EONIA interest rates presents the advantage of not being constrained by the Zero Lower Bound region as would be the case with official policy rates; this avoids the econometric problems associated with censored data.

[3]We have also estimated different models moving the Crisis dummy from 6 months before to 6 months after the proposed date, with no changes either in the detected thresholds and no significant changes in the estimated coefficients.

model with the 2008 financial crisis[4,5].

The MARS specification for i_t^* in (5.1), with possible interaction between explanatory variables, is:

$$
\begin{aligned}
i_t^* = (\beta_0 + \delta_1 d_{Ct}) + \sum_{m_\pi=1}^{M_\pi} (\beta_{m_\pi} + \delta_{1,m_\pi} d_{Ct}) B[\pi_{t-1}, \tau_{m_\pi}] + \\
+ \sum_{m_y=1}^{M_y} (\beta_{m_y} + \delta_{1,m_y} d_{Ct}) B[\widetilde{y}_{t-1}, \tau_{m_y}] + \\
+ \sum_{m_{y\pi}=1}^{M_{y\pi}} (\beta_{m_{y\pi}} + \delta_{1,m_{y\pi}} d_{Ct}) B[\pi_{t-1}, \tau_{\pi,m_{y\pi}}] B[\widetilde{y}_{t-1}, \tau_{y,m_{y\pi}}] + \varepsilon_t \\
d_{Ct}: \text{ crisis dummy}
\end{aligned}
\tag{5.2}
$$

Given a variable x_t and an endogenously detected threshold τ associated to it, each basis function $B[x_t, \tau]$ can be $B[x_t, \tau] = max[x_t - \tau, 0]$ or $B[x_t, t] = max[\tau - x_t, 0]$, to allow for lower and/or upper thresholds. When a threshold in a regressor is detected, MARS splits it into two separable variables (see for instance Keogh (2010)): one with values under the threshold and another with values above it. Hence, from a given matrix of regressors and a set of thresholds, we obtain an enhanced matrix of split regressors. Using lagged values for the explanatory variables tackles the endogeneity problem and is also consistent with the idea that the ECB decisions on nominal interest rates require information that is time-consuming to collect.

Second, we adopt the partial adjustment process of the interest rate considered in Judd and Rudebusch (1998)

$$
\Delta i_t = \rho(i_t^* - i_{t-1}) + (1 - \rho)\Delta i_{t-1} \tag{5.3}
$$

where i* comes from (5.2).

So, for the EONIA, the partial adjustment is:

[4] We checked for possible alterations of the monetary policy decisions as a result of the enlargement of the Eurozone after May 2004, by including a dummy variable that activates from that date onwards; no structural break was detected before and after the enlargement process.

[5] We also introduced dummy variables to distinguish between Duisenberg's, Trichet's and Draghi's chairmanships, but they were non significant.

$$\Delta EONIA_t = \rho_1(i_t^* - EONIA_{t-1}) + \rho_2 \Delta EONIA_{t-1} \tag{5.4}$$

Our estimation procedure comprises two sub-steps:

1. We apply MARS and detect the existence of thresholds, saving the enhanced matrix of split regressors into basis functions[6].

2. We iteratively estimate an ARIMA transfer function with the vectors of the enhanced matrix as regressors. In each loop, the least significant variable is eliminated until the estimation process converges to a model in which all the estimated coefficients are significant at 5% and the errors are compatible with white noise. The objective of this second sub-step is to make a more reliable statistical inference of the parameters of the final model. Our procedure applies MARS on time series data following TS-MARS developed by Keogh (2010). We created codes in R for estimations and processing the results. The main packages for estimation and plotting results are *Earth* and *Plotmo* (Milborrow (2009, 2015)).

Table 5.1 shows our final estimations. We offer the results from TS-MARS and from the Linear Transfer Function estimation as a benchmark (MARS and LTF columns respectively). We also present several goodness of fit measures and the differences between the two estimations to assess the improvements obtained with our approach. Additionally, the autocorrelation functions of the residuals of the TS-MARS estimation and the Box Pierce test, also provided, indicate no left autocorrelation. MARS reliably yields a better goodness of fit per AIC, AICC, BIC, and LogLikelihood measures than linear estimations.

[6] As usual for MARS estimations, we discard detection of possible thresholds in the 10% of extreme values of the sample.

Table 5.1: Estimation of ECB Taylor Rule.

Dependent variable: ΔEONIA	MARS		LTF
Variables	**Coefficient**	**Threshold**	**Coefficient**
Inflation	0.3737**	**> 0.02666**	0.1024*
Output gap	0.0389*	**> -0.0172**	0.0625***
	0.122***	**< -0.0172**	
Crisis	-0.0043*		-0.0046**
AR(3)	0.4177***		0.4006***
ma(1)	-0.2285**		-0.2334**
dof	182		186
Reidual S.E	0.00165		0.0017037
Measures of fit	**Improvements MARS vs linear TF**		
AIC	-1959.60	10.57	-1949.02
AICC	-1956.96	9.62	-1947.34
BIC	-1936.58	7.28	-1929.29
LogLik	986.80	6.29	980.51

```
Signif. codes:  0 '***' 0.001 '**' 0.01 '*' 0.05 '.' 0.1 ' ' 1
```

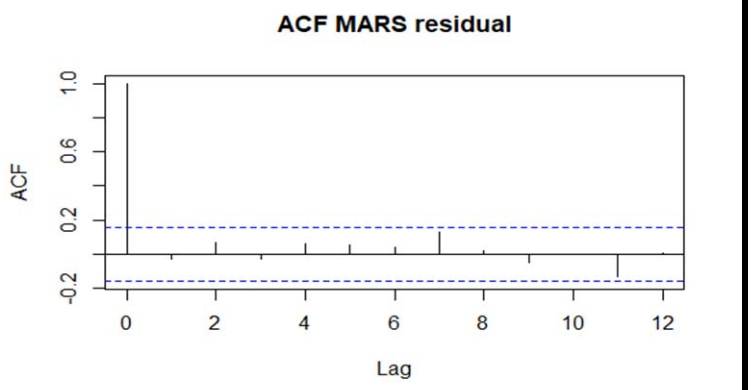


```
Box Pierce test   Chi2= 2.7301, df = 6, p-value = 0.8419
```

Estimated thresholds with their respective 95% confidence interval:
for the inflation rate 2.66%; (2.46%, 2.83%) and for the output gap −0.0172

The first conclusion from 5.1 is that the TR is indeed non linear and characterized by thresholds both in inflation and in output gap. The inflation and output gap coefficients have the expected positive signs. As for the output gap, the ECB reaction is much less intensive with positive or slightly negative output gaps (above -0.0172) than with more negative ones (below -0.0172)[7]. These results reveal that the ECB

[7]Our output gap threshold is close to the threshold detected by Kulikauskas (2014), who separates

cares much more about the economic activity than what is officially declared. On the other hand, the ECB reacts to inflation only when it exceeds 2,66%, more than half a point above its declared 2% inflation target, and its reaction is then, but only then, much stronger than with respect to the output gap. Finally, the 2008 crisis dummy variable does not affect neither the coefficients nor the thresholds; it only shifts the whole Taylor rule downwards by -0.0043. This probably reflects a decrease in the equilibrium interest rate in the ZLB period.

5.1 helps to interpret our results in the light of the historical evolution of the data. The threshold values for inflation and for the output gap are represented with horizontal lines, as well as the official 2% inflation official objective of the ECB; the vertical shaded areas identify the periods of inflation rate above 2.66%. It is worth noting that the periods of intense inflation (above 2,66%) or intense negative output gap (below -0.0172) have been unfrequent and short-lived. These periods are precisely those in which the ECB reacted with more intensity to the determinants of its monetary policy. The rest of the time, our results indicate that the ECB has conducted a moderate policy guided more by the economic activity than by the level of inflation.

the economy into two states according to an output gap value estimated at -0.0135. However, he obtained either non-significant or negative coefficients for ECB response to inflation rates, while we obtain a more complete map of ECB behaviour.

Figure 5.1: Inflation and output gap time series.

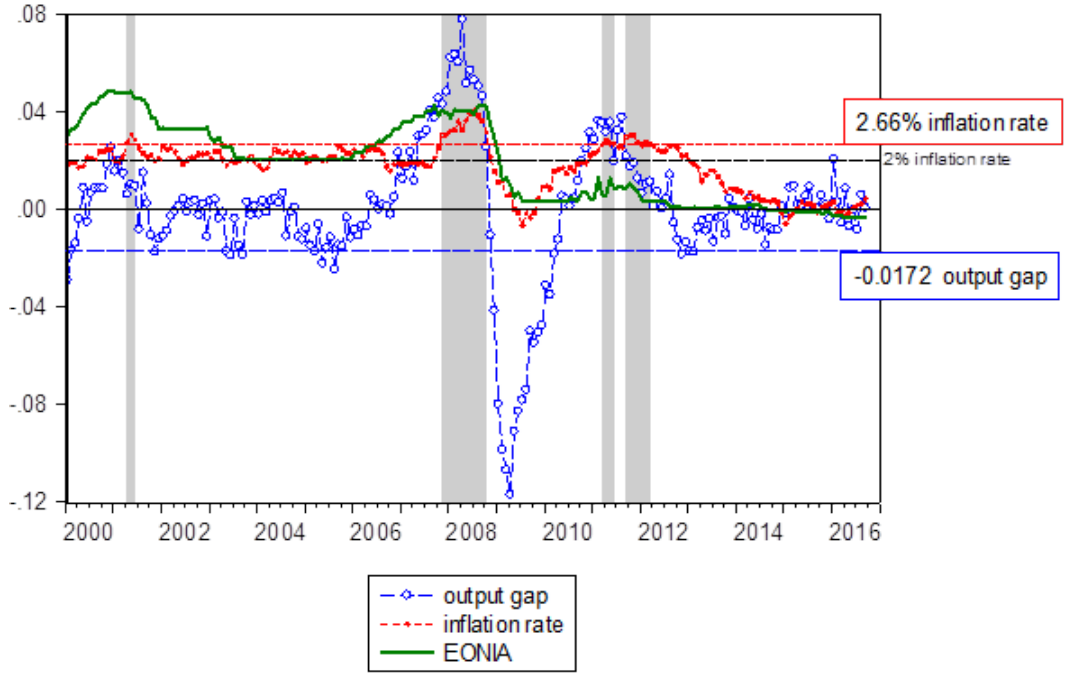

5.3 Conclusion

In this paper we obtain a TR with multiple thresholds, which can be theoretically derived from general and plausible characteristics of CB preferences. We use the MARS procedure adapted to time series to endogenously detect thresholds using the ARIMA transfer function refinement to whiten the error to increase inference reliability.

To summarize our results: a) we detect thresholds both in the output gap and in the inflation rate; b) the threshold level for the output gap is identified at -0.0172; 95%; c) the ECB reaction is three times more intensive for output gaps below -0.0172 than above it; d) the ECB is sensitive to the inflation rate only for high levels of inflation, namely above 2.66%; 95%; e) above that level of inflation the ECB is much more sensitive to inflation than to the output gap; f) the 2008 crisis provoked a more abrupt decrease of the interest rate than expected according to the macroeconomic circumstances, which is consistent with the theoretical literature on optimal monetary policy in the vicinity of ZLB. Our empirical results also indicate that there are no significant policy differences between the three successive chairmanships of the ECB.

We conclude that the ECB cares more about the economic activity than officially declared and reacts intensively to inflation deviations once they sufficiently exceed the official 2% target.

Finally, our results provide empirical support to Nebot et al. (2016) theoretical conjecture and offer a more complete characterization of the ECB Taylor Rule than more conventional approaches used to date.

6 A model for nonlinear Okun's law.

Since Okun (1962) formally stated the existence of an empirical negative relationship between growth and variations of the unemployment rate from US statistical data, numerous studies have focused on verifying the robustness of Okun's law but very few ones attempted to provide a theoretical foundation to identify possible factors that cause the observed patterns. Prachowny (1993); Zerbo et al. (2018) model linear Okun's law from production functions. Adachi et al. (2015) use efficiency wages in a Solow's model to state a linear Okun's law in the steady state. None of them addresses the theoretical foundations of the nonlinearity of Okun's law.

In this section, our purpose consist of developing a simple model that provides nonlinear Okun's law with a theoretical foundation. In their survey, Silvapulle et al. (2004) collect three main theoretical hypotheses to explain asymmetries in Okun's Law:

- Hypothesis 1 (H1) - The "Institutional rigidity hypothesis" has to do with the fact that employers face institutional restrictions to lay off workers, so that employers fire less workers than desired in bad times.
- Hypothesis 2 (H2) - The "Labor hoarding hypothesis" reflects the impact on unemployment of the employer's decision to invest in the training of workers. Firms with trained workers are loath to fire them in recessions.
- Hypothesis 3 (H3) - The "Firm's risk aversion hypothesis" that justifies a stronger response of unemployment in recession than in expansions is related to the fact that employers give more weight to bad news than to good ones.

Taking separately each hypothesis, Okun's law function may show at least two different shapes. Under the "Institutional rigidity hypothesis" and the "Labour hoarding hypothesis" the response of unemployment to economic activity would be less intensive in recessions than in expansions. So that, it implies a concave Okun's law. On the opposite, the "Firm's risk aversion hypothesis" justifies a stronger

response of unemployment in recessions than in expansions. As a result, Okun's law exhibits a convex functional form.

As the main empirical studies point out the convex functional form of Okun's law, in this chapter, we develop a model assuming firm's risk aversion. We introduce the possibility that the risk aversion coefficient can be piecewise step function on economic activity. The result will be a convex Okun's law function with thresholds related to the jumps in the piecewise step function of the risk aversion coefficient.

Let us assume there exist L competitive and risk averse firms maximizing profits in an economy. In the short run, firms face capital cost as a fixed cost and they maximize profits hiring n_t workers at wage w_t .

$$\underset{n_t}{Max}\ ce[y_t] - w_t n_t - rk$$

The output y_t with $p = 1$ corresponds to revenue. It is driven by a stochastic process. The risk averse decision-takers in firms decide taking into account an approach to the certainty equivalent function $ce[y]$ (Sandmo, 1971; Subrahmanyam and Thomadakis, 1980) that we define as:

$$ce[y_t] = E[y_t] - \frac{1}{2} ra Var[y_t]$$

where ra is the Arrow Pratt risk aversion coefficient. (Pratt, 1964)

We assume the risk aversion coefficient ra shall depend on the overall state of the economy, Y_t. It means that firm's decision-takers are concerned about the overall economic activity news of the country or region. We define $ra(\triangle Y)$ as a piecewise step function increasing in its argument. The greater the change in the output, the greater the risk aversion coefficient, ra.

Let us assume that the production of each competitive firm follows the same Cobb Douglas function $y_t = A_t k_t^{\alpha} n_t^{1-\alpha}$ and the total factor productivity A_t is a stochastic process with constant $E(A_t) = \mu_A$ and $Var(A_t) = \sigma_A^2$.

The optimal decision problem will be the following:

$$\underset{n_t}{Max}\ E[A_t k_t^{\alpha} n_t^{1-\alpha}] - \frac{1}{2} ra Var[A_t k_t^{\alpha} n_t^{1-\alpha}] - w_t n_t - rk$$

Denoting $\overline{y}_t = k_t^{\alpha} n_t^{1-\alpha}$ we simplify the problem.

$$\underset{n_t}{Max} \mu_A \overline{y}_t - \frac{1}{2} ra \sigma_A^2 \overline{y}_t^2 - w_t n_t - rk \tag{6.1}$$

We obtain the labor demand of each firm from the first order condition with respect to n_t of the (6.1).

$$E[A_t](1-\alpha)\left(\frac{\overline{y}_t}{n_t}\right) - ra Var(A_t)\overline{y}_t(1-\alpha)\left(\frac{\overline{y}_t}{n_t}\right) - w_t = 0$$

$$\Longrightarrow n_t^d = \frac{1-\alpha}{w_t}[E[A_t]\,(\overline{y}_t) - raVar(A_t)\overline{y}_t^2]$$

Aggregating demands for k symmetrical firms and taking into account that $\sum^{k}\overline{y}_t^2 = k\overline{y}_t^2 = k(\frac{\overline{Y}_t}{k})^2 = \frac{\overline{Y}_t^2}{k}$ we can obtain the aggregate labor demand.

$$N_t^d = \frac{1-\alpha}{w_t}(E[A_t]\overline{Y}_t - raVar[A_t]\frac{\overline{Y}_t^2}{k}) \tag{6.2}$$

In the short term, let us assume sticky wage $\overline{w}$ in the labor market. Therefore, the equilibrium condition in the labour market with an inelastic labor supply L and an aggregated labour demand (6.2) will be:

$$L = N^d(\overline{w}_t) + U_t \tag{6.3}$$
$$L - U_t = \frac{1-\alpha}{\overline{w}}(E[A_t]\overline{Y}_t - raVar[A_t]\frac{\overline{Y}_t^2}{k})$$

$$L - U_t = \frac{1-\alpha}{\overline{w}}(E[A_t]\overline{Y}_t - ra\frac{Var[A_t]}{E[A_t]^2}\frac{(E[A_t]\overline{Y}_t)^2}{k})$$

Denoting volatility as $\phi = \frac{\sqrt{Var[A_t]}}{E[A_t]}$ and using $E[A_t]\overline{Y}_t = E[Y_t]$, the equilibrium condition will be:

$$L - U_t = \frac{1-\alpha}{\overline{w}}(E[Y_t] - ra\phi^2\frac{E[Y_t]^2}{k})) \tag{6.4}$$

With unemployment rate $u_t = U_t/L$, we can obtain Okun coefficient for the output growth rate version of Okun's law by taking logs and derivatives with respect to time from (6.4). The Okun coefficient will depend on ra.

$$\ln(1-u_t) = \ln(\frac{1-\alpha}{\overline{w}}) + \ln(E[Y_t]) + \ln(1 - ra\phi^2\frac{E[Y_t]}{k})) - \ln(L)$$

$$\frac{-\partial u_t/\partial t}{(1-u_t)} = \frac{\partial E[Y_t]/\partial t}{E[Y_t]} - \frac{\partial E[Y_t]/\partial t\frac{ra}{k}\phi^2}{(1-\frac{ra}{k}\phi^2 E[Y_t])}$$

$$\partial u_t/\partial t = -(1-u_t)\frac{\partial E[Y_t]/\partial t}{E[Y_t]}(1 - \frac{E[Y_t]\frac{ra}{k}\phi^2}{1-E[Y_t]\frac{ra}{k}\phi^2})$$

$$\Longrightarrow \partial u_t/\partial t = -\frac{N^*(\overline{w})}{L}\frac{\partial E[Y_t]/\partial t}{E[Y_t]}(1 - \frac{E[Y_t]\frac{ra}{k}\phi^2}{1-E[Y_t]\frac{ra}{k}\phi^2})$$

Denoting $\gamma_t^e = \frac{\partial E[Y_t]/\partial t}{E[Y_t]}$ is the expected growth rate of the economy.

$$\partial u_t/\partial t = -\frac{N^*(\overline{w})}{L}(1 - \frac{E[Y_t]\frac{ra}{k}\phi^2}{1 - E[Y_t]\frac{ra}{k}\phi^2})\gamma_t^e$$

The Okun coefficient ($\mathcal{OL}$) will be:

$$\mathcal{OL} = -\frac{\mathrm{N}^*(\overline{\mathrm{w}})}{\mathrm{L}}(1 - \frac{\mathrm{E}[\mathrm{Y_t}]\frac{\mathrm{ra}}{\mathrm{k}}\phi^2}{(1 - \mathrm{E}[\mathrm{Y_t}]\frac{\mathrm{ra}}{\mathrm{k}}\phi^2)}) \tag{6.5}$$

and its absolute value is decreasing with ra.

For a constant risk aversion firms for all output growth rate in the domain, we get a simple linear negative relationship between output growth and unemployment rate variation.

It is easy to see that if ra is an increasing piecewise step function on economic growth rate, we get an Okun's law with thresholds. Its shape will be convex according to the firm's risk aversion hypothesis (H3).

For instance, a risk aversion function such that $ra(\gamma_t^e) = \begin{cases} a & \gamma_t^e \leq 0 \\ b > a & \gamma_t^e > 0 \end{cases}$ reflects a greater risk aversion for positive output growth rates than for a negatives, the absolute value of the Okun coefficient will be lower for positive economic growth rate than for negative ones. See Figure 6.1.

Figure 6.1: Okun's law under firm's risk aversion hypothesis with a threshold at $\tau_{\gamma_t^e} = 0$.

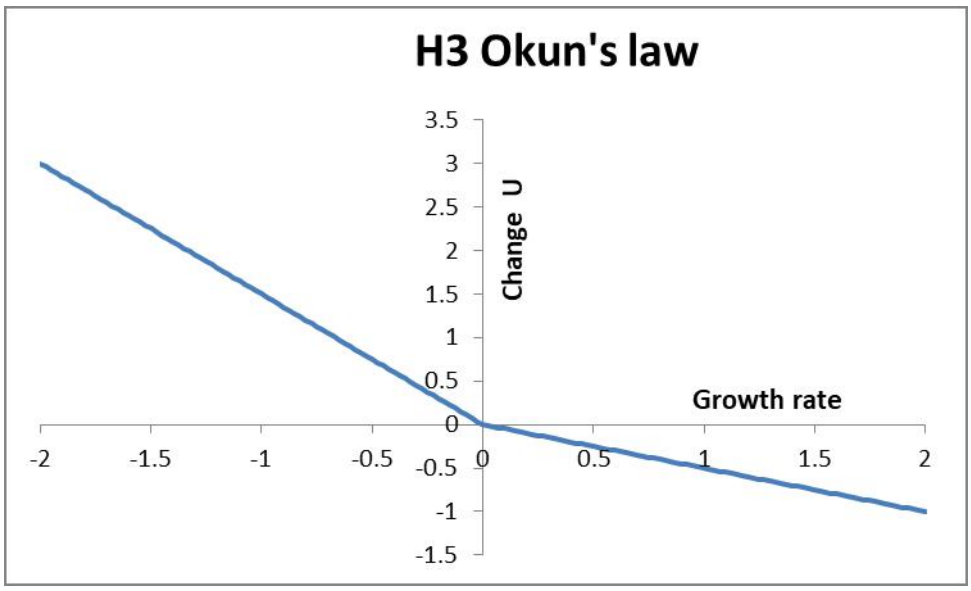

Okun coefficient for the output gap Okun's law version can be obtained by taking partial derivatives from the equilibrium condition (6.4).

$$L - U_t = \frac{1-\alpha}{\overline{w}}(E[Y_t] - ra\phi^2\frac{E[Y_t]^2}{k}))$$

$$-\partial u_t = \partial E[Y_t]\frac{1-\alpha}{\overline{w}L}(1 - 2ra\phi^2\frac{E[Y_t]}{k})$$

$$\frac{\partial u_t}{\partial E[Y_t]} = -\frac{1-\alpha}{\overline{w}L}(1 - 2ra\phi^2\frac{E[Y_t]}{k}) \tag{6.6}$$

The absolute value of this Okun coefficient (6.6) depends negatively on ra. Indeed, for a constant ra such that $ra < \frac{k}{2E[Y_t]\phi^2}$ we get a linear Okun's law with a negative Okun coefficient.

For a risk aversion piecewise step function such that $ra \begin{cases} a & Y_t \leq Y_t^P \\ b > a & Y_t > Y_t^P \end{cases}$, where Y_t^P corresponds to the potential output, we get a greater risk aversion coefficient for positive output gaps than for negative. As the absolute value of the Okun coefficient negatively depends on ra

$$\frac{\triangle|\frac{\partial U}{\partial E[Y_t]}|}{\triangle ra} = -\frac{1-\alpha}{\overline{w}}2\phi^2\frac{E[Y_t]}{kL}) \tag{6.7}$$

consequently we obtain that the greater the output gap, the greater the ra and so the lower the absolute value of the Okun coefficient.

Flexibility of our model lays on how employer's risk aversion depends on economic growth rate or the output gap of the economy. So that, risk aversion preference function with different steps may provide more than one threshold in Okun's law with different locations than zero growth rate or output gap.

If we restrict Okun's law to have only one threshold at zero growth rate, only H3 "Firm's risk aversion hypothesis" generates Okun's law shape sustained by evidence, as Silvapulle et al. (2004) point out. However, our flexible model allows to overcome

this restriction. For instance, different threshold locations can reconcile evidence with a combination of theoretical hypotheses. Let us consider that hypotheses H1 and H2 also may intervene together with H3 shaping Okun's law. "Institutional rigidity hypothesis", H1, may be easily combined with H3 with a threshold on negative values. Risk averse employers would be more reluctant to fire workers when facing higher costs of laying off them. Therefore, employer's risk aversion coefficient increases even for negative growth rates. The higher the firing costs and institutional rigidity, the more negative the threshold above which the employer becomes more cautious and below which more intensively fire workers. Thus, our model can combine H1 and H3 simply letting threshold lay on negative values of the growth rate or the output gap when the unemployment rate is increasing. (See Figure 6.2).

Figure 6.2: Okun's law under firm's risk aversion and institutional rigidity hypotheses with a threshold $\tau_{\gamma_t^e} < 0$.

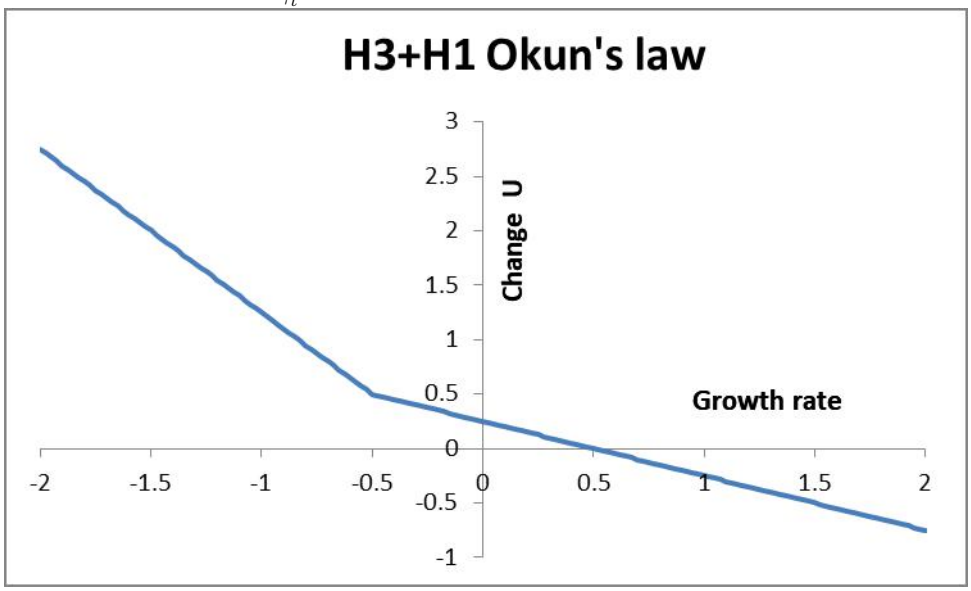

Similarly H2, "Labor hoarding hypothesis", may be easily combined with H3 with a threshold on positive values. It may result into a non-linear convex Okun's law with at least a threshold in the expansion zone (positive growth and decreasing unemployment rate). It means that in an economy where firms invest on training their workers, the absolute value of the Okun coefficient decreases when the expansion turns to be sufficiently intensive; so that, firms decelerate workers contracting rate

for investing in training them. Thus, our model can combine H2 and H3 simply letting threshold lay on positive growth rates or output gaps when the unemployment rate is decreasing. (See Figure 6.3).

Figure 6.3: Okun's law under firm's risk aversion and "Labor hoarding hypotheses with a threshold $\tau_{\gamma_t^e} > 0$.

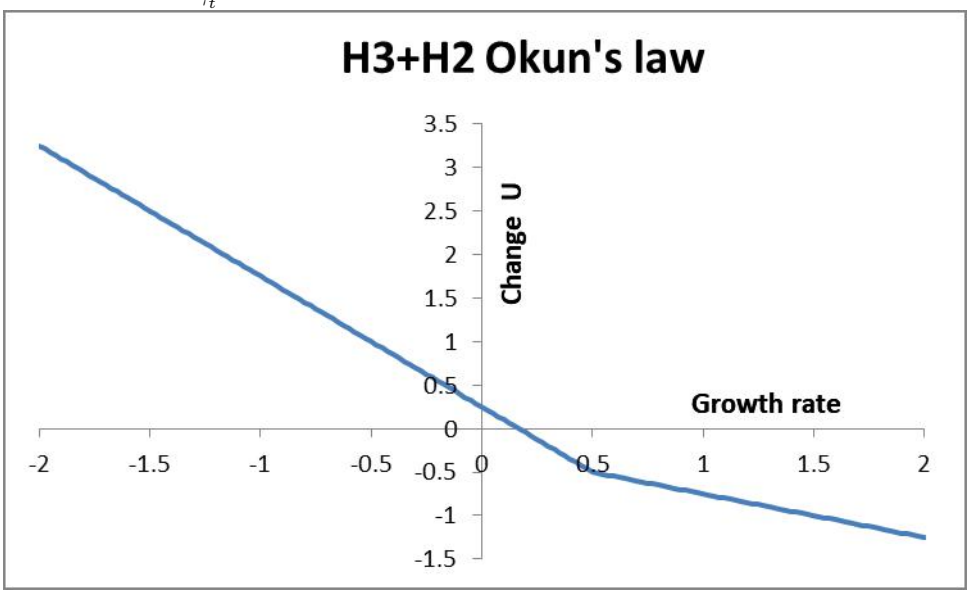

Therefore, our flexible model let us reconcile theoretical hypotheses combination in Okun's law by the difference between Okun coefficients for each region and by the location of thresholds on the growth rate or the output gap. Consequently, in order to estimate Okun's law in which the different theoretical hypotheses could intervene, it is required an empirical methodology sufficiently flexible that not previously impose the number of thresholds an their locations.

7 New insights into the nonlinearity of Okun's law.

We estimate Okun's law for four European countries (France, Germany, the Netherlands and Spain) with a nonparametric procedure, without imposing a previous specific functional form. We apply the non parametric MARS methodology that endogenously detects multiple thresholds and therefore is able to identify multiple possible regimes. In addition, we control for the Euro area crisis to capture possible effects of the economic activity of neighbour countries on domestic unemployment rate variations. Our results confirm the existence of two regimes in each country but significantly different thresholds across countries. The form of Okun's law for Germany, France and the Netherlands are similar and quite different from Spain where it is much steeper. Differences between Okun coefficients below and above the threshold are consistent with the "firm's risk aversion hypothesis", but different thresholds across countries may be related to the "labour hoarding hypothesis". The negative value of the threshold in Spain may reflect the "institutional rigidity hypothesis". Finally, the fact that the Euro area crisis may affect the domestic Okun's law is consistent with decision makers with risk aversion who use information from the economic area they are operating in. These results not only potentially enrich Okun's law estimations but also opens the debate over how the different theoretical hypothesis intervene and shape Okun's law for each country.

7.1 Introduction.

The empirical validity of Okun's law has been extensively explored in the literature. Recent studies have provided theoretical explanations of responsiveness of unemployment to output growth depending on whether the economy is in a recession or an expansion, resulting in an asymmetric Okun´s law. In such a framework, a

correct identification of the non-linear characteristics of the relationship between unemployment and output is crucial for the correct design, the implementation and the effectiveness of economic policies aimed at improving the labour market operation. This may be particularly important to better understand why after the recent crisis, some European countries are facing high unemployment rates in spite of the recovery.

Most of the empirical studies that investigate the nonlinearity of Okun's law use parametric models, often with exogenously imposed thresholds. To cite some of the most recent ones, Economou and Psarianos (2016) find that the stronger the labour market protection of a country the weaker its Okun coefficient, but some countries as Spain contradict this finding. Huang and Chang (2005) also estimate for Canada two regimes in output gap around a threshold but previously estimate a structural break to capture the instability of the Okun's coefficient over time. Owyang and Sekhposyan (2012)also check with rolling regressions the instability over time of the Okun coefficients. But non constant coefficients over time can be related to different regimes in the explanatory variables rather than directly due to a structural change associated with time; therefore, restricting the estimation to detect only one threshold may induce to misleading detection of structural changes instead of additional thresholds. Using a methodology similar to Holmes and Silverstone (2006), Valadkhani and Smyth (2015) estimate asymmetric Okun's laws for the USA, although they do so around an exogenously fixed zero value of cyclical unemployment; they also detect two distinct Markow switching regimes of asymmetries but these switching regimes have much to to do with a structural change from 1982 onwards. Tang and Bethencourt (2017) estimate asymmetries with nonlinear autoregressive distributed lag modeling but they previously and exogenously impose the two regimes. The use of exogenously fixed thresholds is also the case of the study for Greece carried out by Koutroulis et al. (2016). Jardin and Gaétan (2012) use a more flexible Kernel semiparametric approach on a panel of data for 16 European countries and confirm nonlinearity in the average Okun's law of all these countries. However, their approach neither quantifies the relationship between output growth and unemployment variations, nor estimates the thresholds positions at which this relationship suffers modifications. Moreover, their results refer to the whole group of countries of the panel, without distinction in nonlinearities between the individual members.

In our opinion, both a flexible and comprehensive estimation procedure is required to reach three important objectives: to quantify the nonlinear relationship bet-

ween output growth and unemployment, to endogenously detect and locate various thresholds if they exist and possible structural breaks, and to allow for different non-linearities in different countries. For that purpose, in this paper we estimate Okun's relationship for several individual European countries using the nonparametric Multiple Adaptive Regression Splines (MARS) methodology (Friedman, 1991; Lewis and Stevens, 1991; Keogh, 2010), which is particularly suited to estimate models with multiple and endogenously detected thresholds and transition variables with possible interactions. Since our underlying interest is to understand the functioning of labour markets under different institutional setups of the Eurozone, we examine Okun's law in four EMU countries: three considered part of the core, France, Germany and the Netherlands, and one generally ranked as peripheral, Spain. The periods covered by our analysis runs from 1970Q1 to 2018Q1 for France and the Netherlands; from 1992Q1 to 2018Q1 for Germany, and from 1995Q1 to 2018Q1 for Spain, depending on the availability of homogeneous statistics. The time spans of our analysis allow us to investigate whether Okun's relationship changes in each country in recession periods of the Euro area as a whole, controlling for the Euro area crisis variable created by CEPR.

We obtain several interesting findings. As a first immediate result, Okun's law for the three core countries is very similar and quite flat, whereas it is much steeper for Spain. On the other hand, our empirical findings help us discerning which explanatory theory of Okun's law asymmetries, as synthetized by Silvapulle et al. (2004), fits better into the estimated coefficients and thresholds of each country. Concretely, in the first place, for each country, differences between Okun coefficients below and above the threshold are consistent with the firm's "risk aversion hypothesis", according to which unemployment responds more strongly during recessions than during expansions. In the second place, differences between the threshold positions across countries can be related to the "labour hoarding hypothesis", which establishes that firms with trained workers are reluctant to fire them in recessions; our results indicate in which countries firms are more reluctant to do so. In the third place, the fact that the breaking point in unemployment deceleration for the Spanish economy takes place at a negative rate of output growth is consistent with the institutional obstacles the employers find in bad times to fire workers ("institutional rigidity hypothesis"). Finally, the periods of economic crisis in the Euro area affect Okun's law in France, supporting the idea that decision makers in this country are also concerned about the information from the economic area they are operating in,

which gives further support to the firm's risk aversion hypothesis.

The rest of the paper is set up as follows. In section 2, we discuss some new considerations of the main theoretical hypothesis. The empirical methodology and data are explained in section 4; in this section we explain an innovative procedure to compute confidence intervals for the threshold locations. The results are presented in section 5, and section 6 concludes and derives some policy prescriptions.

7.2 New considerations on the main theoretical hypotheses of nonlinearities in Okun's law.

Several studies attempted to explain theoretically the nonlinearities in Okun´s law. Courtney (1991) attributes non linear responses of unemployment to the existence of a non constant factor substitution rate during cycles. Harris and Silverstone (2001) formulate asymmetric responses due to heterogeneity in plants in terms of job creation and job destruction facing shocks. Mayes and Viren (2002) attribute asymmetry to the behavior of the labour market due to mismatching between jobs and unemployment in different regions and sectors. Campbell and Fisher (2000) focus on aggregate asymmetries in job creation and destruction attributable to microeconomic asymmetries in adjustment costs so that firing workers responds more than hiring new ones to positive external shocks. Summarizing all these theoretical considerations in a survey, Silvapulle et al. (2004) characterise three theoretical explanations for asymmetries in Okun's law. According to the "institutional rigidity hypothesis" (H1) employers face institutional restrictions to lay off workers, so that employers fire less workers than desired in bad times. The "labour hoarding hypothesis" (H2) reflects the impact on unemployment of the employer's decision to invest in the training of workers: firms with trained workers are reluctant to fire them in recessions. And the "firm's risk aversion hypothesis" (H3) justifies a stronger response of unemployment in recession than in expansions. This third hypothesis has to do with the fact that employers give more weight to bad news than to good ones. Although the studies tend to focus on one of these hypothesis excluding the other ones, the debate over how the different theoretical hypotheses may intervene together and shape Okun's law is, however, desirable.

Under the "institutional rigidity hypothesis" and the "labour hoarding hypothesis" the response of unemployment to economic activity would be less intensive in re-

cession than in expansions. This on its own would imply a concave Okun's law. On the opposite, the "firm's risk aversion hypothesis" justifies a stronger response of unemployment in recession than in expansions. As a result, in expansion times, firms would be reluctant to hire workers by fear of a possibly not long lasting recovery. Under this third hypothesis on its own, Okun's law would exhibit a convex functional form. In Figure 7.1, we reflect the different shapes under hypothesis H1, H2 and H3 separately.

Figure 7.1: Shapes of Okun's law with the different underlying theoretical hypotheses.

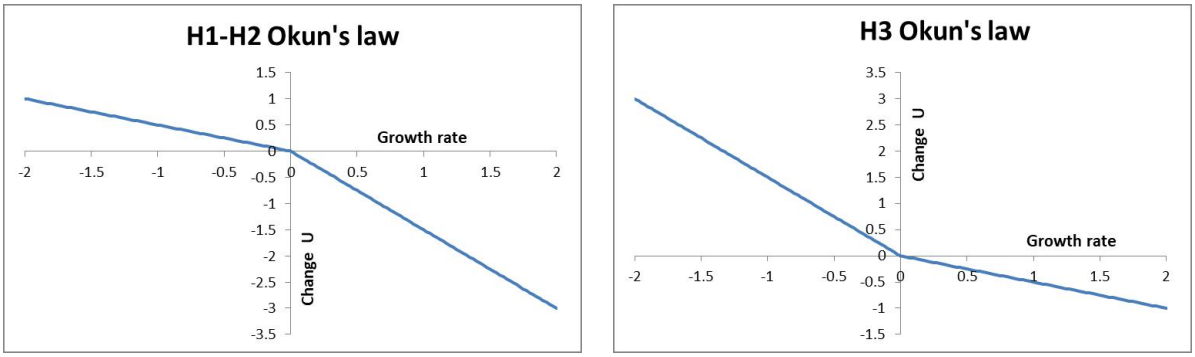

However, as mentioned by Jardin and Gaétan (2012), there is no reason why nonlinearities in Okun's law have to be attributed to only one of these hypotheses. In fact, a combination of them might give rise to Okun's laws that are more complex than the one derived from one single hypothesis. If more than one hypotheses intervene, and interact, more than two regimes might exist and so more complex Okun's laws might emerge from the data. Moreover, we argue that an hypothesis can affect not only the Okun coefficient but also the position of thresholds. For instance, in Figure 7.1 the shape under H3 with the threshold at a negative value could reflect institutional rigidity in the labour market of the country. This would be the case with firms facing high firing cost that would be reluctant to reduce their workforce even for some negative values of economic growth; they would start firing workers only when output growth exhibits sufficiently negative rates, that is rates below a negative threshold. Furthermore, differences across countries in training workers may justify different values of threshold along the growth rate axis. Although the results from Jardin and Gaétan (2012) do not allow to estimate the thresholds positions and quantify Okun coefficients, their semiparametric approach empirically opens the possibility that different hypothesis may simultaneously intervene to ex-

plain Okun's law shape. From the preceding reasoning we conclude that Okun's law should be estimated with a data-driven and very flexible methodology that allows for possible multiple thresholds along with their precise location, completed with a procedure able to compute confidence intervals for these locations; otherwise, imposing parametric functions could difficult a correct identification of the nonlinear characteristics of the unemployment-output tradeoff.

7.3 Methodology and data.

Threshold regression models considered so far in the empirical literature consider the existence of only one threshold variable and only one set of disjoint threshold-defined regions. These are serious limitations for our purpose since we do not want to previously restrict the number of regimes derived from the theoretical hypothesis in Okun's law. Lewis and Stevens (1991) criticize the limitations of traditional threshold models and propose the MARS methodology from Friedman (1991) to endogenously detect and estimate possibly multiple thresholds for each independent variable of the model, and even possible interactions if suspected..

MARS is a nonparametric estimation procedure that selects and fits the model endogenously detecting and quantifying thresholds and complex nonlinearities if they exist. Given a set of explanatory variables, MARS fits a model as an expansion in products of truncated linear spline functions (hinge functions), which are selected through a recursive partitioning strategy with forward and backward passes. By using products of hinge functions, the procedure accommodates both nonlinearities and interactions among the explanatory variables as a generalization of Recursive Partitioning (RP) (Friedman, 1977). MARS for time series (TSMARS) initiated by Lewis and Stevens (1991) has been extensively explored by Keogh (2010). While SETAR and the self-exciting open-loop threshold autoregressive (TARSO) models of Tong (1990) identify piecewise linear functions over disjoint subregions, with discontinuities at the boundaries of the regions, TSMARS methodology obtains nonlinear threshold models that are continuous in the domain of the predictor variables, and with possible interactions among lagged predictor variables. Therefore TSMARS constitutes a further generalization of Tong's models (Chung, 2012).

MARS seeks to model the dependence of variable y_t on a set of explanatory variables $x_t^1, ..., x_t^p$ (where some of these variables may be lagged values of other, i.e. x_t^p might

be x_{t-1}^1 for instance). The true unknown model is

$$y_t = f(x_t^1, ..., x_t^p) + \varepsilon_t$$

where the error term ε_t is assumed to be independently distributed with $E(\varepsilon_t) = 0$ and variance $E(\varepsilon_t^2) = \sigma^2$. The function $f(x)$ is the true relationship between outcome time-series (y_t) and a vector of p explanatory variables $x_t = (x_t^1 \ldots .x_t^p)$ that we want to estimate from the data.

MARS procedure approximates this function as:

$$y_t = \beta_0 + \sum_{m=1}^{M} \beta_m b_m (x_t) + \varepsilon_t \tag{7.1}$$

where;

β_0 is a constant

β_m is the coefficient for the m^{th} basis function, $m = 1, ..., M$

$b_m(x_t)$ is the m^{th} basis function, $m = 1, ..., M$

ε_t is an independently distributed error term with $E(\varepsilon_t) = 0$ and $E(\varepsilon_t^2) = \sigma^2$

The basis functions are products of up to a maximum interaction order mi truncated linear splines or hinge functions (we usually restrict $mi = 2$), describing the relationship between one or more explanatory variables and the outcome in terms of segments of stable association separated by knots or threshold values. These interacting hinge functions allow us to identify possible interactions between variables. Namely, for $mi = 2$ the m^{th} basis function takes one of the following two forms:

No interaction: $b_m (x_t) = h_m \left(x_t^k, \tau_{k,m}\right)$ for some $k = 1, \ldots, p$

With interaction: $b_m (x_t) = h_m \left(x_t^k, \tau_{k,m}\right) \cdot h_m \left(x_t^j, \tau_{j,m}\right)$

for some $k,\ j = 1, \ldots, p,\ k \neq j$

where $\tau_{k,m}$ is the threshold value of x_t^k in the m^{th} basis function and where $h \left(x_t^k, \tau_{k,m}\right)$ is a hinge function (or truncated linear spline) that takes the following form depending on whether the basis function takes effect above or below the threshold $\tau_{k,m}$(See Figure 2.1)

a) above the threshold: $h_m \left(x_t^k, \tau_{k,m}\right) = max(x_t^k - \tau_{k,m},\ 0)$

b) below the threshold: $h_m\left(x_t^k, \tau_{k,m}\right) = max(\tau_{km} - x_t^k,\ 0)$

Figure 7.2: Graph of the two truncated linear spline or hinge functions.

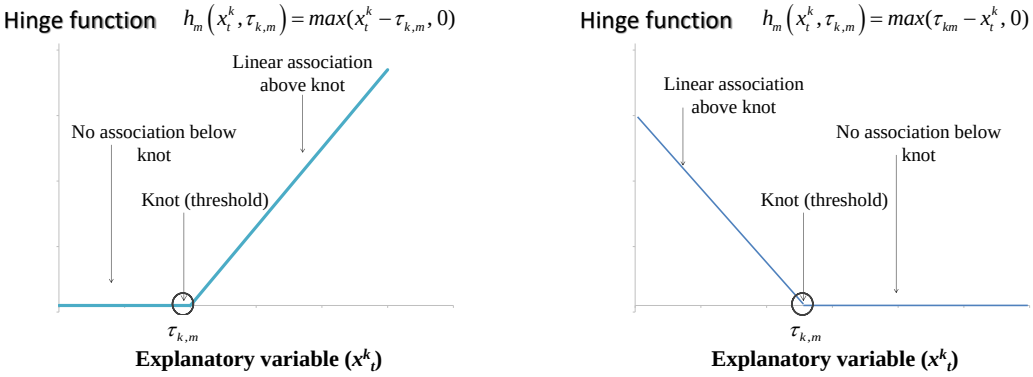

If no knot (threshold) is detected in a given variable, then a simple linear association between the explanatory and outcome variables can be specified as a single function applied across the total range of values of that explanatory variable.

In the algorithm, once we define $x_t = (x_t^1 \ldots . x_t^p)$ with all potentially significant explanatory variables, including the associated lags, the model identification and estimation proceed by an automated, iterative, process. The description that follows is mainly based on Friedman (1991, 1993); Chung (2012).

Forward pass: In general terms, starting with the simplest model containing only a constant basis function, MARS iteratively generates a matrix of basis functions in a forward stepwise manner. Candidate basis functions are added according to their ability to improve the model fit by minimizing the residual sum of squares (RSS), until the model reaches a predefined limit of complexity. The candidate basis functions are identified by a nested exhaustive search looping over the existing set of basis functions, and all other possible explanatory variables (or interactions) and knot (threshold) positions.

This forward pass procedure provides a model that overfits the data. Therefore, a pruning process is required to remove the subregions whose product basis functions do not sufficiently contribute to the accuracy of the model.

Backward (pruning) pass: During the backward pass, MARS iteratively prunes the model obtained from the forward pass. It removes basis functions to reduce the

value of a modified form of the generalized cross validation ($MGCV$) criterion that penalizes model complexity, based on Craven and Wahba (1979). This pruning pass runs until MGCV cannot be further reduced. This criterion is defined as

$$\text{MGCV} = \frac{\frac{1}{T}\ \sum_{t=1}^{T}(y_t - \hat{f_M}\left(x_t\right))^2}{\left[1 - C\left(M\right)/T\right]^2}$$

where T is the number of observations; $C(M)$ is the model complexity penalty function which is defined as $C(M) = (M+1) + dM$, where M is the number of basis functions retained in the model, M+1 the number of parameters in $\hat{f_M}\left(x_t\right)$) and d represents the degree of additional contribution brought by a basis function to the model complexity. Friedman (1991) suggests a value for d between 2 and 4; usually $d = 3$.

Therefore, this MGCV criterion accounts for the inherent improvement in explained variance associated with increasing numbers of basis-functions, and its calculation allows estimates of the relative importance of each basis function so the model selection process converges on a set of basis functions that most efficiently explain variation in the dependent variable.

For easier understanding, we provide Figure 7.3 that schematize OLS procedure in the left column and MARS procedure in the right one. While OLS directly proceeds to estimate model parameters using the data, MARS uses them in each iteration of forward and backward passes to select and estimate the final model. During these passes, each variable x may be splitted into two variables $z_1 = max(x - \tau, 0)$ and $z_2 = max(\tau - x, 0)$; therefore, at the end, MARS estimates a linear model with a matrix of split explanatory variables corresponding to each basis function detected for the final model. Consequently, OLS can be understood as a particular case of MARS where forward and pruning passes do not detect any threshold for any of the explanatory variables.

For the estimation of Okun's law, we propose a procedure to apply MARS methodology that comprises four steps:

Step 1. For each country, we check the integration order of the unemployment rate using the unit root test with multiple structural changes (up to 5) proposed by Carrion-i Silvestre et al. (2009). In case of the existence of a unit root, we use the MARS cointegration test proposed by Sephton (1994) to check for cointegration

Figure 7.3: Comparison between the Ordinary Least Squares (OLS) estimation and Multiple Adaptive Regression Spline (MARS) procedure.

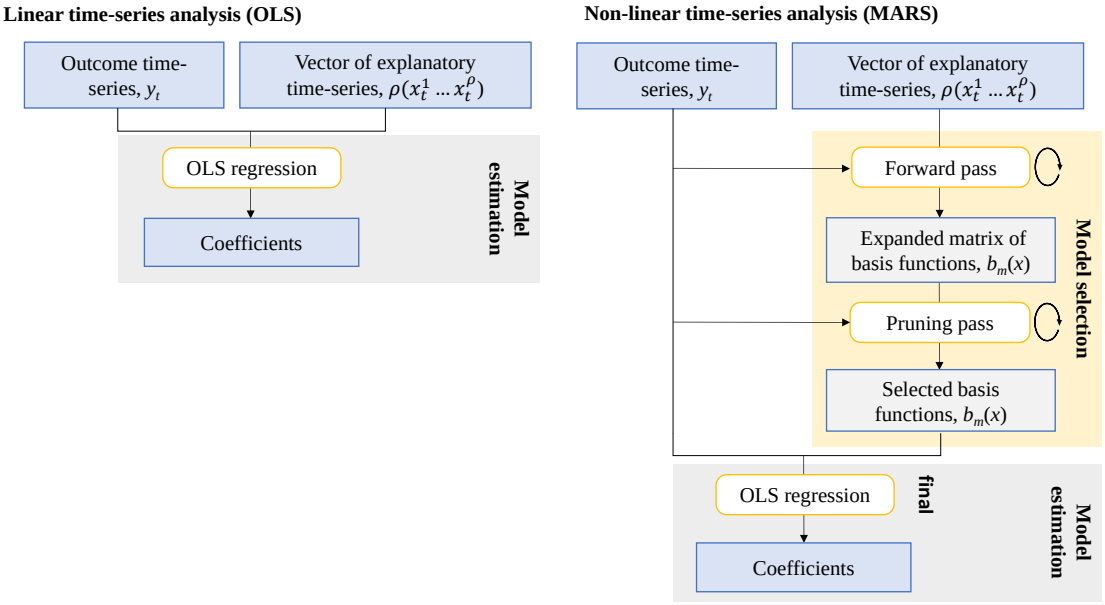

between the unemployment rate and real GDP, to determine whether we have to discriminate between long term and short term effects in Okun's law.

Step 2. Given the results of step 1, if cointegration is not detected we apply the nonparametric procedure MARS to model 7.2, to allow for complex nonlinearities: from the linear version of Okun's law $\triangle u_t = \beta_0 + \beta_{m_\pi}\gamma_t + \rho_1 \triangle u_{t-1} + \rho_2 \triangle u_{t-2} + \varepsilon_t$, the corresponding MARS specification would be:

$$\triangle u_t = (\beta_0 + \delta_1 d_{Ct}) + \sum_{m=1}^{M} \beta_m b[\gamma_t, \tau_m] + \rho_1 \triangle u_{t-1} + \rho_2 \triangle u_{t-2} + \varepsilon_t \tag{7.2}$$

u_t : unemployment rate d_{Ct}: crisis dummy, γ_t : quarterly growth rate

In the proposed specification we include the dummy variable d_{Ct} for the Euro area crisis created by CEPR Euro Area Business Cycle Dating Committee that establishes the chronology of recessions and expansions in the Eurozone, to allow the model to capture the idea that employers also take into account the information of the whole economic area they are operating in to take their employment decisions[1].

In the case that cointegration were detected in Step 1, we would apply the MARS

[1] As usual for MARS estimations, we discard detection of possible thresholds in the 10% of extreme values of the sample.

specification of the Error Correction Model on the original variables. In both cases (with or without cointegration), the MARS procedure gives us an enhanced matrix of split regressors corresponding to each basis function detected (and finally selected after the backward pruning pass). It is also interesting to estimate the linear version of the model as a benchmark for comparative purposes.

Step 3. It is necessary to compute the autocorrelation function (ACF) of the MARS residuals to verify that they are whitened; otherwise statistical inference on the parameters of the final model would not be reliable. For that purpose, we run the Box Pierce test to detect possible autocorrelations in the residuals. If so, we iteratively estimate an ARIMA transfer function with the vectors of the enhanced matrix as regressors. In each loop, the least significant variable is eliminated until the estimation process converges to a model in which all the estimated coefficients are significant and the errors are compatible with a white noise to make a more reliable statistical inference of the parameters of the final model. In this sense, our procedure applies MARS on time series data following TS-MARS developed by Keogh (2010)[2].

Step 4. Finally we construct 95% confidence intervals for each threshold applying an innovative approach. In the absence of an existing method for deriving measures of uncertainty around thresholds derived from non-parametric MARS models, we adapt to MARS model a procedure inspired by Hansen (2000)[3]. Hansen considers a simple threshold model with only one variable affected by a threshold effect, and obtains a distribution theory for the threshold parameter (τ) from which asymptotic confidence intervals can be built. He first derives the limiting distribution of a Likelihood Ratio test (LR) for the null hypothesis $\tau = \tau_0$ for the threshold parameter . He then builds confidence intervals through the inversion of LR: the $(1 - \alpha)$ Inverted Likelihood Ratio (ILR) confidence interval consisting of all the possible values of τ for which the null hypothesis would not be rejected at the α level. Donayre et al. (2018) examine improvements of Hansen's ILR confidence interval, increasing its quality in finite samples with large threshold effects (i.e. when the change in slope from one side of the threshold to the other is large). They show that a "conservative modification" enlarging Hansen's ILR confidence interval is optimal. In this "conservative ILR confidence interval" the lower end of the interval

[2]We created codes in R for estimations and the processing of the results. The main packages for estimation and plotting results are *Earth* and *Plotmo* (Milborrow (2009, 2015)).

[3] To the best of our knowledge, the computation of confidence intervals for thresholds parameters in MARS model is an innovation of this thesis.

is enlarged from the first value lower than τ_l (lower bound of the confidence interval) for which the null hypothesis is rejected, up to τ_l; at the upper end, it is enlarged from τ_u (upper bound of the confidence interval) up to the first value greater than τ_u for which the null hypothesis is rejected. According to Donayre et al. (2018), this modification provides intervals at a confidence level at least as high as the nominal one that are still informative.

We adapted this procedure for MARS estimations with possibly more than one explanatory variable containing thresholds, and/or possibly one or more thresholds per variable, by using the partial residuals – i.e. the variation in the outcome not explained by other explanatory variables and their thresholds. To simplify the explanation, let us suppose that in modeling y, we have two explanatory variables, x_1 and x_2, and that a threshold has been detected by MARS for each one, at $\tau_{x_1}\hat{}$ and $\tau_{x_2}\hat{}$ respectively. To obtain the confidence interval associated with τ_{x_1}, we obtain the "partial residuals relative to x_1" , say $y(x_1)$, which is the part of y not explained by x_2 (and its threshold). We obtain it by subtracting from y the part of the full model related exclusively with x_2. Once $y(x_1)$ is obtained, we can apply on the data of $y(x_1)$ and x_1 the procedure of Hansen (2000) improved by Donayre et al. (2018). In that way we obtain a conservative ILR confidence interval for $\tau(x_1)$ conditional on the estimated values of the parameters (slopes and thresholds) related to x_2. We then repeat the same procedure interchanging the roles of x_1 and x_2, and we now obtain the conservative ILR confidence intervals for $\tau(x_2)$ conditional on the estimated values of the parameters related tox_1[4].

The present study use data for 4 European countries: France, Germany, the Netherlands and Spain[5].

[4]Our Monte Carlo simulations, available on request, show that this procedure produce confidence intervals with a confidence level at least equal to the nominal one and short enough to be informative for the empirical analyst.

[5]We use harmonized unemployment rate and real GDP, both extracted from OECD Quarterly National Accounts. The series for France and the Netherlands started from Q1:1970 and end in Q1:2018. For the purpose of this study we avoid using retropolated data provided by OECD. Consequently, Spain's series start from Q1:1995 and end in Q1:2018. Germany's series start from Q1:1992 and end in Q1:2018.

7.4 Results.

The first step in our procedure consists of testing for a unit root in the unemployment rate of each country. We use the test proposed by Carrion-i Silvestre et al. (2009) (henceforth, C-B-P test) that allows to consider multiple structural breaks under the null hypothesis of unit root. Considering the possibility of multiple structural breaks is important to avoid detecting spurious unit roots. Table 7.1 shows the values of C-B-P test with up to 5 possible structural breaks, and the 5 percent critical value for each country. This is a left-tailed test; therefore we cannot reject the null hypothesis of unit root of unemployment rate for any country. Consequently, we run the MARS cointegration test proposed by Sephton (1994) between unemployment rate and the real GDP in a MARS model with a maximum of 10 possible basis functions, which 5% critical value is -4.46. It is also a left-tailed test under the null hypothesis of no cointegration; therefore we find no evidence of cointegration between unemployment rate and real GDP in all four countries.

Table 7.1: C-B-P test and MARS Cointegration test for each country.

	C-B-P test	C-B-P test cv(5%)	unit root?	MARS Cointegration test	Cointegration? cv(5%)=−4.46
France	58.68	8.90	yes	-3.45	no
Germany	47.20	9.34	yes	-3.57	no
Netherlands	73.50	9.26	yes	-2.83	no
Spain	90.60	9.32	yes	-2.17	no

In accordance with these results, we proceed to estimate Okun's law as specified in equation (7.2). Table 7.2 provides the main results of estimation for each country from steps 2 to 4 of our procedure. The first block, on the top of the table, offers the significant coefficients of MARS estimation for each country. The "Thresholds" row contains the detected thresholds; the next two rows contain the significant Okun coefficients below and above the threshold, respectively. For comparison purposes we include in the last row the Okun coefficient from fitting a linear Okun's law. The 95% confidence intervals are provided in brackets below each coefficient and threshold. At the bottom of the table, we provide the improvements in measures of fit when using our MARS procedure instead of a linear approach. Additionally, the p-value from the Box-Pierce tests indicate no left autocorrelation.

Although our estimation procedure is able to endogenously detect more than one threshold, Table 7.2 reports only one detected threshold in the quarterly real growth rate for each country. Figure 7.4 provides graphical representation of the results. It is important to stress that all four Okun's laws exhibit a steeper slope (in absolute value) below the threshold than above it, which is consistent with the "firm's risk aversion hypothesis".

Table 7.2: Main results of estimations.

	France	**Germany**	**Netherlands**	**Spain**
intercept	-0.0163 (-0.035, 0.002)	-0.034 (-0.059, -0.008)	-0.053 (-0.084, -0.022)	0.2086 (-0.019, 0.436)
Δu_{t-1}	0.6376 (0.489, 0.786)	0.771 (0.669, 0.873)	0.766 (0.663, 0.869)	0.3906 (0.122, 0.659)
Δu_{t-2}	-	-	-	0.2574 (-0.036, 0.551)
$ma1$	-0.2444 (-0.468, -0.021)	-	-	-
Thresholds τ	0.4342 (0.39, 0.5)	0.385 (0.35, 0.46)	0.71 (0.63, 0.76)	-0.4073 (-0.96, -0.08)
Okun coeff. above τ	-	-	-	-0.2912 (-0.51, -0.072)
Okun coeff. below τ	-0.1279 (-0.197, -0.059)	-0.094 (-0.132,. -0.056)	-0.135 (-0.195,-0.075)	-1.04367 (-1.582, -0.505)
Eurozone Crisis	0.0558 (0.00, 0.12)	-	-	.
Box Pierce Test p-value	0.9397	0.1585	0.099	0.2255
Linear Okun coeff.	-0.0637 (-0.103,-0.024)	-0.0577 (-0.085,-0.03)	-0.0856 (-0.131,-0.04)	-0.1399 (-0.245,-0.035)
Improvements of goodness of fit (MARS - OLS)				
AIC	2.452	3.552	4.5712	3.77
AICC	2.452	3.388	4.5712	3.22
BIC	2.452	0.9076	4.5712	1.21
LogLik	1.226	2.776	2.2856	3.89

The results in Table 7.2 and Figure 7.4 also show that Okun's laws are very similar

Figure 7.4: Graphs of Okun's law estimation for each country.

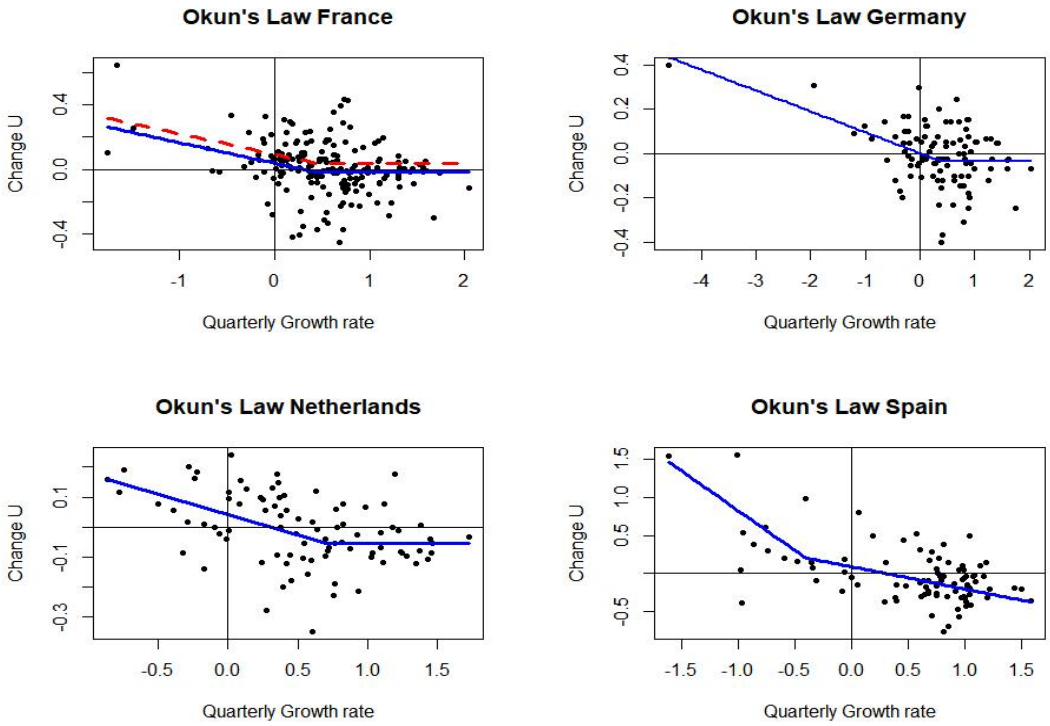

for Germany, France and the Netherlands. By contrast, Okun's law in Spain is strikingly different: in this country, Okun coefficients are higher in absolute value than those for the rest of the countries. If we consider the difference between the coefficient below and above the threshold as an approach to the degree of firm's risk aversion in the economy, risk aversion in Spain would be six times greater than in France and eight times greater than in Germany.

Differences among the detected thresholds are also remarkable. Okun's law for France, Germany and the Netherlands exhibit thresholds at significantly positive output growth rates (as reflected by their 95% confidence intervals all located at positive values), and their differences could be related to differences on "labour hoarding" described in H2: Germany and France would be more reluctant to fire trained workers than the Netherlands (this is reflected not only in the point estimates of the threshold but also in the CCILR interval estimation; the threshold for the Netherlands is significantly higher than those of France and Germany which are much closer - both algebraically and statistically- to each other). On the other hand, the threshold in Spain takes place at a significantly negative output growth

rate, and substantially below the threshold values of the other three countries: not only the threshold takes a negative value but the whole 95% CCILR confidence interval covers negative values, in contrast with the point and interval estimates of the thresholds of the other three countries. This might be due to the special rigidity of the Spanish labour market, which is in turn directly related to the "institutional rigidity" hypothesis. In other words, these results allow us to interpret that in Spain the "institutional rigidity" hypothesis on Okun's law gives rise to a threshold at a negative rate of output growth instead of creating a linearly decreasing Okun's coefficient during recessions.

Figure 7.5 contains the graphs for all the countries at the same scale for comparison purposes. France, Germany and the Netherlands show a much flatter Okun law than Spain. The level of growth a country needs to start reducing unemployment (the cut point in the x-axis) also differs among countries. The Netherlands, France and Spain start reducing unemployment around 0.3 (1.2% annual growth rate). In contrast, Germany starts reducing unemployment at a quarterly growth rate very close to zero (0.025).

Another relevant point is the constant and small reduction of unemployment when France, Germany and the Netherlands grow at a rate that exceeds their respective thresholds. By contrast in Spain again, unemployment reduction takes place at a linear increasing rate after the threshold, even for quarterly rates of output growth higher than 1.5%. France Okun's law deserves a final comment: it is the only one affected by the Euro area crisis periods, that move it slightly upwards, as shown by the results in Table 7.2 and reflected in the graph of Figures 7.4 and 7.5 by the dashed line.

Figure 7.5: Comparative of Okun's law across countries (Spain scale).

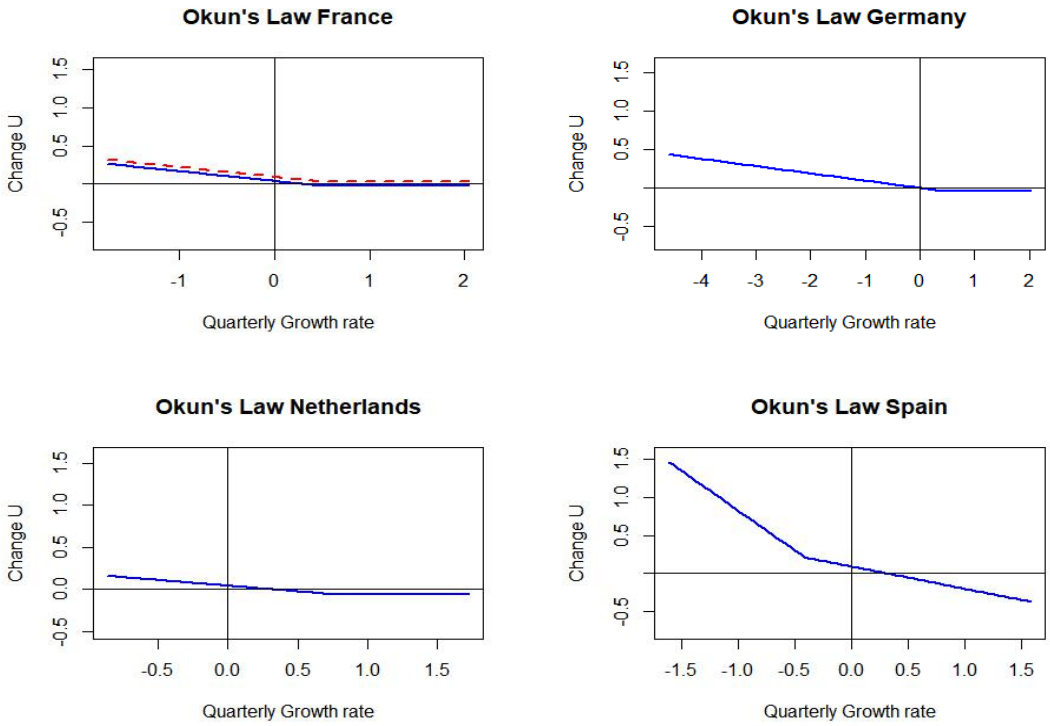

Figure 7.6 shows the unemployment (dashed line) and the quarterly growth rate (solid line) historical time series for each country, together with the detected threshold for each country. The shaded vertical bands correspond to the Euro area crisis periods when our dummy variable takes value 1. In each country graph, the horizontal dot-dashed straight line corresponds to the detected threshold of the quarterly growth rate as reported in Table 7.2. As already commented, all thresholds, except for Spain, are located above zero.

As far as the influence of the Euro area crisis in France is concerned, time series for France in Figure 6 shows that, in general terms, during Eurozone crisis periods the increase in French unemployment is more intensive than outside these periods. This reflects the idea that, at least in France, decision makers under the "firm's risk aversion hypothesis" are not only concerned by their own country economic information but also by the information from the economic area they are operating in.

Figure 7.6: Quarterly growth and unemployment rate time series with Eurozone crisis periods (shaded fringes) and the detected threshold.

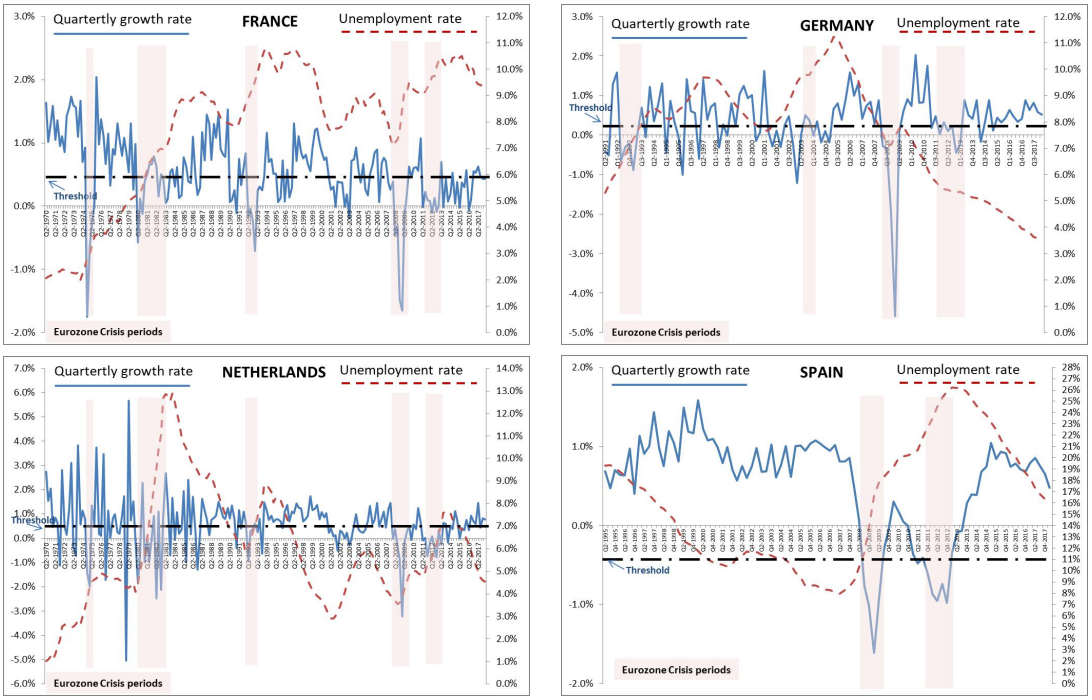

7.5 Conclusions.

In this paper we estimate Okun's law for four European countries (France, Germany, the Netherlands and Spain) with the MARS procedure adapted to time series, to endogenously detect possibly multiple thresholds. We use the ARIMA transfer function refinement to whiten the error to increase inference reliability, and we compute confidence intervals for the thresholds which inform us about the accuracy of the estimates and allow us to test the significance, the sign and the value of the thresholds. We also include the dummy variable for the Eurozone crisis created by CEPR Euro Area Business Cycle Dating Committee, that establishes the chronology of recessions and expansions in the Euro area.

To summarize our results: a) for each country we detect only one threshold in quarterly growth rate; b) Okun's law for Germany, France and the Netherlands are very similar and quite flat, whereas Okun's law for Spain is much steeper; c) for each

country, differences between Okun coefficients below and above the threshold are consistent with the firm's risk aversion hypothesis, and reveal particularly high risk aversion in the Spanish firms; d) the differences between thresholds across countries can be related to the "labour hoarding hypothesis", and show that the German and French firms are more reluctant to fire trained workers than the Dutch ones; e) the fact that the detected threshold for Spain takes place at a significant negative output growth rate, and is substantially lower than the significantly positive threshold value for the other countries, is also consistent with the "institutional rigidity hypothesis"; f) the Euro area crisis affects Okun's law in France, reflecting the idea that decision makers under firm's risk aversion hypothesis are also concerned about the information from the economic area they are operating in.

Our results potentially enrich not only Okun's law estimations and interpretations but also the debate over how the different theoretical hypothesis intervene and shape the Okun's law in each country. Combining nonlinearity and threshold location may be helpful to better understand how the diverse theoretical hypotheses intervene in the recovery after the recent crisis of some European countries facing high unemployment rates. Since we are not imposing previously a fixed number of thresholds, this data-driven procedure offers empirical results of the Okun's law much more general than those published to date.

The application of this approach to other European and/or OECD countries is left for further research, with the hope of improving the understanding of how the different hypotheses about nonlinearities of Okun's law combine and interact with each other.

Finally, a direct implication follows from our findings: the remarkable differences between Okun's law of the Eurozone countries, in particular between the core and Spain, demonstrate the need to erode the institutional differences and of regulation of the implied national labour markets. Otherwise, any demand policy at the European level, and in particular the monetary policy of the ECB, which is necessarily the same for all countries of the Eurozone, will have a very different impact on the labour markets and on the macroeconomic magnitudes of the countries under study.

8 Finding population antibiotic use thresholds to control antibiotic resistance.

Balancing the need for antibiotic use with the containment of antibiotic resistance is a global public health priority. To date, both empirical evidence and antibiotic stewardship policy have tended to consider use-resistance relationships to be linear. However, theoretical and mathematical models give several reasons for relationships being non-linear. One explanation is that resistance genes are commonly associated with 'fitness costs', impairing the replication or transmissibility of the pathogen. Therefore, resistant genes and pathogens may only gain a survival advantage, and proliferate within populations, where antibiotic selection pressures exceed critical thresholds. These thresholds may provide optimal targets for containing antibiotic use while avoiding over-restriction. We evaluated the generalisability of a non-linear time-series analysis approach for identifying thresholds using historical monthly data on population use of antibiotics and rates of infection with different resistant pathogens from five European settings in Hungary, Spain (two sites), France, and Northern Ireland. We frequently identified minimum thresholds in relationships between use of selected antibiotic groups and resistance outcomes in both hospital and community populations, and at different epidemiological phases. Utilising the increasing availability of electronic data and surveillance systems, non-linear time-series can identify context-specific quantitative targets for rationalising population antibiotic use and controlling resistance.

8.1 Introduction.

Antimicrobials have been a catalyst for improvements in health and food-security worldwide. However, excessive use has led to increasing antimicrobial resistance (AMR), undermining many aspects of healthcare and generating new disease burdens (Laxminarayan, 2014; Laxminarayan et al., 2013; Group, 2016; O'Neill, 2017). A key challenge is that while decisions around antimicrobial use are made by individual prescribers and patients, consequences of over-use are only fully apparent across populations (Millar, 2012). As with other global common goods, such as climate stability, competing needs and non-exclusivity can lead to a 'tragedy of the commons'(Laxminarayan, 2014; Laxminarayan et al., 2013). The Global Action Plan on AMR therefore highlights the importance of cross-societal efforts to conserve the effectiveness of current antimicrobials (WHO, 2017). In healthcare, antimicrobial stewardship aims to control AMR by reducing inappropriate use, while ensuring access to effective therapy (Laxminarayan et al., 2013). There is growing evidence that reducing the use of antimicrobials strongly selecting for resistance, can effectively reduce AMR (Davey et al., 2013). However, over-restriction may be counter-productive. For example, use of alternative antimicrobials may increase in response, leading to new selection pressures or resistance problems (Peterson, 2005). Balancing the benefits and risks of antimicrobials in healthcare requires understanding of their effects on AMR at population scales (Levy, 1994; Levin et al., 1997; Austin et al., 1999).

To date, empirical evidence has generally considered use-resistance relationships as linear (López-Lozano et al., 2000; Vernaz et al., 2011; Aldeyab et al., 2008; Monnet et al., 2004; Aldeyab et al., 2012). These are useful for identifying the most salient selection pressures in a population (López-Lozano et al., 2000), but theoretical and mathematical models suggest that non-linear relationships are more likely (Levy, 1994; Levin et al., 1997; Austin et al., 1999; Haber et al., 2010). In particular, selection pressures may only have notable impact on resistance rates, where volumes of antibiotic use in the population are above minimum thresholds. Potential explanations for minimum thresholds, include: antibiotic substitution with changes in use (Peterson, 2005); associations between the strength of selection pressure and induction of co-resistance (Oz et al., 2014); differential effects on sub-populations within bacterial species (Arepyeva et al., 2017), or ecological niches (Kiffer et al., 2011); and the 'total use thresholds' hypothesis Levy (1994). The latter concept

arises from the observation that resistance genes are commonly associated with 'fitness costs' impairing pathogen replication or transmissibility (Vogwill and MacLean, 2015). Resistant pathogens may therefore only gain a survival advantage over susceptible organisms, where selection pressures from antibiotic use outweigh fitness costs (Levy, 1994). If identified, minimum thresholds may offer important targets for antibiotic stewardship, indicating an upper limit of safe population antibiotic use which does not substantially increase rates of resistance at population scales.

Non-linear relationships between fluoroquinolone use and resistant E.coli and Staphylococcus aureus have been reported using different methods (Kiffer et al., 2011; Berger et al., 2004). We have previously shown that reducing antibiotic use to below minimum thresholds predicted shifts in the molecular and clinical epidemiology of S. aureus and Clostridium difficile (Lawes et al., 2015b,a, 2017). However, these studies suggest antibiotic use-resistance relationships are likely to depend upon the clinical population (Levy, 1994; Lawes et al., 2015b, 2017), pathogen genotypes (Lawes et al., 2015a), intensity of infection control (Lawes et al., 2015a), and transmission dynamics (Austin et al., 1999). Moreover, fitness costs associated with different resistance genes are variable (Vogwill and MacLean, 2015). If 'fitness costs' are low, or attenuated through epistasis (Wong, 2017) or compensatory mutations (Levin et al., 2000), resistance may persist despite removing previously important antibiotic selection pressures (Andersson and Hughes, 2010). A generalisable method for finding minimum thresholds should therefore provide context-specific information, have relatively low-informational demands, and allow for iteration.

Here, we examined the generalisability of a non-linear time-series analysis methodology for identifying minimum threshold in use-resistance associations. Using routinely generated healthcare data from five European centres, we show this pragmatic approach can provide population-specific quantitative targets for antimicrobial stewardship for a variety of resistance outcomes, epidemiological phases, transmission dynamics, and clinical populations.

8.2 Results.

Identifying nonlinear temporal relationships: from experiment to application.

We used a Monte Carlo experiment to compare the ability of linear and non-linear time-series analysis (Multivariate Adaptive Regression Splines, MARS) to identify pre-defined relationships between simulated explanatory and outcome time-series (See Appendix A Figure 8.7). Non-linear time-series analysis (NL-TSA) accurately identified both truly linear and non-linear associations. However, linear time-series analysis provided biased estimations and overall poorer data-fit if relationships were non-linear. NL-TSA models applied to retrospective time-series data from five European study populations (Examples 1-5)[1], frequently identified non-linear relationships between explanatory and resistance time-series, including minimum thresholds in antibiotic use-resistance relationships, (8.1, Figures 1-6). 'Ceiling effects', in which further increases in explanatory variables did not further affect resistance rates, were found at high-levels of use of some antibiotics and hand hygiene. Non-linearities in autoregression and population interaction terms further indicated the complexity of transmission dynamics within and between clinical populations.

[1]These results have been presented at 28th European Congress of Clinical Microbiology and infectious Diseases in Madrid, and the results for Debreçen at Liverpool University.

Table 8.1: Results of non-linear time-series analysis (MARS) models.

Predicting variable	Lag[a]	Threshold (95% CI)[b]	Relation to threshold[c]	Coefficient (95% CI)[d]	T-ratio	p value
1: Carbapenem-resistant *Acinetobacter baumannii* (CRAb)‡ Debrecen, Hungary [R2 0.859; MAPE 45.3%; MGCV 2.254]						
Constant	-	-	-	6.962 (6.157 to 7.767)	16.9	<0.0001
Previous CRAb incidence density	1	6.2 (4.7 to 8.0)	Below	0.563 (0.326 to 0.801)	4.64	<0.0001
Previous CRAb incidence density	1	9.4 (7.0 to 11.2)	Above	0.932 (0.478 to 1.386)	4.02	0.0001
Previous CRAb incidence density	2	9.4 (7.8 to 12.3)	Below	0.397 (0.235 to 0.559)	4.79	<0.0001
Carbapenem use	3	15.4 (8.1 to 23.9)	Above	0.067 (0.028 to 0.106)	3.39	0.0007
Piperacillin-tazobactam use	3	7.0 (5.0 to 14.0)	Above	0.296 (0.070 to 0.523)	2.56	0.0102
Fluoroquinolone use	1	85.2 (65.6 to 103.0)	Above	0.060 (0.019 to 0.100)	2.89	0.0038
2: Extended-spectrum β-lactamase producing *E. coli* (%Ec-ESBL+)^ Orihuela, Spain						
***a) Hospital* [R^2 0.622; MAPE 57.1%; MGCV 19.97]**						
Constant	-	-	-	5.858 (3.288 to 8.428)	4.46	<0.0001
Previous %Ec-ESBL+ (hospital)	3	9.9 (6.3 to 13.3)	Below	0.266 (0.488 to 0.045)	2.51	0.0129
Previous %Ec-ESBL+ (hospital)	3	9.9 (6.3 to 13.3)	Above	-0.254 (-0.45 to -0.058)	2.77	0.0061
%Ec-ESBL+ (community)	2	10.1 (5.9 to 20.0)	Below	0.359 (0.579 to 0.138)	3.08	0.0024
%Ec-ESBL+ (community)	2	10.1 (5.9 to 20.0)	Above	-1.291 (-2.066 to -0.516)	3.26	0.0013
Third-gen. ceph. use (hospital)	1	65.15 (36.5 to 95.5)	Above	0.061 (0.029 to 0.093)	3.28	0.0012
Fluoroquinolone use (hospital)	2	82.28 (70.5 to 101.1)	Above	0.122 (0.085 to 0.159)	6.07	<0.0001
Fluoroquinolone use (hospital)	2	150.83 (145.5 to 155.2)	Above	-0.269 (-0.495 to -0.044)[e]	-2.34	0.0203
Fluoroquinolone use (hospital)	2	160.32 (153.3 to 168.0)	Above	0.010 (-0.300 to 0.319)[e]	0.06	0.9522
***b) Community* [R^2 0.768; MAPE 46.2%; MGCV 4.715]**						
Constant	-	-	-	4.828 (3.774 to 5.883)	8.97	<0.0001
Previous %Ec-ESBL+	3	7.3 (5.9 to 10.3)	Below	0.423 (0.266 to 0.597)	5.11	<0.0001
Previous %Ec-ESBL+	4	4.1 (2.1 to 5.8)	Above	0.473 (0.302 to 0.645)	5.40	<0.0001
Previous %Ec-ESBL+	5	1.1 (0.9 to 4.7)	Above	0.167 (0.062 to 0.273)	3.10	0.0021
%Ec-ESBL+ (hospital)	1	5.5 (1.61 to 12.50)	Below	0.286 (0.106 to 0.466)	3.11	0.0020
Co-amoxiclav use (community)	4	6.7 (5.0 to 10.0)	Above	0.549 (0.223 to 0.875)	3.30	0.0010
Fluoroquinolone use (community)	6	2.8 (1.4 to 5.2)	Above	0.635 (0.174 to 1.100)	2.70	0.0070
3: Cefepime-resistant *E. coli* (%EcFepR)* Seville, Spain [R^2 0.301; MAPE 41.6%; MGCV 12.11]						
Constant	-	-	-	6.163 (5.164 to 7.161)	12.1	<0.0001
Previous %EcFepR	12	11.6 (1.2 to 21.9)	Above	0.580 (0.254 to 0.907)	3.48	0.0005
Audit 2*%EcFepR	1	5.8 (4.6 to 7.0)	Above	-2.801 (-4.669 to -0.994)	-2.93	0.0033
Audit 2*%EcFepR	1	7.1 (5.8 to 8.4)	Above	3.301 (0.923 to 5.680)	2.72	0.0065
Fluoroquinolone use	3	138.2 (79.5 to150.4)	Above	0.105 (0.012 to 0.198)	2.2	0.0272
3rd/4th gen cephalosporin use	4	45.8 (29.1 to 55.6)	Above	0.197 (0.103 to 0.291)	4.1	<0.0001
4: Gentamicin-resistant *Pseudomonas aeruginosa* (GRPa)§ Besançon, France [R^2 0.857; MAPE 27.3%; MGCV 2.66]						
Constant	-	-	-	3.236 (2.894 to 3.577)	18.5	<0.0001
Previous GRPa incidence density	1	4.8 (3.4 to 5.8)	Above	0.670 (0.563 to 0.773)	12.4	<0.0001
Previous GRPa incidence density	12	2.7 (1.6 to 5.1)	Above	0.170 (0.073 to 0.268)	3.43	<0.0001
Gentamicin and tobramycin use	1	8.0 (3.9 to 10.6)	Above	0.221 (0.077 to 0.365)	4.18	<0.0001
Fluoroquinolone use	1	81.0 (78.0 to 84.0)	Above	0.045 (0.029 to 0.061)	3.01	0.003
5: Methicillin-resistant *Staphylococcus aureus* (MRSA)§ Antrim, Northern Ireland [R^2 0.561; MAPE 15.1%; MGCV 0.331]						
Constant	-	-	-	1.982 (1.762 to 2.202)	17.6	<0.0001
Previous MRSA incidence density	3	1.9 (1.1 to 2.5)	Above	0.273 (0.086 to 0.460)	2.86	0.0042
Fluoroquinolone use	3	16.8 (14.2 to 20.7)	Above	0.003 (0.000 to 0.006)	2.13	0.0299
Third-gen. cephalosporin use	3	4.9 (4.3 to 5.7)	Above	0.026 (0.015 to 0.037)	4.51	0.0005
Co-amoxiclav use	1	224.9 (132.8 to 296.6)	Above	0.003 (0.002 to 0.005)	4.39	<0.0001
Alcohol-based hand rub use	2	6.9 (3.9 to 16.1)	Below	-0.133 (0.047 to 0.218)	3.04	0.0024

DDDs Defined Daily Doses; MGCV Modified Generalised Cross Validation criteria (a lower value indicates a more efficient model; MAPE Mean Average Percentage Error (observed/predicted × 100); OBDs Occupied Bed Days; R^2 indicates the percentage of total variation in outcome explained.

a average delay (in months) between change in predictive time-series and associated change in outcome time-series

b value of the predicting variable at which the association with the outcome changes, with 95% conditional conservative inverted likelihood ratio (CCILR) confidence intervals (see Methodology section for details).

c Indicator of whether the association is seen below or above the threshold.

d Coefficient refers to the change in the outcome for a 1 unit (e.g. DDD) increase in the explanatory variable

e contribution above this threshold derived from sum of coefficients operating above current and any other lower thresholds for same variable and lag combination.

‡ Cases per 10 000 OBDs. § Cases per 1000 OBDs. ^ Percentage of all non-duplicate *E. coli* isolates positive for ESBL. * Percentage of all non-duplicate *E. coli* isolates resistant to cefepime.

Table 8.2: Translation of thresholds identified in non-linear models into population-specific antibiotic stewardship policy suggestions.

Antibiotic	Patient treatments per month[a]			
	Maximum suggested by threshold (95% CI)	Average use in last 12 months of study	Suggested reduction in use (%)	
			Standard (using point estimate for threshold)	Conservative (using lower limit of 95% CI for threshold)
1. Carbapenem-resistant *Acinetobacter baumannii* (CRAb)‡ Debrecen, Hungary				
Carbapenems	86 (45 to 134)	226	140 (62%)	181 (80%)
3rd generation cephalosporins	203 (169-229)	299	96 (32%)	130 (57%)
Fluoroquinolones	478 (367-576)	375	Maintain below threshold	9 (2%)
Piperacillin-tazobactam	39 (28-78)	41	2 (5%)	13 (32%)
2. Extended-spectrum β-lactamase producing *Escherichia coli* (%Ec-ESBL+) Orihuela, Spain				
a) Hospital population				
Fluoroquinolones	78 (67 to 96)	165	68 (41%)	87 (53%)
Third-generation cephalosporins	62 (35 to 91)	78	16 (21%)	43 (55%)
b) Community population				
Fluoroquinolones	80 (40 to 148)	66	Maintain below threshold	26 (39%)
Co-amoxiclav	191 (142 to 284)	277	86 (31%)	135 (49%)
3. Cefepime-resistant *Escherichia coli* (%EcFepR) Seville, Spain				
Fluoroquinolones	392 (225 to 426)	351	Maintain below threshold	126 (36%)
3rd/4th generation cephalosporins	130 (83 to 158)	211	87 (41%)	128 (61%)
4. Gentamicin-resistant *Pseudomonas aeruginosa* (GRPa) , France				
Gentamicin and tobramycin	75 (36-99)[b]	68[b]	Maintain below threshold	32 (47%)
Fluoroquinolones	324 (316 to 330)	223	Maintain below threshold	Maintain below threshold
5. Methicillin-resistant *Staphylococcus aureus* (MRSA) Antrim, Northern Ireland				
Fluoroquinolones	24 (20 to 29)	39	15 (39%)	19 (49%)
3rd generation cephalosporins	7 (6 to 8)	6	Maintain below threshold	Maintain below threshold
Co-amoxiclav	320 (189 to 422)	320	Maintain below threshold	131 (41%)

a Derived by multiplying the threshold in table 1, expressed in DDDs per 1000 OBDs, by the size of the population (in 1000 OBDs or IDs), and then dividing by an average patient treatment (considered as 7 DDDs unless otherwise specified)
b Average treatment course considered as 3 DDDs.

Example 1: Carbapenem-resistant *Acinetobacter baumannii* (Debrecen, Hungary)

Scenario: We examined ecological determinants of carbapenem-resistant *Acinetobacter baumannii* (CRAb) in a tertiary hospital population in Debrecen, Hungary (Figure 1). Between Oct 2004 and Aug 2016 (n=143 months), incidence density of CRAb increased from a 12-month average of 0.14 to 9.43 cases per 10000 OBDs, while that of carbapenem susceptible *A. baumannii* (CSAb) remained relatively constant. There were no planned antibiotic stewardship interventions in the study period, but we observed increasing use of broad-spectrum antibiotics, including a tripling in carbapenem use, and rising colistin use in later study months.

Hypothesis: Carbapenem resistance in this setting was conferred predominantly by$bla_{OXA-23-like}$ carbapenemases, while $bla_{OXA-24-like}$ genes occurred sporadically (Mózes et al., 2014). CRAb were significantly more likely to be resistant to ciprofloxacin, gentamicin, amikacin, piperacillin-tazobactam and ceftazidime than CSAb (Figure 1a), although susceptibility testing for the latter two agents was discontinued in 2013 as recommended by EUCAST. Colistin resistance was rare in both

CRAb and CSAb (1% *vs.* 2%; p=0.06). Vector autoregression (VAR) models, suggested that colistin use followed, rather than predicted, variation in CRAb incidence density. We identified population use of carbapenems, fluoroquinolones, piperacillin-tazobactam, third generation cephalosporins, and aminoglycosides as potentially important explanatory variables.

Model estimation: Previous CRAb incidence density and recent hospital use of carbapenems, piperacillin-tazobactam, and fluoroquinolones were explanatory variables in the best-fit ($R^2 = 0.86$) non-linear TSA model (Table 8.1). In an almost identical model, but with poorer trade-off of data fit and model complexity (higher Modified Generalised Cross Validation, MGCV), fluoroquinolone use was replaced by the effect of third-generation cephalosporin use above a threshold of 36 (95% CI, 30 to 41) DDDs per 1000 OBDs (coefficient, 95% CI: 0.111, 0.018 to 0.203; p=0.019; lag 3).

Policy implications: In this setting increases in CRAb added to, rather than replaced, clinical burdens from CSAb, suggesting CRAb occupied new ecological niches. Strong autoregression in the CRAb time-series was consistent with previous evidence for substantial within-hospital transmission (Mózes et al., 2014). CRAb incidence density increased when population use of carbapenems, piperacillin-tazobactam, fluoroquinolones, and third-generation cephalosporins exceeded minimum thresholds. By the end of the study period, use of fluoroquinolones had reduced to below threshold. However, CRAb could be further controlled by reducing use of carbapenems (-63%), third-generation cephalosporins (-32%) and piperacillin-tazobactam (-2%) from present levels to respective thresholds (Table 8.2).

Figure 8.1: Carbapenem-resistant A. baumannii and antibiotic use.

a

Antibiotic in antibiogram	CRAb (% I/R)	CSAb (%I/R)	Difference in % non-susceptible	p-value
Cefotaxime	98%	72%	26.0 (22.7 to 29.2)	<0.001
Ciprofloxacin	97%	67%	28.3 (24.9 to 31.6)	<0.001
Piperacillin-tazobactam	94%	22%	72.4 (69.1 to 75.6)	<0.001
Ceftazidime	93%	56%	36.8 (33.0 to 40.6)	<0.001
Gentamicin	91%	55%	36.0 (32.4 to 39.6)	<0.001
Amikacin	89%	43%	46.6 (43.1 to 50.2)	<0.001
Colistin	1%	2%	-1.2 (-2.7 to 0.3)	0.053

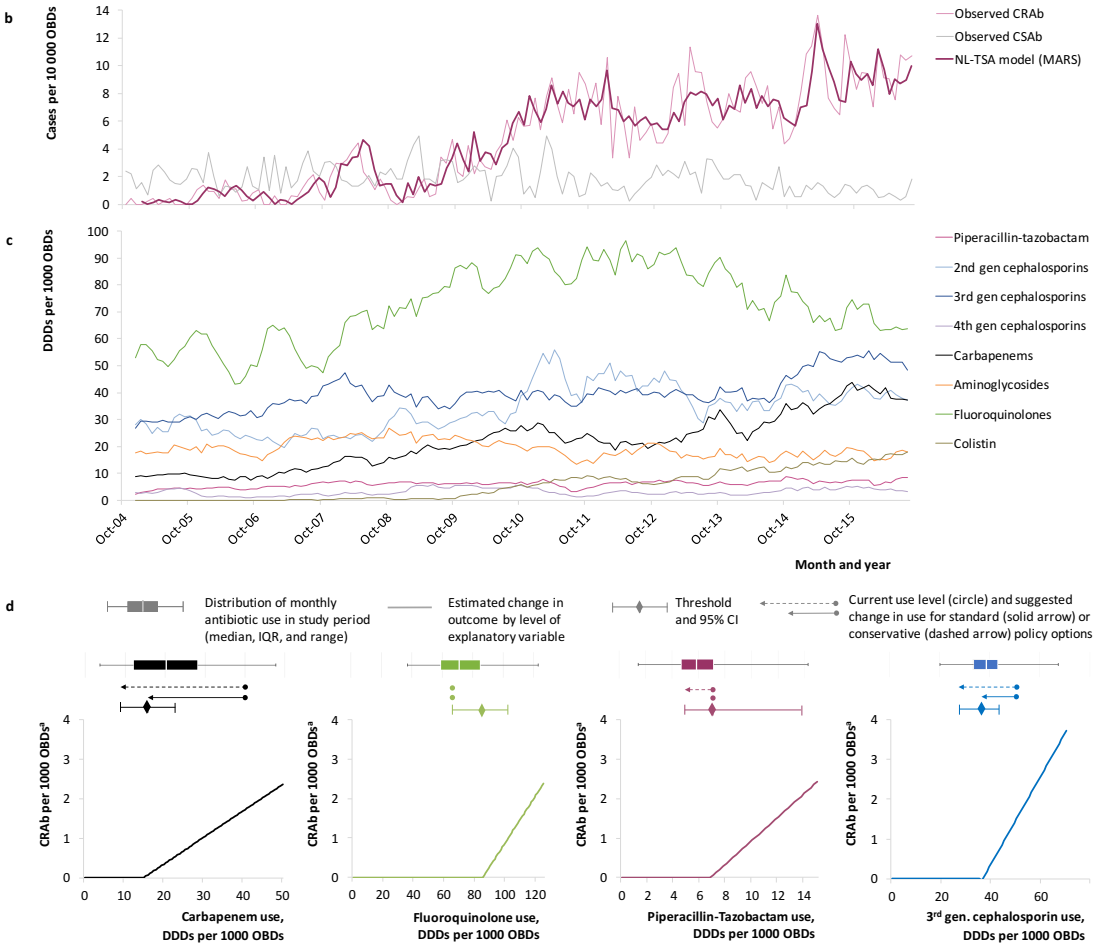

(a) Frequency of co-resistances to other antibiotics in CRAb and CSAb (b) Time series for observed and predicted incidence density of CRAb, with observed incidence density of CSAb (c) Time series for use of potential explanatory antibiotic groups (5-month moving averages) (d) Contribution charts illustrating the relationship between explanatory variables and CRAb incidence density. a Change relative to median monthly CRAb incidence density for study period. CRAb, carbapenem-resistant A. baumannii. CSAb, carbapenem-susceptible A. baumannii. DDDs, defined daily doses. IQR, Interquartile range. MARS, Multivariate Adaptive Regression Splines. NL-TSA, non-linear time series analysis. OBDs, occupied bed days.

Example 2: Extended spectrum β-lactamase producing *E. coli* (Orihuela, Spain)

Scenario: We examined ecological determinants of % *E. coli* infections producing ESBL (%Ec-ESBL+) in connected district general hospital and community populations in Orihuela, Spain, between Jul 1991 and Oct 2016 (n=304 months, Figure 8.2). Limited outbreaks of ESBL-producing *E. coli* were noted in both community and hospital from 1998, but from the last quarter of 2002 the %Ec-ESBL+ increased rapidly alongside escalating use of fluoroquinolones and co-amoxiclav (Figure 2b and 2c). While use of these agents later stabilised or declined, hospital use of third-generation cephalosporins continued to increase.

Hypothesis: Over the study period, bla_{CTX-M} genes were common in *E. coli* across Spain, with both dissemination of the $CTX-M-15$ producing $O25b-ST131$ clone and clonally unrelated strains harbouring $CTX-M-14$ identified (Díaz et al., 2010; Rodríguez-Baño et al., 2008). Acquisition of fluoroquinolone resistance was a key step in the evolution of dominant $bla_{CTX-M-15}$ containing sub-clones of $O25b-ST13$ (Branger et al., 2005). In line with this, 81% of ESBL-producing *E. coli* in Orihuela were non-susceptible to ciprofloxacin (Figure 2a). ESBL-producing *E. coli* were also significantly more likely to be resistant to co-trimoxazole, co-amoxiclav and aminoglycosides compared to non-ESBL *E. coli*. Preliminary vector autoregression models identified bidirectional interactions between community and hospital %Ec-ESBL+ and showed that use of piperacillin-tazobactam and carbapenems followed, rather than predicted, changes in %Ec-ESBL+. We built separate models for hospital and community considering %Ec-ESBL in the other population, as an explanatory variable.

Model estimation: The best-fit model ($R^2 = 0.62$) hospital %Ec-ESBL+ was predicted by prior %EcESBL in hospital and community, and hospital use of third-generation cephalosporins, and fluoroquinolones exceeding minimum thresholds. A potential 'ceiling' effect was noted at high-levels of fluoroquinolone use, meaning that when use exceeded a second upper threshold, further increases in %Ec-ESBL+ were marginal. An initial decrease in %Ec-ESBL+ where fluoroquinolone use was between 151 and 161 DDDs per 1000 OBDs reflected uncertainty around this ceiling threshold, which may be resolvable with additional data. In the model for community %Ec-ESBL+ ($R^2 = 0.767$), associations were identified with hospital %Ec-ESBL+, and community use of fluoroquinolones and co-amoxiclav above mi-

nimum thresholds.

Policy implications: Autoregressive and population interaction effects suggested the importance of horizontal transmission of ESBLs, with spread from community to hospital particularly strong. Population use of broad-spectrum beta-lactams and fluoroquinolones were also important in shaping the epidemiology of ESBL+ *E. coli* in both settings. In the community, use of fluoroquinolones had fallen below threshold levels and %Ec-ESBL+ had started to decrease by the end of the study. However, translating thresholds into antibiotic stewardship targets (Table 8.2) suggested further restricting community co-amoxiclav use by 31% and hospital use of fluoroquinolones (-41%) and third-generation cephalosporins (-21%).

Using the fitted non-linear TSA model, we created projections for %Ec-ESBL+ in the hospital and community over the next 24-months under different antibiotic stewardship options, and compared these to expected %Ec-ESBL+ under a 'business as usual' scenario of continuing antibiotic use patterns observed in the last year of study (See Appendix A Figure 8.8). Immediate restriction of hospital fluoroquinolones and third-generation cephalosporin use to thresholds was predicted to cause an abrupt and sustained reduction in hospital %Ec-ESBL+ from 9.89% to 2.35% (mean difference, 95% CI: -7.54, -7.94 to -7.19 percentage points; $p<0.0001$) and, due to population interactions, a gradual reduction in community %Ec-ESBL+ from 7.11% to 3.69% (-3.42, -3.60 to -3.18 percentage points; $p<0.0001$). Controlling co-amoxiclav use in community was predicted to have a small but significant impact in reducing community %Ec-ESBL+, but not to significantly affect hospital burdens.

Figure 8.2: Extended-spectrum β-lactamase (ESBL)-producing Escherichia coli and antibiotic use in hospital and community.

a

Co-resistance	ESBL+ E.coli (I/R%)	ESBL- E.coli (I/R%)	Difference in % resistance	p-value
Cefuroxime	100%	2%	98.1 (96.2 to 100.0)	<0.001
Ceftazidime	100%	7%	93.0 (90.1 to 95.9)	<0.001
Aztreonam	99%	2%	96.9 (94.1 to 99.7)	<0.001
Ciprofloxacin	81%	31%	49.8 (47.3 to 52.3)	<0.001
Cefepime	78%	3%	74.6 (72.0 to 77.2)	<0.001
Cotrimoxazole	53%	32%	21.1 (18.3 to 23.9)	<0.001
Co-amoxiclav	31%	15%	16.2 (13.8 to 18.6)	<0.001
Gentamicin	29%	10%	18.9 (15.8 to 22.0)	<0.001
Piperacillin-tazobactam	5%	2%	2.8% (-0.2 to 5.8)	0.067

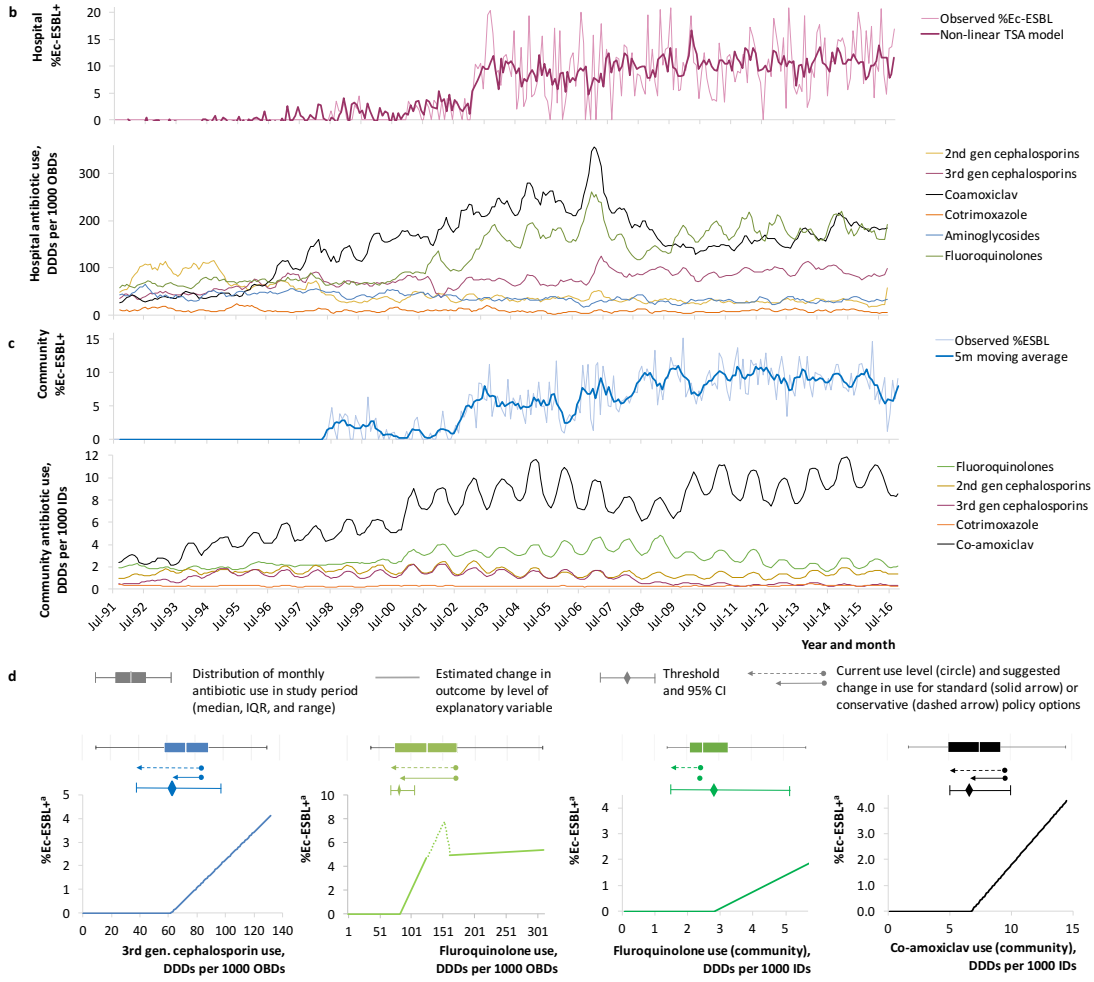

(a) Frequency of co-resistances to other antibiotics in ESBL+ and non-ESBL E. coli isolates. (b) Time series for observed %Ec-ESBL+ with model fit and for use of potential explanatory antibiotic groups in hospital population (5-month moving averages) (c) Time series for observed %Ec-ESBL+ with model fit and use of potential explanatory antibiotic groups in community population (5-month moving averages) (d) Contribution charts illustrating the relationship between explanatory variables and hospital or community %Ec-ESBL+ a compared to median monthly %Ec-ESBL+ for study period. %Ec-ESBL+, percentage of E. coli isolates producing extended-spectrum beta-lactamases. DDDs, defined daily doses. IQR, Interquartile range. MARS, Multivariate Adaptive Regression Splines. NL-TSA, non-linear time series analysis. OBDs, occupied bed days.

Example 3: Cefepime-resistant *Escherichia coli* (Seville, Spain)

Scenario: We examined ecological predictors of cefepime resistance among all *E. coli* urinary or invasive infections (%Ec-FepR) in a tertiary hospital in Seville, Spain. Between March 2008 and December 2016 (n=108 months) %Ec-FepR fell from 12.6% to 7.9% (Figure 8.3). Cefepime use was low, declining from 4.4 to 1.6 DDDs per 1000 OBDs with thrice-weekly (Jan 2012, audit1) and daily (Jan 2014, audit2) prescription audits. By contrast, previously declining use of third-generation cephalosporins increased from January 2013 when they replaced co-amoxiclav and ciprofloxacin as first-line empirical therapy for intra-abdominal or urinary infections.

Hypothesis: Resistance to cefepime in *E. coli* is mostly conferred by ESBLs with high affinity for cefepime (TEM-, SHV- and CTX-M-types). In addition to those agents hypothesised to predict ESBL+ *E. coli* (see Example 2), we considered the role of piperacillin-tazobactam, previously found to predict cefepime resistance in *E. coli* (Vernaz et al., 2011). Due to low rates of cefepime prescribing, we grouped this with third-generation cephalosporin use. We introduced variables for antibiotic auditing interventions and for revised susceptibility breakpoints (Oct 2014) (Rodríguez-Baño et al., 2012).

Model estimation: The final non-linear model ($R^2 = 0.30$) identified associations with %Ec-FepR 12 months prior (seasonal effect) and use of third- or fourth-generation cephalosporins and fluoroquinolones above minimum thresholds. A significant interaction term between %Ec-FepR in the previous month (autoregression, lag 1) and the second antibiotic auditing intervention suggested a gradual effect of the audit in reducing %Ec-FepR.

Policy implications: Reductions in third- and fourth-generation cephalosporins and fluoroquinolone use to below minimum thresholds explained modest declines in %Ec-FepR between 2008 and 2012. Partial reversal in this trend was consistent with increasing use of third-generation cephalosporins towards the end of the study period. From the scenario in the last year of study, our model suggested %Ec-FepR could be controlled further by reducing third- and fourth-generation cephalosporin use by 41% (Table 8.2).

Figure 8.3: Cefepime-resistant Escherichia coli and antibiotic use.

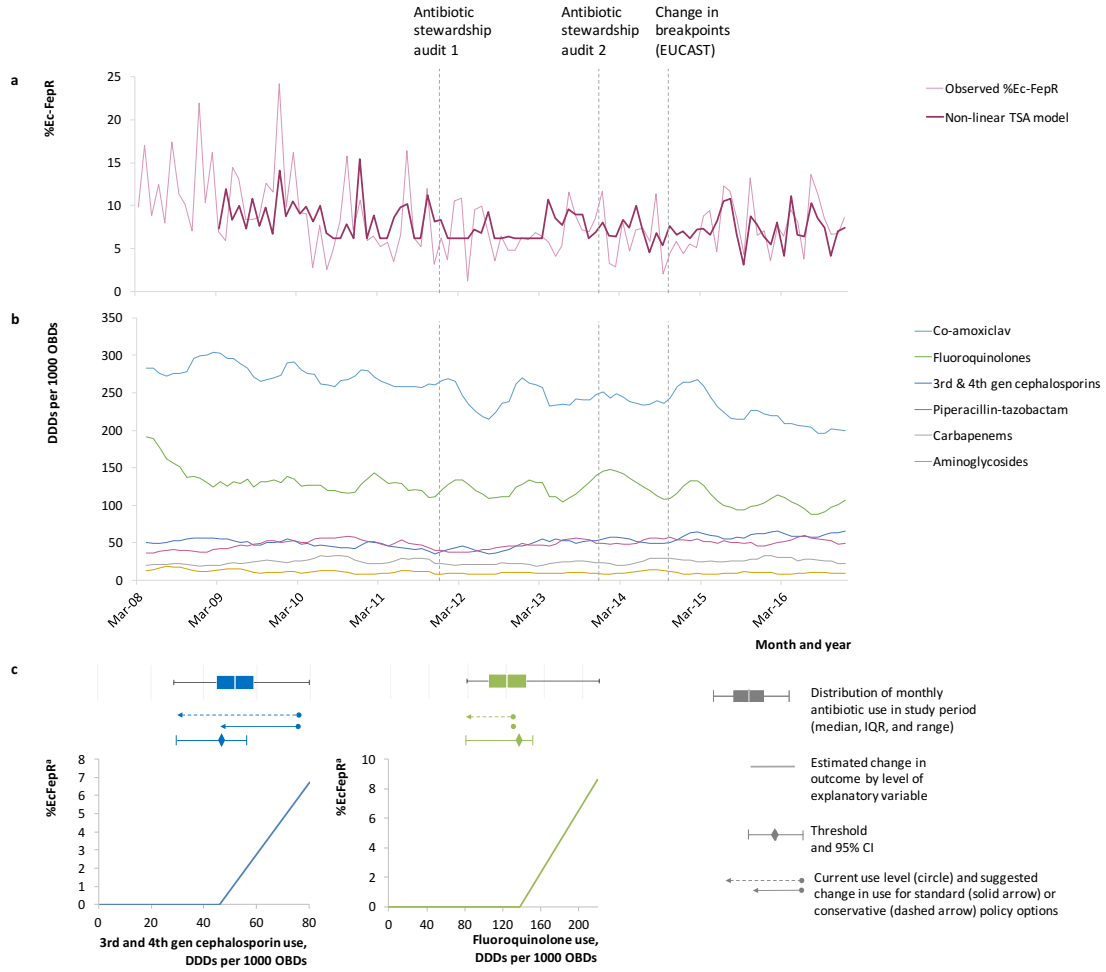

(a) Time series for observed and model predicted incidence density of %Ec-FepR and total number of E.coli isolates per month; (b) Time series for potential explanatory antibiotic groups (5-month moving averages) (c) Contribution charts illustrating the relationship between explanatory variables and %Ec-FepR

[a]compared to median monthly %Ec-FepR for study period. DDDs, Defined Daily Doses. IQR, interquartile range. %Ec-FepR, percentage of E. coli isolates resistant to cefepime. OBDs, Occupied Bed Days.

Example 4: Gentamicin-resistant *Pseudomonas aeruginosa* (Besançon, France)

Scenario: We examined ecological variables explaining rates of gentamicin-resistant *P. aeruginosa* (GRPa) among adult and paediatric admissions to a tertiary hospital in Besançon, France (Figure 8.4). Between Jan 1999 and Dec 2014 (n=192 months), incidence density of GRPa decreased from a 12-month average of 14.0 to 3.4 cases per 1000 OBDs, and the proportion of *P. aeruginosa* isolates resistant to gentamicin declined from 63% to 16%.

Hypothesis: Aminoglycoside modifying enzymes (AMEs) are the most common mediators of aminoglycoside resistance in *P. aeruginosa*; with acetyltransferases (e.g. *aac(6')-Ib*) and nucleotidyltransferases (e.g *ant(2")-Ia*) most frequent in Europe (Poole, 2011). Since common genes encode AMEs and -lactamases, β-lactam use may also predict aminoglycoside resistance (Dubois et al., 2008). In previous analyses from Besançon, aminoglycosides, cefepime and fluoroquinolones were predictors of MexXY-OprM overproduction in *P. aeruginosa* (Hocquet et al., 2008). GRPa isolates were also more likely to overproduce the chromosomally-encoded AmpC cephalosporinase (56% *vs.* 20%; p<0.001) and be multi-drug resistant (65% *vs.* 13%; p<0.001). We hypothesized that GRPa incidence density may be predicted by use of aminoglycosides, fluoroquinolones, extended-spectrum penicillins with β-lactamase inhibitors, carbapenems, monobactams, and third- and fourth-generation cephalosporins. Given potential intra-class differences in promoting resistance, we grouped use of gentamicin and tobramycin separately from that of amikacin.

Model estimation: In the best-fit model ($R^2 = 0.86$), GRPa incidence density was strongly predicted by incidence density in the previous month, and hospital use of gentamicin/tobramycin and fluoroquinolones above minimum thresholds. No independent association with Amikacin use was identified.

Policy implications: Declining clinical burdens from GRPa were explained largely by reductions in inpatient use of gentamicin/tobramycin, and, to a lesser extent, fluoroquinolones. Use of both drug groups was maintained below minimum thresholds from around 2007. Continuing decreases in GRPa incidence density were at least partially explained by autocorrelation when incidence density fell <14 cases per 1000 OBDs. Reciprocal increases in gentamicin-susceptible *P. aeruginosa* over the same period, and moderate inverse correlation ($r = -0.55$), suggest competition for the same niche as GRPa. Gentamicin/tobramycin and fluoroquinolone use

should be maintained at, or below, identified thresholds to control GRPa.

Figure 8.4: Gentamicin-resistant Pseudomonas aeruginosa and antibiotic use.

a

Co-resistance	GRPa (I/R%)	GSPa (I/R%)	Difference in % resistance	p-value
Ciprofloxacin	65%	23%	42.0 (40.2 to 43.8)	<0.001
ESBL+	56%	20%	36.1 (34.3 to 38.0)	<0.001
Ticarcillin / clavulinic acid	56%	20%	36.1 (34.3 to 38.0)	<0.001
Imipenem	47%	13%	34.4 (32.6 to 36.2)	<0.001
Aztreonam	45%	19%	26.2 (24.4 to 28.1)	<0.001
Cefepime	40%	5%	34.9 (33.3 to 36.6)	<0.001
Piperacillin-tazobactam	33%	6%	27.2 (25.6 to 28.8)	<0.001
Ceftazidime	25%	5%	19.7 (18.2 to 21.1)	<0.001

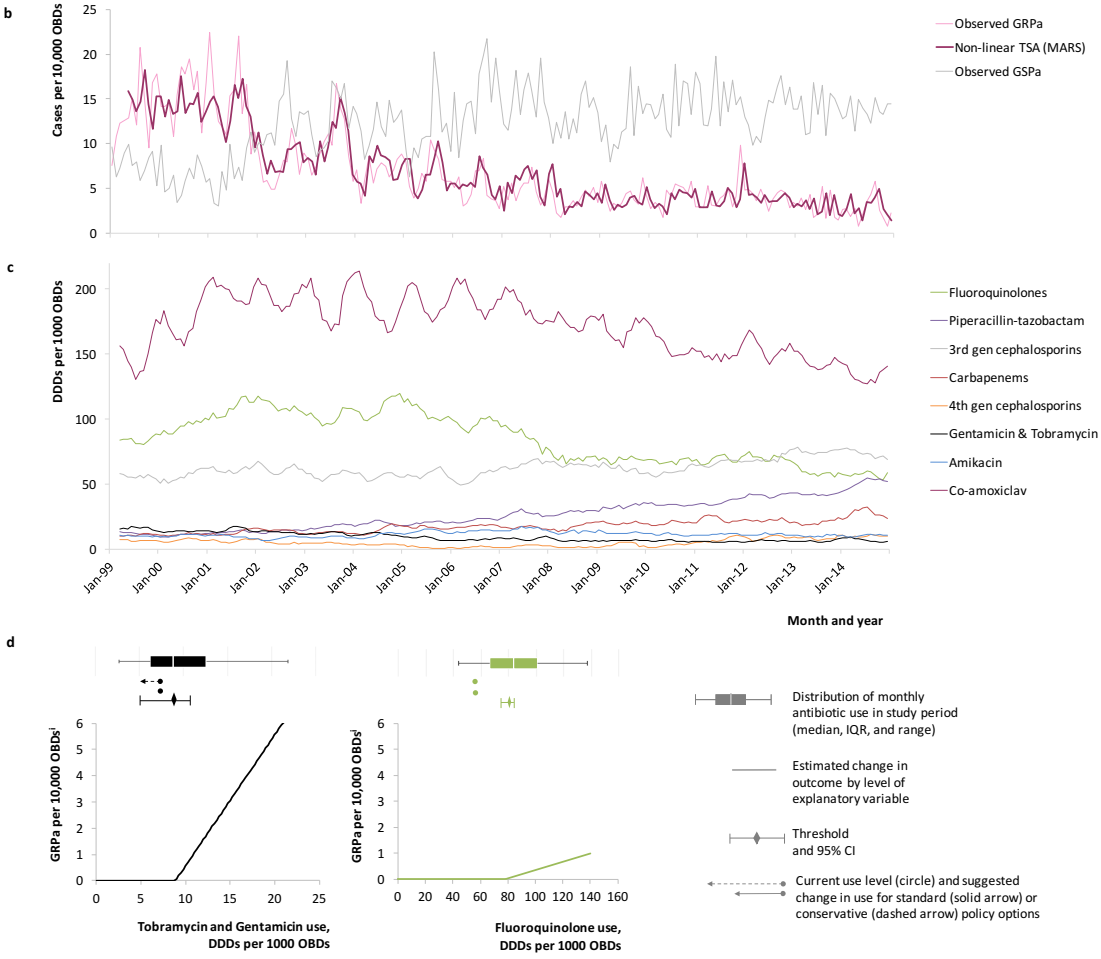

(a) Frequency of co-resistances to other antibiotics in gentamicin-resistant (GRPa) and gentamicin-susceptible (GSPa) P. aeruginosa isolates in population. (b) Time series for observed and model predicted incidence density of GRPa; (c) Time series for potential explanatory antibiotic groups (5-month moving averages) (d) Contribution charts illustrating the relationship between explanatory variables and GRPa incidence density[a]

[a]compared to median monthly GRPa incidence density for study period. DDDs, Defined Daily Doses. GRPa, gentamicin-resistant P. aeruginosa; GSPa, gentamicin-susceptible P. aeruginosa isolates. IQR, Interquartile range. MARS, multivariate adaptive regression splines OBDs, Occupied Bed Days.

Example 5: Methicillin-resistant *Staphylococcus aureus* (Antrim, Northern Ireland)

Scenario: We evaluated incidence density of all MRSA clinical isolates in adult admissions to a district general hospital in Antrim (Jan 2005 to Sep 2013, n=105 months). Between 2005 and mid-2008, incidence density of MRSA clinical isolates remained stable at c.3.0 per 1000 OBDs (Figure 8.5). Following an intervention restricting fluoroquinolones (January 2008) and intensification of infection control, burdens gradually fell to 1.64 cases per 1000 OBDs in 2013.

Hypothesis: The epidemic hospital MRSA clonal complex CC22, predominated in Northern Ireland during the study period: its success attributed to an ability to acquire mobile genetic elements carrying multiple resistance genes, with limited fitness costs (Horváth et al., 2012). Moreover, persistence of fluoroquinolone-resistance mutations in CC22 explain its strong associations with prescribing fluoroquinolones. Consistent with previous linear analyses from the region (Aldeyab et al., 2008), we hypothesised MRSA burdens may be predicted by use of fluoroquinolones, third-generation cephalosporins, co-amoxiclav, and macrolides.

Model estimation: In the best-fit model ($R^2 = 0.53$), MRSA incidence density was positively associated with rates of MRSA in the previous month and use of fluoroquinolones, third-generation cephalosporins, and co-amoxiclav exceeding minimum thresholds. An inverse relationship was seen with increased hospital use of alcohol-based hand rub (ABHR) up to 6.9 Litres per 1000 OBDs, above which further increases in ABHR use was not associated with further declines in MRSA (ceiling effect).

Policy implications: Declines in MRSA incidence density could be partly attributed to deliberate restriction of fluoroquinolone use, and concurrent declines in co-amoxiclav and third-generation cephalosporin use, intended to control *C. difficile*. Strong autoregression and inverse relation to ABHR use were consistent with importance of infection prevention and control measures in interrupting horizontal transmission. Reversal of previous declines in fluoroquinolone use were seen by the last year of study. MRSA could be best controlled by maintaining antibiotic use under thresholds, use of ABHR at, or above, threshold levels and reducing fluoroquinolone use by 39% (Table 8.2).

Figure 8.5: Methicillin-resistant Staphylococcus aureus, hand hygiene, and antibiotic use.

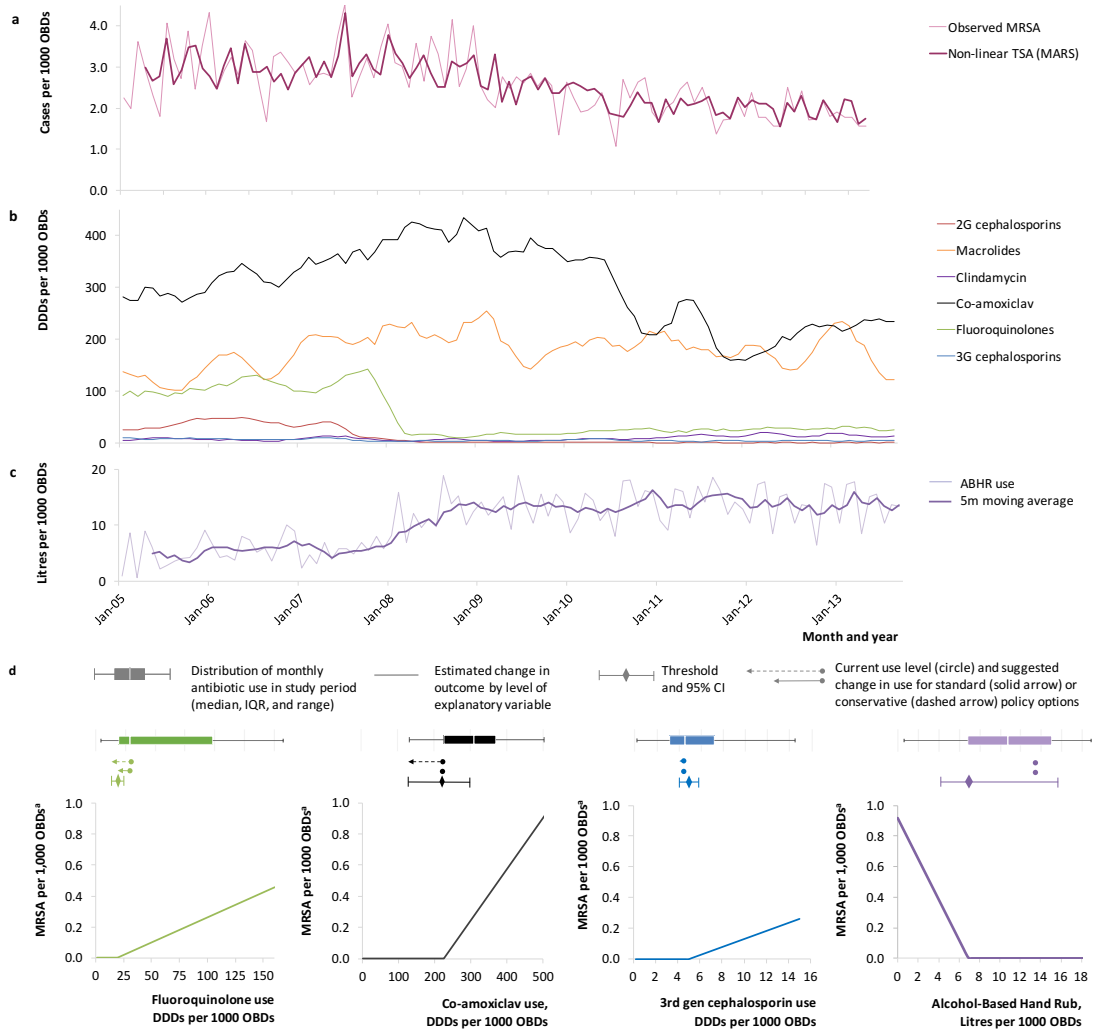

(a) Time series for observed and model predicted incidence density of MRSA (b) Time series for potential explanatory antibiotic groups (5-month moving averages) (c) Time series for alcohol-based hand rub (ABHR) use; (d) Contribution charts illustrating the relationship between explanatory variables and MRSA incidence density[a]

[a]compared to median monthly MRSA incidence density for study period. ABHR, alcohol-based hand rub. DDDs, Defined Daily Doses. ECDC, European Centre for Disease Prevention and Control. MRSA, Methicillin-resistant Staphylococcus aureus. OBDs, Occupied Bed Days.

Discussion.

Using a non-linear time-series analysis (NL-TSA) approach, we found empirical evidence of non-linear relationships between population antibiotic use and resistance outcomes in five European settings. The method was generalisable to different clinical populations, resistant pathogens, definitions of resistance burdens, and epidemiological phases. We demonstrated that identification of minimum thresholds could provide population-specific quantitative targets for antibiotic stewardship, balancing the need for use with control of resistance.

Our approach builds upon earlier work using linear time-series analysis to explain temporal relationships between antibiotic use and resistance (López-Lozano et al., 2000; Vernaz et al., 2011; Aldeyab et al., 2008; Monnet et al., 2004; Aldeyab et al., 2012). NL-TSA shares a number of strengths with linear models, including: low-informational demands, requiring only aggregate prescribing and resistance data; ease of reiteration as new data becomes available, providing context-specific results; adjustment for the non-independence of serial observations and stochasticity inherent to time-series of communicable diseases; identification of temporality in associations and 'lagged' effects; and integration of impacts of multiple exposures (López-Lozano et al., 2000). Additionally, NL-TSA reveals non-linear relationships between exposures and resistance, providing more accurate understanding of how modifying antibiotic use, infection control or other exposures is likely to effect resistance. General limitations of NL-TSA include: the need for longer time-series than linear TSA; the potential for spurious thresholds in areas of limited data, including at extremes of the exposure variable range; and difficulty in identifying thresholds in associations in situations of stable resistance and prescribing. We note the poorer predictive performance of some models (e.g. Example 3), may be explained by absence of data on infection prevention and control activities, and resistance levels in interacting populations.

Non-linear relationships between population antibiotic use and clinical burdens from resistance may have important implications for antibiotic stewardship. In general, impacts of changes in antibiotic use on resistance vary dependent upon the antibiotic use level. More specifically, minimum thresholds may be interpreted as an upper limit for 'safe' population antibiotic use which does not appear to substantially increase resistance rates at the population level. Alternative theories may suggest the threshold indicates: a maximum level of selection pressure not conferring a survival

advantage to resistant pathogens to spread within populations or ecological niches (Peterson, 2005; López-Lozano et al., 2000), or strong enough to induce resistance (Oz et al., 2014); or a minimum level of use, below which antibiotic substitution creates equivalent or greater selection pressure (Peterson, 2005). Crucially, they may provide quantitative targets for balancing the need to access therapies with control of resistance, analogous to 'quotas' applied to other natural resources (e.g. fisheries, forestries) which seek to maximize extracted value while maintain a non-declining stock (Laxminarayan, 2014; Laxminarayan et al., 2013, 2001). Moving from current qualitative targets of reducing use, to quantitative targets may also aid operational effectiveness. Targets appear to work best if pragmatic, collaborative and iterative (Berry et al., 2015). Complete restriction of use of some agents is not feasible, and in balancing competing needs of use and control of resistance, quantitative targets offer an opportunity to align interests and motivations of clinician and antimicrobial management team (Hulscher et al., 2010).

We emphasise the need for caution with interpretations of thresholds. Firstly, thresholds should offer guidance rather than strict limits. Uncertainty around thresholds is variable, as reflected in width of associated confidence intervals. Narrower confidence intervals around threshold locate with reasonable precision the level of antibiotic use at which effects on resistance are substantially altered. Wider intervals may indicate insufficient data or influence of additional explanatory variables. We suggest a pragmatic approach, as in Table 8.2, of interpreting thresholds depending upon the policy scenario. Where the priority is strict control of resistance a conservative approach of limiting use to the lower limit of the threshold confidence interval is advisable. Where excessive restriction is a concern, the standard approach of limiting use to the point estimate of the threshold is likely to offer the best balance between restriction and control of resistance. Secondly, changes in molecular epidemiology under sustained antibiotic selection pressures, such as compensatory mutations minimising fitness costs (Wong, 2017; Levin et al., 2000), or strain replacement (Lawes et al., 2015a,b), mean thresholds may vary by epidemiological phase and time. Variation in thresholds across populations can be anticipated, reflecting host, environment, and organism factors (Lawes et al., 2015b,a, 2017). Therefore, models based on local data and iterative analysis is necessary to ensure time and context-specific guidance. Thirdly, it is important not to assume that all antibiotic use below thresholds is safe, since antibiotic exposures may be important for individual patients, or cause unseen change in reservoirs of resistant pathogens in

environment or hosts.

Potential foci for further research include: evaluating the consistency of thresholds for specific antibiotic use-resistance combinations across different settings and identifying factors affecting thresholds; providing global recommendations for controlling multiple AMR problems through applications of NL-TSA to composite indices of resistance (Laxminarayan and Klugman, 2011; Hughes et al., 2016); the use of Bayesian approaches to standardise and accelerate selection of explanatory variables and facilitate analysis with shorter time-series or rare resistance outcomes (Murphy et al., 2011); applications to smaller populations, such as intensive care units; and prospective studies to validate the effectiveness of quantitative targets in antibiotic stewardship interventions.

We have illustrated how non-parametric time-series models based on empirical data, can identify non-linear relationships between population antibiotic use and resistance burdens. Further we have shown how identification of population-specific minimum thresholds may guide rational compromises between control of resistance and access to therapeutics. With the increasing availability of electronic surveillance and healthcare systems, this approach offers a useful tool for sustaining the effectiveness of current antimicrobials in many areas of the world.

8.3 Methods.

Design and study populations.

This was a multi-centre time-series study. We used multivariable non-linear time-series analysis to quantify associations between ecological exposures, including population use of antibiotic groups, and rates of antibiotic-resistant infections in five populations from France, Hungary, Northern Ireland (UK), and Spain (See Appendix A Table 8.3)

The populations and resistance outcomes were a purposive sample, chosen to reflect varying epidemiological scenarios, clinical settings, and resistant infections in European centres participating in the THRESHOLDS (THReshold EStimation to Help Optimise Local Decisions on antibiotic Stewardship) study group. This collaborative aims to further the development of time-series analysis for understanding antibiotic resistance and planning antibiotic stewardship. Members included centres

with prior experience in applying linear time-series approaches. Investigators were asked to identify an important resistance problem in a defined clinical population from their region. Minimum data requirements were consistent microbiological and prescribing data across a minimum of 60 monthly observations (5 years). Duration of time-series was defined by the longest period of consistent data for a minimum data set of the outcome and candidate explanatory variables.

For each population we described the regional scenario for the chosen outcomes, the theoretical basis for inclusion of candidate explanatory variables, findings from the non-linear time-series analysis, and how these could inform local antibiotic stewardship policy.

Outcome and explanatory time series.

The outcome time-series for each population were: carbapenem-resistant *Acinetobacter baumannii* (Debrecen, Hungary); extended spectrum β-lactamase producing *Escherichia coli* in hospital and community (Orihuela, Spain); cefepime-resistant *Escherichia coli* (Seville, Spain); gentamicin-resistant *Pseudomonas aeruginosa* (Besançon, France); and methicillin-resistant *Staphylococcus aureus* – MRSA (Antrim, Northern Ireland). Cases were defined microbiologically as isolates from all relevant body sites not identified as infection control specimens and meeting consistent criteria for resistance or resistance mechanism (see supplemental file for details). Isolates from the same patient identified within 30 days of a prior isolate with the same organism were considered part of the same infectious episode and de-duplicated. Outcomes were expressed, where possible, as monthly incidence density of resistant infections (cases per 1000 or 10,000 occupied bed days, OBDs). Where there were large changes in testing frequency or organism identification over time, we defined resistance as a percentage of clinical isolates from the same organism with any susceptibility pattern.

The primary explanatory variables were monthly population use of antibiotic agents classified by pharmacological sub-group of antibacterials for systemic use (J01) in the 2016 WHO/ATC index, and expressed as defined daily doses (DDDs) per 1000 OBDs (hospital) or 1000 inhabitant-days (community). Candidate antibiotic sub-groups were identified *a priori*, on the basis of regional co-resistance profiles, molecular epidemiology in the region, reviews and prior evidence on individual or population

level risk factors for acquisition of the resistant infection. We included separate time-series for individual antibiotic agents or chemical sub-groups only where there were strong theoretical grounds for investigating independent associations, such as prior evidence of variable within-class actions or targeting within antibiotic stewardship interventions.

In addition, we incorporated autoregressive terms capturing association between current incidence density and incidence density in recent months. Where available, we incorporated infection prevention and control (IPC) variables such as use of alcohol-based hand-rub. Dummy variables were added to capture immediate and gradual impacts of changes in laboratory methods or other planned interventions. We considered lags in association of up to 6 months and seasonal autoregressive terms (lag 12).

Data collection and laboratory procedures.

In all centres, microbiological and prescribing and IPC data were extracted from electronic databases maintained for routine healthcare activities. Data were anonymised and aggregated before electronic submission to the THRESHOLDS study group. Meta-data on population characteristics, IPC activities, antibiotic stewardship interventions and resources for control of antibiotic resistance were captured using a standardised questionnaire.

Pathogens were identified using standard laboratory methods. Susceptibility testing was by disc-diffusion (Besançon, Debrecen, Antrim) or broth microdilution (Seville, Orihuela). Isolates were defined as resistant if not susceptible to an antibiotic agent according to zone diameter (for disc-diffusion) or minimum inhibitory concentration (MIC, for broth microdilution) breakpoints as recommended by the European Committee on Antimicrobial Susceptibility Testing (EUCAST) or Clinical & Laboratory Standards Institute (CLSI). Details of standards used, and deviations from EUCAST or CLSI criteria are detailed in Table 8.3. Known changes in breakpoints and laboratory methods were adjusted for in time-series analysis.

Statistical methods.

In the following sections we provide a technical exposition of the statistical methods used. We offer here, a brief description for the general reader.

Before applying non-linear time-series analysis (NL-TSA) to real-world datasets from study populations, we performed a statistical, Monte-Carlo, experiment to illustrate its advantages over, more familiar, linear TSA. We applied both linear and non-linear TSA to computer-simulated time-series, where the relationship between the outcome and explanatory time-series was known. Three types of relationship were explored: a linear relationship; a non-linear relationship without correlations between successive data points in time-series (autoregression), and a non-linear relationship with autoregression; By running this experiment over 10,000 simulated datasets for each type of relationship we evaluated the typical ability of linear and non-linear TSA to describe the relationships accurately.

We next applied a seven-step non-linear time-series analysis approach to resistance problems in study populations (Figure 8.6).

Figure 8.6: Summary of the 7-step non-linear time-series methodology and potential pitfalls.

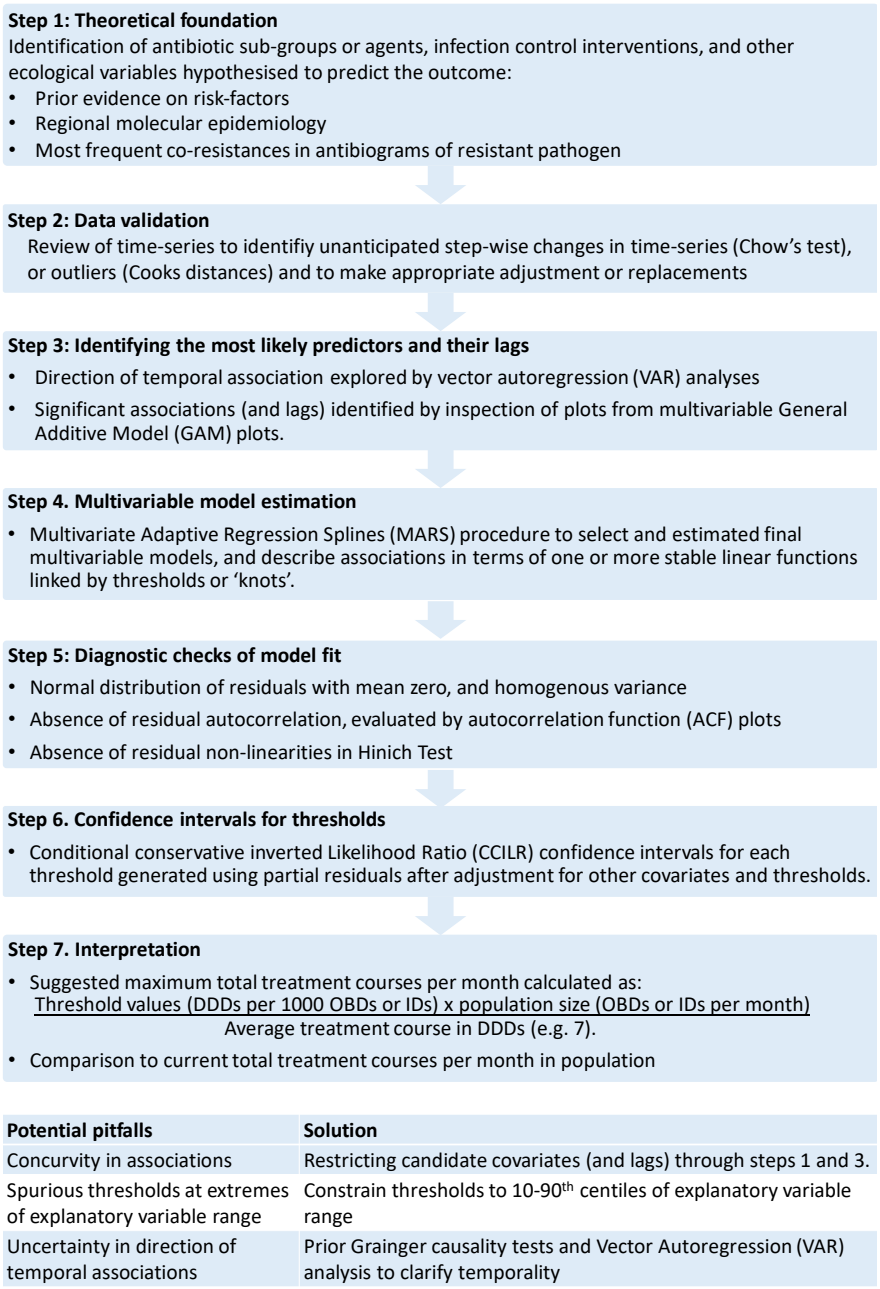

Potential pitfalls	Solution
Concurvity in associations	Restricting candidate covariates (and lags) through steps 1 and 3.
Spurious thresholds at extremes of explanatory variable range	Constrain thresholds to 10-90th centiles of explanatory variable range
Uncertainty in direction of temporal associations	Prior Grainger causality tests and Vector Autoregression (VAR) analysis to clarify temporality

Mirroring the approach with more familiar regression techniques, we started by defining a set of explanatory variables (antibiotic use, infection control time-series, population interactions, resistance in previous months – autoregression, etc.). This set was defined by (a) expert opinion informed by prior risk-factor studies, molecular epidemiology in the region; and (b) inspection of resistance profiles of the patho-

gen of interest. We consider delays between changes in explanatory time-series and associated change in outcome time-series (lags) of up to 6 months. Before analysis we checked time-series and make adjustments for extreme values (outliers) or unexpected shifts in mean (structural changes). We also used vector autoregression (VAR) models to help distinguish any reverse causality in relationships between explanatory and outcome series: this might occur, for example, if prescribing behaviour was altered by resistance rates in the population in previous months. Next we restrict the set of explanatory variables, and lags, to be put into final multivariable models. We use a procedure that fits smooth functions to relationships between explanatory and outcome time-series, and allows visual inspection of likely significant associations. After identifying the most promising explanatory variables (and lags of effects) we enter these into a Multivariate Adaptive Regression Splines (MARS) model which both identifies significant predictors, and defines any non-linear relations as a series of linear relationships connected by 'knots' or thresholds. Model fit for MARS is checked by ensuring residuals were normally distributed without unexplained non-linearities. Confidence intervals around each threshold were fit by a conditional conservative inverted likelihood ratio (CCILR) method, using partial residuals. Finally we converted thresholds from models into suggested maximum total treatment courses per month in the population by multiplying model thresholds by the size of the population and dividing by an average treatment course.

To provide an example of how model findings can inform policy, for the Orihuela population, we predicted the effects of restricting antibiotic use to threshold levels compared to a 'business as usual' scenario of prescribing based on the last months of study. We quantify impacts of immediate restriction sustained over two years.

A technical explanation follows:

a) Comparing linear and non-linear time-series model performance.

We used a Monte-Carlo experiment to compare the ability of linear (Ordinary Least Squares, OLS) and non-linear (Multivariate Adaptive Regression Splines, MARS) time-series models in identifying various pre-defined functional relationships between simulated explanatory and outcome time-series. We hypothesised that for time-series related by simple linear processes MARS and OLS regression methods would perform equally well, but that only MARS would accurately identify non-linear associations. We generated 10,000 simulated datasets using simple stochastic

processes incorporating the following pre-defined functional relationships:

- Non-autoregressive without threshold

$$y_t = -4 + 2x_t + u_t \quad u_t \sim N\left(0, \sigma^2 = 0.02\right) \quad \forall t = 1, \cdots, 200$$

- Non-autoregressive with threshold

$$\begin{cases} if\ x_t \leq 2 \ \ y_t = u_t & u_t \sim N\left(0, \sigma^2 = 0.5\right) \\ if\ x_t \leq 2_t \ \ y_t = -4 + 2x_t + u_t & u_t \sim N\left(0, \sigma^2 = 0.5\right) \end{cases} \forall t = 1, \cdots, 200$$

- Autoregressive with threshold

$$\begin{cases} if\ x_t \leq 0 \ \ y_t = 0 + \rho y_{t-1} + u_t & u_t \sim N\left(0,\ \sigma^2 = 0.05\right) \\ if\ x_t > 0 \ \ y_t = 0 + \rho y_{t-1} + 1x_t + u_t & u_t \sim N\left(0,\ \sigma^2 = 0.05\right) \end{cases} \forall t = 1, \cdots, 200$$

Where:

x_t is the explanatory (independent) time-series variable at time t

y_t is the outcome (dependent) time-series variable at time t

u_t is the error term at time t , with Normal distribution, zero mean and variance σ^2

ρy_{t-1} is an autoregressive term or order 1 (i.e. dated at *t-1*) with $\rho = 0.25$

For each dataset we fitted both linear and non-linear time-series analyses, and recorded sample parameter estimates (a constant, b slope, and s^2 as the estimate of population variance) and a measure of goodness of fit (R^2). Histograms were created illustrating the distributions of R^2 values and parameter estimates from both linear and non-linear models. Visual comparison was made to pre-defined parameter values to identify bias in parameter estimates. We used a t-test of mean difference for independent samples to compare model performance based on R^2 values.

b) Applications of non-linear time-series analysis to real-world datasets.

We applied a seven-step approach to generate non-linear time-series models describing how contemporaneous and prior population antibiotic use, and other ecological variables, explain monthly variation in clinical burdens from antibiotic-resistant infections in five European centres.

Step 1: Theoretical foundation.

Participating centres identified *a priori* a minimum dataset of antibiotic sub-groups or agents they considered most likely to affect the epidemiology of the resistant organism under investigation (target organism). Decisions were based upon: previous empirical evidence of risk factors and molecular epidemiology in the study region or related contexts. Additionally, using antibiogram data from the study period and population, we reviewed co-resistances to other antibiotics among isolates of the target organism with and without the resistance under investigation. We considered antibiotics with the largest absolute rates of co-resistance in the resistant isolates to be most likely to exert significant selection pressures (Søgaard, 1989; Møller, 1989). Consensus on the list of potential predictive variables was found through discussion among all THRESHOLDS study group members.

Where data was available we integrated additional explanatory variables on hospital activity or infection control activities, associated with the outcome variable in previous studies.

Step 2: Data validation.

To ensure consistent time-series we first accounted for known changes in exogenous conditions, such as changes in laboratory method. We captured immediate and gradual effects by entering a dummy variable (0 in months before the change, 1 in months after change) and its interaction with an autoregressive term, as explanatory variables. We then reviewed time-series to detect possible unknown measurement errors as follows. Visual inspection identified potential structural changes (seen as large step-wise change in mean for instance) or outliers (seen as values deviating substantially from surrounding values). Successive Chow tests were applied to automatically detect the most probable dates of structural changes in the time-series and, where necessary, to disaggregate the sample into two or more segments, each with a stable mean. For each segment we applied an outlier detection technique using the following criterion: an observation was considered as an outlier if Cook's distance at this point was greater than five times the mean of Cook's distances of all the observations of the segment. Finally, we replaced outlier values with the mean of the three preceding and three following observations.

Step 3 Identifying the most likely predictors and their lags.

Given the potentially complex relationships between ecological variables under investigation we sought to refine our understanding of potential associations before

applying final multivariable non-linear models.

Firstly, situations of reverse causality could exist when ecological exposures - such as rates of infections with resistant pathogens connected populations, or use of some antibiotic groups in a given population - respond to, rather than predict, rates of resistance. In order to minimise this risk, we tested direction of temporal relationships between explanatory and outcome time-series by applying Granger-causality analysis and Vector Autoregression (VAR) models. Secondly, non-linear models of the type used in this study are potentially complex and difficult to extract form the data if too many predictors are used at the same time. Therefore, we carried out an additional *a priori* data-based selection of candidate explanatory variables and lags (the lag refers to the delay in months between change in exposure and associated change in outcome). This was done through inspection of outputs from fitting a General Additive Model (GAM) to the data. GAM is a very general procedure that can be used for the identification of the most likely predictors, since it runs a non-parametric estimation of the functional relationships between explanatory (x) and outcome (y) time-series, based upon iterative data fitting, rather than prior assumptions. It also allows for variability in the functional relationships across different values of the explanatory variables and can therefore capture non-linear associations between ecological variables and resistance outcomes (Donayre et al., 2018). In particular, we used the GAM procedure in the SCAB34S Splines module (available in SCA Workbench, Scientific Computing Associates Corp, Illinois, USA) to define the relationship between p explanatory (x) and the outcome (y) time-series as a sum of smooth, or spline, functions:

$$E(y \mid x_1, x_2, \ldots, x_p) = s_0 + \sum_{j=1}^{p} s_j(x_j)$$

where $(s_j(x_j))$ are the spline functions; they were standardised such that, after removal of free constants (s_o) their expected contribution to the outcome (y) is zero (i.e. $E[s_j(x_j)] = 0$ for each j).

The splines were derived by a process of splitting the time-series into sections, joined at knot points, and fitting simple curves described by cubic functions to the data in each section. The GAM methodology identified the optimal combination of spline functions $s_j(x_j)$, following the iterative procedure suggested by Hastie and Tibshirani (1990). Combining a local scoring algorithm and a backfitting procedure, this method converges on a solution balancing data fit with smoothness.

To identify the most relevant explanatory time-series, for each centre we started

with a multivariable GAM model including all theoretically relevant variables at lags of 1 to 6 months and autoregressive terms at lags 1 and 2. We limited lags to 6-months based on widespread evidence of declining relevance of antibiotic exposures by time-since exposure, and prior experience that considerations of longer lags lead to problems of concurvity. On the basis of the GAM outputs, an explanatory variable with a specific lag was retained in the model only if its contribution was significant at a 5% level of probability (identified on contribution charts by the zero line of non-association falling outside of 95% confidence intervals around the estimate). The process was run iteratively by removing first those variables and lag combinations whose contributions were non-significant before re-running the GAM model on a reduced subset of variables and lags. The process stopped when the model contained only significant contributions of variables and lags. These constituted the restricted set of explanatory variables for entry into MARS analysis.

A further objective of applying the GAM procedure was to determine whether consideration of non-linear associations is justified in terms of improvement in predictive performance. For each explanatory variable (and lag), GAM provides a comparison of the data fit of a non-linear spline function (nl) with an analysis in which this relationship is restricted to a linear function (l). Significant improvement in goodness of fit over a linear fit is defined by an F-test, as follows:

$$F_0 = \frac{(SSR_l - SSR_{nl}) \,/\, (p_{nl} - p_l)}{SSR_{nl}/(n - p_{nl})} \sim F_{(df_{nl}-df_l),(n-p_{nl})}$$

where; SSR= Sum of squares of residuals, n= number of observations, p= number of parameters, l= linear function, and nl= non-linear spline function.

The null hypothesis that estimates from an enhanced (non-linear) model do not provide a significantly better fit than those from a linear model can be rejected where F exceeds a critical value ($a = 0.05$) from an F-distribution with $(p_{nl} - p_l, n - p_{nl})$ degrees of freedom.

Step 4. Multivariable model estimation.

After identifying the most likely explanatory variables (and lags), and whether associations with the outcome series were linear or non-linear, we used the MARS procedure (in the SCAB34S Splines module) to obtain an easily interpretable characterization of these associations(Friedman, 1991). MARS is a non-parametric regression approach suitable for situations of non-linear associations that can provide

more interpretable and interesting empirical results than GAM. Given our research aims, its particular advantages were: (i) the ability to identify distinct threshold values ('knots') of the explanatory variables delimiting regions (ranges of values) of individual or interacting explanatory variables within which associations with the outcome differs substantially from those in other regions; and (ii) a systematic approach for model identification and estimation, which automatically selects the combination of explanatory variables and threshold values which most efficiently explain variation in outcomes. (See Appendix A Figure 8.9)

MARS approximates the functional relationship between an outcome time-series (y_t) and a vector of p explanatory variables $x_t = (x_t^1 \ldots .x_t^p)$ as:

$$y_t = \beta_0 + \sum_{m=1}^{M} \beta_m b_m (x_t) + \varepsilon_t$$

where;

β_0 is a constant

β_m is the coefficient for the m^{th} basis function, $m = 1, ..., M$

$b_m(x_t)$ is the m^{th} basis function, $m = 1, ..., M$

ε_t is an independently distributed error term.

The basis functions are products of up to two truncated linear or hinge functions, describing the relationship between one or more explanatory variables and the outcome in terms of segments of stable association separated by knots or thresholds values. These interacting hinge functions allow us to identify possible interactions between variables as in Figure 8.1C(ii). Namely, the m^{th} basis function takes one of the following two forms:

No interaction: $b_m (x_t) = h\left(x_t^k, t_{k,m}\right)$ for some $k = 1, \ldots, p$

With interaction: $b_m (x_t) = h_m\left(x_t^k, t_{k,m}\right) \cdot h_m\left(x_t^j, t_{j,m}\right)$ for some $k, j = 1, \ldots, p,\ k \neq j$

where $t_{k,m}$ is the threshold value of x_t^k in the m^{th}basis function and where $h\left(x_t^k, t_{k,m}\right)$ is a hinge function that takes the following form depending on whether the basis function takes effect above or below the threshold $t_{k,m}$

a) above the threshold: $h_m\left(x_t^k, t_{k,m}\right) = max(x_t^k - t_{k,m},\ 0)$

b) below the threshold: $h_m\left(x_t^k, t_{k,m}\right) = max(t_{km} - x_t^k,\ 0)$

If no knot (threshold) is detected, then a simple linear (and therefore constant) association between explanatory and outcome variable can be specified as a single function applied across the total range of values of the explanatory variable.

All potentially significant explanatory variables, and associated lags, identified in previous steps, were incorporated into models. Model identification and estimation proceed by an automated, iterative, process:

Forward pass: starting with the simplest model containing only a constant basis function, MARS generates a matrix of basis functions in a forward stepwise manner. Candidate base functions are added in order of ability to improve model fit, until the model reaches a predefined limit of complexity. The candidate basis functions are identified by a nested exhaustive search looping over the existing set of basis functions, and all other possible explanatory variables (or interactions) and knot positions.

Backwards (pruning) pass: During the subsequent pruning pass MARS removes basis functions contributing least to model fit, until no significant improvement is seen in a modified form of the generalized cross validation (MGCV) criterion:

$$\text{MGCV} = \frac{\frac{1}{N}\ \sum_{i=0}^{n}(y - f\,(x))^2}{1 - ((C\,(M) + dM)/n)^2}$$

Where; N is the number of observations,

$\sum_{i=0}^{n}(y - f(x))^2$ is the sum of square of residuals (observed - estimated y).

$C(M)$ is the number of parameters being fitted, M the number of non-constant basis functions and $d = 3$ (conventional value).

The MGCV incorporates a complexity penalty accounting for the inherent improvement in explained variance associated with increasing numbers of basis-functions, and its calculation allows estimates of the relative importance of each basis function. Model selection therefore converges on a set of basis functions that most efficiently explain variation in antibiotic resistance before a final model fit by OLS estimation.

From the output of each MARS model we generated contribution charts illustrating the change in the outcome time-series across the observed ranges of explanatory variables.

Step 5. Diagnostic checks

Adequacy of model fit was defined by three criteria: (i) *Normally distributed residuals* – with homogeneous variance and mean equal to zero, as evaluated by a

Normality test; (ii) *absence of significant residual autoregression* – identified in lags 0 to 6 on an autocorrelation function (ACF) plot; and (iii) *absence of residual non-linearities* – as evaluated by a Hinich test. In addition to the MGCV we reported more familiar measures of model performance such as R^2 and the mean absolute percentage error (MAPE).

Step 6: Confidence intervals for thresholds values

In the absence of an existing method for deriving measures of uncertainty around thresholds derived from non-parametric MARS models, we develop a procedure inspired by Hansen (2000). His procedure considers a simple threshold model with only one variable affected by a threshold effect, and obtains a distribution theory for the threshold parameter (τ) from which asymptotic confidence intervals can be built. He first derives the limiting distribution of a Likelihood Ratio test (LR) for the null hypothesis that the threshold parameter $\tau = \tau_0$. He then builds confidence intervals through the inversion of LR: the (1-α) Inverted Likelihood Ratio (ILR) confidence interval consisting of all the possible values of τ for which the null hypothesis would not be rejected at the α level. Donayre et al. (2018) examine improvements of Hansen's ILR confidence interval, increasing its quality in finite samples with large threshold effects (i.e. when the change in slope from one side of the threshold to the other is large). They show that a 'conservative modification' enlarging Hansen's ILR confidence interval is optimal. In this "conservative ILR confidence interval" the lower end of the interval is enlarged from the first value lower than τ_l for which the null hypothesis is rejected, up to τ_l; at the upper end, it is enlarged from τ_u up to the first value greater than τ_u for which the null hypothesis is rejected. This modification provides intervals at a confidence level at least as high as the nominal one that are still informative.

We adapted this procedure for MARS estimations with more than one explanatory variable containing thresholds, and one or more thresholds per variable, by using the partial residuals –i.e. the variation in the outcome not explained by other explanatory variables and their thresholds. This allowed us to identify conservative ILR confidence intervals for each explanatory variable, conditional on all the estimated coefficients and thresholds other than the one for which the confidence interval is computed. Since in MARS all thresholds and slope coefficients are anyway selected and estimated to optimise overall model fit using conditional inference, identifying these 'conditional conservative ILR (CCILR) confidence intervals' does not impose

costs to reliability.

We adapted this procedure for MARS estimations with more than one explanatory variable containing thresholds, and one or more thresholds per variable, by using the partial residuals –i.e. the variation in the outcome not explained by other explanatory variables and their thresholds. This allowed us to identify conservative ILR confidence intervals for each explanatory variable, conditional on all the estimated coefficients and thresholds other than the one for which the confidence interval is computed. Since in MARS all thresholds and slope coefficients are anyway selected and estimated to optimise overall model fit using conditional inference, identifying these 'conditional conservative ILR (CCILR) confidence intervals' does not impose costs to reliability. Computing confidence intervals conditional only on other thresholds, but with re-estimation of coefficients describing piece-wise associations (slopes), offers a valid alternative. In a Monte Carlo experiment (results available on request) we found both approaches resulted in adequate coverage (>95% of intervals including the actual value of the threshold) but CIs were wider with a procedure with slope re-estimation, and less informative for a given coverage rate. As a result, we recommend the partial residual approach. Other alternatives, such as bootstrapped methods, are not likely to give satisfactory results. On the one hand, given the presence of multiple thresholds, they may be prohibitively time-consuming; on the other hand, even in the case of only one threshold, bootstrapping is very time consuming and has been shown to yield non informative confidence intervals (seeEnders et al. (2007)) .

Step 7. Interpretation

The minimum thresholds identified for each significantly associated antibiotic group were translated into suggested maximum numbers of patient treatment courses per month not expected to adversely affect resistance at population levels. We multiplied the threshold, expressed in DDDs per 1000 OBDs (or IDs), by the size of the monthly patient population (in thousands of OBDs or IDs), and then divided by an average patient treatment course of 7 DDDs (except for aminoglycosides which were considered as 3 DDDs). These maximums were further compared to contemporary levels of antibiotic use in the last year of study, to provide indications of how current use of antibiotics should be modified to avoid resistance spread.

Projections for alternative antibiotic stewardship policy options.

To illustrate the potential effects of restricting antibiotics associated with %Ec-ESBL+ to threshold levels in populations of Orihuela, we compared the expected evolution of %Ec-ESBL+ under a 'business as usual' scenario in which antibiotic use continued as in last year of study, to projected time-series with antibiotics restricted to threshold levels.(Figure 8.8)

Firstly, we used a breakpoint analysis to identify the last stationary segment in %Ec-ESBL+ time-series from the study period. We recursively estimated MARS models using means from these stationary segments as starting points to derive steady states for %Ec-ESBL+ in community and hospital populations. Based on steady state values and MARS models for the study period (baseline) we simulated 1000 samples of 24-month projections, incorporating random error term with variance as derived in the baseline MARS model. For each sample projection we entered mean antibiotic levels in the last year of the study period ('business as usual') and alternative levels set at identified thresholds (antibiotic stewardship options). We calculated the mean difference between business as usual and each policy option for every month along with 95% confidence intervals. Finally, we illustrated alternative projections and differences using medians of distributions from the 1000 sample projections.

8.4 Appendix.

Extended data file.

Figure 8.7: Monte-Carlo experiments comparing linear and non-linear time-series analyses-

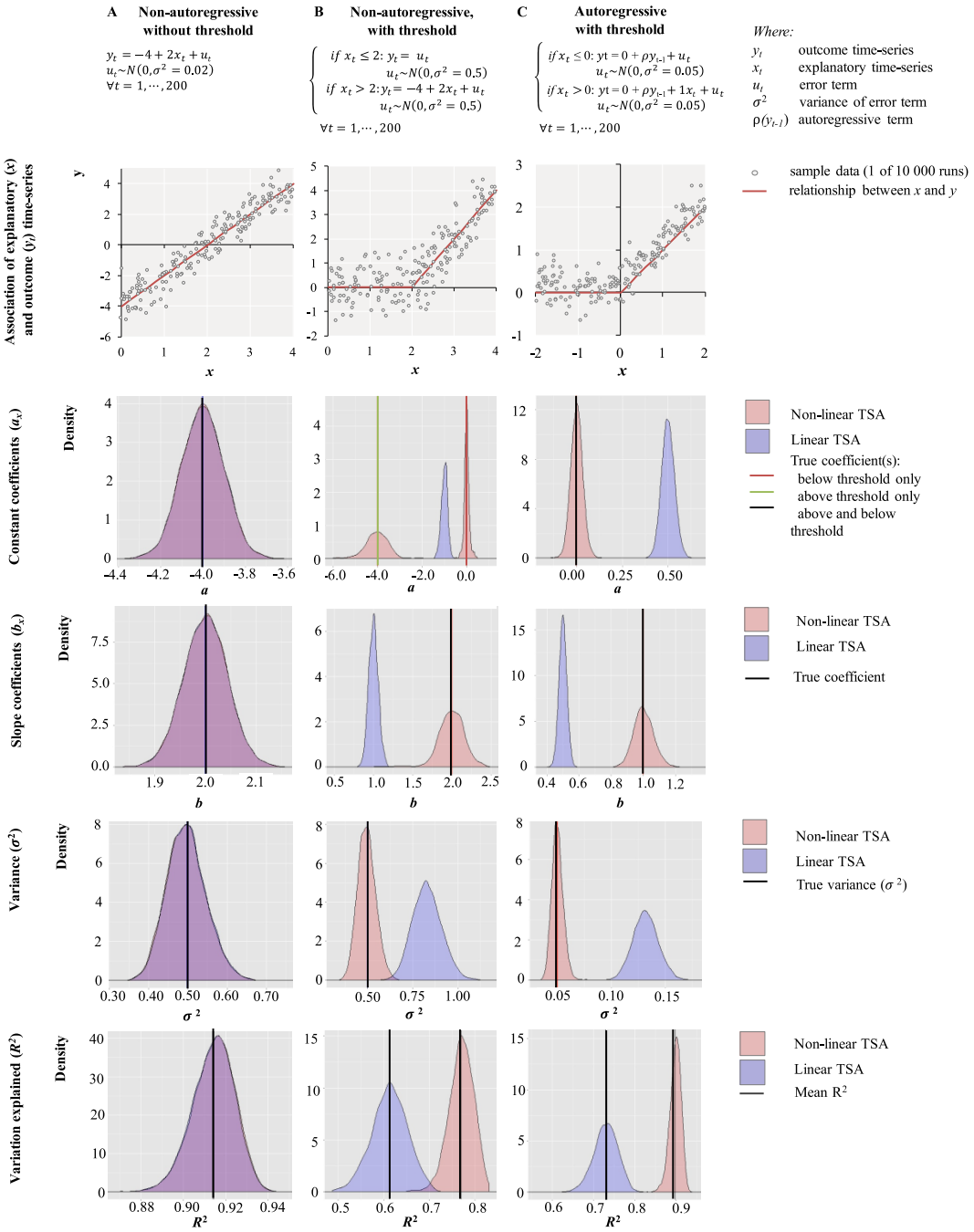

Ability to identify known relationships between explanatory (x) and outcome (y_t) time-series was assessed by applying both linear (ordinary least squares, OLS) and non-linear (Multivariate Adaptive Regression Splines, MARS) models to 10000 datasets generated through simple pre-defined stochastic processes (A) to (C). Frequency distributions indicate estimates from these 10000 models of coefficients (constant a, slope b), and variance (s^2) as well as summary of model fit (R^2). Comparison can be made to pre-defined values for coefficients and variance. (TSA, time-series analysis).

Figure 8.8: Projections of the percentage of extended-spectrum β-lactamase-producing Escherichia coli (%Ec-ESBL) for hospital and community over next 24 months according to antibiotic stewardship intervention options.

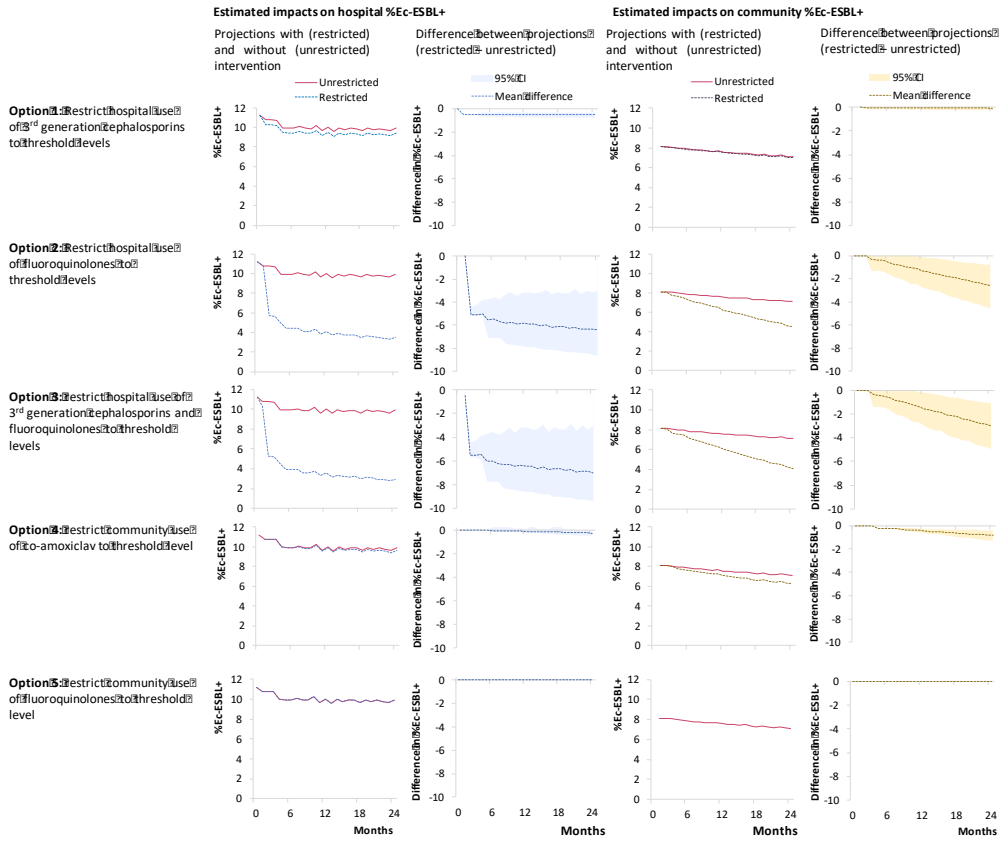

'Business as usual' scenario reflects expected %Ec-ESBL if antibiotic use patterns persist at levels seen in last 12-months of study period. Other projections based on immediate reduction of indicated antibiotic to level of minimum threshold. Note potential indirect effects due to population interactions.

Figure 8.9: Illustrations of GAM and MARS procedures for non-linear time-series analysis

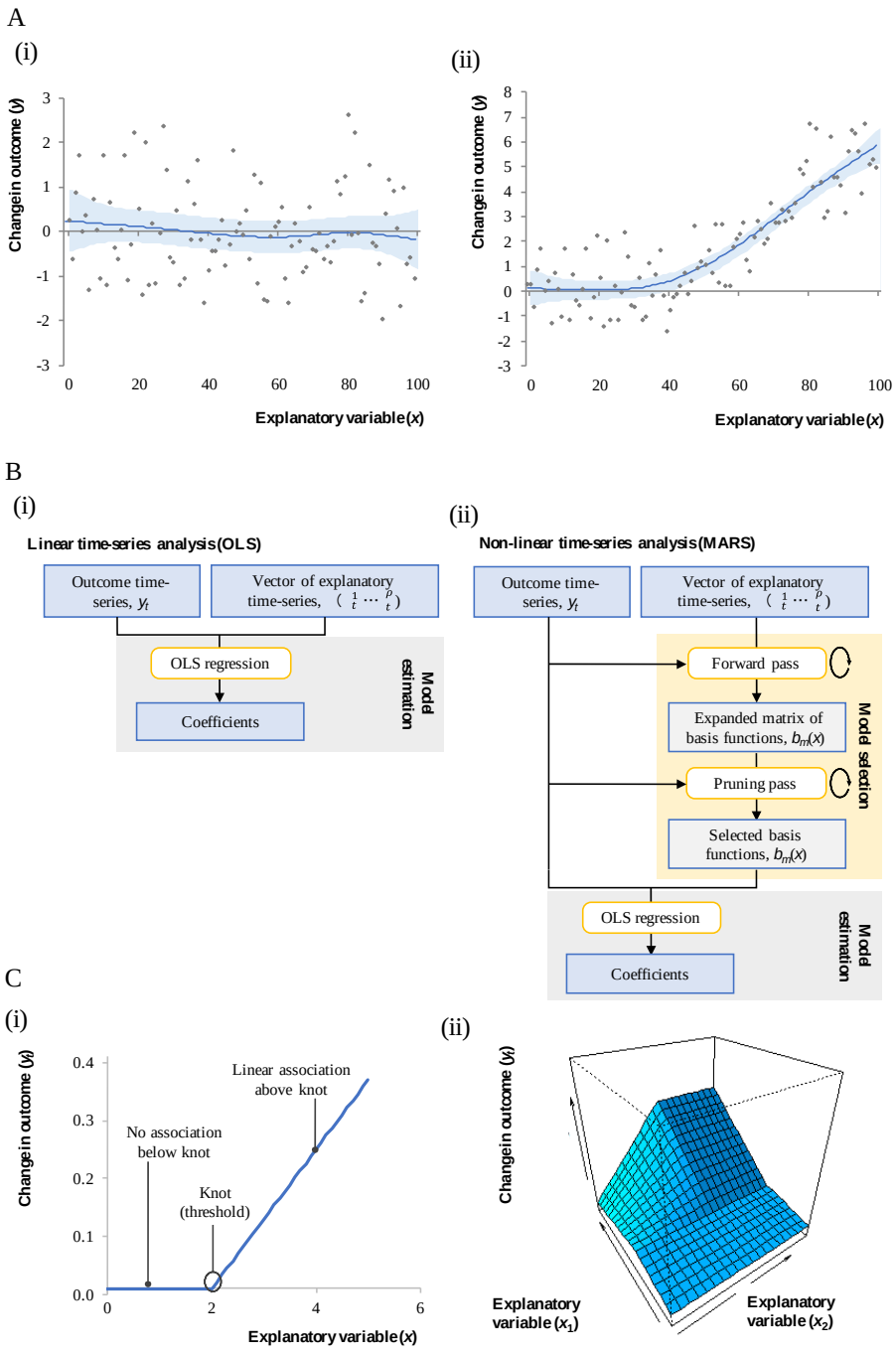

(A) Examples of contribution charts from GAM procedure in (i) the absence and (ii) the presence of significant relationships between (x) and the outcome (y) variables. (B) Schematic comparing (i) linear (OLS) and (ii) non-linear (MARS) regression analyses. (C) Contribution charts illustrating the case of basis (spline) functions of the relationship between the outcome (y_t) and (i) a single explanatory variable with positive impact only above threshold and (ii) interacting explanatory variables (x_1, x_2) with various types of impact depending on the regions of the interacting variables

Table 8.3: Summary of study populations, outcomes and exposures

Centre	1. Debrecen (Hungary)	2. Orihuela (Spain)	3. Seville (Spain)	4. Besançon (France)	5. Antrim (N.Ireland)
Months of study (No.)	Oct 2004 to Aug 2016 (N=143)	July 1991 to Oct 2016 (N=304)	Feb 2008 to Dec 2016 (N=108)	Jan 1999 to Dec 2014 (N=192)	Jan 2005 to Sep 2013 (N=105)
Setting	1559-bed tertiary hospital. Serving population of 1 500 000	a) 350-bed district hospital b) Primary care (community) services for 199 000.	778 bed hospital Serving population of 481 000	1200-bed tertiary hospital. Serving population of 1 200 000.	340-bed teaching hospital. Serving population of 147 103.
Population	General adult and paediatric inpatients, 75 ICU beds, 100 chronic-care beds, haematology, oncology, transplantation services 39 300 OBDs per month	General adult inpatients, 10-bed ICU. Oncology services. 6 670 OBDs per month	General adult and paediatric inpatients, 6-bed PICU, 6-bed NICU, 50-bed ICU. Renal, oncology services. 21 300 OBDs per month	General adult and paediatric inpatients, including 40-bed ICU and 12-bed NICU. 27 710 OBDs per month	General adult inpatients including 7-bed ICU and oncology services, renal replacement therapy. 9 750 OBDs per month
Primary Outcome	Carbapenem-resistant *Acinetobacter baumannii* isolates per 10 000 OBDs (CRAb)	% *Escherichia coli* producing extended-spectrum ß-lactamases (%Ec-ESBL+)	% *Escherichia coli* resistant to cefepime (%Ec-FepR)	Gentamicin resistant *Pseudomonas aeruginosa* cases per 1000 OBDs (GRPa)	Methicillin-resistant *Staphylococcus aureus* per 1000 OBDs (MRSA)
Laboratory methods /susceptibility testing	Disc-diffusion Breakpoint: - CLSI (to Aug 2013) - EUCAST (from Sep 2013) - Non-susceptible if zone diameter <23mm (for imipenem).	Microdilution Breakpoint - CLSI (to Dec 2015) - EUCAst (from Jan 2016). - ESBL+ if: (i) MIC >1mg/L for cefotaxime or ceftazidime. and; (ii) ≥3 two-fold decrease in MIC when combined with clavulanic acid.	Microdilution Breakpoint: - CLSI (to Dec 2015) - EUCAST (from Jan 2016) - Non-susceptible if MIC ≤8mg/L (to Sep 2014) ≤2mg/L (from Oct 2014) ≤1mg/L (from Jan 2016)	Disc-diffusion Breakpoint: - EUCAST (all months) - Non-susceptible if zone diameter <16mm.	Disc-diffusion (Oxicillin to Nov 2007, Cefoxitin from Nov 2007). Breakpoint: -NCCLS from (Jan 2005- Mar 2007) -CLSI (Mar 2007 - Nov 2011) -EUCAST (from Nov 2011) - Non-susceptible if zone diameter <22mm (Cefoxitin)
Isolate types	All body sites (excluding infection control isolates)	All body sites (excluding infection control isolates)	All body sites (excluding non-clinical isolates)	All body sites	All body sites
Hypothesised explanatory variables	Carbapenems Fluoroquinolones Piperacillin-tazobactam Cephalosporins Aminoglycosides Glycopeptides	2nd/3rd gen cephalosporins Co-amoxiclav Fluoroquinolones Co-trimoxazole Aminoglycosides %EcESBL+ in other population	Fluoroquinolones 3rd/4th gen cephalosporins Clindamycin Co-amoxiclav Carbapenems	Aminoglycosides Fluoroquinolones Carbapenems 3rd/4th gen cephalosporins Piperacillin-tazobactam	Fluoroquinolones 3rd/4th gen cephalosporins Clindamycin Co-amoxiclav Macrolides Alcohol-Based Hand Rub (Litres per 1000 OBDs)
Antibiotic stewardship					
Resources	None specific.	Local AMT 0.5 WTE antibiotic pharmacist	0.5 WTE antibiotic pharmacist, 0.5 WTE stewardship doctor	Regional and local AMT 1.0 WTE antibiotic pharmacist.	Regional AMT. 1.5 WTE antibiotic pharmacists
Restrictive interventions	None.	Permissions for use required for fluoroquinolones, linezolid, vancomycin, 3rd gen cephalosporins (from Jan 1995)	None	Permissions for use required for carbapenems, daptomycin (from Jan 2012)	Removal of stock and permissions for use (from Jan 2008) for: clindamycin fluoroquinolones, cephalosporins, vancomycin, linezolid, colistin, amikacin, chloramphenicol, co-trimoxazole, meropenem, Limited disclosure of antibiograms (all years)
Persuasive interventions	Voluntary consultation with clinical microbiologist available throughout study period	Empirical guidelines	Empirical guidelines Education & reminders (from Jan 2012-) Ward-based audit (from Jan 2013-) Root cause analysis for HCAIs (all months)	Empirical Guidelines Ward-based audit of antibiotic use	Empirical guidelines Ward-based audit Root-cause analysis for HCAIs (all study months)
Infection prevention & control					
Resources	3.0 WTE ICN, 1.0 WTE ICD	1.0 WTE ICN, 1.0 WTE ICD	4 WTE ICN, 0.5 WTE ICD	4 WTE ICNs, 2 WTE ICDs	10 WTE ICNs, 2 WTE ICDs
Hand-hygiene	ABHR throughout study period	ABHR (Jan 2000 ongoing) Regional / National Hand Hygiene campaign (Jan 2000 ongoing)	ABHR (2001-) Auditing of compliance (2006-) Regional hand-hygiene campaign (2008-)	ABHR (Jan 2000 ongoing) Auditing of compliance.	ABHR throughout study period, monthly hospital-wide consumption measured.
Isolation practices	MRSA cases isolated. Other multiresistant pathogens depend on isolation room availability	As per CDC recommendations. Nasal mupirocin / chlorhexidine washes for MRSA (Jan 1991 -)	Of all CRE,VRE cases Nasal mupirocin for MRSA	Isolation of MRSA, ESBLE, VRE, CRE, CDI and CRAb cases.' Nasal mupirocin for MRSA	Isolation or cohorting of MRSA and CDI cases
Admission screening for outcome pathogen	No	ICU (Jan 2013 -)	No	*P. aeruginosa* screening in both adult ICUs (Jan 2000-)	Risk-factor based screening for MRSA in all wards (all study months)
Environmental interventions	None	Audit of hospital cleanliness (Jan 1995 -) Hospital Environment Inspections –continuous (Jan 1995 -)	Audit of hospital cleanliness Hospital environment inspections	None	None

Supplementary information.

Acknowledgements

Additional members of the THRESHOLDS study group contributing to this paper include:

María Núñez-Núñez, Ana I. Suárez (Hospital Virgen de la Macarena, Sevilla, Spain); Michelle Thouverez (Centre hospitalier régional et universitaire, Besançon, France); María Navarro Cots, Emilio Borrajo, Carlos Devesa, Joan Gregori, Inmaculada García Cuello, Isabel Pacheco, María Cerón (Hospital Vega Baja, Orihuela, Spain); and Hajnalka Tóth (Department of Medical Microbiology, Faculty of Medicine, University of Debrecen, Debrecen, Hungary).

All authors acknowledge Dominique L. Monnet, from the European Centre for Disease Prevention and Control (ECDC) for his continuous support, guidance and intellectual contributions to the THRESHOLDS project. J-M.L-L., acknowledges the continuous support of the Management Team of the Hospital Vega Baja, and the technical support of Carlos Quiles (Cabosoft SL), in the development of time-series analysis techniques in the field of antimicrobial resistance, and in particular the WebResist project (www.webresist.org) which provided a framework for the development of this study. G.K., acknowledges funding from the Bolyai Research Scholarship of the Hungarian Academy of Sciences. T.L., acknowledges funding from the Wellcome Trust.

Author information

José-María López-Lozano, Timothy Lawes, César Nebot, Arielle Beyaert, Xavier Bertrand, Didier Hocquet, Mamoon Aldeyab, Michael Scott, Geraldine Conlon-Bingham, David Farren, Gábor Kardos, Adina Fésűs, Jesús Rodríguez Baño, Pilar Retamar, Nieves Gonzalo-Jiménez, Ian M Gould, and the THRESHOLDS study group.

Affiliations

Medicine Preventive-Infection Control Team, Hospital Vega Baja, Orihuela-Alicante, Spain. José-María López-Lozano.

The Wellcome Trust Centre for Global Health Research, Liverpool, UK. Timothy Lawes

Centro Universitario de la Defensa (CUD) de San Javier, Murcia, Spain. César Nebot

Departamento de Métodos Cuantitativos para la Economía y la Empresa, University of Murcia, Spain. Arielle Beyaert

Centre hospitalier régional et universitaire (CHRU) and UMR 6249 Chrono-environnement, Université de Bourgogne-Franche-Comté, Besançon, France. Xavier Bertrand and Didier Hocquet

Northern Health and Social Care Trust/School of Pharmacy and Pharmaceutical Science, University of Ulster, Northern Ireland, UK. Mamoon Aldeyab

Pharmacy Department, Northern Health and Social Care Trust and Regional Medicines Optimisation Innovation Centre, Antrim, Northern Ireland ,UK. Michael Scott, Geraldine Conlon-Bingham

Department of Medical Microbiology, Antrim Area Hospital, Antrim, Northern Ireland, UK. David Farren

Department of Medical Microbiology, Faculty of Medicine, University of Debrecen, Hungary. Gábor Kardos

Clinical Pharmacy, University of Debrecen, Debrecen, Hungary. Adina Fésűs

Infectious Diseases and Clinical Microbiology Unit, Instituto de Biomedicina de Sevilla (IBiS), Hospital Universitario Virgen Macarena and University of Seville, Seville, Spain. Jesús Rodríguez Baño and Pilar Retamar

Medical Microbiology Department, Hospital Vega Baja, Orihuela-Alicante, Spain. Nieves Gonzalo-G Jiménez

Medical Microbiology Department, Aberdeen Royal Infirmary, Aberdeen, Scotland, UK. Ian M Gould

Contributions

J-M.L-L., T.L., C.N., A.B., and I.M.G., proposed the original idea and designed the study. X.B., D.H., M.A., G.C-B., M.S., D.F., G.K., J.R-B., P.R., and N.G., collated centre-specific data, situational analysis, and hypotheses. J-M.L-L., T.L.,

C.N., A.B., contributed to statistical analysis, with C.N and AB, the principal analysts. All authors discussed the results and commented on the manuscript.

9 Conclusions

This thesis pretends to contribute to the ongoing debate on Macroeconomics about the nonlinearity of the Taylor rule and of Okun's law. For this purpose, we develop a protocol to implement a methodology able to estimate multiple thresholds on the explanatory variables in a very flexible manner. In the field of Public Heath, since the uprising antimicrobial resistance has become one of the most important current concerns of the World Health Organization (WHO), we also apply this methodology to detect thresholds in the relationship between the intensity of use of different antibiotics in several European medical centres and the antimicrobial resistance. Both Macroeconomics and Public Health debates are of major interest; we hope our humble contributions can be helpful to shed some light on them and may contribute to the design of public policies.

Given the suspicion that these relationships are nonlinear, we are interested in estimating possible and multiple thresholds with an appropriate and flexible data-driven methodology that allows not only the estimation of the model but also its selection. Unlike parametric methods that estimate the parameters of an a priori selected model, non-parametric methods provide the greater flexibility needed to estimate and analyse the relationships that are the object of this thesis. The nonparametric Multiple Adaptive Regression Splines (MARS) methodology developed by Friedman (1991) allows selecting and estimating models by detecting thresholds in the main effects of several explanatory variables and even in interaction effects between them, if they exist.

In Chapter 2, we described MARS methodology and proved its comprehensiveness and its adequacy. We proposed a basic estimation protocol that exploits MARS advantages and we particularize it for each relationship that we analyse. In the absence of an existing method for deriving measures of uncertainty around thresholds derived from non-parametric MARS models, we develop a new procedure inspired by Hansen (2000) and (Donayre et al., 2018) to complete the usefulness of our basic

estimation protocol. To the best of our knowledge, the computation of confidence intervals for thresholds parameters in MARS model is an innovation of this thesis. Our Monte Carlo experiments indicate that our procedure is relevant since it generates confidence intervals that are more informative than alternative procedures.

In order to address the analysis of the first nonlinear macroeconomic relationship, i.e. the Taylor rule, we first present a simple theoretical framework that generalises Svensson's model to allow possible thresholds in explaining variables, even in interactions between them. Unlike the traditional approach, which imposes specific functional forms, we propose using central bank's generic piecewise-defined social preferences. We show that the social preferences of the central bank may be a source of multiple thresholds and interaction effects in the resulting Taylor rule. Using this theoretical framework, we present two research papers estimating the Taylor rule for the Federal Reserve in United States and that for the European Central Bank.

We estimate the TR for the United States from 1970 to 2014 with monthly data and we detect thresholds for the inflation rate at 4.31%; 95% and for the output gap at 0.0012;. As the theoretical framework predicts, we also find an interaction between inflation and output gap. We also confirm the stronger sensitivity of the Fed's reaction during the Volcker -Greenspan period to the inflation rate; the Bernanke period is also characterized by a less intensive reaction to inflation as well as to the output gap. One of the contributions of the paper consists of estimating not only a stronger Fed's reaction in the Volcker -Greenspan period but also highlighting the fact that this sensitivity is triggered at an even lower threshold than in the other periods. Our results provide a more complete characterization of the nonlinear Taylor rule than alternative empirical techniques applied so far in the literature.

Our research paper that analyses the Taylor rule for the European Central Bank also provides some interesting results. We detect thresholds both in the output gap and in the inflation rate. Threshold level for the output gap is identified at -0.0172; 95%, and the ECB reaction is three times more intensive for output gaps below this threshold than above it. On the other hand, the ECB is sensitive to the inflation rate only for high levels of inflation, namely above 2.66%; 95%; and above that level of inflation rate the ECB is much more sensitive to inflation than to the output gap. Finally, we confirm that the 2008 crisis provoked a more abrupt decrease of the interest rate than expected according to the macroeconomic circumstances, which is consistent with the theoretical literature on optimal monetary policy in

the vicinity of the Zero Lower Bound. In contrast with what happens between presidencies of the US Federal Reserve, our empirical results for the ECB show no significant policy differences between the three successive chairmanships. One of the contribution of our research paper is an empirical support to the idea that the ECB cares more about the economic activity than officially declared and reacts intensively to inflation deviations once they sufficiently exceed the official 2% target.

Our methodology and findings open some further research on estimating Taylor rule for other central banks, to check if operating with thresholds is common practice outside the Federal Reserve Bank or the ECB. It is also of interest for future research the existence of possible nonlinear association with thresholds between the policy rate decisions taken by ECB or by the Federal Reserve and the Taylor rule for central banks from smaller economic areas. Finally, the identification of institutional or political factors that could affect the thresholds is presently outside the scope of this thesis but should be retained for further research.

Regarding nonlinear Okun's law, we present a simple and flexible theoretical model based on the hypothesis that the firm employers are risk averse. This theoretical model is a contribution by its self because not many efforts have been devoted to offering theoretical foundation to Okun's law nonlinearity. Although the evidence of nonlinearity in Okun's is mainly attributed to the firm's risk aversion hypothesis, there is no reason why it must be attributed to only one hypotheses. In fact, firm's risk aversion hypothesis combined with the institutional rigidity or labour hoarding hypotheses might give rise to more complex Okun's laws than the one derived from one single hypothesis. Our flexible methodology allows for endogenous threshold detections and locations; it may thus reconcile the empirical evidence with the combined influence of different theoretical hypotheses.

In this research paper, we estimate Okun's law for four European countries (France, Germany, the Netherlands and Spain) and we include the dummy variable for the Eurozone crisis created by CEPR Euro Area Business Cycle Dating Committee, that establishes the chronology of recessions and expansions in the Euro area. For each country we detect only one threshold in quarterly growth rate. We also find that Okun's law for Germany, France and the Netherlands are very similar and quite flat, whereas Okun's law for Spain is much steeper. For each country, differences between Okun coefficients below and above the threshold are consistent with the firm's risk aversion hypothesis, and reveal particularly high risk aversion in the Spanish

firms. On the other hand, the differences between thresholds across countries can be related to the "labour hoarding hypothesis", and show that the German and French firms are more reluctant to fire trained workers than the Dutch ones. The estimated threshold for Spain takes place at a significant negative output growth rate, that is substantially lower than the significantly positive threshold value for the other countries. It is also consistent with the "institutional rigidity hypothesis". Finally, the Euro area crisis affects Okun's law in France, reflecting the idea that decision makers under firm's risk aversion hypothesis are also concerned about the information from the economic area they are operating in. These results enrich Okun's law estimations and give relevance to the differences among countries and their possible causes.

A direct implication follows from our findings: the remarkable differences between Okun's law of the Eurozone countries, in particular between the core and Spain, demonstrate the need to erode the institutional differences and of regulation of the implied national labour markets. Otherwise, any demand policy at the European level, and in particular the monetary policy of the ECB, which is necessarily the same for all countries of the Eurozone, will have a very different impact on the labour markets and on the macroeconomic magnitudes of the countries under study.

Our research paper contributes to the debate over how the different theoretical hypothesis intervene and shape the Okun's law in each country. Combining nonlinearity and threshold location may be a helpful strategy to better understand how the diverse theoretical hypotheses intervene in the recovery after the recent crisis of some European countries facing high unemployment rates. On the other hand, since we are not previously imposing a fixed number of thresholds, this data-driven procedure offers empirical results of the Okun's law much more general than those published to date.

Our findings open some further research on nonlinear Okun's law from different economic areas, for instance, by analysing differences between thresholds from European and American countries; further research on identifying economic and political factors affecting thresholds, or research on the specific effect of the labour market regulations in the shape of Okun's law and its threshold locations, would also be of interest .

Finally, we address the analysis of the Antimicrobial resistance because it has been constituted as one of the most important current concerns of the World Health

Organization (WHO) in the field of Public Health. We present in this thesis an interdisciplinary research paper that analyses the relationship between the pressure of antibiotic use in different European hospitals and primary care centers and the emergence of resistant strains to these antibiotics. We find strong empirical evidence of non-linear relationships between population antibiotic use and resistance outcomes in five European settings and confirms the existence of minimum thresholds in the intensity of use of antibiotics in the hospital and primary care centres we have analysed. Our pathbreaking findings in this field may have important implications for the design of Public Health policies regarding antibiotic stewardship. Minimum thresholds may be interpreted as an upper limit for "safe" population antibiotic use which does not appear to substantially increase resistance rates at the population level. Crucially, they may provide quantitative targets for balancing the need to access therapies with control of resistance, analogous to "quotas" applied to other natural resources.

Our research paper contributes with several empirical innovations to the debate on the rationalization in the use of antibiotics to cope with the threat of bacterial resistance. Our findings encourage us to explore a research line that could help to orientate the design of Public Health policies about antibiotic stewardship.

Our results open some potential further research. One consists of evaluating the consistency of thresholds for specific antibiotic use-resistance combinations across different settings and identifying factors affecting thresholds. It is interesting to provide global recommendations for controlling multiple antimicrobial resistance problems. Another further line of research could be employing Bayesian approaches to compensate the scarcity of available resistance time series or facilitate analysis with shorter time-series or rare resistance outcomes; yet another direction of research would consist of applications of the methodology to smaller populations, such as intensive care units; and finally, prospective studies could be carried out to validate the effectiveness of quantitative targets in antibiotic stewardship interventions.

Faithfully, we hope the results of this thesis may humbly contribute to shed some light in the design of public policies to face the current challenges in Macroeconomics and Public Health.

Bibliography

Adachi, H., Imoto, S., and Inagaki, K. (2015). Economic Growth and Unemployment: Theoretical Foundations of Okun's Law. In *Studies in Medium-Run Macroeconomics: Growth, Fluctuations, Unemployment, Inequality and Policies*, pages 69–85. World Scientific.

Aguiar, A. and Martins, M. M. F. (2008). Testing for asymmetries in the preferences of the euro-area monetary policymaker. *Applied Economics*, 40(13):1651–1667.

Ahmad, S. (2016). A multiple threshold analysis of the Fed's balancing act during the Great Moderation. *Economic Modelling*, 55:343–358.

Akaike, H. (1987). Factor analysis and AIC. In *Selected Papers of Hirotugu Akaike*, pages 371–386. Springer.

Aldeyab, M. A., Harbarth, S., Vernaz, N., Kearney, M. P., Scott, M. G., Darwish Elhajji, F. W., Aldiab, M. A., and McElnay, J. C. (2012). The impact of antibiotic use on the incidence and resistance pattern of extended-spectrum beta-lactamase-producing bacteria in primary and secondary healthcare settings. *British journal of clinical pharmacology*, 74(1):171–179.

Aldeyab, M. A., Monnet, D. L., López-Lozano, J. M., Hughes, C. M., Scott, M. G., Kearney, M. P., Magee, F. A., and McElnay, J. C. (2008). Modelling the impact of antibiotic use and infection control practices on the incidence of hospital-acquired methicillin-resistant Staphylococcus aureus: a time-series analysis. *Journal of Antimicrobial Chemotherapy*, 62(3):593–600.

Alvarado, S. A., Silva, C. S., and Cáceres, D. D. (2010). Modelación de episodios críticos de contaminación por material particulado (PM10) en Santiago de Chile. Comparación de la eficiencia predictiva de los modelos paramétricos y no paramétricos. *Gaceta Sanitaria*, 24(6):466–472.

Andersson, D. I. and Hughes, D. (2010). Antibiotic resistance and its cost: is it possible to reverse resistance? *Nature Reviews Microbiology*, 8(4):260.

Arepyeva, M. A., Kolbin, A. S., Sidorenko, S. V., Lawson, R., Kurylev, A. A., Balykina, Y. E., Mukhina, N. V., and Spiridonova, A. A. (2017). A mathematical model for predicting the development of bacterial resistance based on the relationship between the level of antimicrobial resistance and the volume of antibiotic consumption. *Journal of Global Antimicrobial Resistance*, 8:148 – 156.

Assenmacher-Wesche, K. (2006). Estimating central bank preferences from a time-varying empirical reaction function. *European Economic Review*, 50(8):1951–1974.

Austin, D. J., Kristinsson, K. G., and Anderson, R. M. (1999). The relationship between the volume of antimicrobial consumption in human communities and the frequency of resistance. *Proceedings of the National Academy of Sciences*, 96(3):1152–1156.

Balke, N. S. and Fomby, T. B. (1997). Threshold cointegration. *International economic review*, pages 627–645.

Ball, L. (1999). Efficient Rules for Monetary Policy. *International Finance*, 2(1):63–83.

Baum, C. F. and Karasulu, M. (1997). Modelling federal reserve discount policy. *Computational Economics*, 11(1-2):53–70.

Berger, P., Pascal, L., Sartor, C., Delorme, J., Monge, P., Ragon, C. P., Charbit, M., Sambuc, R., and Drancourt, M. (2004). Generalized additive model demonstrates fluoroquinolone use/resistance relationships for Staphylococcus aureus. *European journal of epidemiology*, 19(5):453–460.

Berry, N., Gardner, T., and Anderson, I. (2015). *On targets: how targets can be most effective in the English NHS*. Health Foundation.

Box, G. E. P. and Pierce, D. A. (1970). Distribution of residual autocorrelations in autoregressive-integrated moving average time series models. *Journal of the American statistical Association*, 65(332):1509–1526.

Bozdogan, H. (2003). *Statistical data mining and knowledge discovery*. CRC Press.

Branger, C., Zamfir, O., Geoffroy, S., Laurans, G., Arlet, G., Thien, H. V., Gouriou, S., Picard, B., and Denamur, E. (2005). Genetic background of Escherichia coli and extended-spectrum β-lactamase type. *Emerging infectious diseases*, 11(1):54.

Briand, L. C., Freimut, B., and Vollei, F. (2000). Using multiple adaptive regression splines to understand trends in inspection data and identify optimal inspection ra-

tes. International Software Engineering Research Network (ISERN). *International Software Engineering Research Network. Technical report ISERN-00-07.*

Campbell, J. R. and Fisher, J. D. M. (2000). Aggregate employment fluctuations with microeconomic asymmetries. *American Economic Review*, 90(5):1323–1345.

Carrion-i Silvestre, J. L., Kim, D., and Perron, P. (2009). GLS-based unit root tests with multiple structural breaks under both the null and the alternative hypotheses. *Econometric theory*, 25(6):1754–1792.

Castro, V. (2011). Can central bank monetary policy be described by a linear (augmented) Taylor rule or by a nonlinear rule? *Journal of Financial Stability*, 7(4):228–246.

Chan, K. S. and Tong, H. (1986). On estimating thresholds in autoregressive models. *Journal of time series analysis*, 7(3):179–190.

Christiano, L. J., Eichenbaum, M., and Evans, C. L. (1999). Monetary policy shocks: What have we learned and to what end? In *Handbook of Macroeconomics*, volume 1, Part A of *Handbook of Macroeconomics*, pages 65 – 148. Elsevier.

Chung, S. S. (2012). A class of non-parametric volatility models: Application to financial time series. *Journal of Econometrics*.

Clarida, R., Gali, J., and Gertler, M. (2000). Monetary policy rules and macroeconomic stability: evidence and some theory. *The Quarterly journal of economics*, 115(1):147–180.

Clarida, R. H. and Gertler, M. (1997). How the Bundesbank conducts monetary policy. In *Reducing inflation: Motivation and strategy*, pages 363–412. University of Chicago Press.

Courtney, H. G. (1991). *The Beveridge Curve and Okun's law: a re-examination of fundamental macroeconomic relationships in the United States*. PhD thesis, Massachusetts Institute of Technology.

Craven, P. and Wahba, G. (1979). Smoothing noisy data with spline functions: estimationg the correct degree of smoothing by the method of generalized cross-validation. *Numerische Mathematik*, 31:377–403.

Cukierman, A. and Muscatelli, A. (2008). Nonlinear Taylor rules and asymmetric preferences in central banking: Evidence from the United Kingdom and the United States. *The BE Journal of macroeconomics*, 8(1).

Davey, P., Brown, E., Charani, E., Fenelon, L., Gould, I. M., Holmes, A., Ramsay, C. R., Wiffen, P. J., and Wilcox, M. (2013). Interventions to improve antibiotic prescribing practices for hospital inpatients. *Cochrane Database Syst Rev*, 4(4).

Díaz, M. A., Hernández-Bello, J. R., Rodríguez-Baño, J., Martínez-Martínez, L., Calvo, J., Blanco, J., Pascual, A., and for Nosocomial Infections (GEIH), S. G. (2010). Diversity of Escherichia coli strains producing extended-spectrum beta-lactamases in Spain: second nationwide study. *Journal of clinical microbiology*, 48(8):2840–2845.

De Gooijer, J. G., Ray, B. K., and Kräger, H. (1998). Forecasting exchange rates using TSMARS. *Journal of International Money and Finance*, 17(3):513–534.

De Sá, R. d. and Portugal, M. S. (2015). Central bank and asymmetric preferences: An application of sieve estimators to the US and Brazil. *Economic Modelling*, 51:72–83.

Deo, R. C., Kisi, O., and Singh, V. P. (2017). Drought forecasting in eastern Australia using multivariate adaptive regression spline, least square support vector machine and M5Tree model. *Atmospheric Research*, 184:149–175.

Dey, P. and Das, A. K. (2016). Application of Multivariate Adaptive Regression Spline- Assisted objective function on optimization of heat transfer rate around a cylinder. *Nuclear Engineering and Technology*, 48(6):1315 – 1320.

Dolado, J., Maria-Dolores, R., and Ruge-Murcia, F. J. (2004). Nonlinear monetary policy rules: some new evidence for the US. *Studies in Nonlinear Dynamics & Econometrics*, 8(3).

Dolado, J. J., Maria-Dolores, R., and Naveira, M. (2005). Are monetary-policy reaction functions asymmetric?: The role of nonlinearity in the Phillips curve. *European Economic Review*, 49(2):485–503.

Donayre, L., Eo, Y., Morley, J., et al. (2018). Improving likelihood-ratio-based confidence intervals for threshold parameters in finite samples. *Studies in Nonlinear Dynamics & Econometrics*, 22(1):1–11.

Dubois, V., Arpin, C., Dupart, V., Scavelli, A., Coulange, L., André, C., Fischer, I., Grobost, F., Brochet, J.-P., Lagrange, I., et al. (2008). β-Lactam and aminoglycoside resistance rates and mechanisms among Pseudomonas aeruginosa in French general practice (community and private healthcare centres). *Journal of antimicrobial chemotherapy*, 62(2):316–323.

Economou, A. and Psarianos, I. N. (2016). Revisiting Okun's law in European Union countries. *Journal of Economic Studies*, 43(2):275–287.

Enders, W., Falk, B. L., and Siklos, P. (2007). A threshold model of real US GDP and the problem of constructing confidence intervals in TAR models. *Studies in Nonlinear Dynamics & Econometrics*, 11(3).

Frank, I. E. (1995). Modern nonlinear regression methods. *Chemometrics and intelligent laboratory systems*, 27(1):1–19.

Friedman, J. H. (1977). A recursive partitioning decision rule for nonparametric classification. *IEEE Transactions on Computers*, (4):404–408.

Friedman, J. H. (1991). Multivariate Adaptive Regression Splines. *The Annals of Statistics*, 19(1):1–67.

Friedman, J. H. (1993). *Fast MARS.* Stanford University. Laboratory for Computational Statistics.

Friedman, J. H., Olshen, R. A., Stone, C. J., et al. (1984). Classification and regression trees. *Belmont, CA: Wadsworth & Brooks*.

Friedman, J. H. and Roosen, C. B. (1995). An introduction to multivariate adaptive regression splines.

Gerdesmeier, D. and Roffia, B. (2004). Taylor rules for the euro area: the issue of real-time data. Technical report, Deutsche Bundesbank, Research Centre.

Gerlach, S. and Lewis, J. (2014a). ECB reaction functions and the Crisis of 2008. *International Journal of Central Banking*, 10(1):137–158.

Gerlach, S. and Lewis, J. (2014b). Zero lower bound, ECB interest rate policy and the financial crisis. *Empirical Economics*, 46(3):865–886.

Gerlach, S. and Schnabel, G. (2000). The Taylor rule and interest rates in the EMU area. *Economics Letters*, 67(2):165–171.

Gnabo, J.-Y. and Moccero, D. N. (2015). Risk management, nonlinearity and aggressiveness in monetary policy: The case of the US Fed. *Journal of Banking & Finance*, 55:281–294.

Goh, A. T. C., Zhang, W., Zhang, Y., Xiao, Y., and Xiang, Y. (2018). Determination of earth pressure balance tunnel-related maximum surface settlement: a multivariate adaptive regression splines approach. *Bulletin of Engineering Geology and the Environment*, 77(2):489–500.

Granger, C. W. J., Terasvirta, T., et al. (1993). Modelling non-linear economic relationships. *OUP Catalogue*.

Group, W. B. (2016). Drug-resistant infections: A threat to our economic future (discussion draft). Technical report, World Bank, Washington DC.

Haber, M., Levin, B. R., and Kramarz, P. (2010). Antibiotic control of antibiotic resistance in hospitals: a simulation study. *BMC infectious diseases*, 10(1):254.

Hamilton, J. D. (2010). Regime switching models. In *Macroeconometrics and Time Series Analysis*, pages 202–209. Springer.

Hansen, B. E. (2000). Sample splitting and threshold estimation. *Econometrica*, 68(3):575–603.

Hansen, B. E. (2011). Threshold autoregression in economics. *Statistics and its Interface*, 4(2):123–127.

Harris, R. and Silverstone, B. (2001). Testing for asymmetry in Okun's law: A cross-country comparison. *Economics Bulletin*, 5(2):1–13.

Hastie, T. (2013). gam: Generalized Additive Models, R Package, version 0.98. *R Foundation for Statistical Computing: Vienna, Austria*.

Hastie, T. and Tibshirani, R. (1987). Generalized additive models: some applications. *Journal of the American Statistical Association*, 82(398):371–386.

Hastie, T. J. (2017). Generalized additive models. In *Statistical models in S*, pages 249–307. Routledge.

Hastie, T. J. and Tibshirani, R. J. (1984). Generalized aditive models. Department of Statistics. Technical report, Stanford University, Technical Report 98.

Hastie, T. J. and Tibshirani, R. J. (1990). *Generalized Additive Models*. Chapman & Hall/CRC Monographs on Statistics & Applied Probability. Taylor & Francis.

Hayat, A. and Mishra, S. (2010). Federal reserve monetary policy and the non-linearity of the Taylor rule. *Economic Modelling*, 27(5):1292–1301.

Hinich, M. J. (1982). Testing for Gaussianity and linearity of a stationary time series. *Journal of time series analysis*, 3(3):169–176.

Hocquet, D., Muller, A., Blanc, K., Plésiat, P., Talon, D., Monnet, D. L., and Bertrand, X. (2008). Relationship between antibiotic use and incidence of MexXY-OprM overproducers among clinical isolates of Pseudomonas aeruginosa. *Antimicrobial agents and chemotherapy*, 52(3):1173–1175.

Hodrick, R. J. and Prescott, E. C. (1997). Postwar US business cycles: an empirical investigation. *Journal of Money, credit, and Banking*, pages 1–16.

Holmes, M. J. and Silverstone, B. (2006). Okun's law, asymmetries and jobless recoveries in the United States: A Markov-switching approach. *Economics Letters*, 92(2):293–299.

Horváth, A., Dobay, O., Kardos, S., Ghidan, A., Toth, A., Pászti, J., Ungvári, E., Horváth, P., Nagy, K., Zissman, S., et al. (2012). Varying fitness cost associated with resistance to fluoroquinolones governs clonal dynamic of methicillin-resistant Staphylococcus aureus. *European journal of clinical microbiology & infectious diseases*, 31(8):2029–2036.

Huang, H.-C. and Chang, Y.-K. (2005). Investigating Okun's law by the structural break with threshold approach: Evidence from Canada. *The Manchester School*, 73(5):599–611.

Hughes, J. S., Hurford, A., Finley, R. L., Patrick, D. M., Wu, J., and Morris, A. M. (2016). How to measure the impacts of antibiotic resistance and antibiotic development on empiric therapy: new composite indices. *BMJ open*, 6(12).

Hulscher, M. E. J. L., Grol, R. P. T. M., and van der Meer, J. W. M. (2010). Antibiotic prescribing in hospitals: a social and behavioural scientific approach. *The Lancet infectious diseases*, 10(3):167–175.

Hurvich, C. M. and Tsai, C.-L. (1989). Regression and time series model selection in small samples. *Biometrika*, 76(2):297–307.

Ikeda, T. (2010). Time-varying asymmetries in central bank preferences: the case of the ECB. *Journal of Macroeconomics*, 32(4):1054–1066.

Jardin, M. and Gaétan, S. (2012). How Okun's law is non-linear in Europe: a semi-parametric approach. *Rennes, University of Rennes*.

Jin, R., Chen, W., and Simpson, T. W. (2001). Comparative studies of metamodelling techniques under multiple modelling criteria. *Structural and multidisciplinary optimization*, 23(1):1–13.

Judd, J. P. and Rudebusch, G. D. (1998). Taylor's rule and the Fed: 1970-1997. *Economic Review-Federal Reserve Bank of San Francisco*, (3):3.

Kazanas, T., Philippopoulos, A., and Tzavalis, E. (2011). Monetary policy rules and business cycle conditions. *The Manchester School*, 79:73–97.

Keogh, G. (2010). *Univariate time series modelling and forecasting using TSMARS*. Theory of probability, stochastics, mathematical statistics. LAP LAMBERT Academic Publishing.

Kiffer, C. R. V., Camargo, E. C. G., Shimakura, S. E., Ribeiro, P. J., Bailey, T. C., Pignatari, A. C. C., and Monteiro, A. M. V. (2011). A spatial approach for the epidemiology of antibiotic use and resistance in community-based studies: the emergence of urban clusters of Escherichia coli quinolone resistance in Sao Paulo, Brasil. *International journal of health geographics*, 10(1):17.

Kilinc, B. K., Malkoc, S., Koparal, A. S., and Yazici, B. (2017). Using multivariate adaptive regression splines to estimate pollution in soil. *INTERNATIONAL JOURNAL OF ADVANCED AND APPLIED SCIENCES*, 4(2):10–16.

Kim, D. H., Osborn, D. R., and Sensier, M. (2005). Nonlinearity in the Fed's monetary policy rule. *Journal of applied Econometrics*, 20(5):621–639.

Klose, J. (2011). Asymmetric Taylor reaction functions of the ECB: An approach depending on the state of the economy. *The North American Journal of Economics and Finance*, 22(2):149–163.

Koutroulis, A., Panagopoulos, Y., and Tsouma, E. (2016). Asymmetry in the response of unemployment to output changes in Greece: Evidence from hidden co-integration. *The Journal of Economic Asymmetries*, 13:81–88.

Kuhnert, P. M., Do, K.-A., and McClure, R. (2000). Combining non-parametric models with logistic regression: an application to motor vehicle injury data. *Computational Statistics & Data Analysis*, 34(3):371–386.

Kulikauskas, D. (2014). Nonlinear Taylor rule for the European Central Bank. *Economics Bulletin*, 34(3):1798–1804.

Lamarche, J.-F. and Koustasy, Z. (2012). Estimation of a nonlinear Taylor rule using Real-Time US data. *Studies in Nonlinear Dynamics & Econometrics*, 16(5).

Lawes, T., López-Lozano, J.-M., Nebot, C., Macartney, G., Subbarao-Sharma, R., Dare, C. R. J., Edwards, G. F. S., and Gould, I. M. (2015a). Turning the tide or riding the waves? Impacts of antibiotic stewardship and infection control on MRSA strain dynamics in a Scottish region over 16 years: non-linear time series analysis. *BMJ open*, 5(3):e006596.

Lawes, T., López-Lozano, J.-M., Nebot, C. A., Macartney, G., Subbarao-Sharma, R., Dare, C. R. J., Wares, K. D., and Gould, I. M. (2015b). Effects of natio-

nal antibiotic stewardship and infection control strategies on hospital-associated and community-associated meticillin-resistant Staphylococcus aureus infections across a region of Scotland: a non-linear time-series study. *The Lancet Infectious Diseases*, 15(12):1438–1449.

Lawes, T., López-Lozano, J.-M., Nebot, C. A., Macartney, G., Subbarao-Sharma, R., Wares, K. D., Sinclair, C., and Gould, I. M. (2017). Effect of a national 4C antibiotic stewardship intervention on the clinical and molecular epidemiology of Clostridium difficile infections in a region of Scotland: a non-linear time-series analysis. *The Lancet Infectious Diseases*, 17(2):194–206.

Laxminarayan, R. (2014). Antibiotic effectiveness: balancing conservation against innovation. *Science*, 345(6202):1299–1301.

Laxminarayan, R., Brown, G. M., et al. (2001). Economics of antibiotic resistance: a theory of optimal use. *Journal of Environmental Economics and Management*, 42(2):183–206.

Laxminarayan, R., Duse, A., Wattal, C., Zaidi, A. K. M., Wertheim, H. F. L., Sumpradit, N., Vlieghe, E., Hara, G. L., Gould, I. M., Goossens, H., et al. (2013). Antibiotic resistance- the need for global solutions. *The Lancet infectious diseases*, 13(12):1057–1098.

Laxminarayan, R. and Klugman, K. P. (2011). Communicating trends in resistance using a drug resistance index. *BMJ open*, 1(2):e000135.

Leathwick, J. R., Elith, J., and Hastie, T. (2006). Comparative performance of generalized additive models and multivariate adaptive regression splines for statistical modelling of species distributions. *Ecological modelling*, 199(2):188–196.

Levin, B. R., Lipsitch, M., Perrot, V., Schrag, S., Antia, R., Simonsen, L., Moore Walker, N., and Stewart, F. M. (1997). The population genetics of antibiotic resistance. *Clinical infectious diseases*, 24(Supplement_1):S9–S16.

Levin, B. R., Perrot, V., and Walker, N. (2000). Compensatory mutations, antibiotic resistance and the population genetics of adaptive evolution in bacteria. *Genetics*, 154(3):985–997.

Levy, S. B. (1994). Balancing the drug-resistance equation. *Trends in microbiology*, 2(10):341–342.

Lewis, P. A. and Stevens, J. G. (1991). Nonlinear modeling of time series using mul-

tivariate adaptive regression splines (mars). *Journal of the American Statistical Association*, 86(416):864–877.

Lewis, P. A. W. and Ray, B. K. (1997). Modeling long-range dependence, nonlinearity, and periodic phenomena in sea surface temperatures using TSMARS. *Journal of the American Statistical Association*, 92(439):881–893.

López-Lozano, J.-M., Monnet, D. L., Yagüe, A., Burgos, A., Gonzalo, N., Campillos, P., and Saez, M. (2000). Modelling and forecasting antimicrobial resistance and its dynamic relationship to antimicrobial use: a time series analysis. *International journal of antimicrobial agents*, 14(1):21–31.

Mayes, D. G. and Viren, M. (2002). Asymmetry and the problem of aggregation in the Euro Area. *Empirica*, 29(1):47–73.

Mehdizadeh, S., Behmanesh, J., and Khalili, K. (2017). Using MARS, SVM, GEP and empirical equations for estimation of monthly mean reference evapotranspiration. *Computers and Electronics in Agriculture*, 139:103–114.

Milborrow, S. (2009). Earth: Multivariate Adaptive Regression Spline Models.

Milborrow, S. (2015). Plotmo: Plot a model' s response and residuals. R package.

Millar, M. (2012). Constraining the use of antibiotics: applying Scanlon's contractualism. *Journal of medical ethics*, 38(8):465–469.

Møller, J. K. (1989). Antimicrobial usage and microbial resistance in a university hospital during a seven-year period. *Journal of Antimicrobial Chemotherapy*, 24(6):983–992.

Monnet, D. L., MacKenzie, F. M., López-Lozano, J. M., Beyaert, A., Camacho, M., Wilson, R., Stuart, D., and Gould, I. M. (2004). Antimicrobial drug use and methicillin-resistant Staphylococcus aureus, Aberdeen, 1996–2000. *Emerging infectious diseases*, 10(8):1432.

Morlini, I. (2006). On multicollinearity and concurvity in some nonlinear multivariate models. *Statistical Methods and Applications*, 15(1):3–26.

Mózes, J., Ebrahimi, F., Gorácz, O., Miszti, C., and Kardos, G. (2014). Effect of carbapenem consumption patterns on the molecular epidemiology and carbapenem resistance of Acinetobacter baumannii. *Journal of medical microbiology*, 63(12):1654–1662.

Mukkamala, S., Sung, A. H., Abraham, A., and Ramos, V. (2006). Intrusion detection systems using adaptive regression spines. In *Enterprise information systems VI*, pages 211–218. Springer.

Muñoz, J. and Felicísimo, Á. M. (2004). Comparison of statistical methods commonly used in predictive modelling. *Journal of Vegetation Science*, 15(2):285–292.

Murphy, T. E., Van Ness, P. H., Araujo, K. L. B., and Pisani, M. A. (2011). Bayesian time-series analysis of a repeated-measures Poisson outcome with excess zeroes. *American journal of epidemiology*, 174(11):1230–1237.

Nebot, C., García-Solanes, J., and Beyaert, A. (2016). *Thresholds in the nonlinear Taylor rule*. SAE 2016.

Neftci, S. N. (1984). Are economic time series asymmetric over the business cycle? *The Journal of Political Economy*, pages 307–328.

Okun, A. (1962). Potential GNP: Its measurement and significance. In *Proceedings of the Business and Economic Statistics Section of the American Statistical Association*, volume 7, pages 89–104.

O'Neill, J. (2017). Antimicrobial Resistance: Tackling a crisis for the health and wealth of nations. 2014. *Review on Antimicrobial Resistance, London, United Kingdom*.

Orphanides, A. and Wieland, V. (2000). Inflation zone targeting. *European Economic Review*, 44(7):1351–1387.

Owyang, M. T. and Sekhposyan, T. (2012). Okun's law over the business cycle: was the great recession all that different? *Federal Reserve Bank of St. Louis Review*, 94(September/October 2012).

Oz, T., Guvenek, A., Yildiz, S., Karaboga, E., Tamer, Y. T., Mumcuyan, N., Ozan, V. B., Senturk, G. H., Cokol, M., Yeh, P., et al. (2014). Strength of selection pressure is an important parameter contributing to the complexity of antibiotic resistance evolution. *Molecular biology and evolution*, 31(9):2387–2401.

Pesaran, M. H. and Potter, S. M. (1997). A floor and ceiling model of US output. *Journal of Economic Dynamics and Control*, 21(4-5):661–695.

Petersen, K. et al. (2007). Does the Federal Reserve follow a non-linear Taylor rule? Technical report.

Peterson, L. R. (2005). Squeezing the antibiotic balloon: the impact of antimicrobial classes on emerging resistance. *Clinical Microbiology and Infection*, 11:4–16.

Poole, K. (2011). Pseudomonas aeruginosa: resistance to the max. *Frontiers in microbiology*, 2:65.

Potter, S. M. (1995). A nonlinear approach to US GNP. *Journal of applied econometrics*, 10(2):109–125.

Prachowny, M. F. J. (1993). Okun's law: theoretical foundations and revised estimates. *The review of Economics and Statistics*, pages 331–336.

Pratt, J. W. (1964). Risk aversion in the small and in the large. *Econometrica*, 32(1/2):122–136.

Robert Nobay, A. and Peel, D. A. (2003). Optimal discretionary monetary policy in a model of asymmetric Central Bank preferences. *The Economic Journal*, 113(489):657–665.

Rodríguez-Baño, J., Alcalá, J. C., Cisneros, J. M., and et al (2008). Community infections caused by extended-spectrum β-lactamase-producing escherichia coli. *Archives of Internal Medicine*, 168(17):1897–1902.

Rodríguez-Baño, J., Picón, E., Navarro, M. D., López-Cerero, L., Pascual, A., Group, E. S. B. L.-R. E. I. P. I., et al. (2012). Impact of changes in CLSI and EUCAST breakpoints for susceptibility in bloodstream infections due to extended-spectrum β-lactamase-producing Escherichia coli. *Clinical Microbiology and Infection*, 18(9):894–900.

Ruge-Murcia, F. J. (2002). A prudent central banker. *IMF Staff Papers*, pages 456–469.

Sandmo, A. (1971). On the theory of the competitive firm under price uncertainty. *The American Economic Review*, 61(1):65–73.

Schwarz, G. et al. (1978). Estimating the dimension of a model. *The annals of statistics*, 6(2):461–464.

Sephton, P. (2001). Forecasting recessions: Can we do better on MARS. *Federal Reserve Bank of St. Louis Review*, 83(March/April 2001).

Sephton, P. S. (1994). Cointegration tests on MARS. *Computational Economics*, 7(1):23–35.

Shen, C.-H. et al. (1995). Monetary policy as a decision-making hierarchy: The case of Taiwan. *Journal of Macroeconomics*, 17(2):357–368.

Silvapulle, P., Moosa, I. A., and Silvapulle, M. J. (2004). Asymmetry in Okun's law. *Canadian Journal of Economics/Revue canadienne d'économique*, 37(2):353–374.

Sims, C. A. and Zha, T. (2006). Were there regime switches in US monetary policy? *The American Economic Review*, 96(1):54–81.

Søgaard, P. (1989). The epidemiology of antibiotic resistance in three species of the Enterobacteriaceae and the relation to consumption of antimicrobial agents in Odense University Hospital. *Danish medical bulletin*, 36(1):65–84.

Stokes, H. H. and Lattyak, W. J. (2005). Multivariate Adaptive Regression Spline (MARS) modeling using the B34S proseries econometric system and SCA a workbench. *Scientific Computing Associates Corp.*

Stokes, H. H. and Lattyak, W. J. (2008a). Generalized Additive Modeling (GAM) Using SCAB34S SPLINES and SCA WorkBench. *Scientific Computing Associates Corp.*

Stokes, H. H. and Lattyak, W. J. (2008b). Multivariate Adaptive Regression Spline modeling using SCAB34S SPLINES and SCA Workbench. *Scientific Computing Associates Corp.*

Subrahmanyam, M. G. and Thomadakis, S. B. (1980). Systematic risk and the Theory of the firm. *The Quarterly Journal of Economics*, 94(3):437–451.

Surico, P. (2002). US monetary policy rules: the case for asymmetric preferences.

Surico, P. (2007a). The Fed's monetary policy rule and US inflation: The case of asymmetric preferences. *Journal of Economic Dynamics and Control*, 31(1):305–324.

Surico, P. (2007b). The monetary policy of the European Central Bank. *The Scandinavian Journal of Economics*, 109(1):115–135.

Svensson, L. (1997). Inflation Forecast Targeting. *European Economic Review*, pages 111–146.

Svensson, L. E. O. (1999). Inflation targeting as a monetary policy rule. *Journal of monetary economics*, 43(3):607–654.

Svensson, L. E. O. (2010). Inflation targeting. In *Handbook of monetary economics*, volume 3, pages 1237–1302. Elsevier.

Tang, B. and Bethencourt, C. (2017). Asymmetric unemployment-output tradeoff in the Eurozone. *Journal of Policy Modeling*, 39(3):461–481.

Taylor, J. B. (1993). Discretion versus policy rules in practice. In *Carnegie-Rochester conference series on public policy*, volume 39, pages 195–214. Elsevier.

Taylor, J. B. (1999). A Historical Analysis of Monetary Policy Rules. In *Monetary Policy Rules*, NBER Chapters, pages 319–348. National Bureau of Economic Research, Inc.

Tong, H. (1983). Threshold models in non-linear time series analysis. *New York*.

Tong, H. (1987). Non-linear time series models of regularly sampled data: a review.

Tong, H. (1990). *Non-linear time series: a dynamical system approach*. Oxford University Press.

Tong, H. and Lim, K. S. (1980). Threshold autoregression, limit cycles and cyclical data. *Journal of the Royal Statistical Society. Series B (Methodological)*, pages 245–292.

Ture, M., Kurt, I., Kurum, A. T., and Ozdamar, K. (2005). Comparing classification techniques for predicting essential hypertension. *Expert Systems with Applications*, 29(3):583–588.

Valadkhani, A. and Smyth, R. (2015). Switching and asymmetric behaviour of the Okun coefficient in the US: Evidence for the 1948–2015 period. *Economic Modelling*, 50:281–290.

Vanegas, J. and Vásquez, F. (2017). Multivariate Adaptative Regression Splines (MARS), una alternativa para el análisis de series de tiempo. *Gaceta sanitaria*, 31:235–237.

Vernaz, N., Huttner, B., Muscionico, D., Salomon, J.-L., Bonnabry, P., López-Lozano, J. M., Beyaert, A., Schrenzel, J., and Harbarth, S. (2011). Modelling the impact of antibiotic use on antibiotic-resistant Escherichia coli using population-based data from a large hospital and its surrounding community. *Journal of Antimicrobial Chemotherapy*, 66(4):928–935.

Vogwill, T. and MacLean, R. C. (2015). The genetic basis of the fitness costs of antimicrobial resistance: a meta-analysis approach. *Evolutionary applications*, 8(3):284–295.

WHO (2017). Global action plan on antimicrobial resistance. 2015.

Wong, A. (2017). Epistasis and the evolution of antimicrobial resistance. *Frontiers in microbiology*, 8:246.

Zerbo, A. et al. (2018). A Theorem for Okun's Law. Technical report, Groupe d'Economie du Développement de l'Université Montesquieu Bordeaux IV.

Zhang, Y. and Hepner, G. F. (2017). Short-term phenological predictions of vegetation abundance using Multivariate Adaptive Regression Splines in the Upper Colorado River Basin. *Earth Interactions*, 21(1):1–26.